

PLUTONIC AND VOLCANIC ROCKS FROM CENTRAL CHILE
(33° - 42°S): GEOCHEMICAL EVIDENCE REGARDING
THEIR PETROGENESIS

by

LEOPOLDO LOPEZ ESCOBAR

B.A., Catholic University of Chile (1963)

M.S. in Chemistry, M.I.T. (1972)

M.S. in Earth and Planetary Sciences, M.I.T. (1972)

SUBMITTED IN PARTIAL FULFILLMENT
OF THE REQUIREMENTS FOR THE
DEGREE OF DOCTOR OF
PHILOSOPHY

at the

MASSACHUSETTS INSTITUTE OF TECHNOLOGY

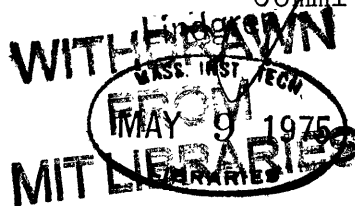
November, 1974

(i.e. February 1975)

Signature of Author.....
Department of Earth and Planetary Sciences
November 27, 1974

Certified by.....
Thesis Supervisor

Accepted by.....
Chairman, Departmental
Committee on Graduate Students



PLUTONIC AND VOLCANIC ROCKS FROM CENTRAL CHILE
(33° - 42°S): GEOCHEMICAL EVIDENCE REGARDING
THEIR PETROGENESIS

by

LEOPOLDO LOPEZ ESCOBAR

SUBMITTED TO THE DEPARTMENT OF EARTH AND PLANETARY SCIENCES
IN PARTIAL FULFILLMENT OF THE REQUIREMENTS FOR THE
DEGREE OF DOCTOR OF PHILOSOPHY

ABSTRACT: The Miocene Coastal volcanic belt in central-south Chile (37-42°S) is geochemically similar to the calc-alkaline suite of Circumpacific island arcs. Andesites from central-south Chile do not have the high abundances of large-ion-lithophile elements that characterize northern Chile andesites. These geochemical differences correlate with differences in Benioff zones; in the north, intermediate-depth earthquakes are abundant and the down-going slab dips ~25°, whereas in the central-south, the dip is <15° and intermediate-depth earthquakes are rare.

Unaltered Nazca plate basalt does not contain enough K, Rb, Sr, and Ba to generate andesites by fractional melting of amphibolite or eclogite. Amphibolite models also fail to account for the fractionated rare earth element (REE) distributions of andesites. Partial melts of garnet-bearing assemblages, e.g., eclogite, have fractionated REE distributions, and two calc-alkaline suites (Ancud in central-south Chile, and the Cascades) have decreasing heavy REE with increasing SiO₂ as expected in such melts. Small amounts (<10%) of peridotite (with REE two times chondrites) melting can also account for the REE distribution of andesites, but peridotite melts are likely to be deficient in K, Rb, Sr, and Ba relative to andesites. None of the simple melting models of oceanic ridge basalt (altered or unaltered) or peridotite account for all aspects of andesite trace element geochemistry.

In the High Andean Range, the plateau series at Pino

Hachado is alkali-rich ($\text{Na}_2\text{O} > \text{K}_2\text{O}$) and has trace element abundances similar to differentiated rocks of the alkali-olivine basalt series. Stratovolcanoes are superimposed on the plateau series. Partial melting of peridotite (2-10%) offer the best explanation for the REE abundances in the high-alumina basalts from these stratovolcanoes. The high-alumina basalts have undergone extensive plagioclase fractionation. Such differentiation does not develop andesitic composition.

Granodiorite is the most abundant rock type in the Central and Andean batholiths outcropping in the central part of Chile between latitudes 33-34°S. These granodiorites have geochemical characteristics similar to the average circumpacific granodiorite (Taylor, 1969). They are also similar to granodiorites from the Sierra Nevada batholith. Some eastward chemical trends, similar to those observed in the western USA batholiths, are also observed between the Central and Andean batholiths. Geochemical similarities between Chilean plutonic and volcanic rocks suggest a similar origin for both kinds of rocks. The Coastal batholith granodiorites can be derived by a fractional crystallization process, involving mainly plagioclase and amphibole, from the Coastal batholith tonalites. These tonalites can be derived by a fractional crystallization process, involving plagioclase and clinopyroxene, from andesitic magmas. The REE of the Central Chile plutonic rocks are not consistent with a generation by fractional melting of the subducted Nazca Plate tholeiitic basalts.

THESIS SUPERVISOR: Frederick A. Frey

TITLE: Associate Professor

To my wife, Ana Rosa, and to my children Marcelo
Andres, Gonzalo Alberto, Leopoldo Patricio and Ana
Carolina.

TABLE OF CONTENTS

	Page
ABSTRACT	2
CHAPTER I	7
INTRODUCTION	7
EXPERIMENTAL	9
SAMPLE LOCALITIES	11
MAJOR ELEMENT COMPOSITION	11
TRACE ELEMENTS	13
DISCUSSION	15
Geochemical Comparison of Calc-alkaline Suites	15
Origin of Andesites	18
Fractional Crystallization of Basaltic Magma	19
Fractional Melting of Amphibolite	22
Fractional Melting of Eclogite	25
Fractional Melting of Garnet Amphibolite and Garnet Granulite	29
Fractional Melting of Peridotite	30
Genetic Relationship Between Temuco Andesites	32
SUMMARY AND CONCLUSION	33
CHAPTER II	37
INTRODUCTION	37
SAMPLE LOCALITIES	38
RESULTS AND DISCUSSION	39
Major Element Composition	39
Rare-earth Element Composition	41
Origin of the High Andean Calc-alkaline Rocks	44
Samples with La/Yb ~ 2-3	45
Samples with La/Yb ~ 5	46
Samples with La/Yb ~ 10	47
SUMMARY AND CONCLUSION	48

TABLE OF CONTENTS (continued)

	Page
CHAPTER III	50
INTRODUCTION	50
COASTAL BATHOLITH	53
CENTRAL BATHOLITH	54
ANDEAN BATHOLITH	56
RESULTS AND DISCUSSION	57
Sample Localities	57
Mineralogy	57
Major Element Geochemistry	58
Trace Element Geochemistry	61
Compatible Trace Elements	61
Incompatible Trace Elements	67
Relationships Between Tonalites, Granodiorites and Granites of the Central Chile Batholiths. Evidences for a fractional crystallization model.	74
Relationships Between Chilean Tonalites and Andesites	80
SUMMARY AND CONCLUSION	85
APPENDIX I	89
APPENDIX II	98
REFERENCES	123
TABLES	136
FIGURES	177
ACKNOWLEDGEMENTS	268
BIOGRAPHICAL INFORMATION	269

CHAPTER I

ANDESITES FROM CENTRAL-SOUTH CHILE:
TRACE ELEMENT ABUNDANCES AND PETROGENESIS

INTRODUCTION

The Andes can be divided into three main regions: the Southern Andes, south of 47°S ; the Central Andes from 47°S to near the Peru-Ecuador border; and the Northern Andes (Gansser, 1973). The Central Andes are characterized by the north-south trending Coastal Cordillera and the parallel High Andean Cordillera which are typically separated by a longitudinal valley. In central-south Chile ($37^{\circ}30' - 42^{\circ}\text{S}$), a deeply-eroded Tertiary Coastal volcanic belt borders the western side of the valley (Illies, 1970; Vergara, 1974). This belt which overlies Paleozoic metamorphic rocks contains andesitic lava flows and pyroclastics which form volcanic necks and nearly horizontal layers occasionally interfingered with Miocene marine sediments (Vergara, 1970; Vergara and Munizaga, 1974). Approximately 100 km east of the Coastal volcanic belt is the High Andean Cordillera. Here two volcanic units are distinguished: 1) an andesitic plateau series composed of subhorizontal andesite flows and pyroclastics resting unconformably on Mesozoic basement, and 2) stratovolcanoes superimposed on

the plateau series (Vergara and Munizaga, 1974). These volcanoes are dominantly andesite and high alumina basalt; the latter are not found in the High Andean Cordillera of northern Chile (Pilcher and Zeil, 1969, 1972; Katsui, 1972). In central-south Chile both volcanic units of the High Andean Cordillera are Pliocene to Holocene in age (Vergara and Munizaga, 1974).

The Peru-Chile Trench west of the continent is an important geological feature, although its topography is minimized south of 33°S because of sedimentary filling (Hayes, 1966). Underthrusting of the Nazca plate in central-south Chile is implied by numerous shallow-focus earthquakes (up to 120 km) forming a 15° dipping Benioff zone. Compared to northern Chile this region has abundant shallow-focus earthquakes offset to the west with extensive activity underneath the trench, fewer intermediate-focus earthquakes, and no deep-focus earthquakes (Figures 9 and 10, Stauder, 1973).

The study in this chapter compares the geochemical characteristics of Upper Cenozoic volcanics from the central-south Chile Coastal Range with other continental and island-arc calcalkaline provinces. The major objective is an understanding of andesite petrogenesis.

EXPERIMENTAL

Major elements were determined by wet chemical analysis at the Department of Geology of the University of Chile (Lopez-Escobar and Oyarzun, 1974). The precision of this technique was estimated from the results of a triplicate analysis of the USGS standard rock G2 (Oyarzun, personal communication). The precisions are generally better than $\pm 5\%$. For TiO_2 , MnO and P_2O_5 the precision is better than $\pm 15\%$. The accuracy of the measurements is estimated to be equal to the precision. Ni was analyzed by atomic absorption. Its precision is better than $\pm 20\%$. Rb and Sr were determined by x-ray fluorescence. The precision and accuracy of this technique is $\pm 10\%$. The rest of the trace elements were obtained by instrumental neutron activation analysis (INAA) at M.I.T. The precision of this technique was estimated from the results of a triplicate analysis of the USGS standard rock G2 (Table 1). The errors indicated in Table 1 are the standard errors of the mean. These were calculated in the following way:

- a) A number "n" of determinations for each element was made. Generally the value of "n" was 3, but in those cases, such as La, in which more than one peak was used for its determination, the value of "n" was greater than 3.
- b) The values " x_i " obtained in those "n" determinations were added and then divided by "n" in order to get

an average value \bar{x} .

c) The deviation of each determination from the average, i.e. $(x_i - \bar{x})$, was calculated and then squared. These values were added, i.e. $\sum (x_i - \bar{x})^2$ was obtained. This sum was divided by $(n-1)$ and the square root of the ratio was calculated. This corresponds to the standard deviation of the mean, "s", i.e.:

$$s = \sqrt{\frac{\sum (x_i - \bar{x})^2}{n-1}}$$

d) The standard error of the mean, "e", which is a measure of the precision of the measurements, was calculated by dividing the standard deviation by the square root of the number of determinations "n", i.e.:

$$e = \frac{s}{\sqrt{n}}$$

The precision of the INAA is generally better than $\pm 5\%$. The precisions of Yb and Lu are respectively 7 and 8%. The precision of Gd is poorer ($\pm 20\%$). The accuracy of the measurements is believed to be equal to the precision. Further details on the analytical procedure used at M.I.T. are found in Appendix II.

SAMPLE LOCALITIES

Four andesites and two dacites were obtained from Temuco and Los Angeles, respectively. The seven Ancud samples from the northern part of Chiloe Island are from andesitic flows intercalated with large sequences of subaerial pyroclastics (Figure 1).

Petrographic descriptions of all samples are included in Appendix I.

MAJOR ELEMENT COMPOSITION

The majority of samples studied have chemical features expected of calc-alkaline volcanics (Table 2). For example, in an FMA diagram (Figure 2), central-south Chilean volcanics fall within or below the field designating Kuno's hypersthene (calcalkaline) andesite series (Kuno, 1968a). This field includes most of the Circumpacific andesitic suites (Kuno, 1968b; Irvine and Baragar, 1971). In a total alkalis versus silica plot, central-south Chilean volcanics are intermediate between the alkaline and subalkaline fields (Figure 3); that is, within the field of the high-alumina basalt series (Kuno, 1960). As observed by Irvine and Baragar (1971), Al_2O_3 abundance is the most prominent major element difference between the basic members of the calcalkaline and tholeiitic series. The high Al_2O_3 abundances of these Chilean volcanics

relative to fresh and altered tholeiitic rocks (e.g., Nazca plate basalts) are seen in Figure 4.

Taylor (1969) proposed the following nomenclature for calc-alkaline rocks:

1. High-alumina basalt ($<53\%$ SiO_2)
2. Low-silica andesite ($53-56\%$ SiO_2 , $0.7-2.5\%$ K_2O)
3. Low-K andesite ($53-62\%$ SiO_2 , $< 0.7\%$ K_2O)
4. Andesite ($56-62\%$ SiO_2 , $0.7-2.5\%$ K_2O)
5. High-K andesite ($53-62\%$ SiO_2 , $> 2.5\%$ K_2O)
6. Dacite ($62-68\%$ SiO_2)
7. Rhyolite ($>68\%$ SiO_2)

Thus the Coastal belt volcanics (on an anhydrous basis) include one high-alumina basalt, three low-silica andesites, eight andesites, and two dacites.

Calc-alkaline rocks may also be subdivided by a plot of normative color index (sum of mafic normative minerals) against normative plagioclase composition (Irvine and Baragar, 1971). On this basis, three samples are high-alumina basalts since two of the previously defined low-silica andesites have color indexes greater than 26, and thus lie just above the andesite-basalt boundary (Figure 5). Several of these basalts contain calcic plagioclase ($>\text{An } 50$) but have very low $\text{Mg}/\text{Mg}+\Sigma\text{Fe}$. In fact, this ratio varies only from 0.48 to 0.61 as the SiO_2 varies from 49.6 to 63.2%. Pichler and Zeil (1972) defined basalt as

having a color index >40 , and stated that true basalts are lacking in both northern and central-south Chile.

TRACE ELEMENTS

For petrogenetic purposes trace elements can be divided into two broad groups: 1) compatible elements (Sc, Cr, Co, and Ni) which are readily accommodated into mafic phases, and 2) incompatible elements, typically large-ion-lithophile (LIL) elements such as Rb, Sr, Ba, rare-earth elements (REE), Hf, Ta, Th, and U. The following discussion outlines the trace element characteristics of each sample locality.

Ancud

Several trace element abundance trends occur as SiO_2 and K_2O increase in the sequence high-alumina basalt to low-silica andesite to andesite (Tables 2 and 3).

1. Rb, Hf, Ta, Th, and U increase. The two andesites (CH-15 and GVO-63) with groundmass biotite have unusually high Rb abundances (300 and 120 ppm).

2. Sr and Ba decrease or remain approximately constant probably as a result of plagioclase fractionation since at Ancud, as in most calc-alkaline suites, plagioclase is the principal phenocryst mineral.

3. Light rare earth elements (LREE) increase and a negative Eu anomaly develops. However, the heavy rare

earth elements (HREE) reach a maximum in the low-silica andesites (Figure 6a). The high-alumina basalt has a positive Eu anomaly indicating preferential accumulation of plagioclase phenocrysts.

4. Compatible trace elements decrease. Notable exceptions are the anomalously high Cr and Ni abundances in the andesites with very high Rb abundances.

Temuco

The samples with amphibole phenocrysts (T-3 and T-13) are the most differentiated. They have the highest normative quartz, LREE, Ba, Hf, and Th abundances, the lowest Sc and Co abundances, and significant Eu depletions (Table 2 and 3, Figure 6b). In all these aspects T-3 is considerably more differentiated than T-13.

Compared to Ancud andesites, the Temuco andesites have higher Sr abundances and similar Ba abundances (except for T-3). Also Hf, Ta, and U abundances (except for T-3) are comparable to or lower than in the Ancud high-alumina basalt, whereas Rb and Th abundances are intermediate between the Ancud low-silica andesites and andesites. The average REE abundances in the Temuco andesites are nearly identical to the Circumpacific average (Figure 6b).

Los Angeles

The dacites differ significantly in major and trace

element compositions. Relative to T-18, T-17 has higher Mg, Fe, Ca, Cr, Co, and Ni abundances, but lower abundances of Na, K, P, and LIL elements (Tables 2 and 3).

Compared to Ancud andesites, the dacites have higher abundances of LIL elements (except Sr and Ta) and similar relative Eu depletions (Figure 6c). Nevertheless, the high $Mg/Mg+\Sigma Fe$, Cr, and Ni abundances in T-17 preclude derivation of these dacites by fractional crystallization of Ancud or Temuco andesites.

DISCUSSION

Geochemical Comparison of Calc-alkaline Suites

Jakes and White (1972) summarized the major and trace element abundance characteristics of island arc, calc-alkaline rocks, and proposed geochemical criteria to distinguish calc-alkaline rocks of continental margins (Andean-type) from those in island arcs. Data from northern Chile were used to define the calc-alkaline continental margin suite (Siegers et al., 1969; El-Hinnawi et al., 1969; Pichler and Zeil, 1972). High FeO/MgO , K_2O/Na_2O , and LIL-element abundances are associated with continental margin environments (Table 4); however, some continental margin areas, e.g. the North American Cascades, are classed with island-arc suites.

Brousse and Oyarzun (1973) found that in Chile, K_2O ,

Rb, and Sr abundances in Pliocene and Quaternary andesites increase from 37°S to 18°S (Sr 405 to 960 ppm, Rb 12 to 69 ppm). A difference between northern and central-south Chile calc-alkaline rocks can also be seen in $\text{K}_2\text{O}-\text{SiO}_2$ trend lines (Figure 8). Based on other LIL-element differences, northern Chile andesites are expected to have higher REE abundances and La/Yb than the Circumpacific average. No REE data is available for northern Chile andesites, but average REE abundances in Temuco andesites are nearly identical to the Circumpacific average (Figure 6 b). It is evident that the geochemical characteristics (Figure 6, Table 4) of central-south Chile Coastal belt andesites are more similar to island-arc andesites than northern Chile andesites (continental margin or Andean type of Jakes and White, 1972). An exception are the very high Rb abundances and resulting low K/Rb of the Ancud andesites. It is likely that the high Rb in these biotite-bearing rocks results from alteration (Armbrust et al., 1971).

Although abundances of compatible trace elements are important in understanding andesite petrogenesis (Taylor et al., 1969), no consistent differences between island-arc and continental margin andesites have been established (Jakes and White, 1972). Large variations in Ni abundance and Ni/Co are found in Chilean andesites, but there is

no correlation with latitude. In the central south Miocene volcanics, Ni abundance ranges from normal (20 ppm at Temuco) to high (25-90 ppm at Ancud and Los Angeles), and Ni/Co ratios exceed unity which is unusual for andesites (Taylor et al., 1969). Oyarzun (1971) found an average Ni content of 35 ppm and Ni/Co of 1.9 in Chilean Tertiary andesites and 19 ppm Ni and Ni/Co of 0.9 in the Chilean Quaternary andesites. Because of large standard deviations, these differences may be insignificant. Similar large variations are found in northern Chile. Rhodes and Ridley (1971) determined an Ni average of 21 ppm in 17 northern Chile andesites and Siegers et al., (1969) reported an Ni average of 50 ppm with Ni/Co=2.1 for 24 northern Chile andesites.

The geochemical differences between northern and central-south Chile andesites correlate with marked tectonic and volcanic differences (Brousse and Oyarzun, 1973). There is an absence of recent volcanism in Chile between approximately 27°S and 33°S; basic calc-alkaline volcanics are more abundant south of this gap (Katsui and Gonzalez, 1968; Pichler and Zeil, 1969, 1972; Katsui, 1972). In the north (18°-22°S), a well developed Benioff zone with abundant intermediate depth earthquakes and a few deep (600 km) earthquakes dips 25° beneath the continent. In the central-south (34-42°S) intermediate and deep earth-

quakes are absent; abundant shallow earthquakes indicate a 15° dipping Benioff zone bottoming at 120 km (Figures 9 and 10, Stauder, 1973). Between north and central-south Chile there is a silent zone ($25-27^{\circ}\text{S}$) which lacks intermediate depth earthquakes (Santo, 1969; Figure 10a, Stauder, 1973). This silent zone nearly overlaps the lack of recent volcanism between 27° and 33°S . The subducting lithosphere is apparently broken into discrete sections which behave differently north and south of the quiet zone (Stauder, 1973). Therefore, the geochemical differences between north and central-south Chile andesites correlate with depth of the Benioff zone in a north-south direction rather than perpendicular to the cordillera-trench system. In fact, in the north there is ambiguity concerning the presence of a relationship between K_2O abundance and depth to the Benioff zone (cf. James et al., 1973; Rhodes and Ridley, 1971; Lefevre, 1973). In contrast, Vergara (1970) has presented evidence for increasing alkalinity towards the east in the High Andes and extra-Andean region of central-south Chile and Argentina.

Origin of Andesites

Two recent papers (Boettcher, 1973; Ringwood, 1974) have reviewed alternative models for the origin of

andesite. Constraints on theories of andesite petrogenesis arise from geophysical, petrological, and geochemical data. Trace element data provide sensitive tests for alternative models (e.g., Taylor, 1969). A rapid increase in trace element data for calc-alkaline rocks (Taylor et al., 1969; Jakes and White, 1972; Ewart and Bryan, 1973; Church, 1973b; Condie and Swenson, 1973; Gill, 1974; DeLong, 1974) has led to increased discussion of trace element constraints on andesite petrogenesis. The central-South Chile trace element data has been evaluated in relation to the following models for andesite origin:

1. fractional crystallization of basaltic magma,
2. anatexis of oceanic lithosphere in subduction zones,
3. anatexis of hydrous peridotite.

Models involving sialic crust have not been considered because central-south Chilean andesites are similar to andesites developed in areas devoid of such crust (i.e., island arcs).

Fractional Crystallization of Basaltic Magma

Plagioclase is the dominant phenocryst mineral in andesites, and at low pressures it is the only liquidus phase over a wide temperature interval (Ringwood, 1974). At the oxygen fugacities of andesitic magmas (Drory and

Ulmer, 1974), plagioclase fractionation would cause significant relative Eu depletions in the residual magma (Weill and Drake, 1973). Nevertheless, calc-alkaline rocks with Eu anomalies are unusual (Jakes and White, 1972; Condie and Swenson, 1973). Chilean samples with relative Eu depletions have probably undergone low-pressure plagioclase fractionation (Figure 6).

The following discussion of fractional crystallization is limited to the least differentiated andesites; that is, those with the lowest LIL-element abundances and no Eu anomaly (low-silica andesites of Ancud and T2, T9, and T13 from Temuco).

Low pressure fractionation models for generating andesites usually involve magnetite or amphibole. However, magnetite fractionation is unlikely as a dominant process (Boettcher, 1973). Two parent basaltic magma compositions are conceivable: 1) high-alumina basalt and 2) oceanic ridge basalt, possibly with an altered chemical composition.

Basalts termed high-alumina do not form a coherent class, and they are the subject of considerable controversy (summarized by Irvine and Baragar, 1971). For example, the Warner basalt of California (termed high alumina by Kuno, 1960) has mineralogical and chemical features quite different from Japanese high-alumina basalts (Figure 7, this paper, Smith and Carmichael, 1968). In calc-alkaline

provinces the most distinctive chemical features of high-alumina basalts are high Al_2O_3 and low $\text{Mg}/\text{Mg} + \Sigma\text{Fe}$ relative to tholeiitic basalts (Wilkinson, 1967).

The Rayleigh fractionation law, expressed in the formula $C_D/C_P = (1-x)^\lambda^{-1}$ (Gast, 1968; Haskin et al., 1970) is valid in crystallization situations where crystals are removed from contact with the liquid as soon as they are formed. In this expression C_P is the concentration of a given trace element in the initial liquid; C_D is the concentration of that element in the residual liquid; x is the weight fraction of the crystals fractionated; λ is, in case that a single phase is crystallizing, the partition coefficient for the trace element between the phase crystallizing and the liquid; if more than one phase is involved in the process, λ is the average of individual partition coefficients weighed according to the proportions in which different phases crystallize (Gast, 1968). The application of this expression shows that the REE pattern observed in Temuco andesites cannot be explained by fractionation either of plagioclase or clinopyroxene or amphibole (or any combination of these three minerals) from a magma of REE composition of CH6 (high-alumina basalt from Ancud). For example, relative to CH6, the Temuco andesites are depleted in HREE. Fractionation

involving the above minerals cannot explain this fact since the partition coefficients for HREE between those minerals and liquids of basaltic composition are generally <1 (Schnetzler and Philpotts, 1970; Table 4, this work). Therefore, a fractionation of these minerals enrich (instead of deplete) the residual magma in HREE. Evidently, as concluded by Taylor et al. (1971) fractional crystallization of high-alumina basalt does not commonly yield andesite magma.

Fractionation of low-silica amphibole from oceanic ridge basalt (or melting of oceanic ridge basalt in amphibolite mineralogy) remains a viable mechanism for andesite generation (e.g., Holloway and Burnham, 1972). In order to evaluate oceanic ridge basalt as parental material for andesite, trace element abundances have been calculated for fractional melts of this basalt in amphibolite and eclogite facies. If andesites are liquids derived from oceanic ridge basalt, the models can be evaluated by comparing the ratios: C^A/C^B (C^A and C^B are abundances of trace element in andesite and oceanic ridge basalt, respectively) and C^L/C_0 (C^L = average concentration of element in aggregate liquid formed during fractional melting (Shaw, 1970), C_0 = concentration in initial solid). Partition coefficients used for these calculations are in Table 5.

Fractional Melting of Amphibolite

Approximately 30-40% melting of tholeiitic basalt in

amphibolite facies yields liquids with the major element composition of andesite (Holloway and Burnham, 1972). Since amphibolite composed only of amphibole represents the end member mineralogy of oceanic crust in a shallow (<100 km) hydrous environment, the results of amphibole melting were calculated (Figures 9 and 10). This model accounts for the abundances of Sc, Cr, and Ni in andesites, but Co in the calculated liquid is too high (Figure 9). However, Co partition coefficients range widely (7.5, Ewart and Taylor, 1969; 1.1, Gunn, 1972), and an average value would provide better agreement.

Concordance between calculated and observed values is very poor for K, Rb, Sr, and Ba; Rb and Ba abundances in andesites are approximately a factor of 10 greater than predicted. Such discrepancies decrease substantially if the parent oceanic ridge basalt is highly altered. For example, Frey et al. (1974) found a two-fold Sr enrichment and a seven-fold Ba enrichment in some highly altered Deep Sea Drilling Project basalt cores; similar enrichments in K and Rb have been found (Hart, 1969). Altered basalt also explains strontium isotopic differences between andesites and oceanic ridge basalts (Church, 1973a; Dasch et al., 1973). In addition, the lower K/Rb of andesites can be accounted for since 1) alteration of oceanic ridge basalts decreases K/Rb (Hart, 1969), and 2) liquids in

equilibrium with amphibole have lower K/Rb than the source rock (Figure 9). These results imply that only upper altered portions of oceanic crust are involved in andesite formation, perhaps as suggested by Fitton (1971).

However, REE abundances in liquids derived by fractional melting of amphibole are not consistent with andesite data. The slope of the calculated REE distribution is not large enough to account for andesite REE abundances (Figure 9 and 10), and, more importantly, the model does not predict the HREE depletion (relative to oceanic ridge basalts) of the Temuco andesites (Figure 6b). Similar discrepancies for Tonga andesites led Ewart and Bryan (1973) to discard an amphibolite model.

A more realistic, less hydrous, source rock than pure amphibole would be composed of plagioclase and clinopyroxene in addition to amphibole. Liquids formed in equilibrium with plagioclase would be Eu depleted; thus residual plagioclase could explain the Eu-depleted Los Angeles dacites and Ancud andesites (Figures 6a and 6c). However, in this model most andesitic liquids would coexist with only clinopyroxene and amphibole since plagioclase is not a near-liquidus phase at hydrous conditions (Green, 1972). Inclusion of clinopyroxene as a residual phase has the following effects on the derived liquid (Figure 9):

- 1) Cr abundance decreases markedly,
- 2) K, Rb, Sr, and Ba

abundances increase, but are still far below levels in andesites, and 3) REE abundances change only insignificantly. For example, REE abundances were determined in a liquid derived from partial melting of a Hawaiian tholeiite at 5kb and 1000°C (Holloway and Burnham, 1972). This liquid which coexisted with a solid of 86% amphibole, 7% clinopyroxene, and 7% olivine plus opaques has REE abundances (normalized to the initial basalt) similar to those calculated for pure amphibole melting (Figure 9). As a result, amphibolite models of fresh or altered oceanic basalt are not suitable for andesites such as at Temuco.

Fractional Melting of Eclogite

At high pressures (>25 kb) and under anhydrous conditions subducted oceanic crust transforms primarily to clinopyroxene plus garnet (eclogite facies, Green and Ringwood, 1968; Green, 1972). Fitton (1971) and Ringwood (1974) have proposed that eclogite-controlled fractionation is important in the generation of calc-alkaline magmas. Specifically, this mechanism is believed to cause an increase in K/Na relative to the source rock and a development of LREE enrichment relative to chondrites.

Relative to the Temuco andesites, a melt formed by 40% fractional melting of eclogite has one tenth the Rb and Ba, less than one half the K, Sc, and Cr, similar Sr and Co, and three times the Ni (Figure 9). Although

subsequent olivine fractionation would lower the high Ni abundance, the deficiencies in K, Rb, Ba, Sc, and Cr are difficult to explain. For calc-alkaline magmas possibly derived from the Nazca plate, it is tempting to cite the abundant metalliferous sediments (Bostrom et al., 1973; Dymond et al., 1973; Hart et al., 1974) as a source for elements deficient in oceanic ridge basalt. However, when the role of sediment has been investigated by isotopic studies, the sediment contribution to calc-alkaline magmas is 2% (Church, 1973a). Thus, as for the amphibolite model altered basalt is required to account for K, Rb, and Ba abundances of andesites.

Similar conclusions were reached by Gill (1974), who evaluated the hypothesis that Fijian calc-alkaline rocks have been derived by partial melting of average oceanic ridge basalt in an eclogite mineralogy. He found, 1) altered basalt was required to generate the K, Rb, Sr, Pb, Th, and U abundances and Sr isotopic data of the calc-alkaline rocks. However, even altered basalt could not account for the Ba abundance of andesites, 2) Sc, Cr, and Co abundances in the theoretical melts were consistent with andesite abundances, but V, and especially Ni, abundances were too high. DeLong (1974) observed a similar Ni discrepancy for Aleutian andesites.

The most sensitive test for eclogite fractionation

is REE abundances. This is because in a basaltic composition at crustal and upper mantle pressures, garnet is the only major mineral which has HREE solid/liquid partition coefficients greater than unity. Thus, as an eclogitic assemblage undergoes melting, the first dacitic liquids (Green and Ringwood, 1968; Green, 1972), should be HREE depleted but LREE enriched relative to the source rock. As melting increases, HREE and LREE abundances in the liquid approach the source rock abundances. A literature survey (Gill, p. 42, 1974) showed that calc-alkaline suites do not have this REE behavior. This result precludes eclogite fractionation as an important model for generating the range of compositions (basalt-andesite-dacite) comprising calc-alkaline suites.

Nevertheless, eclogite fractionation is the obvious and commonly invoked mechanism (e.g., Ringwood, 1974) for explaining HREE abundances in andesites which are depleted in HREE relative to oceanic ridge basalts (e.g., Temuco andesite average and Circumpacific average in Figure 6b). There is considerable uncertainty about garnet HREE solid/liquid partition coefficients, but all likely eclogite fractionation models predict HREE depletion relative to the source rock (Figure 10). However, as Gill (1974) observed, the predicted chondrite-normalized slope in the HREE region is too steep to match observed andesites.

Also, the chondrite-normalized LREE depletion of oceanic ridge basalt is retained by the theoretical melts (Figure 10). Such LREE depletion (La and Ce < Pr and Nd) is not observed in andesites. Because neither garnet nor clinopyroxene retain significant amounts of LREE, this feature is inherent in an eclogite model (also the amphibolite model). Thus, a simple eclogite partial melting model cannot account for andesite trace element abundances if the eclogite has formed from average oceanic ridge basalt.

Calc-alkaline magmas of the Cascades exhibit the HREE trends expected for eclogite melting. For example, rocks from Mount St. Helens (Washington) decrease in HREE from basalts (HREE 11-14 x chondrites) to andesites (9 x chondrites) to dacites (6.5 - 7.5 x chondrites; Figure 11). The data of Condie and Swenson (1973) for Mt. Shasta, Mt. Rainier, and Mt. Jefferson volcanics and the data for Ancud exhibit the same trend: in each case the most silicic rocks have the lowest HREE abundances. An alternative explanation for these HREE trends is fractional crystallization of an HREE enriched accessory phase such as zircon or apatite. Zircon fractionation is unlikely because Hf abundances increase as HREE decrease (Table 3). Although P_2O_5 typically decreases from basalt to dacite (Anderson and Gottfried, 1971), apatite fractionation is unlikely because 1) P_2O_5 contents of calc-alkaline rocks

rarely exceed 0.50 wt.%, 2) apatite phenocrysts are not observed in the basalts and andesites, and 3) apatite removal would not selectively deplete HREE (Nagasawa, 1970). Among the calc-alkaline suites studied in detail, the Cascades are the most likely to have been derived by partial melting of eclogite. The Franciscan eclogites (Coleman et al., 1965) may be representative of the source rocks (Church, 1973b). Relative to oceanic ridge basalts, these eclogites have higher alkali metal, Ba (factor of 10), and LREE abundances (Figure 11, this study; Coleman et al., 1965; Church, 1973b). Because of such differences, these eclogites are more suitable source rocks than oceanic ridge basalt.

Fractional Melting of Garnet Amphibolite and Garnet Granulite

Oceanic ridge basalt contains amphibole at intermediate pressures in addition to garnet and clinopyroxene (Green, 1972). Ewart and Bryan (1973) found that fractional melting of such as assemblage (70% amphibole, 20% clinopyroxene and 10% garnet) is a feasible mechanism for producing calc-alkaline andesite REE distributions. They used very high HREE garnet/liquid partition coefficients (Schnetzer and Philpotts, 1970); thus 10% garnet caused HREE depletion in the derived liquids (Figure 5, Ewart and Bryan, 1973). With lower garnet partition coefficients,

the proportion of garnet in the residual solids can be increased (Figure 10). However, garnet amphibolite is not a significantly better model than eclogite because in both models the melts are deficient in K, Rb, Ba, and La relative to andesites.

To account for K, Rb, and Sr abundances in Aleutian Islands andesites, DeLong (1974) utilized a model of 10% fractional melting of altered basalt as garnet granulite (30% clinopyroxene, 35% garnet, 25% plagioclase, and 10% quartz). This model closely matches the K, Rb, and Sr abundance of the central-south Chilean andesites (Figure 9), but the melts would be relatively deficient in Eu. Thus, the model is applicable only for the small number of calc-alkaline rocks with negative Eu anomalies.

Fractional Melting of Peridotite

The controversy regarding the SiO_2 contents of equilibrium partial melts of hydrous peridotite has been summarized by Boettcher (1973) and Ringwood (1974). Kushiro et al. (1972) and Mysen et al. (1974) propose that andesite is formed directly by small degrees ($\leq 20\%$) of peridotite melting. If mantle peridotite trace element abundances are estimated (see Figures 10 and 12) from Mercy and O'Hara (1967), Goles (1967), Gast (1968), Fisher et al. (1969), Carter (1970), and Frey and Green (1974), 5% fractional melts of such peridotite are enriched

relative to circumpacific andesites (Taylor, 1969) by factors of 1.8, 8, and 10 for Co, Cr, and Ni, respectively, but depleted in Rb, Sr, and Ba by factors of 0.5, 0.8, and 1.2, respectively. However, the predicted K, Rb, Sr, and Ba abundances are close to the average abundances in the Ancud low-silica andesites (Figure 12). Moreover, REE abundances in a 5% peridotite melt parallel the REE abundances of andesites (Figure 10). It is evident that if the peridotite has twice chondritic REE abundances, garnet fractionation is not necessary to account for andesite REE distributions.

Nicholls and Ringwood (1973) believe that hydrous melting of peridotite will not yield SiO_2 -rich andesitic liquids. They propose that 10-30% melts of hydrous peridotite are quartz-tholeiites which differentiate by olivine fractionation to form the island-arc tholeiite series. Their model is consistent with REE abundances because $\geq 10\%$ melts of peridotite have the nearly unfractionated REE patterns characteristic of the island-arc tholeiite series (Jakes and Gill, 1970). All degrees of peridotite melting yield liquids enriched in Cr, Co, and Ni relative to island-arc tholeiite or calc-alkaline rocks. In order to generate andesitic liquids from peridotite, extensive olivine (\pm spinel) fractionation is required (Jakes and Gill, 1970; DeLong, 1974). It is the low

concentration of ferromagnesian elements (e.g., Cr, Co and Ni) in calc-alkaline andesites which led Taylor (1969) to adopt a two-stage model for andesite origin.

Genetic Relationship Between Temuco Andesites

Sample T3, the most differentiated Temuco andesite, has the highest normative quartz, LREE, Ba, Hf and Th abundances, the lowest Sc and Co abundances and a significant Eu anomaly (Table 2 and 3 ; Figure 6b). In this section, I will evaluate the possibility that this sample was derived by fractional crystallization from a magma composition equivalent to sample T2, one of the most undifferentiated Temuco andesites. REE abundances offer a way of testing this hypothesis. Computations using the expression $C_D/C_P = (1-x)^{n-1}$ (Gast 1968; Haskin et al., 1970) show that it is possible to derive a REE pattern similar to that of sample T3 from a magma of REE composition similar to that of T2 by fractionating approximately 50% of this magma as clinopyroxene and plagioclase in equal proportions (Figure 35). The partition coefficients for REE in clinopyroxene used in these computations are shown in Table 5 and Figure 34. The partition coefficients for REE in plagioclase are 0.4 for Eu and 0.1 for the rest. The model predicts for T3 a Ba, Co and Sc content of 490, 11.2 and 15.4 ppm respectively. The Ba, Co and Sc contents in T3 are respectively 560, 11.2 and 18.7 ppm. The partition coefficients used for Ba, Co

and Sc in clinopyroxene are those in Table 5. The partition coefficient is 0.25 for Ba in plagioclase and 0.06 for Co and Sc in plagioclase. The partition coefficient shown for Cr in Table 5 is not suitable to explain the Cr abundance observed in T3. It would produce a strong Cr depletion. A value of 4 for the partition coefficient would yield a more realistic number.

Major element abundances do not fit well with this model, possibly because of the uncertainty in the major element composition of the plagioclase and pyroxene involved in this process. Computations using the chemical composition of plagioclase An 40 and the composition of a clinopyroxene from an andesite from the Islands of Tonga (Ewart, et al., 1973) are shown in Table 22. TiO_2 is not explained by this model. Clinopyroxene and plagioclase contain too little TiO_2 to account for the abundances observed in sample T3.

SUMMARY AND CONCLUSIONS

Calc-alkaline rocks from Chile's central-south Coastal volcanic belt differ significantly from those of the andesitic suite in northern Chile, but they are similar to those in island arcs. The marked geochemical differences between

northern and central-south Chile andesites correlate with differences in their respective Benioff zones (Stauder, 1973).

Based on the occurrence of negative Eu anomalies, plagioclase fractionation is more common in central-south Chile volcanics than in the Cascades or Circumpacific island-arc rocks. However, the Ancud high-alumina basalt does not develop andesitic compositions by extensive plagioclase and pyroxene fractionation.

It is apparent that the small amount of data available for Andean calc-alkaline rocks precludes construction of detailed petrogenetic models. The inherent difficulty is demonstrated by the Cascade stratovolcanoes which do not exhibit long-term, systematic compositional changes (Wise, 1969; Condie and Swenson, 1973). Moreover, each volcano has unique geochemical characteristics, apparently reflecting differences in source composition. Similar results have been found in central-south Chile. For example, the Los Angeles dacites are not related by igneous fractionation to Temuco or Ancud andesites, and even at a single locality (Ancud) low pressure igneous fractionation cannot relate the andesites to low-silica andesites.

Although detailed models cannot be made, trace element data for calc-alkaline rocks do provide broad constraints on petrogenetic models. Results of fractional melting models

lead to the following conclusions:

1. Fractional melting of unaltered oceanic ridge basalt in various assemblages (amphibolite to eclogite) does not yield enough K, Rb, Sr, and Ba to account for their abundances in andesites. As hypothesized by Armstrong (1971) and Church (1973b), a source such as altered basalt or sediment is required for these LIL elements. Amphibolite melting can account for Sc, Cr, Co, and Ni abundances in calc-alkaline andesites, but it cannot explain their REE distribution. Eclogite models can intrinsically cause the REE fractionation in andesites. In particular, the decreasing HREE abundances with increasing SiO_2 content (observed in Cascades and at Ancud) result from eclogite melting. However, when compared to Temuco andesites, eclogite fractional melts are too enriched in Ni and too depleted in Cr and La. In several geochemical aspects (flat REE distributions relative to chondrites, and enriched alkalis relative to oceanic ridge basalt), Franciscan eclogites are suitable sources for andesite magmas (Figure 11, this paper; Church, 1973b). A combination of ocean ridge basalt with other materials (alkali-olivine basalt? oceanic sediment? lower continental crust?) is implied.

2. Fractional melts (~5%) of peridotite, with estimated trace element abundances for the upper mantle, have LIL-element abundances similar to the Ancud low-silica

andesites. However, compatible trace element abundances exceed those in andesites, and subsequent olivine fractionation is required. Major problems for this hypothesis are threefold: a) even small amounts of peridotite melt are deficient in K, Rb, Sr, and Ba relative to most andesites; b) it is not proven that small amounts of hydrous peridotite melting yield SiO_2 -saturated, andesitic liquids; c) in areas of shallow Benioff zones such as central-south Chile, the model may not provide sufficient andesite because only small quantities of andesitic liquid can be derived from large amounts of mantle.

These conclusions, and those of Gill (1974), imply that the geochemical details of calc-alkaline andesites cannot be explained by simple melting of an oceanic lithosphere slab. The petrogenetic processes must be complex and a large amount of additional data are required from areas such as Chile before the models may be improved.

CHAPTER II

RARE-EARTH AND MAJOR ELEMENT ABUNDANCES IN SOME VOLCANIC
ROCKS FROM THE CHILEAN ANDEAN RANGE BETWEEN
LATITUDES 33° - 42° S

INTRODUCTION

Three main physiographic units are characteristic in Chile between latitudes 33° - 42° S: the Andean range, the Central valley and the Coastal range (Vergara, 1974). Between latitudes 33° - $37^{\circ}30'S$ the Upper Cenozoic volcanism is confined to the Andean range. Between latitudes $37^{\circ}30'S$ - 42° S two units of Upper Cenozoic volcanism are distinguished: the Coastal volcanic belt (Miocene) and the Andean volcanic belt (Pliocene and Quaternary) (Vergara and Munizaga, 1974). Samples from the Coastal volcanic belt were discussed in the previous chapter.

In the Andean volcanic belt two volcanic series are distinguished: a) an andesitic plateau series composed of horizontal andesite flows and pyroclastics resting unconformably on Mesozoic basement and b) stratovolcanoes superimposed on the plateau series (Vergara and Munizaga, 1974).

The volcanic activity in the Andean range began in the Pliocene and continues today. This volcanic activity

has formed numerous stratovolcanoes, and twenty-one are now active (Moreno, 1974a). Andesites predominate from latitude 33°S to 37°S , but from 37°S to 42°S there is a predominance of high-alumina basalt (Moreno, 1974a). Rhyolites are scarce. This latitude variation in lava composition seems to be related to the thickness of the crust (~ 65 km at $33^{\circ}30'\text{S}$ and 25-30 km at $41^{\circ}30'\text{S}$) and subduction angle of the Benioff zone (Oyarzun, 1971; Moreno, 1974a).

Nine samples from eight different stratovolcanoes and three samples from the plateau series have been analyzed for major and REE. Six samples were also analyzed for Sc, Cr, Co, Ba, Hf, Ta, Th and U. The major objective of this study is to obtain an understanding of Andean volcanic rock petrogenesis.

SAMPLE LOCALITIES

Andesitic Plateau Series

Three samples from the andesitic plateau series at Pino Hachado pass (east of Temuco, Figure 1) were studied. The samples are from flows outcropping on a nearly horizontal volcanic plain formed by rhyolitic pyroclastics.

Stratovolcanoes

Nine samples from the following stratovolcanoes were studied: Tupungato ($\sim 33^{\circ}15'\text{S}$), Antuco ($\sim 37^{\circ}30'\text{S}$),

Callaquen ($\sim 37^{\circ}50'S$), Llaima ($\sim 38^{\circ}45'S$), Villarrica ($\sim 39^{\circ}30'S$), Lanin (two samples) ($\sim 39^{\circ}40'S$), Puyehue ($\sim 40^{\circ}35'S$), and Casablanca ($\sim 40^{\circ}45'S$). Except for Tupungato sample, these volcanic rocks appear to be typical examples of basaltic rocks from central-south Chile stratovolcanoes (Klerkx, 1965).

Petrographic descriptions of all samples are included in Appendix I. This appendix also includes a brief description of the stratovolcanoes.

RESULTS AND DISCUSSION

Major Element Composition

The major element composition of the samples analyzed is shown in Table 6. The composition of samples GV164 (Lanin), GV170 (Puyehue) and GV177 (Casablanca) were determined by wet chemical analysis at the Department of Geology of the University of Chile. The precision and accuracy of these analyses were discussed in Chapter I. The rest of the samples, as fluxed glasses, were analyzed by electron microprobe at the Department of Earth and Planetary Sciences at M.I.T. A description of the method is included in Appendix II. In order to determine the precision and accuracy of this method the USGS standard andesite (AGV-I) was analyzed. The AGV-I fluxed glass was analyzed at 5 different points. The results are shown in

Table 7 . The errors shown are the standard errors of the mean calculated according to the procedure discussed in the previous chapter. This table also includes the results (on a volatile-free basis) recommended by Flanagan (1973). The differences between the results obtained in this work and those of Flanagan are less than 3% for most of the elements. CaO shows a difference of 5.4%; K₂O of 13.5% and MnO of 30%.

In an FMA diagram (Figure 2) the samples studied fall within or below (Tupungato) the field designating Kuno's hypersthene (calc-alkaline) series (Kuno, 1968). In a total alkali versus SiO₂ plot (Figure 3) the Pino Hachado (plateau series) samples fall within the alkaline field; the stratovolcanoes samples are intermediate between alkaline and subalkaline fields; that is, within the field of the high-alumina basalt series (Kuno, 1960). In an Al₂O₃ versus normative plagioclase composition plot (Figure 4) the stratovolcanoes samples fall within the field of calc-alkaline rocks.

According to the classification of calc-alkaline rocks proposed by Taylor (1969) six stratovolcanoes samples (Callaquen, Villarrica, 2 Lanin, Puyehue and Casablanca) are high-alumina basalts (<53% SiO₂), two (Antuco and Llaima) are low-K andesites (53 - 62% SiO₂; <0.7% K₂O) and one (Tupungato) is andesite (56-62% SiO₂; 0.7 - 2.5% K₂O).

In the classification based on a plot of normative color index (sum of normative mafic minerals) against normative plagioclase composition (Irvine and Baragar, 1971; this work; Figure 5), eight samples are basalts and one (Tupungato) is a dacite. The basalts contain calcic plagioclase ($>An\ 50$) and relatively low $Mg/Mg + \Sigma Fe$ ratios (0.34 - 0.47).

The Pino Hachado rocks are not typical andesites. Figures 2, 3, 4, and 5). They are quartz normative with $>8.7\ wt\%$ total alkalis, $>18\%$ normative orthoclase and albite-rich normative plagioclase. Their alkali-rich nature suggests analogy with shoshonitic rocks (Nicholls and Carmichael, 1969; Jakes and White, 1972). However, because of their high Na_2O/K_2O , they have been classed as trachyandesites and trachytes (Vergara, 1970).

Rare-earth element composition

The REE abundances for the plateau series and stratovolcanoes were determined by INAA (Gordon et al., 1968; Appendix II this work) at M.I.T. The results are shown in Table 8. The errors based on counting statistics (see Appendix II) are given for three of the high-alumina basalts.

Plateau Series. In their absolute REE abundances and marked light REE enrichment (Figure 13) the Pino Hachado samples (plateau series) are similar to the

Gough Island trachyandesites (Zielinski and Frey, 1970) and to some shoshonites (Nicholls and Carmichael, 1969; Jakes and Gill, 1970). The trachytic welded tuff (TH 40) has a large Eu depletion and lower REE abundances than TH 31 and TH 34. These geochemical features may be a result of the clastic nature of this sample. However, low REE abundances have been observed in some trachytes (Price and Taylor, 1973). As expected of alkali-rich rocks with low $Mg/Mg + \Sigma Fe$ ratios, the Pino Hachado rocks have very low compatible trace element abundances (elements, such as, Sc, Cr, Co, Ni that are enriched in Major rock-forming minerals relative to coexisting silicate liquid) and high LIL element abundances (Tables 6 and 8).

Stratovolcanoes. According to the La/Yb ratio, it is possible to divide the stratovolcanoes samples into three broad groups: those with La/Yb ratio ~ 10 ; those with La/Yb ratio ~ 5 and those with La/Yb ratio $\sim 2-3$. The Tupungato sample belongs to the first group; Callaquen and the two Lanin samples belong to the second group and the rest belong to the third group. These trends are represented graphically in Figures 14 and 15. In these diagrams, the REE abundances normalized to a chondritic average (Frey *et al.*, 1968) have been plotted against the atomic number. The following features characterize these diagrams:

1. The Tupungato volcano sample has a La/Yb ratio equal to 11.6. This value is similar to the average La/Yb

ratio (10) for the circumpacific island arc dacites (Jakes and White, 1972). However, the La/Yb ratio observed in the Tupungato volcano is more than a factor of 2 higher than the La/Yb ratio observed in the Los Angeles dacites (Chapter I). The REE distribution of the Tupungato sample is similar to the average REE pattern of the granodioritic rocks from the Andean batholith between latitude 33° - 34° S. Both the Los Angeles dacites (Figure 6c) and the Tupungato sample have significant negative Eu anomalies.

2. Callaquen and Lanin samples have light REE abundances similar to the Tupungato sample, but they are relatively enriched in HREE. Sample GV164 from Lanin and the Callaquen sample also have significant negative Eu anomalies.

3. The high-alumina basalts from Antuco, Llaima, Villarrica, Puyehue and Casablanca stratovolcanoes have a REE pattern with La/Yb \sim 2-3. This ratio is similar to that of the high-alumina basalt from Ancud (sample CH6, Chapter I). However, the Ancud high-alumina basalt is slightly enriched in total REE and has a significant positive Eu anomaly. Within the experimental errors, no Eu anomaly is observed in the high-alumina basalts from the Andean range with La/Yb \sim 2-3.

Origin of the high Andean range calc-alkaline rocks

Major element data, such as $K_2O - SiO_2$ trends, indicate no distinctive difference between high Andean range calc-alkaline rocks and Coastal belt volcanic (Figures 6c and 15; this work, Vergara, 1970). Notable is the similarity in most of the major and trace elements between samples CH6 (high-alumina basalt from Ancud) and GV170 (high-alumina basalt from Puyehue).

The plateau series at Pino Hachado is quite different. It is characterized by high Na_2O and K_2O abundances. These samples are furthest from the Peru-Chile Trench (Figure 1). According to the systematics of the subduction zones, their alkalic nature is expected. However, the distinct geochemical features of these rocks imply that it is unlikely they are related to the calc-alkaline series.

The stratovolcanoes trace element data have been evaluated in relation to the following petrogenetic models:

- 1) anatexis of oceanic lithosphere in subduction zones
- 2) anatexis of hydrous peridotite.

As in Chapter I, the estimated average trace element values of Nazca plate were used as initial solid concentrations (C_0) for models involving fractional melting of amphibolite and fractional melting of eclogite (Figure 9 caption, this work; Schilling and Bonatti, 1974). Initial REE concentrations for the peridotite model (Figure 10 caption)

are twice chondritic abundances and for the other trace element are those shown in Figure 12 caption. The procedure followed in the calculations is the same as in Chapter I. The discussion of the petrogenesis of the Andean strato-volcanic samples will be initiated with the less differentiated ones, i.e., those samples with $La/Yb \sim 2-3$.

Samples with $La/Yb \sim 2-3$. This group includes the samples from Antuco, Llaima, Villarrica, Puyehue and Casablanca. Fractional melting of amphibolite (either as pure amphibole or as amphibolite composed of plagioclase and clinopyroxene in addition to amphibole) does not explain the REE pattern observed in these samples. Melts produced according to these models are richer in HREE (Figure 16) and Co by factor of ~ 2 and 1.5 respectively and are depleted in K_2O , Ba, Sc, and Cr by factors of 3.1, ~ 10 (or more), ~ 2 and ~ 4 , respectively.

Melts produced by fractional melting of eclogite (Figure caption 10) are depleted in K_2O , Ba, Sc, Cr, and Co relative to GV170 (Puyehue) and GV177 (Casablanca) by factor of 1.7, ~ 10 , ~ 4 , ~ 7 and ~ 2 respectively. These melts also fail to explain the REE patterns observed in the sample under discussion (Figure 16).

Melts produced by $\sim 10\%$ partial melting of peridotite (Figure 10 caption) have a REE pattern that parallels the REE pattern shown by samples with $La/Yb \sim 2-3$ (Figure 16).

These melts also have K_2O (0.6%) and Ba (200 ppm) abundances that are similar to those of the samples GV170 and GV177 (Tables 6 and 8). However, these melts are enriched in Cr and Co by factors of ~ 4 and 1.3 respectively, and depleted in Sc by a factor of ~ 2 when compared with the Casablanca and Puyehue samples.

Samples with La/Yb ~ 5 . Samples from Callaquen and Lanin belong to this group. The following discussion will be centered on the samples 800 and GV164 since both belong to the same volcano (Lanin). Sample GV164 is richer in total REE than sample 800 and has a negative Eu anomaly. No Eu anomaly is observed in sample 800.

Melts produced by fractional melting either of amphibolite or eclogite do not account for the REE pattern observed in sample 800 (Figure 17). But this pattern can be explained by $\sim 2\%$ fractional melting of peridotite (Figure 17). The peridotite model, however, does not explain the K_2O abundance observed in Lanin. The melts produced according to this model are about a factor of 3 richer in K_2O than sample 800.

The REE pattern observed in the sample 800 is not consistent with a derivation of this sample from a magma of REE composition similar to that of the Villarrica sample by fractional crystallization of clinopyroxene. For example, liquids derived by 50% fractional crystallization of clinopyroxene (using the partition coefficients in

Table 5) have HREE abundances similar to that of sample 800, but they are depleted in LREE.

A model including plagioclase in addition to clinopyroxene would produce a negative Eu anomaly, that is not observed in sample 800.

Table 9 suggests that the major element composition of sample GV164 may be derived from a magma composition similar to that of the sample 800 by fractionating 30% of such magma as plagioclase (composition \sim An 60). The REE are also consistent with such differentiation (Figure 17). The plagioclase partition coefficients are 0.1 for all the REE, but for Eu is \sim 1.

Sample with La/Yb \sim 10. Liquids derived by fractional melting either of amphibolite or eclogite are not consistent with the REE pattern of the Tupungato sample (Figure 18). The slope of the calculated REE distribution in liquids derived by partial melting of amphibolite is not large enough to account for the HREE depletion (relative to oceanic ridge basalts) of the Tupungato sample. Liquids derived by 40% fractional melting of eclogite have HREE abundances similar to the Tupungato sample, but such liquids are depleted in LREE relative to Tupungato sample (Figure 18). Also, liquids derived by fractional melting of eclogite are depleted in K_2O by a factor of \sim 6, (Even

an altered oceanic basalt cannot account for the K abundance of the Tupungato sample) and do not reproduce the Eu anomaly observed in the sample under discussion.

Liquids produced by $\sim 2\%$ fractional melting of peridotite have K_2O and LREE abundances similar to the Tupungato sample. However, these liquids do not have Eu anomaly and they are enriched by almost a factor of 2, in HREE (Figure 18).

In Chapter III, I will present a model for deriving liquids with major elements and REE abundances similar to that of the Tupungato sample from a magma composition equivalent to that of sample T2 (andesite from Temuco, characterized by a lack of Eu anomaly and by a REE pattern similar to the average circumpacific andesite) by extensive fractionation of clinopyroxene ($\geq 10\%$) feldspar ($\geq 20\%$), amphibole ($\sim 12\%$), biotite ($\sim 6\%$), and magnetite ($\sim 0.2\%$).

SUMMARY AND CONCLUSIONS A change in the composition of the lavas is observed in the Andean range as one goes from latitude $33^\circ S$ to latitude $42^\circ S$. Up to about latitude $37^\circ S$ the volcanic rocks are predominantly andesitic; further south, they are predominantly basaltic (Moreno, 1974a). The volcanism in this area began in the Pliocene and continues today. Most of the volcanoes whose samples were studied are superimposed on andesitic plateau series

(Figure 1). The plateau series at Pino Hachado is alkali-rich ($\text{Na}_2\text{O} > \text{K}_2\text{O}$) and has trace element abundances similar to differentiated rocks of the alkali-olivine basalt series. The plateau series at Pino Hachado seems to be unrelated to the calc-alkaline volcanism represented by the stratovolcanoes.

Peridotite models offer the best explanation for the REE pattern observed in the sample 800 (Lanin) and in those samples with $\text{La}/\text{Yb} \sim 2-3$. But in the case of sample 800, this model does not explain the K_2O abundances observed in the rock and in the case of samples with $\text{La}/\text{Yb} \sim 2-3$ the peridotite model does not explain the Cr, Co and Sc abundances. Potentially difficult to explain by this model is the Al_2O_3 content of these rocks. However, Mysen (1973) has obtained experimentally liquids with Al_2O_3 abundances similar to those of the samples under discussion by hydrous partial melting of peridotitic rocks. The low $\text{Mg}/\text{Mg} + \Sigma\text{Fe}$ values of these basalts almost certainly preclude that they are direct melts of mantle peridotite. However, if the melts of hydrous peridotite precipitate olivine and spinel (Ringwood, 1974) as they rise, one would get low $\text{Mg}/\text{Mg} + \Sigma\text{Fe}$, and low Ni, Co, Cr.

CHAPTER III

GEOCHEMISTRY AND PETROGENESIS OF CENTRAL CHILE
BATHOLITHS BETWEEN LATITUDES 33° - 34° S

INTRODUCTION

Chile represents an example of a destructive plate margin. Most of the country faces the Nazca Plate and the Peru-Chile Trench. Features such as the Chilean Andes, Central Valley and Coastal Range are probably a result of Nazca Plate underthrusting beneath the South American Plate. Between latitudes 25° - 27° S there exists a seismic quiet zone which lacks intermediate-depth earthquakes (Santo, 1969; Stauder, 1973). This silent zone nearly overlaps the lack of recent volcanism between 27° and 33° S (Katsui and Gonzalez, 1968). North of this region (18° - 22° S) the Benioff zone dips at 25° and intermediate-depth earthquakes are abundant. South of the seismic quiet zone the Benioff zone dips only 15° and intermediate-depth earthquakes are absent. Apparently, the subducting lithosphere is broken into discrete sections which behave differently north and south of the seismic quiet zone (Stauder, 1973). The present study will be centered on the Chilean plutonic rocks localized between latitudes 33° - 34° S, i.e. immediately south of the seismic quiet zone.

Three batholiths (composite masses of granite rocks having areas ranging from tens of square kms. to tens of thousands of square kms., Hamilton and Myers, 1967) are exposed between latitudes 33° - 34° S (Figure 19). Similar to other geological features of Chile, these batholiths exhibit a N-S elongation parallel to that of the Peru-Chile trench. Their age varies systematically from west to east: the coastal batholith (Upper Paleozoic) is to the west, along the Chilean coast; the Andean batholith (Tertiary), localized in the Andes, is the easternmost, and the Central batholith (Upper Cretaceous) is localized between the Coastal and Andean batholith (Lopez-Escobar and Oyarzun, 1974). A plot of seventeen modal abundances on the APQ (alkali feldspar, plagioclase and quartz) diagram (Figure 20) indicates that the rocks analyzed are predominantly tonalites and granodiorites. According to Corvalan (1974) tonalite is the predominant rock type in the Coastal batholith; adamellite and granodiorite also occur. Aguirre et al. (1974) found that the most common Mesozoic and Cenozoic granitoids between latitudes 30° - 35° S are granodiorite, tonalite and granite; quartz-monzonite, adamellite, and gabbro are also present.

Mineralogical, major and trace element data were obtained in seven samples from the Coastal batholith,

four from the Central batholith and six from the Andean batholith. These samples were selected on the basis of minimum alteration. Trace element determinations include compatible and incompatible elements. Compatible trace elements (elements that are easily accommodated in plagioclase and mafic minerals) include some members of the first transition series, Sc, V, Cr, Ni, and Co. Incompatible trace elements (elements that are enriched in silicate melts relative to coexisting rock-forming minerals) include the alkali metals Rb and Cs, the alkaline earth metals Sr and Ba, some members of the third transition series (La, Hf and Ta), lanthanides and the actinides Th and U. These trace element data in conjunction with the mineralogy and major element composition of the samples are used:

1. to establish a relationship between the Chilean intrusive and extrusive rocks.
2. to compare the geochemistry of the Central Chilean batholiths with that of the more extensively studied western USA batholiths (Sierra Nevada and Southern California).
3. to discuss a model for the origin of the Central Chilean batholiths and compare this model with the current models proposed for the origin of other circumpacific batholiths.
4. to provide information on the relationship of

calc-alkaline rock petrogenesis to subduction processes.

COASTAL BATHOLITH

The portion of the Coastal batholith to be discussed is part of a continuous belt extending along the Chilean coast between latitudes 30°S and $38^{\circ}15'\text{S}$ (Ruiz et al., 1965; Munizaga et al., 1973). North of latitude 30°S up to latitude $25^{\circ}35'\text{S}$ the Coastal batholith crops out discontinuously. Between latitudes 33° - 34°S only the eastern border of the batholith is inland. The outcrops of the batholiths occupy an area of about 2800 km^2 . Compositionally, tonalites are predominant, although granodiorite are important (Oyarzun, 1971; Corvalan, 1974). Geochronological studies yield the following preliminary results (Corvalan and Munizaga, 1972): Pb/U ages range from 386 to 405 my. Measured samples were taken on a traverse through the width of the batholith, between Quintay and Cuesta Ibacache (location of sample G11, see Figure 19). The most significant Pb/alpha values obtained for samples were from different sectors of the Coastal batholith range between 160 and 368 my. K/Ar age determinations on biotite from tonalites exposed at El Quisco (location of sample G3, see Figure 19) give an average of 287 ± 20 my. Corvalan (1974), considering: a) that in its northeastern part the Coastal batholith intrudes stratified rocks of late Paleozoic age; b) the great

dispersion shown by Pb/alpha values and c) that at least, in part, this batholith could be considered of Early Devonian age on the basis of the Pb/U values, suggests that the Coastal batholith may correspond to a complex pluton representing more than one intrusive cycle. On the basis of the close age relationship shown by the Pb/U values obtained for rocks of the Coastal batholith (383-405 my) and for the metamorphic rocks of the Quintay formation (383 my), Corvalan (1974) suggests an epoch of batholithic emplacement and metamorphism of Early Devonian age. Munizaga et al., (1973) made eleven whole rock Rb/Sr age determinations on metamorphic rocks in contact with the Coastal batholith between latitudes 34° - 40° S. They obtained two limiting reference isochrons of 342 and 273 my with a $^{87}\text{Sr}/^{86}\text{Sr}$ initial ratio of 0.711. They concluded that the metamorphism of these rocks occurred during the Upper Paleozoic and probably is related in time with granitic intrusions. The Coastal batholith intrudes a pre-Middle Devonian (possible Pre-Cambrian) complex of amphibolite, gneiss, schist and minor quartzite (Bateman, 1974)

CENTRAL BATHOLITH

This batholith constitutes a longitudinal belt parallel to and to the east of the Coastal batholith.

Outcrops of this batholith have been recognized, at least, from latitude 20°S in the north to latitude 41°S in the south. Unlike the Coastal batholith, the Central batholith outcrops discontinuously between latitude $33^{\circ} - 34^{\circ}\text{S}$. Five units, ranging in area from 15 km^2 up to 550 km^2 have been mapped in this zone (Figure 19). The total exposed area of the Central batholith between latitudes $33^{\circ} - 34^{\circ}\text{S}$ is on the order of 1700 km^2 . Compositionally, this batholith is mostly constituted by granodiorite with minor proportions of tonalite and adamellite (Corvalan, 1974).

Thirteen K/Ar ages on biotite, hornblende, and plagioclase and ten Pb/alpha ages have been obtained in Central batholith granitoids (Aguirre et al., 1974). K/Ar ages vary from 118 my to 66 my; most of the values range between 90 my and 110 my. Pb/alpha age determinations range between 136 my and 89 my. This batholith is associated with the Andean orogenic cycle (Aguirre et al., 1974). The contact between Coastal and Central batholiths are not always clear (Oyarzun, 1971). North of latitude 33°S , i.e., between latitudes $32^{\circ}25'$ and $32^{\circ}40'\text{S}$, Coastal and Central batholiths are separated by Jurassic intrusives (Aguirre et al., 1974). The Central batholith intrudes continental volcanic and sedimentary rocks of Lower and Upper Cretaceous age. The Lower Cretaceous formations

consist of marine sediments intercalated with thick sequences of rhyolitic and andesitic volcanic rocks. The Upper Cretaceous formations are composed mainly of volcanoclastic andesitic sediments with sparse intercalations of acidic volcanic rocks (Vergara, 1972). Levi (1969) studied extensively the alteration phenomena related to the country rocks and concluded that the alteration pattern reflected burial metamorphism and are unrelated to local granitic plutons.

ANDEAN BATHOLITH

The Andean batholith is the easternmost and youngest batholith. It is localized in the pre-Andean and Andean region. It has been recognized between latitudes 18°S and 35°S (Ruiz, et al., 1965). Its outcrops are generally of minor area extent. Nine outcrops have been mapped in the area under study (Figure 19). The largest have areas of about 120 and 180 km^2 ; the others have areas less than 30 km^2 . Between latitudes 33° - 34°S the total outcrops of the Andean batholith are about 210 km^2 . Granodiorites and tonalites are the most important rock types. Seventeen Pb/alpha age determinations on Andean batholith rocks range between 68 my and 14 my (Aguirre et al., 1974). The Tertiary batholith is also associated with the Andean orogenic cycle (Aguirre et al., 1974). The Andean batholith intrudes lower Tertiary sedimentary sequences consisting

of about 90% of rocks of andesitic composition and about 10% of ignimbrites and rhyolitic lavas with intercalations of continental clastic sediments (Vergara, 1972).

RESULTS AND DISCUSSION

Sample Localities

Figure 19 , shows the localities where the analyzed samples were collected. Seven samples belong to the Coastal batholith, four to the Central batholith and six to the Andean batholiths. The samples and their specific localities (in parentheses) are the following: Coastal batholith: G2 (Algarrobo), G3 (El Quisco), G5 (Rocas de Santo Domingo), G6 (Rapel), G10 (El Salto), G11 (Cuesta Ibacache) and G15 (Casablanca). Central batholith: G12 (NW of Penaflor), G13 (Cuesta Zapata), G17 (Penaflor) and G18 (Melipilla). Andean batholith: G27 (La Obra), G22 (Romeral), G25 (N of Romeral), G26 (Rio Colorado), G29 (Estero Plomo) and G30 (Disputada).

Mineralogy

The modal composition of the samples analyzed is given in Table 10 . The results are based on 1000 point counts per sample. Following the recommendations suggested by the IUGS subcommission on the Systematics of Igneous Rocks (Streckeisen et al., 1973), the modal proportions have been plotted on the APQ (alkali feldspar, plagioclase and quartz) diagram (Figure 20). On this

basis, the Coastal batholith samples are one quartz diorite (G3), two tonalites (G10 and G11), two granodiorites (G5 and G6) and two granites (G2 and G15); the Central batholith samples are two tonalites (G18 and G12), one quartz monzodiorite (G17) and one granodiorite (G13); Andean batholith samples are three quartz monzodiorites (G25, G29, and G30) and three granodiorites (G22, G26, and G27). This classification modifies slightly a classification adopted previously for these samples (Lopez-Escobar and Oyarzun, 1974).

Major Element Geochemistry

The major element composition of the plutonic rocks analyzed are shown in Table 11. These results were obtained by wet chemical analysis in the Department of Geology of the University of Chile (Lopez-Escobar and Oyarzun, 1974). The molecular normative compositions are in Table 13. The samples from the Coastal batholith exhibit a wide range of SiO_2 composition (58 - 73 wt%). The SiO_2 content of the samples from the Central and Andean batholith fall within the SiO_2 range of the Coastal batholith.

Most of the samples analyzed plot around the polybaric granitic minima line in the Ab-Q-Or normative diagram (Figure 21). This suggests that the Chilean batholith are igneous in origin and that equilibrium between a liquid silicate melt and crystalline phases such

as feldspars and quartz has played a dominant role in the evolution of these rocks (Turner and Verhoogen, 1970).

In an FMA diagram (Figure 22) the majority of samples fall within the field designating Kuno's hypersthene (calc-alkaline) series (Kuno, 1968a), i.e., these samples have chemical features expected of calc-alkaline rocks. As a comparison, this diagram also includes andesite samples from Chile and Cascades.

In order to search for chemical variations across the batholiths, the major element composition of the samples analyzed were plotted as a function of the longitude (Figure 23). If samples with similar SiO_2 content (67.3 ± 0.5) are compared, the few data available suggest that only Fe_2O_3 tends to increase eastward while CaO tends to decrease. However, if only the batholiths associated with the Andean orogenic cycle (Central and Andean are considered, the data available suggest that Fe_2O_3 , Na_2O , P_2O_5 , and K_2O increase in passing from the Central to the Andean batholith, while FeO , CaO and MnO decrease in the same direction. Aguirre et al. (1974) have also observed an eastward increasing in K_2O among the Chilean batholiths associated with the Andean orogenic cycle. The chemical trends suggested for the Chilean Mesozoic and Cenozoic batholiths have been observed in other circumpacific

Mesozoic batholiths. For example, in the Sierra Nevada batholith K_2O increases systematically eastward (Bateman and Dodge, 1970). Fe_2O_3 and TiO_2 seem to behave as K_2O while FeO , MgO and CaO may decrease. In the Southern California batholith, if the batholithic rocks are considered as a whole, SiO_2 , Na_2O and K_2O increase eastward while CaO , FeO and MgO decrease (Baird et al., 1974). In the latter batholith, the K_2O trend is exceptionally strong; in a distance of approximately 170 km, the K/Si ratio increases eastward by a factor ~ 10 .

In order to compare the major element composition of Chilean plutonic and volcanic rocks, the oxides were plotted as a function of the SiO_2 content of the rocks (Figure 24). It is observed that the SiO_2 content of the granitoids is intermediate between that of Chilean andesites and that of Northern Chile acidic volcanics. The SiO_2 content of tonalites overlaps partially with the SiO_2 content of andesites and dacites. In general, there exists a continuum between the chemical composition of plutonic and volcanic. Except for rare cases, the Na_2O content for andesites, plutonics, and ignimbrites falls within the range 4 ± 1 wt%. The Na_2O content is apparently independent of the SiO_2 content. This fact was also observed in the Sierra Nevada batholith (Bateman and Dodge,

1970). In general, the Na_2O content of the Chilean plutonic rocks is slightly higher than that of the Sierra Nevada plutonic rocks.

Trace Element Geochemistry

Petrogenetically the trace elements can be divided into two groups: a) compatible elements (Sc, V, Cr, Co and Ni) which are enriched in mafic minerals and plagioclase; and, b) incompatible elements (typically large-ion-lithophile, LIL elements such as Rb, Cs, Sr, Ba, REE, Hf, Ta, Th, and U) which are enriched in silicate melt relative to coexisting rock forming minerals. Table 13 shows the trace element abundances in the samples studied.

Compatible trace elements. Nickel exhibits an eastward variation (Figure 25). It increases from about 9 ppm in the Coastal batholith to about 15 ppm in the Andean batholith, i.e., the Ni content differs by a factor of approximately 2. Table 14 shows that differences in Ni abundances are controlled by the ferromagnesian minerals. The magnetite in Chilean granitoids contains, on the average, 130 ppm Ni; the Ni abundance in amphiboles average 54 ppm and in biotite average 36 ppm. These values are relatively high compared with the Ni abundance in quartz and feldspar (<5 ppm). The ferromagnesian minerals contain large

amounts of Ni because they have a relatively high number of octahedral sites in their crystal structure and because Ni has a relatively high crystal field stabilization energy in octahedral coordination (Burns and Fyfe, 1964 and 1969; Burns, 1973).

The increase in Ni abundance from west to east parallel the increase in magnetite (Table 10). This mineral increases by approximately a factor of two in passing from the Coastal to the Andean batholith. Table 14 shows that the main cause for higher Ni abundance in the Andean granitic rocks is amphibole. This mineral contributes about 4.9 ppm to the total Ni content of the Coastal batholith rocks and about 9.5 ppm to the total Ni content of the Andean batholith rocks. The amphibole of the Andean batholith rocks are richer in Ni, by almost a factor of three, than the amphibole of the Coastal batholith rocks. Magnetite contributes about 1.1 ppm to the total Ni content of the Coastal batholith rocks and about 1.9 ppm to the Ni content of the Andean batholith rocks. Biotite contributes about 3 ppm to the total Ni content of the Andean batholith rocks. The biotite of the Andean batholith rocks is richer in Ni by almost a factor of three, than the biotite of the Coastal batholith rocks.

The average Ni content of the Andean batholith is

equal to the average Ni content of the circumpacific granodiorites (the average circumpacific granodiorites are based on data from Turekian and Wedepohl (1961) (high calcium granites), Kolbe and Taylor (1966) (Australian granodiorites, Towell et al. (1965) and Taylor and Capp (in prep.), Taylor, 1969) and is also similar to the average Ni content of the intruded Tertiary andesites which is 18 ppm (Oyarzun, 1971). However, the average Ni content of the Central batholith (10 ppm) is slightly more than a factor of two lower than the average Ni content (24 ppm) of the intruded Cretaceous andesites.

The cobalt abundance in Chilean granitoids is practically independent of the longitude (Figure 25). Table 15 shows that magnetite, amphibole and biotite have relatively similar Co abundances. This explains why the Co content is approximately the same for the three batholiths. The average Co content in Chilean granitoids (10 ppm) is identical to the average Co content in the circumpacific granodiorites (Taylor, 1969) but is lower than the average Co content (18 ppm) of the intruded Cretaceous and Tertiary andesites (Oyarzun, 1971).

The chromium abundance in Central Chile granitoids shows a tendency to increase eastward (Figure 25). On the average, the Tertiary granitoides (Andean batholith) are a factor of two richer in Cr than the Upper Paleozoic

granitoids (Coastal batholith). Arguments similar to those used to explain the behavior of Ni can be used to explain the behavior of Cr. From Table 16 it is possible to deduce that the contribution of biotite, amphibole and magnetite to the average Cr content of the Paleozoic rocks are approximately 4.9, 2.2 and 2.9 ppm respectively; their contribution to the average Cr content of the Cretaceous rocks are about 3.4; 7.1 and 4.4 ppm respectively, and in Tertiary rocks 1.5 ppm of Cr comes from the biotite, 9.2 ppm comes from the amphibole and 7.6 ppm comes from magnetite. Thus, amphibole and magnetite contribute to increase the Cr eastward, while the contribution of biotite is opposite to that of magnetite and amphibole.

The Coastal batholith granitoids have Cr contents similar to the Northern Chile ignimbrites. The Cr abundance in the latter rocks average 8 to 15 ppm (Oyarzun, 1971). The Coastal range andesites are about a factor of four richer in Cr than granitoids of Central Chile. In some andesites from the Coastal Range the Cr content reach 300 ppm. These andesites are localized in a metamorphic belt which also contains ultrabasic rocks (Oyarzun, 1971). In the andesite formation of Northern Chile the Cr abundance of the rocks varies from 15 to 500 ppm with an average of 90 ppm. The Cretaceous andesites intruded by the Central batholith have an average of 34 ppm

of Cr (Oyarzun, 1971) which is approximately a factor of two higher than the Cr content in the Central batholith, but is similar to the Cr content in the Andean batholith. The average Cr content (29 ppm) of the latter batholith is similar to the average Cr content (30 ppm) of the circumpacific granodiorites (Taylor, 1969).

Similar to Cr and Ni, Vanadium has a tendency to increase eastward (Figure 25). On the average, the Coastal batholith has 50 ppm V, the Central batholith has 93 ppm and the Andean batholith has 117 ppm, i.e., there is a difference of about a factor of two between the V content of Coastal and Andean batholith. A similar fact was observed for Ni and Cr. Also, one expects that the behavior of vanadium in the batholiths of Central Chile is controlled mainly by ferromagnesian minerals.

There is no vanadium data available to compare granitoids and central-south Chile andesites. The northern Chile andesites, however, have an average of 135 ppm V (Pilcher and Zeil, 1972) which is higher than the average observed in the Central Chile granitoids. On the other hand, the V content of the rhyolite formation of northern Chile average 40 ppm, which is slightly lower than the average of the Coastal batholith, although it is similar to the vanadium content observed in some Paleozoic granodiorites. On the average, the V content of the

central Chile granitoids (82 ppm) is relatively similar to the average content (75 ppm) of the circumpacific granodiorites (Taylor, 1969).

Similar to Co, Scandium does not show any systematic trend with the latitude (Figure 25). In the Coastal batholith the scandium content of the rocks range between 4 and 27 ppm with an average of about 14 ppm. Central and Andean batholith exhibit a lower degree of scattering than the Coastal batholith and their average are, respectively, 16.6 ppm and 9.3 ppm. No analysis of Sc for the individual minerals is available. Similar to what was observed in Co, a constant concentration of Sc in the ferromagnesian minerals could explain the lack of eastward variation in the central Chile batholiths.

On the average, the Sc abundance (13.3 ppm) in the central Chile granitoids is slightly lower than the average Sc content (18.7 ppm) of the central-south Chile Coastal Range andesites and dacites, and is lower by almost a factor of three than the average Sc content (35 ppm) of the andesite formation of northern Chile (Pilcher and Zeil, 1972). However, the average Sc abundance in these granitoids is similar to the average (14 ppm) of the circumpacific granodiorites (Taylor, 1969).

Incompatible trace elements -- Rubidium and Cesium.

Coastal batholith tonalites have lower Rb abundances than granodiorites. On the average, the tonalites have 40 ppm of Rb, i.e., more than a factor of two lower than the corresponding granodiorites. If both types of rocks are related by a fractional crystallization process, no mineral with a high solid/liquid partition coefficient could be involved in a major way. Rb partition coefficients between plagioclase (An 40) and silicate melt are of the order of 0.05 (Philpotts and Schnetzler, 1970). Therefore, plagioclase fractionation would increase the concentration of the Rb in the residual melt. Rb partition coefficient between K-feldspar and melt is of the order of 0.7. Therefore, K-feldspar fractionation can contribute, although to a lesser extent than plagioclase, to increase the Rb concentration in the residual melt. Biotite is the only major mineral that has partition coefficient for Rb > 1.

In general, the Coastal batholith granodiorites are also richer in Cs than the tonalites.

The Andean batholith rocks tend to be richer in Rb and Cs than the Central batholith rocks. This trend parallels the K_2O trend observed between both batholiths.

The Coastal batholith tonalites have Rb abundances similar to the Temuco andesites (35 ppm), but they are depleted by approximately a factor of two with respect

to the northern Chile andesites whose average Rb content is 80 ppm (Pilcher and Zeil, 1972). The average Rb content of the Cretaceous and Tertiary andesites intruded respectively by the Central and Andean batholith is 70 ppm for the former and 63 ppm for the Tertiary volcanics (Oyarzun, 1971). Thus, the Central and Andean batholiths granodiorites are, on the average, richer in Rb than their respective country rocks.

The average Rb content (96 ppm) of the central Chile granodiorites is similar to the average Rb content (98 ppm) of the Sierra Nevada batholith granodiorites (from Kistler and Peterman, 1973). The average Rb (96 ppm) and Cs (3.6 ppm) content of the central Chile granodiorites are slightly lower than the average Rb (110 ppm) and Cs (4 ppm) content of the circumpacific granodiorites (Taylor, 1969).

Strontium and Barium. In the Coastal batholith, tonalites and granodiorites have similar Sr contents, but the granodiorites tend to be richer in Ba than the tonalites. If tonalites and granodiorites are genetically related, the observed trends are consistent with a fractional crystallization process involving mainly plagioclase and amphibole. The Ba partition coefficients in both minerals are < 1 (Philpotts and Schnetzler, 1970). Therefore, crystallization and separation of plagioclase and amphibole tend to increase the Ba content in the residual magma. The

Sr partition coefficient for plagioclase is >1 , but for amphibole is <1 . Therefore, while plagioclase fractionation tends to deplete the residual magma in Sr, amphibole fractionation produces the opposite effect. The resultant of these two effects could give a bulk Sr partition coefficient equal to 1 which would be consistent with the similarity in Sr abundances between tonalites and granodiorites.

On the average, the Andean batholith granodiorites are richer in Sr and Ba than the Central and Coastal batholiths rocks. The latter two batholiths have similar Sr content (~ 400 ppm), but, on the average, the Central batholith rocks are richer in Ba than the Coastal batholith rocks. The Sr and Ba trends observed between the Central and Andean batholiths parallel the trend in K_2O , Rb and Cs.

The average Sr (~ 470 ppm) and Ba (510 ppm) content of the central Chile plutonic rocks are similar to the average Sr (440 ppm) and Ba (500 ppm) content of the circumpacific granodiorites (Taylor, 1969). The average Sr content of the central Chile batholithic granodiorites (~ 475 ppm) is similar to the average Sr content (460 ppm) of the granodiorites from Sierra Nevada batholith (see Kistler and Peterman, 1973).

Lanthanides (REE). The rare earth element abundances for the samples under study are presented in Table 13 . The longitude variation diagrams for REE, Eu and La/Yb

ratio are shown in Figure 25 . The Eu content and the total REE do not exhibit any systematic variation trend from west to east. The La/Yb ratio is scattered; however, it is possible to divide the samples in three broad groups: those with La/Yb greater than 10, those with La/Yb less than 10 but greater than 4 and those with La/Yb less than 4. The granodiorites and the sample G15 (granite) from the Coastal batholith and the samples from the Andean batholith (excepting G27) belong to the first group. The tonalites and quartz diorite from the Coastal batholith, the samples from the Central batholith (excepting G12) and the sample G27 (granodiorite) from the Andean batholith belong to the second group. The samples G2 (granite) from the Coastal batholith and G12 (tonalite) from the Central batholith belong to the third group. These two samples will be discussed later.

The two kinds of trends in REE pattern suggested by the La/Yb ratio are represented graphically in Figure 26 . In these diagrams, the (REE in samples/REE in chondrites) ratios are plotted as a function of the atomic number. The following features characterize these diagrams:

a) compared with the Coastal batholith quartz diorite and tonalite samples, the Coastal batholith granodiorites samples (including in this term G15) are slightly enriched in La, have similar Ce and Nd abundances, are slightly

depleted in Sm, exhibit larger Eu depletions and are strongly depleted in HREE.

b) on the average, the Central batholith samples (excepting G12) exhibit a REE pattern almost identical to that of the Coastal batholith tonalitic samples. They differ in the magnitude of the Eu depletion, the Central batholith samples have a slightly larger negative Eu anomaly.

c) the average REE pattern of the Andean batholith samples (excepting G27) is identical, within the experimental errors, to the average REE pattern of the Coastal batholith granodioritic rocks (Figure 27).

d) the REE pattern of sample G27 (granodiorite from the Andean batholith) is similar to the other samples of the Andean batholith in Σ REE and in Eu depletion, but is similar to the samples from the Central batholith in HREE abundance (Figure 26). This sample is similar to the Woodson Mt. granodiorite of Southern California batholith (Towell et al., 1963; this work, Figure 28).

e) the average REE pattern of the Coastal batholith tonalitic rocks and Central batholith samples is similar to the REE pattern of some andesites from the central-south Chile Coastal Range especially that of sample T3, the most differentiated from Temuco (Figure 29).

f) the average REE pattern for samples with

$4 < \text{La}/\text{Yb} < 10$ is similar to that of the circumpacific granodiorites (Taylor, 1969). The latter are more enriched in La, Sm and HREE (Figure 28).

g) the average REE pattern for those samples with $\text{La}/\text{Yb} > 10$ is similar to the REE pattern exhibited by some granodiorites from the Sierra Nevada batholith (Figure 27), (H. Noyes, personal communication).

Large highly charged cations are elements characterized by a relatively large ionic radii. For these reasons, they are generally rejected from the common rock-forming minerals and are typically concentrated in the later differentiates and in volatile rich magmas (Taylor, 1969). Hf, Ta, Th and U were determined in this work. The three central Chile batholith have similar Hf concentrations (Figure 25) and their average (4.9 ppm) is higher than the average exhibited by the central-south Chile Coastal Range andesites (3.9 ppm) and by the circumpacific granodiorites (3 ppm, Taylor, 1969). The data for Ta are scattered and no systematic trend is observed from one batholith to the other. The Ta concentration averages 0.6 ppm which is similar to the average concentration observed in the central-south Chile Coastal Range andesites (0.54 ppm). The Th abundance is also similar in the three batholiths and their average (10.4 ppm) is almost identical to the average abundance of the circumpacific granodiorites (10 ppm),

but is higher than the average abundance of the central-south Chile Coastal Range andesites (4.7 ppm). The U is more abundant in the Andean batholith than in the Central and in the Coastal batholiths. The average U abundance in these intrusives (2.6 ppm) is higher than the average abundance observed in the central-south Chile Coastal Range andesites (1.7 ppm), but is almost identical to the average determined for the circumpacific granodiorites (2.7 ppm, Taylor, 1969) and is similar to the average U content in granodiorites from the Southern California batholith (2 ppm) and Idaho batholith (2.4 ppm) (Larsen and Gottfried, 1960).

Samples G2 and G12 exhibit the lowest La/Yb ratios of the plutonic rocks analyzed. They are similar to the samples with La/Yb 10 in HREE (Figure 29), but they are depleted with respect to them in LREE. G12 and G2 are also characterized by K, Rb, Ba and Cs depletions. Since the minerals containing K, Rb, Cs and Ba also tend to concentrate REE, it is possible that such anomalies have a common cause. Biotite, hornblende and K-feldspar are minerals able to concentrate such elements. None of these minerals seems to be anomalous in these samples when compared to other samples exhibiting "normal" abundance of K, Rb, Cs, Ba and REE. These facts suggest that the

reason of the above anomalies could be leaching caused by hydrothermal solutions (Condie and Lo, 1971).

A peculiar characteristic of G12 is its $FeO/MgO < 1$.

Relationships between tonalites, granodiorites and granites of the Central Chile batholiths -- evidences for a fractional crystallization model

Tonalites and granodiorites are the most abundant rocks in the batholiths of central-south Chile. In this sense, the Chilean batholiths are similar to most of the circumpacific batholiths. The most abundant plutonic rock type around the Pacific Ocean is granodiorite, followed by tonalite and quartz monzonite or adamellite; true granite is rare (Roddick, 1974). It has already been mentioned that the samples from the Coastal batholith present a wide range of SiO_2 content (58 - 73 wt%). In this batholith are represented the main rock types found in the other two batholiths. The two main types of REE patterns found in the Chilean batholiths between latitudes $33^\circ - 34^\circ S$ are also found in the Coastal batholith. Thus, the REE patterns observed in the Central batholith samples are also observed in the tonalites of the Coastal batholith and the REE patterns exhibited by most of the Andean batholith samples are observed in the granodiorites of the Coastal batholith. On this basis, the Coastal batholith can be considered as a model to discuss the origin of these batholiths.

The Ab-Q-Or variation diagram (Figure 21) shows that, within the Coastal batholith, the samples G10 (tonalite), G6 (granodiorite) and G15 (granite) are the closest to the polybaric granitic minima line, i.e., they are the closest to the equilibrium conditions of igneous differentiation. In the AFM diagram (Figure 22) they follow the trend expected in the differentiation of calc-alkaline magmas. For these reasons these three samples are selected in order to investigate a possible genetic relationship between tonalites, granodiorites and granites of the Chilean batholiths.

The following features characterize the transition from G10 to G6 to G15:

1. SiO_2 and K_2O increase while the other major and minor elements (TiO_2 , P_2O_5 , and MnO) decrease (Table 11). These trends in major and minor elements are characteristic during the differentiation of a calc-alkaline magma (El Hinnawi, et al., 1969).

2. Ni, Co, Sc and V decrease in passing from G10 to G6 to G15 (Table 13). These trends are consistent with a fractional crystallization process involving ferromagnesian minerals. Cr does not show any systematic trend. This could be due to analytical errors in the determination of this element Cr, or this means that the bulk solid Cr partition coefficient is about 1.

3. Rb, and Ba increase, but Sr decreases in passing from G10 to G6 to G15 (Table 13). The affinity of Rb and Sr for K-feldspar and that of Sr for plagioclase are well known and were already mentioned in a previous section. The observed trends are consistent with a plagioclase fractionation process.

4. Hf decreases and Ta has a tendency to increase. Th and U do not follow any systematic trend (Table 13). Probably other factors, such as tendency to form complexes, have controlled the abundance of these elements and have obscured the tendency for these elements to increase during a fractional crystallization process.

5. The REE patterns change in passing from G10 to G6. There is an increase in La/Yb ratio and in Eu depletion. The latter feature is correlated with decreasing Sr abundance and can also be explained by a plagioclase crystal fractionation model. The first characteristic, depletion of HREE in G6 compared with G10, requires the fractionation of a mineral with affinity for HREE. Among the minerals observed in these rocks, hornblende has partition coefficient values (Figure 30) that could explain the REE pattern exhibited by G6 as derivative of G10.

6. Various element ratios, (Table 17) confirm that a process of plagioclase crystal fractionation may have

played a significant role in the evolution of the central Chile plutonic rocks. Thus, Rb/Sr, Ba/Sr, and K/Sr ratios increase in going from G10 to G6 to G15 while K/Rb, Ba/Rb and Eu/Eu* decrease in the same direction.

In conclusion, qualitatively, the behavior of ferromagnesian elements, alkali and alkaline earth elements, REE and petrogenetically significant ratios are consistent with a process of fractional crystallization involving plagioclase, biotite, hornblende, and magnetite in going from tonalites to granodiorites to granites in Chilean batholiths.

It would be interesting to determine how much of these minerals must crystallize from a magma of composition or rock G10 in order to obtain a magma composition of rocks G6 and G15. Table 18 shows that the mineralogy exhibited by rock G6 can be explained by subtracting 20% of feldspar, 5.5% of biotite, 12% of amphibole and 0.23% of magnetite from a magma of composition of G10.

Similar calculations show that in order to pass from G6 to G15 it is necessary to fractionate about 10% feldspar, 1.7% biotite and 0.17% magnetite.

The major element composition can be used to test this model of fractionation. Unfortunately no major element determinations were carried out on the minerals. However, a good approach would be to use the major element

composition of pure minerals, or the major element composition of minerals of similar rocks. Thus, the chemical composition of plagioclase can be obtained by using the following procedure: the normative plagioclase composition of these rocks is An₃₀ (Figures 4 and 5). A plagioclase composition of An₃₀ is made of 30% An and 70% Ab. Pure An consists of 43.2% SiO₂, 36.7% Al₂O₃ and 20.1% CaO and pure Ab consists of 68.7% SiO₂, 19.5% Al₂O₃ and 11.8% Na₂O. Therefore, a plagioclase of composition An₃₀ consists of 61.0% SiO₂, 24.7% Al₂O₃, 6% CaO and 8.3% Na₂O. The composition of biotite was obtained from analysis of biotites in granitic rocks of the Sierra Nevada batholith (Dodge et al., 1969; Hietanen, 1971). The biotite composition used (normalized to 100% volatile free) is shown in Table 19. The composition of hornblende was obtained from the chemical composition of hornblende-biotite granitic rocks of the Sierra Nevada batholith (Hietanen, 1971). The hornblende composition used (normalized to 100% volatile free) is shown in Table 20). For magnetite (Fe₃O₄) was assumed a composition equal to 100% FeO*. Table 19 shows that using these compositions it is possible to explain quite well the composition of rock G6 as derivative of a magma of composition of rock G10 by subtraction of 20% plagioclase (An₃₀), 6% biotite, 12% hornblende, 0.5% magnetite and 0.1% apatite. The latter mineral was

introduced to account for the difference in P_2O_5 between G10 and G6. The composition of pure apatite was used in these calculations. MgO and Na_2O are the only two oxides that are not explained by this model. Similarly, G15 can be derived from a magma composition of rock G6 by fractionation of about 10% plagioclase (An 30), 1.6% biotite and 0.1% magnetite. Fe and Ca do not fit well in this model. The model predicts 3.3 wt% Ca, but G15 has only 2.4 wt%. To explain Fe it would be necessary to fractionate 1% magnetite instead of 0.1%.

A further way of testing the fractionation model is through the REE composition. The expression $C_D/C_P = (1-x)^{d-1}$ (see Chapter I) was used in the calculations. The partition coefficients were taken from the literature (Schnetzer and Philpotts, 1970, Philpotts and Schnetzler, 1970; Dudas et al., 1971, Nagasawa and Schnetzler, 1971). These partition coefficients are shown in Figures 30, 31, 32, and 33. The REE composition of sample G6 can be explained as derived from a magma of REE composition of rock G10 by fractionation of 20% plagioclase, 12% hornblende and 5.5% biotite (Figure 38). However, the REE data are not consistent with the possibility of a transition between G6 (granodiorite) and G15 (granite). None of the minerals present in both rocks has partition coefficient for REE (excepting Eu) greater than 1. This means that a fractional crystallization

process in which any of these minerals would be involved would increase the REE abundance in the residual magma. Now, the REE abundance of G15 is lower than that of G6 (Figure 26). However, the REE do not eliminate the possibility that G15 be derived from G10 by fractional crystallization of about 26% plagioclase, 12% amphibole and 6.4% biotite if the partition coefficients mentioned above are used (Figure 38). Except for Ca and Na, this model explains quite well the major element composition observed in G15 (Table 20). In conclusion, in order to explain the REE pattern observed in granodiorites as derived from the REE pattern observed in tonalites, amphibole must be involved in the fractional crystallization process.

Relationships between Chilean Tonalites and Andesites

Having determined that in central Chile batholiths it is feasible to derive granodiorites and granites from tonalites it would be interesting to investigate the possible origin of tonalites.

Compared with Temuco andesites, the tonalites exhibit a REE pattern similar to that of sample T3 (see, for example, G10 and T3 in Figure 35). Further investigation shows that tonalites and Temuco andesites are relatively similar in major, minor and other trace elements; they are even similar in petrogenetically significant element ratios (Table 21). Levi (1973) has demonstrated that in the Bustamante Hill area (Central batholith area) minor intrusions and their volcanic host rocks exhibit similar petrography.

These facts imply a similar origin for tonalites and andesite volcanics. Forbes et al. (1968) found that the quartz diorite which composes the subvolcanic basement of many Alaskan Peninsula volcanoes, was compositionally similar to the andesites erupted by those same volcanoes. They proposed that the genesis of continental andesites from quartz dioritic melts of the same composition requires no manipulation of compositional data, other than remelting pre-existent quartz diorite, or venting the same magma to the surface. They admit as a possibility that both quartz diorite and andesites are generated by the anatexis of lower crustal material. Kistler and Peterman (1973) and Doe and Deleraux (1973) based, respectively, on Sr-isotopic and Pb-isotopic data proposed that the granitic rocks of the Sierra Nevada batholith can be derived from lower crust (especially of andesitic or quartz dioritic composition) and continental upper-mantle (low velocity zone) sources. Hamilton and Myers (1966) believe that the andesitic volcanics are the extrusive portions of a deep batholith of calc-alkaline nature. Based on gravity data combined with seismic information and corroborated with heat flow measurement, Hamilton and Myers (1967) concluded that batholiths are thin and form from magmas which typically rise completely through the crust and spread out laterally beneath a cover a few kilometers thick of their own volcanic

ejecta. Hamilton (1969) points out that Andean volcanic and batholithic rocks are compositionally similar calc-alkaline assemblages. He also believes that in some places, as the Andes, batholiths are now being formed.

In order to test the above arguments geochemically, the genetic relationships between G10 (tonalite) and T2 (andesite) were investigated. This pair was chosen because Temuco andesite T2 is less fractionated than the Coastal batholith tonalites, and it is similar to the average circumpacific andesites (Figure 35). Note, that the most evolved Temuco andesite (T3) is very similar to these tonalites (Table 21 and Figure 35). Computations for REE, similar to those discussed in Chapter I for the transition T2-T3, show that it is possible to derive G10 from a magma with the REE abundances of T2 by fractionating approximately 50% of the magma as clinopyroxene and plagioclase in equal proportions (Figure 35). The partition coefficients for clinopyroxene used in this calculation are shown in Figure 34. The partition coefficients for plagioclase are 0.1 for all the REE but Eu that is 0.4. Similar computation for Sr and Ba give 467 ppm and 490 ppm respectively. These values agree quite well with the observed Sr and Ba values in G10 (Table 21). The Sr and Ba partition coefficients for clinopyroxene are those in Table 5; for plagioclase are ~1 and 0.3 respectively (Figure 36 and 37). Rb does not fit well in

the model. The model predicts for G10 a Rb content of about 66 ppm and the Rb content in G10 is only 55 ppm. The Rb partition coefficients are 0.05 for clinopyroxene (Table 5) and 0.08 for plagioclase (see Philpotts and Schnetzler, 1970). Major element abundances do not fit well with this model possibly because of the uncertainty in the major element composition of the pyroxene and plagioclase involved in this process. Computations using a clinopyroxene from an andesite from the Islands of Tonga (Ewart, et al., 1973) and plagioclase An 40 give the best approach for the major element composition of G10 (Table 22). The Ti content in G10 is particularly difficult to explain. Major and trace element models differ in the degree of fractional crystallization (~50% is required by the trace elements and ~20% by the major elements).

The above results indicate that Chilean volcanic and plutonic rocks may have a similar origin. In general, the trace element abundances are consistent with a fractional crystallization model, involving mainly plagioclase and pyroxene, to explain samples T3 (the most differentiated andesite from Temuco, Chapter I) and G10 (tonalite from the Coastal batholith) as derived from a magma of trace element composition similar to that of T2 (andesite from Temuco characterized by a lack of Eu anomaly and by a REE

pattern similar to that of the average circumpacific andesites (Figure 35). However, some major elements are difficult to explain by this model. In the transition T2-T3 the model does not explain the K and Ti abundances observed in T3 and in the transition T2-G10 the model fails to explain the Ti abundance observed in G10.

The similarity between volcanic and plutonic rocks that has been discussed with reference to the Coastal batholith and Temuco andesites, seems to be also true in the Andean region. The Tupungato volcano andesitic sample (latitude $33^{\circ}15'$), for example, has geochemical characteristics similar to those of the granitoids from the Andean batholith between latitudes 33° - 34° S. Its REE pattern is similar to the average REE pattern of these granitoids (Figure 14). The Tupungato sample is particularly similar in major element composition to the sample G30 (quartz-monzodiorite) (Table 23) collected only a few kilometers from the Tupungato volcano (Figure 19). The Tupungato volcano is part of a volcanic complex that includes also the Marmolejo volcano. One sample of the latter volcano was analyzed for REE (Figure 14; Table 23). Its REE pattern is also similar to that of the nearby granitoids of the Andean batholith. The similarity in major and trace elements between volcanic and plutonic rocks between latitudes 33° - 34° S also favor the hypothesis

that plutonic and volcanic rocks from central Chile have a similar origin.

SUMMARY AND CONCLUSIONS

Three batholiths outcrop in the central part of Chile between latitudes 33° - 34° S. They exhibit a N-S elongation parallel to that of the Peru-Chile trench. Their ages vary systematically from west to east: the Coastal batholith (Upper Paleozoic) is to the west; the Andean batholith (Tertiary) is to the east, and the Central batholith (Upper Cretaceous) is located between the Coastal and Andean batholiths. The few data available suggest that some major and trace elements show eastward variations between the Central and the Andean batholith (both batholiths are associated with the Andean orogenic cycle). Elements such as K, Na, Rb, Sr, Ba, V, Cr, and Ni are more abundant in the Andean batholith than in the Central batholith while elements such as Ca and Mn are more abundant in the Central batholith. Similar eastward variations in chemical composition have been observed in other circumpacific batholiths (Sierra Nevada and Southern California).

Coastal batholith granodiorites are generally similar to the Andean batholith granodiorites (Table 24). Exceptions are Fe, Ti, Sc, V and Ni which are more abundant in the

Andean batholith granodiorites and Ca and Ta which are more abundant in the Coastal batholith granodiorites.

Table 25 shows that the trace element abundances in Chilean batholiths are similar to the trace element abundances of the average circumpacific granodiorite. Most of the trace element abundances determined in Chilean batholiths fall within the respective range of trace element abundances determined in the Sierra Nevada batholith.

There exists similarity in major and trace elements between volcanic and plutonic rocks. The Coastal batholith tonalites are similar in most of the major and trace elements to some Temuco andesites. The Tupungato sample (andesite) is also similar in major and REE composition to some nearby Andean granitoids. These similarities in geochemical characteristics between plutonic and volcanic rocks suggest that both kinds of rocks have a similar origin. However, no trends comparable to those observed between Cretaceous and Tertiary batholiths are observed between Cretaceous and Tertiary volcanoes (Table 26).

Most of the major and trace elements (particularly REE) are consistent with a derivation of the Coastal batholith granodiorites from a magma composition similar to that of the Coastal batholith tonalites by fractional

crystallization of plagioclase, amphibole biotite and magnetite. In turn, the Coastal batholith tonalites are genetically related to a magma of andesitic composition, similar to that of the sample T2 (andesite from Temuco) through a fractional crystallization process involving mainly plagioclase and pyroxene. REE are not consistent with an origin of the central-south Chile andesites by fractional melting of subducted Nazca plate tholeiitic basalts. However, liquids derived by fractional melting of upper mantle peridotite have REE patterns that parallel those of the less differentiated andesites. Therefore, if the Chilean granitoids are derived from magmas of andesitic composition they are also not genetically related to the subducted Nazca plate tholeiitic basalts.

Based mainly in strontium isotope data, Kistler and Peterman (1973) have also concluded that the Sierra Nevada igneous rocks are not consistent with a derivation from subducted oceanic tholeiitic basalts and sediments. According to these investigators, most of the products that arrived in and on the upper crust were melted, or at least began their differentiation, in the region that intersected both upper mantle and lower crust. Similar conclusion was reached by Doe and Delevaux (1973) on the basis of lead-isotopic compositions. According to these investigators an attractive origin for the Mesozoic

granitic rocks from the Sierra Nevada batholith involves derivation from the lower crustal (especially of andesitic or quartz dioritic compositional and continental upper mantle (low velocity zone) sources. Doe and Delevaux (1973) also concluded that an origin of the batholith from subducted material, if such material can be represented by graywackes and blueschists of the Fransiscan formation, is permitted by the lead-isotope data, but, as pointed out by Kistler and Peterman (1973), apparently not by strontium-isotope data.

APPENDIX I

PETROGRAPHY AND STRATOVOLCANOES DESCRIPTION

COASTAL RANGE VOLCANIC ROCKS

Temuco

T2 is a porphyritic andesite from Ñielol Hill with phenocrysts of plagioclase (An 40), clinopyroxene, and orthopyroxene. The groundmass is hyalopilitic with plagioclase, clinopyroxene, orthopyroxene, magnetite, chlorite, and glass.

T3 is a porphyritic andesite from Ñielol Hill with phenocrysts of plagioclase (35% of An 40), clinopyroxene (3%), orthopyroxene (7%), hornblende (4%) and magnetite (1%). The hyalopilitic groundmass contains plagioclase, orthopyroxene, magnetite, tridymite and glass.

T9A is a porphyritic andesite from 21 km north of Temuco. Phenocrysts are 33% plagioclase (An 35-40) and 0.7% clinopyroxene. The groundmass is dominantly plagioclase with quartz, alkali feldspar, magnetite and glass.

T13 is a porphyritic andesite from 9 km south of Temuco. Phenocrysts are 42% plagioclase (An 45), 2% hornblende, and 0.5% magnetite. The groundmass is dominantly plagioclase with quartz, alkali feldspar, amphibole, magnetite, and chlorite.

Los Angeles

T17 is a porphyritic dacite with phenocrysts of 12% plagioclase (An 40), 5% quartz, and 4% magnetite. The hyalopilitic groundmass is plagioclase, clinopyroxene, magnetite and glass.

T18 is a porphyritic dacite with phenocrysts of 23% plagioclase (An 45), 2% orthopyroxene, and 1.5% clinopyroxene. The groundmass is hyalopilitic with minor calcite veins.

Ancud

CH6 is a porphyritic high-alumina basalt with plagioclase phenocrysts (An 35) in a groundmass of plagioclase, clinopyroxene, magnetite and chlorite.

CH8 is an aphyric low-silica andesite with 67% plagioclase, 15% quartz and alkali feldspar, 10% chlorite, 5% magnetite and 3% alteration products.

CH21 is an aphyric low-silica andesite with 40% glass, 8% pyroxenes, 51% plagioclase and 1% sphene plus chlorite.

CH30 is a porphyritic low-silica andesite with phenocrysts of 5% plagioclase (An 50), 1% clinopyroxene and 1% orthopyroxene. The intersertal groundmass is plagioclase, clinopyroxene, magnetite, chlorite and glass.

CH19C is a porphyritic andesite with phenocrysts of plagioclase (2.4%) and orthopyroxene (0.1%). The

hyalopilitic groundmass is glass (40.4%), plagioclase (36.7% pyroxenes, magnetite, and chlorite.

CH15 is a porphyritic andesite with phenocrysts of 20% plagioclase (An 40) and 5% orthopyroxene. The groundmass is glass (53%), plagioclase (40%) with clinopyroxene, orthopyroxene, biotite, and alkali feldspar. GV063 is an aphyric andesite with 25% plagioclase (An 15), 70% glass and quartz, magnetite, and biotite.

HIGH ANDEAN RANGE VOLCANIC ROCKS

Pino Hachado

TH31 is an aphyric trachyandesite with an intersertal groundmass of 93.5% plagioclase with olivine, amphibole, magnetite, alkali feldspar and glass.

TH34 is a porphyritic trachyandesite with 1.5% plagioclase (An 40) phenocrysts in a groundmass of plagioclase (An 15), alkali feldspar, clinopyroxene, hornblende, magnetite and apatite.

TH40 is a trachytic welded tuff with vitroclastic texture. The rock is 20% clastic plagioclase (An 15 and 35), 41% glass, 37% volcanic clasts, 1% biotite and 0.5% clinopyroxene.

Stratovolcanoes

797 is a porphyritic andesite from Tupungato Volcano. It consists of ~65% groundmass; 15% of plagioclase phenocrysts

(An ~68 near the core and ~30 in the rim); 15% of brown hornblende phenocrysts (sometimes altered to opaques); ~5% phenocrysts of clinopyroxene; 1% phenocrysts of biotite and ~1% phenocrysts of orthopyroxene. Apatite and opaques are observed as accessory minerals.

The Tupungato Volcano is located approximately at latitude $33^{\circ} 15'S$ (Figure 1). Tupungato is a strato-volcano with lava flows and pyroclastic material that is part of a volcanic complex which also includes the Tupungatito, San Jose and Marmolejo Volcanoes (Moreno, 1974_a). The volcanic activity in this area began in the Pliocene and continued up to the recent. The main rock types are calc-alkaline andesites and possibly trachytes. Oxihornblende is a typical phenocryst in the lavas. Plagioclase and clinopyroxene are also present as phenocrysts. Sometimes augite, olivine and biotite are observed in the groundmass.

801 is a porphyritic low-K-andesite from Antuco Volcano. It consists of ~25% groundmass; 60% plagioclase phenocrysts (An 65-60); 10% olivine phenocrysts and ~5% clinopyroxene phenocrysts.

The Antuco Volcano is located approximately at latitude $37^{\circ} 30'S$. This volcano is part of a volcanic complex formed by the Sierra Velluda, Cerro Condor and Antuco volcanoes (Vergara and Katsui, 1969; Vergara, 1974).

Two units are observed in the Antuco Volcano: the Somma (also called Laja Volcano) and the Central cone (which is properly the Antuco Volcano). According to Vergara and Katsui (1969), the activity of the Antuco Volcano started with the formation of a large strato volcano (~10 km in diameter). Subsequent to its formation, the area around the crater collapsed forming a caldera type structure (Antuco I). After the formation of this caldera a new cone developed inside the caldera (Antuco II) and a parasitic cone appeared in the NE flank of the volcano. The main cone consists of a central crater and two subsidiary craters. The principal cone is a typical stratovolcano whose lavas and pyroclastic flows are mainly of olive basaltic andesite composition. Typical of these volcanic materials are phenocrysts of plagioclase, clinopyroxene and olivine (Vergara and Katsui, 1969).

799 is a porphyritic high alumina basalt from Callaquen Volcano. It consists of ~70% groundmass; 25% plagioclase phenocrysts (An ~70) and ~5% olivine phenocrysts partially altered to iddingsite.

The Callaquen Volcano is located at latitude $37^{\circ}50'S$ (Figure 1). It forms a volcanic complex with the Copahue Volcano. The volcanic activity began in the Pliocene and continues today (Moreno, 1974). The activity of Callaquen is of fumarollic type. The lavas of these

volcanoes are basalts with phenocrysts of labradorite, augite and Mg-olivine in a intergranular groundmass, and andesites with phenocrysts of labradorite and augite in a hyalopilitic groundmass.

798 is a porphyritic low-K andesite from Llaima Volcano. It consists of ~60% groundmass; 35% plagioclase phenocrysts (An~55) and ~5% olivine phenocrysts.

The Llaima Volcano is a large stratovolcano that form a volcanic group with the Villarrica and Quetrupillan and Lanin Volcanoes (Figure 1). It is located at latitude 39°43'S. Its volcanic material is mainly of basaltic composition although andesites and dacites are also found (Moreno, 1974).

802 is a porphyritic high-alumina basalt from Villarrica Volcano. It consists of 50% groundmass; 35% plagioclase phenocrysts (An 53) and 15% olivine phenocrysts.

The Villarrica Volcano is located approximately at latitude 39°30'S (Figure 1). It is a well-shaped stratovolcano with a large somma displaced toward the SE (Moreno, 1974). Today the volcanic activity is manifested through parasitic cones since the main crater is blocked up (Moreno, 1974). Its lavas are mainly of olivine andesites and olivine basaltic andesites (Klerkx, 1965). Rhyodacite and alkaline rhyolite have also been

found. Similar to other volcanoes of this zone, the lavas are porphyritic with phenocrysts of plagioclase, clinopyroxene and olivine. The plagioclase phenocrysts are generally zoned (An~55 in the center and An~30 in the rim) and corroded. The clinopyroxene is augite and the olivine phenocrysts are generally small and surrounded by a rim consisting of small grains of pyroxene. Sometimes this rim is double, the internal rim consisting of opaque minerals and the external of clinopyroxene.

800 is a porphyritic high-alumina basalt from Lanin Volcano. It consists of ~30% groundmass; ~55% plagioclase phenocrysts (An~58) and ~15% olivine phenocrysts.

GV164 is a porphyritic high-alumina basalt from Lanin Volcano with phenocryst of 40% plagioclase (An 75-80) and 10% olivine. The plagioclase phenocrysts (1-2 mm) are subhedral with glassy inclusions, and the olivine is euhedral to subhedral. The groundmass is 10% plagioclase microlites, 4% olivine, and 86% glass (refractive index 1.57).

The Lanin Volcano is a large stratovolcano that form a volcanic group with the Villarrica, Quetrupillan and Llaima Volcanoes (Figure 1). It is located at latitude 39°43'S. Its volcanic material is mainly of basaltic composition although andesites and dacites are also found (Moreno, 1974).

GVL77 is a porphyritic high-alumina basalt from Casablanca Volcano with 25% plagioclase (An₇₀), 5% olivine and scarce clinopyroxene.

The Casablanca Volcano is located at latitude 40°45'S (Figure 1). It forms a volcanic complex with the Antillanca, Fiucha and Sarnoso stratovolcanoes. Volcanic activity extends from late Pliocene to Holocene (Moreno, 1974a). Volcanic materials are of basaltic composition and they rest unconformably on Mesozoic and Paleozoic bedrocks consisting mainly of granitoid rocks (Moreno, 1974a). In general the basalts contain phenocrysts of Mg-olivine, augite and labradorite in an iron-rich groundmass with clinopyroxene, olivine and labradorite.

GVL70 is a aphyric high alumina basalt from Puyehue Volcano with scarce microphenocryst (less than 0.5 m) of plagioclase (8%, An₇₀) and olivine (90.5%) partially altered to iddingsite. The groundmass is plagioclase microlites (25%), clinopyroxenes (5%), opaque (0.5%) and glass (61.9%).

The Puyehue Volcano is located at latitude 40°35'S (Figure 1). It forms a volcanic complex together with the Carran, Los Venados, Mencheca, Cordon Caulle and Cordillera Nevada Volcanoes (Moreno, 1974a). The volcanic activity in this area began in the late Pliocene and

continues up to date. Moreno (1974c) has distinguished three different sets of volcanic rocks: basalts, andesites and dacites. Carran, Los Venados and Mencheca consist of basalts, Cordillera Nevada is composed mainly of andesites and Puyehue Cordon Caulle volcanic group is mainly dacitic.

APPENDIX II

ANALYTICAL PROCEDURE: INSTRUMENTAL
NEUTRON ACTIVATION ANALYSIS BY USING Ge (Li) DETECTORS

INTRODUCTION

The determination of the abundances of the elements studied was carried out by Instrumental Neutron Activation Analysis. The Neutron Activation Analysis technique, its importance and its applications, has been discussed in different works and papers (Wahl and Kramer 1967; Wayne-Meinke, 1955; Mapper, 1960; and Schoeder et al., 1966). The Instrumental Neutron Activation Analysis and its applications to the study of igneous rocks has been discussed by Gordon et al. (1968) and Hertogen and Gijbels (1971). This technique allows the exact and precise determination of some 25 to 30 elements to the ppm level.

Radioactivation Analysis is any process of nuclear bombardment which enables a particular element in a sample to be determined by its induced radioactivity. When neutrons are used as the bombarding particles, the method is generally called neutron activation analysis (Wayne-Meinke, 1966).

The interaction between a neutron and a target nucleus depends upon the energy of the neutron and the nature of the target nucleus. The nuclear reaction proceeds in two steps, both being separated by an interval of time of about 10^{-16} sec. During the first step, neutron and target

nucleus form a compound nucleus. This is highly energetic, since it contains the kinetic energy of the incident neutron plus its binding energy which is about 7 MeV. This high energy content makes the compound nucleus unstable and in a second step it starts decaying by emission of one or more particles or by emission of gamma radiation. The kind of radiation emitted by this compound nucleus depends in great part on the energy of the incident neutron. The greater the incident neutron energy the greater the probability that the emitted radiation is a particle instead of a gamma ray. Therefore if one's interest is centered in a (n, γ) process, the sample must be irradiated with slow neutrons.

The intensity of the gamma radiation emitted by the compound nucleus is proportional to the amount of element present in the sample, irrespective of its state of chemical combination since the process is entirely nuclear in nature.

The activity which has been induced in a given isotope at the end of an irradiation time, t_i , is given by the following relation:

$$A_0 = \phi \cdot \sigma \cdot \theta \cdot N_0 \cdot M^{-1} \times w [1 - \exp(-\lambda t_i)] \quad (I)$$

ϕ = neutron flux at which the sample has been subjected. This quantity is expressed in neutrons $\times \text{cm}^{-2} \times \text{sec}^{-1}$.

σ = cross sections of the given isotopes expressed in barns.

θ = isotopic abundance of the isotope that is activated.

N_0 = Avogadro's Number.

M = Atomic weight of the element.

w = amount of the element in the sample irradiated.

λ = radioactive decay constant of the isotope formed during the irradiation time = $0.693/t_{1/2}$.

t_i = irradiation time.

The product of $(\phi \cdot \sigma \cdot \theta \cdot N_0 \cdot M^{-1})$ for a given ϕ and a given isotope is generally tabulated under the name of "saturation activity". So, the expression (I) can be written simply as:

$$A_0 = SA \cdot w \cdot 1 - \exp(-\lambda t_i) \quad (II)$$

A given radioactive nuclei emits a gamma ray or a set of gamma rays whose energies are characteristic of that particular nuclei and thus it is possible to distinguish one isotope from another. Sometimes the gamma rays emitted by different radionuclides are so similar in energy that they cannot be adequately resolved in the gamma ray spectra. When this happens, it is necessary to isolate the radio-nuclei by using chemical methods such as precipitation, solvent extraction, ion exchange separation etc. The

application of Instrumental Neutron Activation Analysis with high-resolution lithium-drifted germanium detectors gives very good resolution for gamma ray energies, reducing the need for wet chemistry after irradiation. This means that the neutron irradiation is followed by counting without any chemical separation and it is possible to determine by this method at least 30 elements in rocks (Allen et al., 1962).

The activity, A_c , after a time t_c after the irradiation is given by the following relation also derived from the relationship for the radioactive decay process:

$$A_c = A_0 \cdot \exp(-\lambda t_c) = SA \cdot w [1 - \exp(-\lambda t_i)] \cdot [\exp(-\lambda t_c)] \quad \text{(III)}$$

If equation II is remembered it is possible to see that, at least theoretically, neutron activation analysis is an absolute technique, since it is possible to calculate w if all the other quantities are known. In practice, complications arise from uncertainties connected with the irradiation process, such as variation in the flux during the irradiation time, changes in the energy distribution of the bombarding neutrons, etc. For this reason neutron activation analysis is carried out in a comparative way: a standard containing a known amount of the nuclide to be determined is irradiated together with the unknown. Since all the terms in equation III, but w and A_c are the same

for the sample and for the standard, the unknown amount of nuclide can readily be calculated from the relative activities (or some other quantity that is proportional to the activities such as the relative intensities) at a common time t_c .

The relative character of the neutron activation analysis also requires that sample and standard be counted in the same position relative to the radiation detector, so the fraction of the emitted radiation which is detected is the same for sample and standard. Since it is not possible to count the radiation from one sample and standard at the same time, it is necessary to correct the counts to the same time. Later on in this chapter this point will be discussed again.

EXPERIMENTAL

The present work was carried out through the following steps:

1. Preparation of samples and standard for irradiation.
2. Irradiation.
3. Gamma ray spectrometry.
4. Determination of elemental concentrations.

1. Preparation of samples and standard for irradiation

This step can be subdivided into the following steps.

- 1.1 Preparation of stock solutions. Before starting

with this substep one has to have in mind the following three factors: First, Instrumental Neutron Activation Analysis is a comparative method and the best results are obtained when the amount of the element of interest in the standard is approximately equal to the amount of the same element in the amount of sample to be irradiated. This means that it is necessary to have an idea of the abundance of that element in the rock to be studied. In this work it was assumed that the abundance of the elements of interest in the Chilean plutonic rocks was approximately equal to that of the average circumpacific granodiorites (Taylor, 1969).

Second it is necessary to know what the concentration of the standard solution will be for the element of interest. The procedure to determine this is: into one of the polyethylene vials used for irradiation was put about 0.5 gr of rock sample. In another vial of the same dimensions silica (specpure) was added to reach the same height that the rock sample attained in its respective vial. Then, a minimum volume of water necessary to wet the silica was added. The same volume of standard solution must have the element of interest in about the same amount as is found in the 0.5 gr of rock sample. With this in hand one knows the concentration that the standard solution must have in a given element.

Silica is used as the carrier because it is a low cross section material and is the dominant oxide in rocks. This reduces one of the principal errors that can be produced during the irradiation, the self shielding or lack of uniformity of the flux within the sample. This error is proportional to the cross section that a given material offers to incident neutrons. On the other hand the requirement that the height of the silica in the vial must be equal to the height of the sample in its respective vial, assuming both vials are equal, is due to geometric reasons mentioned before.

Third, before starting the preparation of the stock solutions it is necessary to determine the volume of the standard solution to be prepared. It is advisable that this volume be greater (in ml.) than $10 \times$ the number of elements that the standard solution is going to contain. The reason for this will be discussed next.

Now one is ready to start the preparation of the different stock solutions. The concentration of each of the stock solutions must be such that 10 ml. contains the amount of element necessary to prepare the volume of standard solution in the required concentration for that element. The reason for this is simple: the error one makes when pipetting 10 ml. of solution is less than the error one makes when pipetting 5 ml. or less. With this

reasoning one might think: why not pipette 15 ml. or more instead of 10 ml.? The error one can make pipetting 10 ml. is already small enough that it is not justifiable to pipette a volume greater than 10 ml.

The method used to prepare the stock solutions was the following:

A. The stock solutions of REE were prepared from their respective oxides of high purity (99.99%). Since some of the REE can form non-stoichiometric oxides, ultimate standardization was by titration.

The necessary amount of REE oxide was weighed to five places and then transferred to a teflon beaker. The oxide was dissolved with 1:1 vycor distilled HNO_3 and the solution was evaporated almost to dryness. The solution was then diluted in a volumetric flask, to 250 ml. with deionized water and transferred to a clean, dry, polyethylene bottle.

B. To obtain a stock solution of Th, the necessary amount of this element was weighed and transferred to a Teflon Beaker. About 10 ml. of HCl concentrate was added and the result is a black precipitate of ThCl_4 ? This is treated with about 10 ml. of HNO_3 and the formation of a green residue is noticed. With a further addition of one drop of HF appears a white precipitate. The addition of 10 ml. of H_2O and heating makes the solution completely

clear. Then the procedure continues as before: evaporation to almost dryness, dilution to 250 ml. and transferring to a clean, dry, polyethylene bottle.

C. The stock solutions of Hf and Ta were prepared by dissolving the necessary amount of Hf and Ta in HF. This solution was evaporated almost to dryness, diluted to 250 ml. with deionized H₂O and then transferred to a polyethylene bottle.

D. The stock solutions of Cs and Rb were prepared from Cs and Rb acetate respectively 99.9% pure. These acetates are very hygroscopic, therefore it is necessary to subject them to successive heating to 110°C and cooling to reach constant weight. Then the substances were transferred to a teflon beaker to be subjected to the same treatment given to the REE oxides.

E. The stock solution of Fe was prepared from Fe wire standard. Iron was not determined because the samples were contaminated with Fe during their preparation. The Fe wire was treated with very dilute HNO₃ in order that the only possible reaction be that of electronic interchange between H and Fe. It is difficult to accomplish this. The absolute standardization of Fe was by Atomic Absorption.

F. Stock solutions of Ba and Mg were not prepared because the abundance of these elements in rhyolites is

high and one must use a lot of reagent. The necessary amount of Ba (as BaCO_3) and Mg to prepare the standard solution were weighed accurately, then treated with an adequate amount of HNO_3 in order to get a solution of Ba^{++} and Mg^{++} nitrate and this solution was transferred directly to the volumetric flask containing standard solution.

1.2 Standardization of stock solutions. In most of the cases the definite determination of the concentration of the stock solution was done by back titration of copper standard solution against EDTA. The method applied were those described by Welcher (1958). Reagent grade copper foil was carefully weighed to five places, dissolved in 1:1 vycor distilled HNO_3 and diluted with distilled water to a convenient volume. This solution was transferred to a clean, dry polyethylene bottle and was used as the copper standard solution. An EDTA solution was prepared and standardized with respect to the copper solution. After that most of the stock solution was standardized with respect to the copper solution by titration.

An illustration of the procedure used to standardize the stock solution of REE is described: to a 50 ml erlenmeyer flask was introduced a small amount (10-20 ml.) of water. The pH value was adjusted to 4 with a concentrated

solution of acetic acid and NaOH. The success of the titration depends on proper adjustment of pH. Then a given amount of stock solution is added. As one has an idea of the concentration of the stock solution the amount of it used in the process must be such that EDTA reacts mainly with the element of interest and only the excess of EDTA reacts with Cu^{++} . An excess of EDTA is added together with two or three drops of PAN indicator. The solution is heated to facilitate the reaction of EDTA with the element of interest. The normal concentration of the stock solution is calculated by applying the following relation:

$$N_{ss} = \frac{N_{\text{EDTA}} \times V_{\text{EDTA}} - N_{\text{Cu}^{++}} \times V_{\text{Cu}^{++}}}{V_{ss}} \quad (\text{IV})$$

where ss means stock solution.

The normal concentration expressed in $\text{eq} \cdot \text{l}^{-1}$ is later expressed in $(\mu\text{gr} \times \text{ml}^{-1})$ by applying the following relation:

$$C(\mu\text{gr} \times \text{ml}^{-1}) = \frac{\text{At.w.}}{\text{valence}} (\text{gr eq}^{-1}) \times N(\text{eq} \times \text{l}^{-1}) \times 10^{-3} \\ (1 \times \text{ml}^{-1}) \times 10^6 (\mu\text{gm} \times \text{ml}^{-1}) \\ C(\mu\text{gr} \times \text{ml}^{-1}) = \frac{\text{At.w.}}{\text{valence}} \times N \times 10^3 \quad (\text{V})$$

As EDTA always reacts with REE, Th, Hf, etc. in the ratio 1:1 the value of the valence is the unity and therefore for these cases one has:

$$C(\mu\text{gr} \times \text{ml}^{-1}) = \text{atomic weight} \times N \times 10^3 \quad (\text{VI})$$

1.3 Preparation of standard solution or flux monitor.

This procedure is very simple. It consists in taking from the stock solution the volume containing the necessary amount of the element of interest to prepare the standard solution and adding this volume into the volumetric flask in which the standard solution is being prepared. After all the elements to be analyzed are in the volumetric flask in the required amount, the final volume of the standard solution is completed with deionized water.

Even when the process itself is simple it is advisable to follow the following order when adding the different elements: First, introduce all those solutions containing F^- . Second, introduce the solution of Ba^{++} . After this the formation of a white precipitate of BaF_2 occurs. This is soluble in HNO_3 . Third, introduce those solutions containing NO_3^- .

1.4 Preparation of vials to be irradiated.

Into three vials of polyethylene were put approximately 0.5 gr of powdered rock sample. Assuming that the diameters of the vials are equal, it is important that the height of the sample be equal in all three. It must be remembered that the NAA is a comparative method of analysis and for this reason, the geometry is an important factor. Then the amount of sample in each vial was weighed accurately.

Into a fourth vial was put silica (specpure) to reach the same height as the samples have in their respective vials (in order to keep the same geometry). Then the vials are placed under the infrared lamp to evaporate the water present. This process must be carried out carefully. Placing the lamp too close to the vial can cause deformations of the capsule which affects the geometry in subsequent counting.

In all the processes carried out in this step, one has to avoid any kind of contamination of the samples and of the reagents used.

2. Irradiation

The four vials were sealed, placed in a sample carrier ("rabbit") and subjected to a flux of 2×10^{13} neutrons $\times \text{cm}^{-2} \times \text{sec}^{-1}$ in the core of the M.I.T. nuclear reactor. Following the irradiations the rabbit was delivered from the reactor within a few seconds via a pneumatic tube. After short irradiations (2 minutes) the samples were allowed to "cool" two hours before observation of species with half lives from 2.32 h (Dy) to 15 H (Na). After long irradiation (2 hrs.) the samples were allowed to "cool" 5 days before observation of species with half lives from a few days to many years.

3. Gamma Ray Spectrometry

Before counting, each vial was placed unopened in

another special vial that fits in the holder in front of the detector.

Gamma ray spectra of each sample were taken several times after irradiation in order to study each of the elements of interest according to their respective half lives. Following the experiences of Gordon et al. (1968) and Buma (1970) the schedule of counting is given in Table 27.

This table also contains the detector and photopeak (expressed in kiloelectron volts) used in the determination of the abundance of the element of interest.

A block diagram of the counting equipment is shown in Figure 39 (Zoller and Gordon, 1970). Two different Ge (Li) detectors were used: one of effective volume of 18 cm^3 and the other of effective volume of 0.5 cm^3 . The first one has greater efficiency than the small one and was used for observing high energy gamma rays. The FWHM (full width at half maximum) of the photopeak produced by 661.6 KeV gamma rays from ^{137}Cs was about 2.5 KeV. The small detector, LEPS, (low energy photon spectrometer, FWHM approximately 0.4 KeV at 14.4 KeV (Zoller and Gordon, 1970), has better resolution than the 18 cc and is most effective for photons from about 10 to

150 KeV. It was used up to 400 KeV.

Pulses from the detector were passed through preamplifiers and linear amplifiers which include a baseline restorer to maintain better resolution of the pulses at high count rates. The amplifier pulses were fed to a 4096-channel analog to digital converter (Packard) and the digital information was stored in a 4096-word core memory (Packard) (Zoller and Gordon, 1970). The information from the analyzer memory was printed and it took about two minutes to empty the full memory. The output information is a tape that exhibits the number of the channel and the number of counts in that channel.

Radioactive nuclides were identified on basis of energies and intensities of the peaks. Most species emit several gamma rays, so the intensity pattern of the several gamma rays can be used as a help for identification. Energy calibration is determined from a calibration curve for each detector. These calibration curves were obtained by making use of the standards given in Table 28. This table also includes the detector used to get the curves, and the energy of the gamma rays emitted from the different standards. The last column includes the relative intensity of the ^{241}Am peaks.

The calibration curve is nothing other than an energy

vs. channel curve. This is indispensable in the identification of the species. In these curves it was assumed that the variation of the energy with the channel number is linear over small energy regions.

In order to maintain constant geometry, samples and standard were placed in the same position for counting.

4. Determination of elemental abundances

In order to determine the abundance of the elements of interest, the data given by the instrument were treated following the method proposed by Denechaud (1969). In this method, instead of comparing the total area under a given peak in the sample and standard (this area is proportional to the activity induced during the irradiation in the particular isotope) only a fraction of the peak is analyzed. This fraction generally corresponds to one FWHM. This method tends to minimize the statistical counting error and the error in the placement of the baseline. The fundamentals of the method are discussed by the mentioned author. Therefore I will describe only briefly the mechanics of the method.

The data output is graphed on a three-cycle semilog paper. The axis of the ordinates represents the number of counts per channel, and the axis of the abscissas the channel number.

The number of counts in each channel of a given peak

includes those that are associated with gamma rays of the isotope of interest and those which are associated with higher energy gamma rays (via Compton interactions). Therefore it is necessary to subtract from the total number of counts in each channel those counts in that channel at the base of the peak. It is very important to trace the baseline as exactly as possible. The first step in this task is to find the peak channel, x_0 , which is generally the channel with the highest number of counts, but in those cases where the peak is not smooth. x_0 is taken as the channel which corresponds to the maximum of a smooth curve drawn through the data. When everything works properly, x_0 is the same for each sample (i.e., no gain shifts).

Smooth curves are then penciled in through the data points at the beginning and end of the peaks. Tentative baselines are drawn in such a way that they start at the last channel before the peak and are tangent to the curve just past the peak. These tentative baselines are then compared between the four samples and the definitive baseline is drawn from the best value for the last channel before the peak and the best point of tangency to the curve just past the peak.

The half maximum of the peak under study is calculated in the standard. This is given by the following relation:

$$HM = \frac{B + B'}{2}$$

B is the number of counts corresponding to x_0 .

B' is the number of counts under the baseline at x_0 .

B' is read from the graph.

Once HM has been calculated, one determines the number of channels in the peak which have a number of counts equal or greater than HM. This number is W. The area under the peak in the range of W and above the baseline is the area that is compared between sample and standard. W must be equal for samples and standard and correspond to those channels in the peak with the largest individual counts.

To calculate the peak areas (Gordon et al., 1968) it is necessary to determine the median channel in the range W. From the graph, the number of counts under the baseline at the median channel is read. This number is designated as Y. Then the product $Z = W \cdot Y$ is determined. This number represents the area under the baseline in the range of W. Then the sum of the gross counts in the range W is calculated. This number, that is designated as V, represents the area under the peak in the range W. Therefore the net peak area of interest, S is equal to the difference $V - Z$.

Samples and standard are counted at different times

(always the standard was counted first). Therefore if one wants to compare the net area of the sample with that of the standard, one has to correct to a common counting time by applying the decay law through the following relation:

$$S_c = S \times \exp(\lambda t) \quad \text{(VII)}$$

S_c is the area the peak would have if the sample would have been counted at the same time as the standard. S_c is the corrected area.

S is the area of the peak calculated from the data provided by the instrument and from the graph.

λ is the decay constant for the given isotope.

This is equal to $0.693/t_{\frac{1}{2}}$ where $t_{\frac{1}{2}}$ is the half life of the isotope.

t is the time which has passed between the counting of the sample and that of the standard.

Note: if t is expressed in minutes, λ must be expressed in inverse minutes.

t of equation VII is calculated through the following relation:

$$t = (B_i + X_i) - (B_o + X_o)$$

B_o is the time at which the counting of the standard

started (provided the standard was counted first).

B_i is the time at which the counting of the sample started.

It is advisable to use the 24-hour time of day method to determine the values for B_0 and B_i . For instance, suppose that the counting of the standard began at 10 PM of July 27 and that of the sample at 7 AM of July 28. In this case $B_0 = 22$ hours and $B_i = 24 + 7 = 31$ hours.

The values for X_i and X_0 are calculated in a different way according to the half life of the isotope of interest. If the half life of this is much greater than the counting period X_i represents the midpoint of the counting period of the sample and X_0 represents that of the standard. They are calculated according to these relations:

$$X_i = 0.5 (CP + CP \times DT_i) \quad (IX)$$

$$X_0 = 0.5 (CP + CP \times DT_0)$$

CP is the counting period set by the operator.

DT_0 and DT_i are the dead times when the counting of standard and sample start respectively.

If the half life of the radioactive isotope being determined is of the same order of the counting period (Dy, for example, if it is counted for one hour), X_0 and X_i of the expression (IX) are calculated through the following

relation given by Kerstin Low (1964).

$$X_o = 0.5 CP - \frac{1}{\lambda_o} \ln \left(\frac{1-DT_o}{1-DT_o e^{-\lambda CP}} \right) \quad (X)$$

$$X_i = 0.5 CP - \frac{1}{\lambda_i} \ln \left(\frac{1-DT_i}{1-DT_i e^{-\lambda CP}} \right)$$

Once one has the corrected value for the areas of samples (provided the standard was counted first) the final step is to determine the abundance of the element under study and express it in ppm. This can be done by applying the following relation:

$$C_E(\text{ppm}) = \frac{S_E \text{ sample} / S_{\text{std}} \times L_E}{A_s} \quad (XI)$$

E stands for the element of interest.

C_E is the concentration of the element of interest, expressed in ppm, in the rock under study.

S_E is the corrected area for the element in the sample.

S_{std} is the net peak area of the std.

A_s is the amount (expressed in grams) of the rock irradiated.

L_E is the amount of element V in the standard.

L_E can be calculated from the following relation:

$$L_E = \frac{C_{E_{\text{ss}}} \times V_{\text{ssupst.s}} \times V_{\text{stE}}}{V_{\text{tst.sp}}}$$

C_E^{ss} is the concentration of the stock solution in element E.

$V_{ssupst.s}$ is the volume of stock solution used to prepare the standard solution.

$V_{st.sE}$ volume of standard solution put in the vial to be irradiated.

$V_{tst.sp}$ is the total volume of the standard solution prepared.

At this point one has finally reached the aim of the analytical procedure, i.e., to determine the trace element abundance in a given rock sample. It is advisable to calculate the counting statistical error involved in the determination of each element. This error gives an idea of how good was the peak used in the determination of the element and therefore measured the precision of such determination. The following expression (Quittner, 1972) is applied:

$$\text{Area} = S \pm \sqrt{V + (w/2 + 1/2)^2 \times 2y}$$

An example will illustrate the application of this expression. Let's calculate the statistical error involved in the determination of Hf in the sample GV164. This sample was irradiated with the standard labeled U13. The data for Hf in the standard are the following:

$$S = 13342 \quad V = 16042 \quad w = 5 \quad y = 540$$

Therefore:

$$\text{Area Std} = 13342 \pm \sqrt{16042 + (5/2 + 1/2)^2 \times 2 \times 540} = 13342 \pm 160.5$$

The data for Hf in GV164 is S = 1860, V = 4310,
w = 5, y = 490

Therefore:

$$\text{Area GV164} = 1860 \pm \sqrt{4310 + (5/2 + 1/2)^2 \times 2 \times 490} = 1860 \pm 114.6$$

After applying the time correction for GV164 we have:

$$S_E(\text{GV164}) = 1864.8 \pm 114.9$$

LE = 9.41 and As = 0.36963ge. Therefore, applying the expression λ , the concentration of Hf in the GV164 will be

$$C_{\text{Hf}} (\text{ppm}) = \frac{(1864.8 \pm 114.9) / (13342 \pm 160.5)}{0.36963} \times 9.41$$

$$C_{\text{Hf}} (\text{ppm}) = \frac{(1864.8/13342 \pm 1864.8/13342) \sqrt{(114.9/1864.8)^2 + (160.5/13342)^2}}{0.36963} \times 9.41$$

$$C_{\text{Hf}} (\text{ppm}) = 3.6 \pm 0.2$$

MAJOR ELEMENT DETERMINATION BY ELECTRON MICROPROBE ANALYSIS

The major element compositions of the following samples: 797 (Tupungato), 798 (Llaima), 799 (Callaquen), 800 (Lanin), 801 (Antuco) and 802 (Villarrica) were determined by electron microprobe analysis on fluxed glass. Approximately 1 gr of rock sample ground to 100 mesh was accurately weighed in a porcelain crucible. The sample was heated to 1000°C for an hour in a muffle furnace. Then it was cooled in a desiccator, and weighed again, in order to determine the loss by ignition. 0.5 gr of this sample was mixed with an equal amount of lithium tetraborate flux which had been previously heated to 500°C for one hour. This substance reduces the temperature necessary for the complete fusion of the sample. The flux and the sample were thoroughly mixed, transferred to a graphite crucible, and heated to 1000°C for an hour in a muffle furnace. It has been proved that this temperature and this period of heating are necessary enough for complete melting and homogenization of the sample (Watson, personal communication) with no loss of alkalis. The sample was then quenched on an aluminum plate (1/2 cm thick). The resulting glass was sectioned and checked under the microscope for homogeneity. After this, a selected piece of glass was mounted in epoxy in a hole drilled in a resin disk and polished. The mounted fluxed glass was

stored in a desiccator. Shortly before the determination by electron microprobe, the fluxed glass was carbon coated. Then the glass was analyzed by standard electron microprobe techniques using a low beam current and a 50 micron diameter spot. The USGS standard GSP-1 (granodiorite) was used as standard for K and Al. The USGS standard BCR-1 (basalt) was used as standard for Fe, Mg, Ca, Na, Ti and Mn. The USGS standard AGV 1 (andesite) was used as standard for P and Al. Five point determination were done on each sample. The result is the average.

REFERENCES

- AGUIRRE, L., CHARRIER, R., DAVIDSON, J., MPODOZIS, A., RIVANO, S., THIELE, R., TIDY, E., VERGARA, M., and VICENTE, J.C., 1974.--Andean magmatism: its paleographic and structural setting in the central part (30-35°S) of southern Andes. *Pacific Geology*, 8, p. 1-38.
- ALLEN, R. O., ANDERSON, M.R., and MARVIN, V. B., 1962-- Simultaneous analysis for 30 elements in the Bruderheim chondrite. *Meteoritics*, 4, p. 149.
- ANDERSON, A. T., and GOTTFRIED, D., 1971--Contrasting behavior of P, Ti, and Nb a differentiated high-alumina olivine tholeiite and calc-alkaline andesite suite. *Bull. Geol. Soc. Am.*, 82, p. 1929-1942.
- ARMBRUST, G. A., OYARZUN-MUNOZ, J., ARIAS-FARIAS, J., 1971-- Rubidium as a guide to ore at El Teniente (Braden), Chile. Abstracts with programs. *Geol. Soc. Am. Meetings*, 3, p. 494.
- ARMSTRONG, R. L., 1971--Isotopic and chemical constraints on models of magma genesis in volcanic arcs. *Earth Planet. Sci. Lett.*, 12, p. 137-142.
- BAIRD, A. K., BAIRD, K. W., and WELDAY, E. E., 1974-- Chemical trends across Cretaceous batholithic rocks of southern California. *Geology*, 2, 493-495.
- BATEMAN, P. C., 1974--Circumpacific plutonism project. Meetings in South America. *Geology*, 2, 85-86.
- BATEMAN, P.C., and DODGE, F. C. W., 1970--Variations of major chemical constituents across the central Sierra Nevada batholith. *Bull. Geol. Soc. Am.*, 81, p. 409-420.
- BOETTCHER, A. L., 1973--Volcanism and orogenic belts - the origin of andesites. *Tectonophysics*, 17, p. 223-240.
- BOSTROM, K., JOENSUU, O., MOORE, C., BOSTROM, B., DALZIEL, M., and HOROWITZ, A., 1973--Geochemistry of barium in pelagic sediments. *Lithos*, 6 p. 159-174.

- BROUSSE, R., and OYARZUN-MUNOZ, J., 1973--Les complexes calcoalcalins et la province cuprifere Circum-Pacifique, Colloque Scientifique International. E. Raguin, les roches plutoniques dans leurs rapports avec les gites mineraux. Masson ed., Paris, p. 309-314.
- BUMA, G., 1970--Trace element distribution and the origins of some New England granites. M.S. Thesis, M.I.T.
- BURNS, R. G., 1973--The partitioning of trace transition elements in crystal structures: a provocative review with applications to mantle geochemistry. Geochim. Cosmochim. Acta, 37, p. 2395-2403.
- BURNS, R.G., and FYFE, W. S., 1964--Site preference energy and selective uptake of transition metal ions during magmatic crystallization. Science, 144, p. 1001-1003.
- BURNS, R. G., and FYFE, W. S., 1969--Crystal field theory and the geochemistry of transition elements. In Researches in Geochemistry (Ed. P.H. Ableson), vol.2, p 259-285, Wiley.
- CARTER, J. L., 1970--Mineralogy and chemistry of the earth's upper mantle based on the partial fusion-partial crystallization model. Bull. Geol. Soc. Am., 81, p. 2021-2034.
- CHURCH, S. E., 1973a--Limits of sediment involvement in the genesis of orogenic volcanic rocks. Contr. Mineral. Petrol., 39, p. 17-32.
- CHURCH, S. E., 1973b--Trace element geochemistry of andesites from the Cascade mountains. Abstracts with programs. Geol. Soc. Am. Meetings, 5, p. 576.
- COLEMAN, R. G., LEE, D. E., BEATTY, L. B., and BRANNOCK, W. W., 1965--Eclogites and eclogites: their differences and similarities. Bull. Geol. Soc. Am., 76, p. 483-508.
- CONDIE, K. C., and LO, H. H., 1971--Trace element geochemistry of the Louis lake batholith of early Precambrian age, Wyoming. Geochim. Cosmochim. Acta, 35, p. 1099-1119.
- CONDIE, K. C., and SWENSON, D. H., 1973--Compositional variation in three Cascade stratovolcanoes: Jefferson, Rainier, and Shasta. Bull. Volcanologique, 32, p 205-230.

- CORLISS, J. B., 1970--Mid-ocean ridges basalts, Ph.D. Thesis. Univ. of California at San Diego, 145 pp.
- CORVALAN, J., 1974--Paleozoic crystalline basement complex of central Chile. International symposium on volcanology. Guide book D-6. Dep of Geology. Univ. of Chile, Santiago-Chile, 11 pp.
- CORVALAN, J., and MUNIZAGA, F., 1972--Edades radiometricas de rocas intrusivas y metamorficas de la hoja Valparaiso-San Antonio. Santiago. Instituto de Investigaciones Geologicas. Bol. No. 28.
- DASCH, E. J., HEDGE, C. E., and DYMOND, J., 1973-- Effect of sea water interaction of strontium isotope composition of deep-sea basalts. Earth Planet. Sci. Lett., 19 p. 177-183.
- DELONG, S. E., 1974--Distribution of Rb, Sr, and Ni in igneous rock. Central and western Aleutian Islands, Alaska. Geochim. Cosmochim. Acta, 38, p. 245-266.
- DENECHAUD, E. B., 1969--Rare-earth activation analysis: improvement and application to Stretishorn dike and Duluth complex. Ph.D. thesis. Univ. of Wisconsin.
- DODGE, F. C. W., 1972--Trace-element contents of some plutonic rocks of the Sierra Nevada batholith. USGS prof paper 1314-F.
- DODGE, F. C. W., SMITH, V. C., and MAYS, R. E., 1969-- Biotites from granitic rocks of the central Sierra Nevada batholith, California. J. Petrol., 10, p. 250-271.
- DOE, B. R., and DELEVAUX, M. H., 1973--Variations in lead-isotopic compositions in Mesozoic granitic rocks of California: A preliminary investigation. Bull. Geol. Soc. Am., 84, p 3513-3526.
- DRORY, A., and ULMER, G. C., 1974--Oxygen fugacity determinations for Cascadian andesites, EOS. 55, p. 487.
- DUDAS, M. J., SCHMITT, R. A., HARWARD, M. E., 1971--Trace element partitioning between volcanic plagioclase and dacitic pyroclastic matrix. Earth Planet. Sci. Lett., 11, p. 440-446.

- DYMOND, J., CORLISS, J. B., HEATH, G. R., FIELD, C. W., DASH, E. J., and VEEH, H. H., 1973--Origin of metalliferous sediments from the Pacific Ocean. Bull Geol. Soc. Am., 84, p. 3355-3372.
- EGGLER, D. H., 1972--Water saturated and undersaturated melting relations in a Paricutin andesite and an estimate of water content in natural magma. Contr. Mineral. Petrol., 34, p. 261-271.
- EL HINNAWI, E. E., PICHLER, H., and ZEIL, W., 1969--Trace element distribution in Chilean ignimbrites. Contr. Mineral. Petrol., 24, p. 50-62.
- EWART, A., and TAYLOR, S. R., 1969--Trace element geochemistry of the rhyolitic volcanic rocks, Central north Island, New Zealand, Phenocryst data. Contr. Mineral. Petrol., 22, p. 127-146.
- EWART, A., and BRYAN, W. B., 1973--The petrology and geochemistry of the Tongan islands. In: The western Pacific: Island arcs, marginal seas, geochemistry. P.J. Coleman ed. Univ. of Western Australia press. Australia p. 508-522.
- FISHER, D. E., JOENSUU, O., and BOSTROM, K., 1969--Elemental abundances in ultramafic rock and their relation to the upper mantle. J. Geophys. Res., 74, p. 3865-3773.
- FITTON, J. G., 1971--The generation of magmas in island arcs. Earth Planet. Sci. Lett., 11, p. 63-67.
- FORBES, R. B., RAY, D. K., KATSURA, T., MATSUMOTO, H., HARAMURA, H., and FURST, M. J., 1969--The comparative chemical composition of continental vs. island arc andesites in Alaska. Proc. Andesite Conf. (ed. A. R. McBirney), Dept. Geol. Min. Res. Oregon Bull., 65, p. 111-120.
- FREY, F. A., 1974--Rare-earth element abundances in megacrysts from alkali-olivine basalts, EOS, 55, p. 474.
- FREY, F., HASKIN, M., POETZ, J., and HASKIN, L., 1968--Rare earth abundances in some basic rocks. J. Geophys. Res., 70, p. 6085-6097.
- FREY, F. A., and GREEN, D. H., 1974--The mineralogy, geochemistry and origin of lherzolite inclusions in Victorian basanites. Geochim. Cosmochim. Acta, 38, p. 1023-1059.

- FREY, F. A., BRYAN, W. B., and THOMPSON, G., 1974--Atlantic Ocean floor: Geochemistry of basalts from Legs 2 and 3 of the Deep Sea Drilling Project. J. Geophys. Res., in press.
- GANSSER, A. E., 1973--Facts and theories on the Andes. J. Geol. Soc. Lond., 129, p. 93-131.
- GAST, P. W., 1968--Trace element fractionation and the origin of tholeiitic and alkaline magma types. Geochim. Cosmochim. Acta, 32, p. 1057-1086.
- GILL, J. B., 1974--Role of underthrust oceanic crust in the genesis of a Fijian calc-alkaline suite. Contr. Mineral. Petrol. 43, p. 29-45.
- GOLES, G. G., 1967--Trace elements in ultramafic rocks. In: Ultramafic and related rocks. Wyllie, P. J., ed., John Wiley and Sons, New York, p. 352-362.
- GORDON, G. E., RANDLE, K., GOLES, G. G., CORLISS, J. B., BEESON, M. H., and OXLEY, S. S., 1968--Instrumental activation analysis of standard rocks with high-resolution γ -ray detectors. Geochim. Cosmochim. Acta, 32, p. 369-396.
- GREEN, T. H., 1972--Crystallization of calc-alkaline andesite under controlled high-pressure hydrous conditions. Contr. Mineral. Petrol., 34, p. 150-166.
- GREEN, T. H., and RINGWOOD, A. E., 1968--Genesis of the calc-alkaline igneous rock suite. Contr. Mineral. Petrol., 18, p. 105-162.
- GRIFFIN, W. L., and MURTHY, V. R., 1969--Distribution of K, Rb, Sr and Ba in some minerals relevant to basalt genesis, Geochim. Cosmochim. Acta, 31, p. 877-884.
- GUNN, B. M., 1972--The fractionation effect of kaersutite in basaltic magmas. Canadian Mineral., 11, p. 840-850.
- HAMILTON, W., 1969--The volcanic central Andes. A modern model for the Cretaceous batholiths and tectonic of western North America. Proc. Andesite Conf. (ed. A. R. McBirney), Dept. Geol. Min. Res. Oregon Bull., 65, p. 175-184.

- HAMILTON, W., and MYERS, W. B., 1966--Cenozoic tectonics of the western United States: Reviews. Geophys., 4, p. 509-549.
- HAMILTON, W., and MYERS, W. B., 1967--The nature of batholiths, U.S.G.S. Prof. Paper 554-C, 30 pp.
- HART, S. R., 1969--K, Rb, Cs, contents and Rb/Cs ratios of fresh and altered submarine basalts. Earth Planet. Sci. Lett., 6, p. 295-303.
- HART, S. R., et al., 1974--Oceanic basalt and the Nazca plate, Geotimes, 19, p. 20-24.
- HASKIN, L. A., ALLEN, R. O., HELMKE, P.A., PASTER, T. P., ANDERSON, M. R., KOROTEV, R. L., and ZWEIFEL, K. A., 1970--Rare-earths and other trace elements in Apollo 11 lunar samples. In: Proceedings of Apollo 11 Lunar Science Conference, vo. 2, pp. 1213-1231. Pergamon Press.
- HAYES, D. E., 1966--A geophysical investigation of the Peru-Chile trench. Marine Geol., 4, p. 259-279.
- HEKINIAN, R., 1971--Chemical and mineralogical differences between abyssal hill basalts and ridge tholeiites in the eastern Pacific Ocean. Marine Geol., 11, p. 77-91.
- HERTOGEN, J., and GIJBELS, R., 1971--Instrumental neutron activation analysis of rocks with a low energy photon detector. Anal. Chim. Acta, 56, 61-82.
- HIETANEN, A., 1971--Distribution of elements in biotite-hornblende pairs and in an orthopyroxene-clinopyroxene pair from zoned plutons, northern Sierra Nevada, California. Contr. Mineral. Petrol., 30, p. 161-176.
- HIGUCHI, H., and NAGASAWA, H., 1969--Partition of trace elements between rock-forming minerals and the host volcanic rocks. Earth Planet. Sci. Lett., 7, p. 281-287.
- HO, C. O., 1973--Experimental study of plagioclase/liquid and clinopyroxene/liquid distribution coefficients for Sr and Eu in oceanic ridge basalts system. M.S. Thesis. Columbia Univ. 147 pp.

- HOLLOWAY, J. R., and BURNHAM, C. W., 1972--Melting relations of basalt with equilibrium water pressures less than total pressure. J. Petrol., 13, p. 1-29.
- ILLIES, H., 1970--Geologia de los alrededores de Valdivia y Volcanismo y Tectonica en margenes del pacifico en Chile Meridional. Inst. de Geol. y Geografia. Univ. Austral de Chile. Valdivia, Chile, p. 64.
- IRVINE, T. N., and BARAGAR, W. R. A., 1971--A guide to the chemical classification of the common volcanic rocks. Canadian J. Earth Sci., 8, p. 523-548.
- JAKES, P., and GILL, J. B., 1970--Rare-earth elements and the island arc tholeiitic series, Earth. Planet. Sci. Lett., 9, p. 17-28.
- JAKES, P., and WHITE, A. J. R., 1972--Major and trace element abundances in volcanic rocks of orogenic areas. Bull. Geol. Soc. Am., 83, p. 29-40.
- JAMES, D. E., BROOKS, C., and CUYUBAMBA, A., 1973--Geochemical trends in Andean rocks. Annual report of the Director. Dept. of Terrestrial Magnetism. Carnegie Inst., p. 252-259.
- KATSUI, Y., 1972--Late Cenozoic volcanism and petrographic provinces in the Andes and Antartica. J. Fac. of Science Hokkaido Univ., Series IV, v. XV, p. 27-39.
- KATSUI, Y., and GONZALEZ-FERRAN, O., 1968--Geologia del area neovolcanica de los Nevados de Payachata. Consideraciones acerca del volcanismo Cenozoico superior en los Andes Chilenos. Inst. Geol. Univ. de Chile, 29, p. 61.
- KAY, R., HUBBARD, N., and GAST, P., 1970--Chemical characteristics and origin of oceanic ridge volcanic rocks. J. Geophys. Res., 75, p. 1585-1613.
- KISTLER, R. W., and PETERMAN, Z. F., 1973--Variations in Sr, Rb, K, Na and initial Sr^{87}/Sr^{86} in Mesozoic granitic rocks and intruded wall rocks in central California. Bull. Geol. Soc. Am., 84, p. 3489-3512.

- KLERKX, J., 1965--Etude petrologique de laves des volcans Villarrica, Calbuco, Osorno, Llaima (Chili Central). Ann. Soc. Geologique de Belgique, T88, Bull. 7-8, B451-B471.
- KUNO, H., 1960--High-alumina basalt. J. Petrology, 1, p. 121-145.
- KUNO, H., 1966--Lateral variation of basalt magma type across continental margins and island arcs. Bull. Volcanologique, 29, p. 195 - 222.
- KUNO, H., 1968a--Differentiation of basalt magmas. In: Basalts, v. 2, Hess and Poldervaart, ed., Interscience, New York, p. 623-688.
- KUNO, H., 1968b--Origin of andesite and its bearing on the island arc structure. Bull. Volcanologique, 32, p. 141-176.
- KUSHIRO, I., SHIMAZU, N., NAKAMURA, Y., and AKIMOTO, S., 1972--Composition of coexisting liquid and solid phases formed upon melting of natural garnet and spinel lherzolites at high pressures: A preliminary report. Earth Planet. Sci. Lett., 14, p. 19-25.
- LARSEN, E. S., and GOTTFRIED, D., 1960--Uranium and thorium in selected suites of igneous rocks. Am. Jour. Sci., 258-A, p. 151-169.
- LEFEVRE, C., 1973--Les caracteres magmatiques du volcanisme plioquaternaire des Andes dans le sud du Perou. Contr. Mineral. Petrol., 41, p. 259-272.
- LEVI, B., 1969--Burial metamorphism of a Cretaceous volcanic sequence west from Santiago, Chile. Contr. Mineral. Petrol., 24, p. 30-49.
- LEVI, B., 1973--Eastward shift of Mesozoic and early tertiary volcanic centers in the coastal range of central Chile. Bull. Geol. Soc. Am., 84, p. 3901-3910.
- LOPEZ-ESCOBAR, L., and OYARZUN, J., 1974--Uranium in calc-alkaline granitoids of central Chile. Pacific Geology, 8, p. 47-50.
- MacDONALD, G., 1968--Composition and origin of Hawaiian lavas. Geol. Soc. Am. Mem., 116, p. 477-522.

- MAPPER, D., 1960--Radio activation analysis. In: Methods in Geochemistry (ed. Smales and Wagner), Ch. 9, p. 297. Interscience Publ.
- MASUDA, A., 1968--Geochemistry of lanthanides in basalts of central Japan. Earth Planet. Sci. Lett., 4, p. 284-292.
- MERCY, E. L. P., and O'HARA, M. J., 1967--Distribution of Mn, Cr, Ti, and Ni in co-existing minerals of ultramafic rocks. Geochim. Cosmochim. Acta, 31, p. 2331-2341.
- MORENO, H., 1974a--Airplane flight over active volcanoes of central-south Chile. International symposium on volcanology. Guide Book D-3. Dept of Geology. Univ. de Chile. Santiago, Chile, 56 pp.
- MORENO, H., 1974b--The upper Cenozoic volcanism in the Andes of southern Chile (40°00' to 41°30'S). International symposium on volcanology. Abstracts of papers. Dept. of Geology. University of Chile, Santiago, Chile, p. 51.
- MORENO, H., 1974c--Volcanic landforms and its relations with different magma types in the Puyehue-Carran volcanic area (40°15' - 40°40'S). International symposium on volcanology. Abstracts of papers. Dept. of Geology. Univ. of Chile, Santiago, Chile, p.52.
- MUNIZAGA, F., AGUIRRE, L., and HERVE, F., 1973--Rb/Sr ages of rocks from the Chilean metamorphic basement. Earth Planet. Sci. Lett., 18, 87092.
- MYSEN, G., 1973--Melting in a hydrous mantle: Phase relations of mantle peridotite with controlled water and oxygen fugacitics. Carnegie Institution Year Book, 72, p. 467-478.
- MYSEN, B. O., KUSHIRO, I., NICHOLLS, I. A., and RINGWOOD, A. E., 1974--A possible mantle origin for andesitic magmas: discussion of a paper by Nicholls and Ringwood. Earth Planet. Sci. Lett., 21, p. 221-229.
- NAGASAWA, H., 1970--Rare-earth concentrations in zircons and apatites and their dacites and granites. Earth Planet. Sci. Lett., 9, p. 359-364.

- NAGASAWA, H., and SCHNETZLER, C. C., 1971--Partitioning of rare-earth, alkali and alkali earth elements between phenocrysts and acidic igneous magma. Geochim. Cosmochim. Acta, 35, p. 953-968.
- NICHOLLS, J., and CARMICHAEL, I. S. E., 1969--A commentary on the absarokite-shoshonite-banakite series of Wyoming, U.S.A., Schweiz, Mineral. Petrog. Mitt., 49, p. 47-64.
- NICHOLLS, I. A., and RINGWOOD, A. E., 1973--Effect of water on olivine stability in tholeiites and the production of silica-saturated magmas in the island arc environment. J. Geol., 81, p. 285-300.
- ONUMA, N., HIGUCHI, H., WAKITA, H., and NAGASAWA, H., 1968--Trace element partition between two pyroxenes and the host lava. Earth Planet. Sci. Lett., 5, p. 47-51.
- OYARZUN-MUNOZ, J., 1971--Contribution a l'etude geochimique des roches volcaniques et plutoniques du Chili. These Univ. Paris-Sud, 195 pp.
- PASTER, T. P., 1968--Petrologic variations within submarine basalt pillows. Ph.D. Thesis. Univ. of Florida, 108 pp.
- PHILPOTTS, J. A., and SCHNETZLER, C. C., 1970--Phenocryst-matrix partition coefficients for K, Rb, Sr, and Ba, with applications to anorthosite and basalt genesis. Geochim. Cosmochim. Acta, 34, p. 307-322.
- PHILPOTTS, J., MARTIN, W., and SCHNETZLER, C. C., 1971--Geochemical aspects of some Japanese lavas. Earth Planet. Sci. Lett., 12, p. 89-96.
- PICHLER, H., and ZEIL, W., 1969--Andesites of the Chilean Andes. Proc. Andesite conf. (ed. A. R. McBirney), Dept. of Geol. Min. Res. Oregon Bull., 65, p. 165-174.
- PICHLER, H., and ZEIL, W., 1972--The Cenozoic rhyolite-andesite association of the Chilean Andes. Bull. Volcanologique, 35, p. 424-452.
- PRICE, R. C., and TAYLOR, S. R., 1973--The geochemistry of the Dunedin volcano, East Otago, New Zealand: rare earth elements, Contrib. Mineral. Petrol., 40, p. 195-205.

- QUITTNER, P., 1972--Gamma-ray spectroscopy with particular reference to detector and computer evaluation techniques. Adam Hilger Ltd. London, 111 pp.
- RHODES, J. M., and RIDLEY, W. I., 1971--Trace element abundances in some Andean andesites. Abstracts with programs, Geol. Soc. Am. Meetings, 3, p. 681.
- RINGWOOD, A. E., 1974--The petrological evolution of island arc systems, J. Geol. Soc. Lond., 130, p. 183-204.
- RODDICK, J. A., 1974--Circumpacific plutonism - foreword. Pacific Geology, 8, p. i-ii.
- RUIZ, C., AGUIRRE, L., CORVALAN, J., KLOHN, C., KLOHN, E., and LEVI, B., 1965--Geologia y yacimientos metaliferos de Chile. Inst. Invest. Geologicas. Santiago, Chile. 305 pp.
- SANTO, T., 1969--Characteristics of seismicity in South America, Bull. Earthquake Res. Inst., Tokyo Univ., 47, p. 635-672.
- SCHILLING, J-G., 1971--Sea floor evolution: rare-earth evidence, Roy. Soc. (London) Philos. Trans., 268, p. 663-703.
- SCHILLING, J-G., and BONATTI, E., 1974--East Pacific ridge (2°S-19°S) versus Nazca intraplate volcanism: rare-earth evidence. Earth Planet. Sci. Lett., in press.
- SCHNETZLER, C. C., and PHILPOTTS, J. A., 1970--Partition coefficients of rare-earth elements between igneous matrix material and rock-forming mineral phenocrysts II., Geochim. Cosmochim. Acta, 34, p. 331-340.
- SCHOEDER, G. L., KRANER, H. W., and EVANS, R. D., 1966--Lithium-drifted germanium detectors: Application to neutron activation analysis. Science, 151, p. 815.
- SHAW, D. M., 1970--Trace element fractionation during anatexis, Geochim. Cosmochim. Acta, 34, p. 237-243.
- SIEGERS, A., PICHLER, H., and ZEIL, W., 1969--Trace element abundances in the "andesite" formation of northern Chile, Geochim. Cosmochim. Acta, 33, p. 882-887.
- SMITH, A. L., and CARMICHAEL, I. S. E., 1968--Quaternary lavas from the southern Cascades, Western U.S.A., Contr. Mineral. Petrol., 19, p. 212-238.

- STAUDER, W., 1973--Mechanism and spatial distribution of Chilean earthquakes with relation to subduction of the oceanic plate, J. Geophys. Res., 78, p. 5033-5061.
- STRECKEISEN, A. L., et al., 1973--Plutonic rocks classification and nomenclature recommended by the IUGS subcommission on the systematics of igneous rocks. Geotimes, 18, p. 26-30.
- TAYLOR, S. R., 1969--Trace element chemistry of andesites and associated calc-alkaline rocks. Proc. Andesite Conf. (ed. A. R. McBirney), Dept. Geol. Min. Res. Oregon Bull., 65, p. 43-64.
- TAYLOR, S. R., CAPP, A. E., GRAHAM, A. L., and BLAKE, D. H., 1969--Trace element abundances in andesites II. Saipan, Bougainville and Fiji, Contr. Mineral. Petrol., 23, p. 1-26.
- TAYLOR, S. R., WHITE, A. J. R., EWART, A., and DUNCAN, A. R., 1971--Nickel in high-alumina basalts: A reply. Geochim. Cosmochim. Acta, 35, p. 525-528.
- TOWELL, D. G., WINCHESTER, J. W., SPIRN, R. V., 1965--Rare-earth distributions in some rocks and associated minerals of the batholith of southern California. J. Geophys. Res., 70, p. 3485-3496.
- TUREKIAN, K. K., and WEDEPOHL, K. H., 1961--Distribution of the elements in some major units of the earth's crust. Bull. Geol. Soc. Am., 72, 175-192.
- VERGARA, M., 1972--Note on the paleovolcanism in the Andean geosyncline from the central part of Chile. 24th I.G.C. section 2, p. 222-230.
- VERGARA, M., 1974--Antuco volcano - Sierra Velluda. International symposium on volcanology. Guide book D-1, Dept. of Geology. Univ. de Chile. Santiago, Chile, 22 pp.
- VERGARA, M., 1970--Note on the zonation of the upper Cenozoic volcanism of the Andean area of central-south Chile and Argentina, Conf. on solid earth problems, Buenos Aires, Internat. Upper Mantle Project, 2, p. 381-397.

- VERGARA, M., and KATSUI, Y., 1969--Contribucion a la geologia y petrologia del volcan Antuco. Cordillera de los Andes, Chile central, Depto. Geol. Univ. Chile, 35, p. 25-47.
- VERGARA, M., and MUNIZAGA, F., 1974--Age and evolution of the upper Cenozoic andesitic volcanism in central-south Chile. Bull. Geol. Soc. Am., 85, p. 603-606.
- WAHL, W. H., and KRAMER, H. H., 1967--Neutron activation analysis. Scientific Amer., 216, p. 68.
- WAYNE-MEINKE, W., 1955-Trace element sensitivity: Comparison of activation analysis with other methods. Science, 121, p. 177.
- WEILL, D. F., and DRAKE, M. J., 1973--Europium anomaly in plagioclase-feldspar: experimental results and semiquantitative model, Science, 180, p. 1059-1060.
- WELCHER, F. J., 1958--The analytical uses of EDTA. D. van Nostrand, Publ.
- WILKINSON, J. F. G., 1967--The petrography of basaltic rocks. In: basalts, v. 1, Hess and Poldervaart, ed., Interscience, New York, p. 163-214.
- WISE, W. S., 1969--Geology and petrology of the Mt. Hood area: a study of high Cascade volcanism, Bull. Geol. Soc. Am., 80, p. 969-1006.
- ZIELINSKI, R. A., and FREY, F. A., 1970--Gough Island: evaluation of a fractional crystallization model, Contr. Mineral. Petrol., 29, p. 242-254.
- ZOLLER, W. H., and GORDON G. E., 1970--Instrumental neutron activation analysis of atmospheric pollutants utilizing Ge(Li) x-ray detectors. Anal. Chem., 42, p. 457.

TABLE 1

TRACE ELEMENTS IN USGS STANDARD G-2 DETERMINED BY INAA

	This Work	Lopez-Escobar, M.S. Thesis M.I.T. (1972)	Rey et al., Anal. Chem. Acta. 51 (1970) 163	Rey et al., Anal. Chem. Acta. 51 (1970) 163	Buma, M.S. Thesis M.I.T. (1970)	Gordon et al., Geochim. Cosmochim. Acta. 32 (1968) 369	Flanagan, Geochim. Cosmochim. Acta. 37 (1973) 1189
Sc	3.7±0.08	3.3±0.2			3.12±0.02	3.5±0.2	3.7
Cr	7.9						7
Co	4.8	4.3±0.3				4.3±0.2	5.5
Rb		193±5	191±3	177±5		129±4	168
Cs						1.4±0.3	1.4
Ba	1730±22	2000±80				1800±70	1870
La	86±4	94±2	93±7	93±6	85±2	81±1	96
Ce	136±5	173±3	163±5	177±5	168±5	144±4	150
Nd	52±1	55±3	48±2	51±2			60
Sm	6.8±0.2	7.9±0.3	7.2±0.1	7.3±0.1	7.4	8.7±0.15	7.3
Eu	1.28±0.04	1.48±0.02	1.52±0.02	1.53±0.02	1.29±0.01	1.37±0.05	1.5
Gd	3.7±0.7	3.7±0.1	3.5±0.1	3.9±0.2			5
Ho	0.53±0.01						0.4
Yb	0.71±0.05	0.74±0.02	0.62±0.02	0.81±0.03	0.56±0.05	0.8±0.2	0.88
Lu	0.13±0.01	0.10±0.05	0.12±0.01	0.13±0.01	0.10±0.02	0.18±0.08	0.11
Ta	1.04±0.04	0.97±0.06			0.80±0.04	1.0±0.1	0.91
Hf	8.6±0.2				8.26±0.02	7.8±0.5	7.35
Th	22.5±0.8	23.9±0.5			24.5±1.4	25.9±0.5	24.2
U	2.6±0.1						2.0

TABLE 1 (continued)

TRACE ELEMENTS IN USGS STANDARD G-2 DETERMINED BY INAA

	Randle, K. Chem. Geol. ¹³ (1974) 237-256	Green, Baunfelt and Heier, Geoch. Cosm. Acta ³⁶ (1972) 241-257	Arth, J.G. 1974 (Personal communi- cation)
Sc	3.5 ± 0.09	-	-
Cr	<20	-	-
Co	5.2 ± 0.9	-	-
Rb	164 ± 2	-	169
Cs	1.23 ± 0.14	-	-
Ba	1840 ± 50	-	1872
La	90 ± 4	100	-
Ce	154 ± 10	177	165
Nd	49 ± 7	51	51.1
Sm	7.4 ± 0.2	7.2	6.93
Eu	1.18 ± 0.09	1.51	1.35
Gd	-	4.25	3.73
Ho	-	-	-
Yb	<1	0.76	0.543
Lu	0.113 ± 0.014	0.11	0.0775
Ta	0.84 ± 0.11	-	-
Hf	8.1 ± 0.5	-	-
Th	25.4 ± 0.5	-	-
U	-	-	-

TABLE 2

MAJOR ELEMENT ABUNDANCES IN CENTRAL - SOUTH CHILE COASTAL BELT VOLCANICS

	ANCUD						
	<u>High-Alumina Basalt</u>	<u>Low-Silica Andesite</u>			<u>Andesite</u>		
	<u>CH-6</u>	<u>CH-30</u>	<u>CH-8</u>	<u>CH-21</u>	<u>CH-19</u>	<u>CH-15</u>	<u>GVO-63</u>
SiO ₂	49.61	52.57	52.32	53.97	57.76	59.50	59.89
Al ₂ O ₃	18.20	16.96	19.77	17.04	17.42	16.50	16.54
Fe ₂ O ₃	4.02	2.17	3.66	2.04	2.12	3.21	3.97
FeO	3.10	5.34	1.74	5.58	4.40	1.88	1.26
MgO	5.07	5.22	4.07	4.87	4.07	2.93	3.68
CaO	8.15	7.97	7.20	7.76	6.41	5.80	4.84
Na ₂ O	4.11	4.11	4.39	3.51	3.47	4.28	4.00
K ₂ O	0.76	0.88	0.84	1.08	1.65	2.12	2.37
TiO ₂	1.61	1.21	1.27	1.30	0.70	0.65	0.72
MnO	0.66	0.11	0.02	0.09	0.08	0.04	0.00
P ₂ O ₅	0.19	0.27	0.20	0.31	0.20	0.13	0.26
H ₂ O + CO ₂	4.79	3.85	4.23	2.30	1.48	2.65	2.90
Total	99.67	100.66	99.71	99.85	99.76	99.69	100.43
Mg/Mg+ΣFe	0.57	0.56	0.59	0.54	0.53	0.52	0.58
Normative Quartz	0.14	1.14	3.36	5.47	10.52	12.24	13.24

TABLE 2 (continued)

MAJOR ELEMENT ABUNDANCES IN CENTRAL - SOUTH CHILE COASTAL BELT VOLCANICS

	TEMUCO				LOS ANGELES	
	<u>Andesite</u>				<u>Dacite</u>	
	<u>T-2</u>	<u>T-3</u>	<u>T-9</u>	<u>T-13</u>	<u>T-17</u>	<u>T-18</u>
SiO ₂	58.37	58.61	58.75	59.90	61.31	63.20
Al ₂ O ₃	17.15	17.18	17.50	16.96	14.00	14.40
Fe ₂ O ₃	2.68	2.80	4.02	3.23	2.02	1.48
FeO	3.60	2.66	1.87	2.37	3.43	3.37
MgO	4.73	3.28	3.34	3.53	4.62	2.60
CaO	6.87	6.64	5.77	5.35	4.95	4.02
Na ₂ O	3.78	3.24	3.94	4.00	2.76	4.00
K ₂ O	1.42	1.54	1.22	1.40	2.09	2.51
TiO ₂	0.79	0.69	0.64	0.58	0.56	0.59
MnO	0.14	0.11	0.09	0.10	0.12	0.10
P ₂ O ₅	0.15	0.08	0.14	0.21	0.12	0.18
H ₂ O + CO ₂	1.78	2.66	4.12	0.90	2.90	3.65
Total	100.58	99.49	100.50	100.02	100.10	100.10
Mg/Mg+ $\frac{1}{2}$ Fe	0.58	0.53	0.52	0.54	0.61	0.50
Normative Quartz	9.74	15.72	14.91	15.30	19.97	18.13

TABLE 3

TRACE ELEMENT ABUNDANCES IN CENTRAL - SOUTH CHILE COASTAL BELT VOLCANICS

	ANCUD						
	High-Alumina Basalt	Low Silica Andesites			Andesites		
	<u>CH-6</u>	<u>CH-30</u>	<u>CH-8</u>	<u>CH-21</u>	<u>CH-19c</u>	<u>CH-15</u>	<u>GVO-63</u>
Sc	35.8	32.0	35.7	29.3	19.7	17.0	16.3
Cr	177	120	190	130	70	304	213
Co	34.6	32.6	30.9	28.6	20.7	22.1	16.1
Ni	90	50	55	30	25	80	60
Rb	10	15	10	20	75	300	120
Sr	280	300	330	300	220	200	190
Ba	290	280	200	250	390	205	310
La	9.7	13.1	11.8	16.3	18.1	16.0	18.7
Ce	23.3	27.9	25.7	31.6	38.2	30.3	38.1
Nd	14.4	19.1	15.4	18.2	21.6	15.9	19.6
Sm	3.35	4.95	4.37	5.11	4.16	3.61	4.72
Eu	1.34	1.35	1.29	1.36	0.96	0.86	1.05
Gd	3.7	3.1	3.3	3.8	5.7	3.2	4.8
Ho	0.9	1.2	1.2	1.2	1.0	0.7	0.9
Yb	2.6	2.7	3.0	2.8	2.0	1.7	1.9
Lu	0.38	0.48	0.48	0.48	0.37	0.33	0.32
Eu/Eu*	1.18	1.0	1.0	0.9	0.6	0.8	0.7
Hf	3.3	3.7	3.8	3.8	3.9	4.1	4.6
Ta	0.48	0.51	0.56	0.49	0.76	0.68	0.92
Th	1.8	2.5	2.9	2.6	6.6	5.4	5.8
U	1.0	1.5	2.4	1.8	1.8	3.6	1.9

TABLE 3 (continued)

TRACE ELEMENT ABUNDANCES IN CENTRAL - SOUTH CHILE COASTAL BELT VOLCANICS

	TEMUCO				LOS ANGELES	
	Andesites				Dacites	
	<u>T2</u>	<u>T3</u>	<u>T9</u>	<u>T13</u>	<u>T17</u>	<u>T18</u>
Sc	22.0	18.7	21.8	16.75	18.5	18.3
Cr	73	32	56	73	338	84
Co	22.8	13.2	24.3	15.8	20.6	11.9
Ni	20	-	-	20	60	35
Rb	35	-	-	35	60	75
Sr	350	-	-	420	225	300
Ba	270	560	220	320	410	600
La	10.0	21.8	9.5	11.2	12.8	15.5
Ce	23.1	41.6	21.9	26.2	29.6	31.6
Nd	13.2	21.8	11.7	13.4	18.8	21.2
Sm	2.78	4.37	2.46	2.82	4.85	4.98
Eu	0.84	1.22	0.77	0.75	0.98	1.11
Gd	2.7	5.4	2.6	3.1	4.1	4.9
Ho	0.7	0.9	0.6	0.6	1.1	1.1
Yb	1.8	2.4	1.5	1.5	3.2	3.4
Lu	0.30	0.38	0.23	0.24	0.58	0.58
Eu/Eu*	0.9	0.8	0.9	0.8	0.7	0.7
Hf	2.8	5.1	2.6	3.8	6.7	4.9
Ta	0.30	0.53	0.23	0.39	0.28	0.35
Th	3.1	6.2	2.6	3.1	4.4	4.9
U	1.1	1.7	1.0	0.7	1.7	1.8

All abundances in ppm. Ni, Rb, and Sr abundances from Oyarzun, 1971. Other elements determined by instrumental neutron activation (Gordon *et al.*, 1968). Eu/Eu* is the ratio of the observed chondrite-normalized Eu abundance to that expected by extrapolation from Sm to Gd. The accuracy and precision of the technique have been discussed by Frey *et al.*, 1974.

TABLE 4

GEOCHEMICAL CHARACTERISTICS OF ANDESITES AND DACITES

	FeO*/ MgO	K ₂ O/ Na ₂ O	K/ Rb	Th/ U	La/ Yb	Rb	Sr	Ba	La	Th
<u>Island Arc Andesites</u>										
Average (a)	< 2	< 0.8	430	3.2	6.2	30	385	270	11.9	2.2
Aleutians (b)	-	-	522	-	-	26	434	-	-	-
<u>Central-South Chile Andesites</u> ^(c)										
Ancud	1.5	0.52	103	2.3	9.3	165	203	301	17.6	5.9
Temuco	1.5	0.38	335	3.3	7.2	35	385	341	13.1	3.7
<u>Continental Margin Andesites</u>										
Average (a)	> 2	0.6-1.1	230	> 3.2	> 6.2	> 30	> 385	> 270	> 11.9	> 2.2
Northern Chile (d)	1.8	0.5	{ 225 281	-	-	{ 80 74	{ 700 555	680	-	7
Tupungato (c)	1.6	0.42	-	-	11.6	-	-	-	19.1	-
<u>Island Arc Dacites</u>										
Average (a)	2.6	0.45	380	2.7	10	45	460	520	14	1.7
Aleutians (b)	-	-	479	-	-	45	485	-	-	-
<u>Central-South Chile Dacites</u>										
Los Angeles (c)	1.5	0.68	270	2.6	4.2	67	262	505	14.1	4.6
<u>Continental Margin Dacites</u>										
Northern Chile (d)	-	-	215	-	-	138	416	-	-	19

TABLE 4 (continued)

- a) Jakes and White (1972)
- b) DeLong (1974)
- c) This paper
- d) Siegers et al., (1969), Pichler and Zeil (1972),
Rhodes and Ridley (1971).

All abundances in ppm. FeO* indicates total iron
as FeO.

TABLE 5
SOLID/LIQUID PARTITION COEFFICIENTS USED IN
FRACTIONAL MELTING MODELS

	<u>Amphibole</u>	<u>Clinopyroxene</u>	<u>Garnet</u>
K	0.67	0.06	0.05
Rb	0.25	0.05	0.03
Sr	0.50	0.15	0.008
Ba	0.50	0.08	0.04
Sc	2	3	8.3
Cr	5	33	20
Co	1.1	2	4.0
Ni	3	3	0.7
La	0.2	0.1	0.005
Ce	0.25	0.15	0.007
Nd	0.45	0.35	0.030
Sm	0.60	0.55	0.25
Eu	0.70	0.60	0.35
Ho	0.65	0.65	1.2 - 4
Er	-	-	1.6 - 6
Yb	0.40	0.60	3.0 - 10
Lu	0.35	0.55	- -

Amphibole partition coefficients from Griffin and Murthy (1969), Higuchi and Nagasawa (1969), Gunn (1972), DeLong (1974), and Frey (1974). Clinopyroxene partition coefficients from Onuma *et al.*, (1968), Philpotts and Schnetzler (1970), and Frey (1974). Garnet partition coefficients from Griffin and Murthy (1969), Taylor *et al.*, (1969), Gill (1974), and Frey (1974). Two alternative sets of data were used for HREE (see Figure 10).

TABLE 6

MAJOR ELEMENT ABUNDANCES IN CENTRAL - SOUTH CHILE HIGH ANDEAN VOLCANICS

	STRATOVOLCANOES								
	<u>Tupungato</u>	<u>Antuco</u>	<u>Llaima</u>	<u>*Callaq.</u>	<u>*Vill.</u>	<u>Lanin</u>	<u>Lanin</u>	<u>Puyehue</u>	<u>*Casa.</u>
	<u>Andesite</u>	<u>Low-K Andesites</u>		<u>High Alumina Basalt</u>					
Sample	797	801	798	799	802	GV164	800	GV170	GV177
Latitude	33°15'S	37°30'S	38°45'S	37°50'S	39°30'S	39°40'S	39°40'S	40°35'S	40°45'S
SiO ₂	61.23	53.23	54.40	51.20	52.70	49.76	51.46	51.39	50.94
Al ₂ O ₃	16.61	21.52	19.72	20.46	20.81	19.29	22.02	19.71	19.34
Fe ₂ O ₃	-	-	-	-	-	1.98	-	2.84	1.58
FeO	4.71*	5.66*	7.84*	8.95*	6.11*	7.96	7.33*	5.79	7.15
MgO	3.25	3.22	3.84	4.18	4.80	5.01	3.59	4.73	5.94
CaO	4.48	9.70	9.60	9.56	10.50	8.43	9.38	8.97	9.14
Na ₂ O	5.05	3.87	3.48	3.23	3.32	3.65	3.89	3.26	3.31
K ₂ O	2.11	0.49	0.54	0.57	0.44	1.14	0.70	0.69	0.55
TiO ₂	0.79	0.80	1.08	1.27	0.89	1.16	1.04	1.01	0.86
MnO	0.09	0.18	0.16	0.19	0.17	0.21	0.15	0.22	0.16
P ₂ O ₅	0.21	0.06	0.18	0.33	0.21	0.36	0.14	0.19	0.22
H ₂ O + CO ₂	-	-	-	-	-	0.53	-	0.88	0.71
Total	98.53	100.85	99.95	99.94	99.95	99.48	99.69	99.68	99.90
Mg/Mg+ΣFe	0.53	0.48	0.44	0.43	0.56	0.48	0.44	0.50	0.55
Normative Quartz	7.38	1.27	2.93	-	0.9	-	-	2.19	-
Normative Olivine	-	-	-	0.75	-	11.49	6.69	-	4.17

* Total Fe expressed as FeO

TABLE 6 (continued)

MAJOR ELEMENT ABUNDANCES IN CENTRAL - SOUTH CHILE HIGH ANDEAN VOLCANICS

	Plateau Series		
	Pino Hachado		
	<u>Trachyandesite</u>		<u>Trachyte</u>
	TH31	TH34	TH40
SiO ₂	57.64	59.20	64.95
Al ₂ O ₃	17.06	17.08	16.82
Fe ₂ O ₃	3.74	2.41	3.60
FeO	3.66	3.34	0.23
MgO	2.06	1.48	0.64
CaO	3.18	2.44	1.82
Na ₂ O	6.18	6.00	4.33
K ₂ O	3.05	3.71	4.40
TiO ₂	1.74	1.06	0.52
MnO	0.19	0.15	0.10
P ₂ O ₅	0.71	0.42	0.09
H ₂ O + CO ₂	0.43	2.40	2.22
Total	99.64	99.69	99.72
Mg/Mg+ΣFe	0.34	0.32	0.25
Normative Quartz	1.94	2.86	18.80
Normative Olivine	-	-	-

*Callaq. = Callaquen

*Vill. = Villarrica

*Casa. = Casablanca

TABLE 7

RESULTS OF THE ANALYSIS OF THE USGS-AGV I MADE IN THIS WORK

	<u>This Work</u>		<u>Flanagan</u>	<u>Difference in %</u>
SiO ₂	61.46	0.05	60.47	1.6
Al ₂ O ₃	17.60	0.05	17.68	0.4
FeO*	6.08	0.03	6.26	2.9
MgO	1.56	0.02	1.57	0.6
CaO	4.75	0.02	5.02	5.4
Na ₂ O	4.44	0.11	4.37	1.6
K ₂ O	2.56	0.05	2.96	13.5
TiO ₂	1.10	0.01	1.07	2.8
P ₂ O ₅	0.51	0.01	0.50	2.0
MnO	0.07	0.01	0.10	30.0

The errors shown are the standard error of the mean. The data are compared with those obtained by Flanagan (1973) for the same USGS standard rock. FeO* is total iron expressed as FeO.

TABLE 8

TRACE ELEMENT ABUNDANCES IN CENTRAL - SOUTH CHILE HIGH ANDEAN VOLCANICS

	STRATOVOLCANOES								
	<u>Tupungato</u>	<u>Antuco</u>	<u>Llaima</u>	<u>Callaquen</u>	<u>Villarrica</u>	<u>Lanin</u>	<u>Lanin</u>	<u>Puyehue</u>	<u>Casablanca</u>
	<u>Andesite</u>	<u>Low-K Andesites</u>		<u>High Alumina Basalts</u>					
797	801	798	799	802	GV164	800	GV170	GV177	
Sc	-	-	-	-	-	30.7±0.1	-	36.8±0.2	32.6±0.1
Cr	-	-	-	-	-	25±3	-	116 ±2	99±2
Co	-	-	-	-	-	35.7±0.4	-	31.3±0.3	36.6±0.4
Ni	-	-	-	-	-	-	-	-	-
Rb	-	-	-	-	-	-	-	-	-
Sr	-	-	-	-	-	-	-	-	-
Ba	-	-	-	-	-	510 ±70	-	300 ± 55	170 ± 60
La	19.1	6.7	7.4	16.0	5.9	19.9±0.7	17.6	8.7 ± 0.5	6.4 ± 0.6
Ce	36.4	15.7	16.9	34.8	14.1	47.5±1.1	36.4	21.3 ±0.8	15.2 ±0.8
Nd	17.9	10.3	11.7	23.4	9.0	26.0±1.3	22.3	12.7±1.4	9.5 ±1.1
Sm	3.51	2.49	3.13	4.93	2.43	5.19±0.06	4.09	3.17±0.04	2.25±0.04
Eu	0.98	0.94	1.14	1.23	0.89	1.45±0.05	1.42	1.05±0.04	0.82±0.04
Gd	4.6	2.6	3.2	5.4	2.9	7±1	5.0	3.8 ±0.7	3.1 ± 0.7
Ho	0.5	0.5	0.9	0.8	0.7	1.3 ± 0.3	0.9	0.9 ± 0.2	0.7 ± 0.2
Yb	1.1	1.6	-	2.1	1.7	2.8 ± 0.2	2.3	2.2 ± 0.2	1.8 ± 0.2
Lu	-	0.23	0.37	-	0.27	0.46±0.02	0.32	0.42±0.01	0.33±0.01
Eu/Eu*	0.75	1.1	1.1	0.73	1.0	0.75±0.06	1.0	1.0 ± 0.1	1.0 ± 0.2
Hf	-	-	-	-	-	3.6 ± 0.2	-	2.3 ± 0.2	1.9 ± 0.2
Ta	-	-	-	-	-	0.37±0.03	-	0.24±0.01	-
Th	-	-	-	-	-	5.7 ± 0.2	-	1.7 ± 0.2	1.4 ± 0.2
U	-	-	-	-	-	1.7 ± 0.5	-	1.2 ± 0.4	0.8 ± 0.2

TABLE 8 (continued)

TRACE ELEMENT ABUNDANCES IN CENTRAL - SOUTH CHILE HIGH ANDEAN VOLCANICS

	Plateau Series		
	Pino Hachado		
	Trachyandesites		Trachyte
	TH31	TH34	TH40
Sc	16.3	13.0	9.0
Cr	4	6	9
Co	7.9	5.4	6.3
Ni	20	10	5
Rb	60	100	120
Sr	350	470	285
Ba	940	810	750
La	53.3	44.4	27.8
Ce	122.3	96.2	62.5
Nd	60.3	51.7	28.0
Sm	10.59	9.95	5.05
Eu	2.90	2.56	1.03
Gd	12.0	11.0	6.3
Ho	2.0	2.1	1.4
Yb	4.9	4.4	3.6
Lu	0.77	0.70	0.48
Eu/Eu*	0.8	0.7	0.6
Hf	10.7	12.1	8.5
Ta	2.88	2.95	1.01
Th	8.1	9.4	16.0
U	2.4	3.9	4.9

TABLE 9

FRACTIONAL CRYSTALLIZATION MODEL (MAJOR ELEMENTS) FOR THE
TRANSITION 800 (LANIN) TO GV164 (LANIN)

	<u>800 (Lanin)</u>	<u>0.30 Plagioclase</u>	<u>Result(%)</u>	<u>GV164</u>
SiO ₂	52.0	53.4	51.5	50.4
Al ₂ O ₃	22.3	29.8	19.2	19.5
FeO*	6.7		9.6	9.9
MgO	3.6		5.2	5.1
CaO	9.5	12.1	8.0	8.5
Na ₂ O	3.9	4.7	3.6	3.7
K ₂ O	0.7		1.0	1.2
TiO ₂	1.1		1.6	1.2
P ₂ O ₅	0.15		0.21	0.2
MnO	0.14		0.20	0.36

FeO* is total Fe expressed as FeO. The composition of plagioclase is An 60. (This composition was calculated from the chemical composition of pure Ab and pure An). The number preceding the plagioclase (0.30) indicates the weight fraction of the initial magma that must fractionate as plagioclase. The column Result (%) contains the major element composition predicted by the model. This table also contains the composition of sample GV164 (Lanin).

TABLE 10

MODAL COMPOSITION IN CENTRAL CHILE GRANITOIDS

	COASTAL BATHOLITH							CENTRAL BATHOLITH			
	<u>G3</u>	<u>G10</u>	<u>G11</u>	<u>G6</u>	<u>G5</u>	<u>G2</u>	<u>G15</u>	<u>G18</u>	<u>G17</u>	<u>G13</u>	<u>G12</u>
	<u>Qd</u>	<u>Ton</u>	<u>Ton</u>	<u>Gd</u>	<u>Gd</u>	<u>Gr</u>	<u>Gr</u>	<u>Ton</u>	<u>Qmd</u>	<u>Gd</u>	<u>Ton</u>
Quartz	9.9	18.6	21.6	29.6	29.3	39.8	33.3	19.5	14.8	17.7	26.0
Plagioclase	59.1	56.7	41.2	38.8	39.0	26.9	27.5	56.5	46.5	47.0	54.6
K-Feldspar	-	-	-	20.4	12.7	22.9	28.5	3.9	24.7	11.8	2.2
Biotite	18.3	12.0	9.1	10.6	18.2	8.1	10.1	11.1	-	17.1	6.0
Amphibole	12.2	12.0	27.3	-	-	2.0	-	8.1	12.3	6.0	10.0
Magnetite	0.5	0.6	0.8	0.6	0.8	0.3	0.6	0.9	1.7	0.4	1.2

Qd = Quartz-diorite

Ton = Tonalite

Gd = Granodiorite

Gr = Granite

Qmd = Quartz monzo-diorite

TABLE 10 (continued)

MODAL COMPOSITION IN CENTRAL CHILE GRANITOIDS

	ANDEAN BATHOLITH					
	<u>G30</u>	<u>G22</u>	<u>G23</u>	<u>G29</u>	<u>G26</u>	<u>G27</u>
	<u>Qmd</u>	<u>Gd</u>	<u>Qmd</u>	<u>Qmd</u>	<u>Gd</u>	<u>Gd</u>
Quartz	12.6	27.0	14.6	13.6	19.8	19.8
Plagioclase	52.5	38.0	49.8	44.0	45.4	47.6
K-Feldspar	20.4	18.0	21.5	24.1	17.8	17.9
Biotite	-	3.1	7.1	-	7.2	7.2
Amphibole	13.1	12.3	6.0	16.9	8.2	6.2
Magnetite	1.3	1.5	1.0	1.4	1.6	1.3

Qd = Quartz-diorite

Ton = Tonalite

Gd = Granodiorite

Gr = Granite

Qmd = Quartz monzodiorite

TABLE 11

MAJOR ELEMENT ABUNDANCES IN CENTRAL CHILE GRANITOIDS

	COASTAL BATHOLITH						CENTRAL BATHOLITH				
	<u>G3</u>	<u>G10</u>	<u>G11</u>	<u>G6</u>	<u>G5</u>	<u>G2</u>	<u>G15</u>	<u>G18</u>	<u>G17</u>	<u>G13</u>	<u>G12</u>
	<u>Qmd</u>	<u>Ton</u>	<u>Ton</u>	<u>Gd</u>	<u>Gd</u>	<u>Gr</u>	<u>Gr</u>	<u>Ton</u>	<u>Qmd</u>	<u>Gd</u>	<u>Ton</u>
SiO ₂	58.70	61.44	67.35	67.77	68.78	71.16	73.00	62.51	63.24	67.20	67.37
Al ₂ O ₃	19.18	17.14	16.24	15.71	16.29	14.65	14.33	16.99	17.20	16.59	15.99
Fe ₂ O ₃	0.40	2.54	1.86	1.27	0.89	0.63	1.04	1.74	2.23	2.01	0.34
FeO	6.18	3.15	4.02	2.14	2.09	3.12	1.41	3.57	2.64	4.27	1.60
MgO	1.73	2.27	1.03	1.05	1.08	0.60	0.65	2.34	1.64	1.16	2.56
CaO	6.65	5.15	2.48	3.53	3.15	2.98	2.41	6.51	4.28	2.79	6.69
Na ₂ O	3.98	5.12	4.06	4.21	3.79	3.77	3.78	3.83	3.79	3.19	3.47
K ₂ O	1.22	2.15	1.32	2.94	3.00	2.32	3.43	1.67	2.86	1.14	0.40
TiO ₂	1.04	0.65	0.78	0.48	0.48	0.55	0.38	0.63	0.84	0.77	0.45
P ₂ O ₅	0.30	0.23	0.23	0.18	0.16	0.14	0.16	0.27	0.25	0.18	0.10
MnO	0.12	0.12	0.12	0.08	0.12	0.10	0.06	0.17	0.12	0.12	0.06
H ₂ O + CO ₂	-	-	-	-	-	-	-	-	-	-	-
Total	99.50	99.96	99.49	99.36	99.83	100.02	100.65	100.23	99.09	99.42	99.03

TABLE 11 (continued)

MAJOR ELEMENT ABUNDANCES IN CENTRAL CHILE GRANITOIDS

	ANDEAN BATHOLITH					
	<u>G30</u>	<u>G22</u>	<u>G25</u>	<u>G29</u>	<u>G26</u>	<u>G27</u>
	<u>Qmd</u>	<u>Gd</u>	<u>Qmd</u>	<u>Qmd</u>	<u>Gd</u>	<u>Gd</u>
SiO ₂	61.35	66.06	66.17	66.83	67.52	69.74
Al ₂ O ₃	16.88	15.40	15.99	16.08	16.50	14.84
Fe ₂ O ₃	1.59	1.90	1.77	3.46	2.89	1.70
FeO	3.17	2.47	2.32	2.02	2.09	2.17
MgO	2.47	1.73	1.76	1.31	0.80	0.98
CaO	4.51	3.16	3.26	1.95	1.37	2.83
Na ₂ O	5.85	5.16	4.81	4.50	4.97	3.75
K ₂ O	2.74	3.31	3.13	2.87	2.66	3.11
TiO ₂	0.92	0.57	0.67	0.67	0.70	0.53
P ₂ O ₅	0.27	0.21	0.21	0.25	0.23	0.11
MnO	0.09	0.06	0.06	0.08	0.06	0.12
H ₂ O + CO ₂	-	-	-	-	-	-
Total	99.84	100.03	100.15	100.02	99.79	99.88

TABLE 12

MOLECULAR NORMATIVE COMPOSITION IN CENTRAL CHILE GRANITOIDS

	COASTAL BATHOLITH						CENTRAL BATHOLITH				
	G3	G10	G11	G6	G5	G2	G15	G18	G17	G13	G12
	Qd	Ton	Ton	Gd	Gd	Gr	Gr	Ton	Qmd	Gd	Ton
Qtz	9.92	9.03	28.63	21.17	24.45	29.52	29.43	15.32	17.40	33.09	26.38
Or	7.29	12.64	7.96	17.55	17.86	13.90	20.34	9.90	17.15	6.93	2.40
Ab	36.10	45.73	37.18	38.19	34.29	34.33	34.07	34.49	34.55	29.45	31.59
An	31.19	17.35	11.02	15.45	14.70	14.07	10.96	24.31	19.90	13.03	27.25
Di	0.14	5.27	-	0.86	-	-	-	5.16	-	-	4.60
Hy	12.88	5.99	7.02	4.41	5.16	5.52	2.83	7.62	6.18	7.75	6.61
Mt	0.43	2.65	1.99	1.35	0.94	0.67	1.10	1.83	2.37	2.17	0.37
Il	1.47	0.91	1.11	0.68	0.68	0.78	0.54	0.88	1.19	1.11	0.64
Ap	0.64	0.48	0.50	0.39	0.34	0.30	0.34	0.53	0.54	0.39	0.22
C	-	-	4.65	-	1.61	0.95	0.44	-	0.77	6.14	-
Hm	-	-	-	-	-	-	-	-	-	-	-
Qtz	13.56	10.74	30.05	23.71	27.36	32.66	31.11	17.87	21.08	33.62	27.08
Or	-	8.32	-	12.33	7.29	4.35	15.12	4.21	6.15	-	-
Ab	36.10	45.73	37.18	38.19	34.29	34.33	34.07	34.49	34.55	29.45	31.59
An	27.70	17.35	8.25	14.82	13.02	12.13	9.63	24.31	16.93	10.27	27.25
Mus	-	-	1.66	0.88	8.00	6.03	3.40	-	6.82	-	-
Bio	11.65	6.92	10.85	7.35	7.78	8.40	4.49	9.11	9.82	11.08	3.84
Sphene	2.20	1.36	1.67	1.02	1.02	1.17	0.80	1.32	1.79	1.66	0.96
Mt	0.43	2.65	1.99	1.35	0.94	0.67	1.10	1.83	2.37	2.17	0.37
Ap	0.64	0.48	0.50	0.39	0.34	0.30	0.34	0.53	0.54	0.39	0.22
Andalucite	2.10	-	7.92	-	-	-	-	-	-	10.86	-
Hy	5.67	-	-	-	-	-	-	-	-	0.54	2.51
Actinolite	-	6.49	-	-	-	-	-	6.38	-	-	6.24

TABLE 12 (continued)

MOLECULAR NORMATIVE COMPOSITION IN CENTRAL CHILE GRANITOIDS

		ANDEAN BATHOLITH						
		<u>G30</u>	<u>G22</u>	<u>G25</u>	<u>G29</u>	<u>G26</u>	<u>G27</u>	
		<u>Qmd</u>	<u>Gd</u>	<u>Qmd</u>	<u>Qmd</u>	<u>Gd</u>	<u>Gd</u>	
[Qtz	4.33	13.62	15.50	22.60	23.08	26.20	
	Or	15.97	19.45	18.41	17.07	15.81	18.61	
	Ab	51.83	46.09	43.00	40.67	44.89	34.09	
	An	11.56	9.04	12.74	8.10	5.33	13.49	
	Di	7.03	4.16	1.60	-	-	-	
	Hy	5.85	4.47	5.56	3.65	2.57	4.39	
	Mt	1.64	1.98	1.85	3.51	3.04	1.80	
	Il	1.27	0.79	0.93	0.94	0.99	0.75	
	Ap	0.56	0.44	0.44	0.53	0.49	0.24	
	C	-	-	-	2.89	3.85	0.47	
	Hm	-	-	-	0.10	-	-	
	[Qtz	5.64	14.96	18.74	24.89	24.85	28.76
		Or	11.81	16.03	12.02	3.77	0.78	11.29
Ab		51.83	46.09	43.00	40.67	44.89	34.09	
An		11.56	9.04	12.42	5.75	2.88	11.62	
Mus		-	-	0.46	13.38	16.90	4.26	
Bio		6.66	5.49	9.71	5.99	4.73	6.85	
Sphene		1.90	1.19	1.40	1.41	1.48	1.13	
Mt		1.64	1.98	1.85	3.65	3.04	1.80	
Ap		0.56	0.44	0.44	0.53	0.49	0.24	
Andalucite		-	-	-	-	-	-	
Hy		-	-	-	-	-	-	
Actinolite	8.44	4.84	-	-	-	-		

TABLE 13

TRACE ELEMENT ABUNDANCES IN CENTRAL CHILE GRANITOIDS

	COASTAL BATHOLITH						CENTRAL BATHOLITH				
	<u>G3</u>	<u>G10</u>	<u>G11</u>	<u>G6</u>	<u>G5</u>	<u>G2</u>	<u>G15</u>	<u>G18</u>	<u>G17</u>	<u>G13</u>	<u>G12</u>
	<u>Qd</u>	<u>Ton</u>	<u>Ton</u>	<u>Gd</u>	<u>Gd</u>	<u>Gr</u>	<u>Gr</u>	<u>Ton</u>	<u>Qmd</u>	<u>Gd</u>	<u>Ton</u>
Sc	26.7	15.7	17.9	5.9	6.4	19.6	4.2	14.5	21.2	19.9	18.7
V	60	93	70	32	37	30	25	120	80	110	85
Cr	18	11	11	16	19	10	9	18	17	17	18
Co	15.3	12.6	10.2	5.0	6.9	4.2	4.1	13.4	12.6	17.0	4.2
Ni	10	12	9	6	6	8	6	10	11	11	10
Rb	35	55	30	95	120	40	140	45	85	75	10
Cs	1.3	2.7	1.6	3.3	2.2	0.5	3.0	2.9	2.0	4.0	0.9
Sr	395	490	300	395	540	200	400	465	470	370	390
Ba	230	480	345	465	665	165	640	365	880	455	150
La	2.10	18.2	15.8	25.7	26.5	9.2	23.3	14.5	17.8	21.6	9.4
Ce	47.5	43.0	32.2	44.3	49.5	19.6	42.9	29.9	43.2	41.9	22.4
Nd	23.8	26.1	19.4	18.4	23.4	15.4	16.2	16.2	26.9	23.3	15.7
Sm	4.53	5.01	4.05	3.16	3.72	3.67	2.62	3.86	5.33	4.44	3.31
Eu	1.61	1.18	1.09	0.79	0.95	0.80	0.58	0.95	1.28	1.12	0.85
Gd	6.6	5.7	4.7	4.1	5.1	3.6	3.4	3.6	6.3	6.0	3.2
Ho	1.1	1.0	1.1	0.6	0.8	0.9	0.5	0.9	1.2	1.1	0.9
Yb	2.5	2.6	2.9	1.4	1.6	2.4	1.1	2.5	2.8	2.8	2.7
Lu	0.41	0.40	0.45	0.22	0.19	0.42	0.18	0.37	0.46	0.41	0.39
ΣREE	109.1	103.2	81.7	98.7	111.8	56.0	90.2	72.78	105.3	102.7	58.9
Hf	4.1	5.8	5.3	3.9	4.1	3.9	3.6	4.2	5.3	6.2	4.4
Ta	0.88	0.38	0.41	1.08	0.74	0.45	0.71	0.31	0.55	0.49	0.43
Th	6.2	13.0	3.6	12.2	9.6	4.3	20.1	4.8	16.4	9.2	4.5
U	1.5	2.4	0.7	6.3	1.5	1.1	1.9	1.1	3.2	1.7	1.1

TABLE 13 (continued)

TRACE ELEMENT ABUNDANCES IN CENTRAL CHILE GRANTOIDS

	ANDEAN BATHOLITH					
	<u>G30</u>	<u>G22</u>	<u>G25</u>	<u>G29</u>	<u>G26</u>	<u>G27</u>
	<u>Qmd</u>	<u>Gd</u>	<u>Qmd</u>	<u>Qmd</u>	<u>Gd</u>	<u>Gd</u>
Sc	12.3	7.5	8.1	10.3	8.2	8.7
V	130	100	100	135	120	70
Cr	30	41	22	33	18	17
Co	8.1	7.6	9.8	14.8	10.0	6.6
Ni	15	14	14	20	10	9
Rb	50	115	120	90	115	120
Cs	1.3	3.2	8.9	2.8	3.9	7.0
Sr	600	600	575	690	590	265
Ba	650	650	600	500	540	505
La	20.7	25.4	19.5	16.8	18.3	17.6
Ce	46.7	40.6	39.1	35.1	37.0	33.4
Nd	23.0	18.9	18.7	18.4	18.2	16.8
Sm	4.33	3.52	3.34	3.44	3.16	3.26
Eu	1.00	0.66	0.71	0.73	0.78	0.62
Gd	4.9	4.7	3.9	4.0	3.8	3.3
Ho	0.8	0.6	0.7	0.6	0.6	0.8
Yb	1.5	1.2	1.3	1.2	1.2	2.2
Lu	0.20	0.18	0.22	0.17	0.22	0.35
ΣREE	103.13	95.76	87.47	80.44	83.26	78.33
Hf	6.3	4.1	5.3	4.7	5.9	5.0
Ta	0.48	0.66	0.65	0.43	0.69	0.35
Th	10.0	12.1	14.4	6.8	11.4	10.0
U	4.4	3.8	4.2	2.0	2.9	3.0

NOTE: Sc, Cr, Co, Cs, Ba, REE, Hf, Ta, Th and U were obtained by Instrumental Neutron Activation Analysis; Ni was obtained by Atomic Absorption; V by emission spectrography; Rb and Sr were obtained by x-ray fluorescence. All abundances are in ppm.

TABLE 14

Ni ABUNDANCE IN MINERALS FROM CENTRAL CHILE GRANITOIDS

	Sample	Type	<u>Feldspar - Qtz</u>			<u>Biotite</u>			<u>Amphibole</u>			<u>Magnetite</u>		Ni pred.	Ni Obs.	
			M% x ppm = ppm	A	C	M% x ppm = ppm	A	C	M% x ppm = ppm	A	C	A	C			
Coastal Batholith	G3	Qd	68	5	3.4	18	15	2.7	12	25	3.0	0.5	300	1.5	7.2-10.6	10
	G10	Ton	75	5	3.8	12	25	3.0	13	30	3.9	0.6	110	0.7	7.6-11.4	12
	G11	Ton	62	5	3.1	9	20	1.8	27	30	8.1	0.8	70	0.6	10.5-13.6	9
	G6	Gd	84	5	4.4	10	30	3.0	-	-	-	0.6	220	1.3	4.3-8.7	6
	G5	Gd	80	5	4.0	18	30	5.4	-	-	-	0.8	130	1.0	6.4-10.4	6
	G2	Gr	88	5	4.4	8	15	1.2	2	30	0.6	0.3	220	0.7	2.5-6.9	8
	G15	Gr	88	5	4.4	10	35	3.5	-	-	-	0.6	80	0.5	4.0-8.4	6
Central Batholith	G18	Ton	79	5	4.0	11	20	2.2	8	50	4.0	0.9	95	0.9	7.1-11.1	10
	G17	Qmd	84	5	4.2	-	-	-	12	50	6.0	1.7	85	1.5	7.5-11.7	11
	G13	Gd	76	5	3.8	17	30	5.1	6	40	2.4	0.4	80	0.3	7.8-11.6	11
	G12	Ton	82	5	4.1	6	25	1.5	10	40	4.0	1.2	160	1.9	7.4-11.5	10
Andean Batholith	G30	Qmd	85	5	4.3	-	-	-	13	85	11.1	1.3	160	2.1	13.2-17.5	15
	G22	Gd	81	5	4.1	3	70	2.1	12	75	9.0	1.5	120	1.8	12.9-17.0	14
	G25	Qmd	85	5	4.3	7	80	5.6	6	85	5.1	1.0	110	1.1	11.8-16.1	14
	G29	Qmd	82	5	4.1	-	-	-	17	95	16.2	1.4	210	2.9	19.1-23.2	20
	G26	Gd	81	5	4.1	7	70	4.9	8	80	5.6	1.6	85	1.4	11.9-16.0	10
	G27	Gd	83	5	4.2	7	45	3.2	6	65	3.9	1.3	90	1.2	8.3-12.5	9

M = Mineral Modal Abundance Expressed in wt%

A = Ni Abundance in the Mineral

C = Ni Contribution of the Mineral to the Ni Content of the Whole Rock

NOTE: The data were obtained by Atomic Absorption.

TABLE 15

Co CONTENT IN MINERALS FROM CENTRAL CHILE GRANITOIDS

	Sample	Type	<u>Feldspar - Qtz</u>			<u>Biotite</u>			<u>Amphibole</u>			<u>Magnetite</u>		Co pred.	Co obs.	
			M%	A x ppm	C =ppm	M%	A x ppm	C =ppm	M%	A x ppm	C = ppm	M%	A x ppm			C = ppm
Coastal Batholith	G3	Qd	68	5	3.4	18	35	5.0	12	40	4.8	0.5	40	0.2	13.4	15.3
	G10	Ton	75	5	3.8	12	40	4.8	12	40	4.8	0.8	50	0.4	13.8	12.6
	G11	Ton	62	5	3.1	9	50	0.5	27	30	8.1	0.8	60	0.5	9.1-12.2	10.2
	G6	Gd	84	5	4.4	10	45	4.5	-	-	-	0.6	50	0.3	9.2	5.0
	G5	Gd	80	5	4.0	18	40	7.2	-	-	-	0.8	50	0.4	7.6-11.6	6.9
	G2	G	88	5	4.4	8	30	2.4	2	30	0.6	0.3	40	0.1	7.5	4.2
	G15	G	88	5	4.4	10	45	4.5	-	-	-	0.6	50	0.3	4.8-9.2	4.1
Central Batholith	G18	Ton	70	5	4.0	11	55	5.5	8	35	2.8	0.9	55	0.5	8.8-12.8	13.4
	G17	Qmd	84	5	4.2	-	-	-	12	50	6.0	1.7	40	0.7	6.7-10.9	12.6
	G13	Gd	76	5	3.8	17	45	7.7	6	30	1.8	0.4	45	0.2	9.7-13.5	17.0
	G12	Ton	82	5	4.1	6	30	1.8	10	35	3.5	1.2	45	0.5	9.9	4.2
Andean Batholith	G30	Qmd	85	5	4.3	-	-	-	13	40	5.2	1.3	45	0.6	5.8-10.1	8.1
	G22	Gd	81	5	4.1	3	40	1.2	12	35	4.2	1.5	55	0.8	6.2-10.3	7.6
	G25	Qmd	85	5	4.3	7	80	5.6	6	35	3.3	1.0	70	0.7	9.6-13.9	9.8
	G29	Qmd	82	5	4.1	-	-	-	17	50	8.5	1.4	60	0.8	9.3-13.4	14.8
	G26	Gd	81	5	4.1	7	60	4.2	8	50	4.0	1.6	65	1.0	9.2-13.3	10.0
	G27	Gd	83	5	4.2	7	40	2.8	6	40	2.4	1.3	60	0.8	6.0-10.2	6.6

M = Mineral Model Abundance Expressed in wt%

A = Ni Abundance in the Mineral

C = Ni Contribution of the Mineral to the Ni Content of the Whole Rock

NOTE: The data were obtained by Atomic Absorption except for the data in the last column.

TABLE 16

Cr ABUNDANCE IN MINERALS FROM CENTRAL CHILE GRANITOIDS

	Sample	Type	Feldspar - Qtz			Biotite			Amphibole			Magnetite			Cr pred.	Cr obs.
			M% x	A ppm	C =ppm	M%	A ppm	C ppm	M%	A ppm	C ppm	M%	A ppm	C ppm		
Coastal Batholith	G3	Qd	68	5	3.4	18	10	1.8	12	50	6.0	0.5	500	2.5	13.7	18
	G10	Ton	75	5	3.8	12	25	3.0	12	50	6.0	0.6	500	3.0	12.0-15.8	11
	G11	Ton	62	5	3.1	9	20	1.8	27	35	9.5	0.8	300	2.4	13.7-16.8	11
	G6	Gd	84	5	4.4	10	80	8.0	-	-	-	0.6	600	3.6	11.6-16.0	16
	G5	Gd	80	5	4.0	18	45	8.1	-	-	-	0.8	450	3.0	11.1-15.1	19
	G2	Gr	88	5	4.4	8	30	2.4	2	70	1.4	0.3	600	1.8	5.6-10	10
Central Batholith	G15	Gr	88	5	4.4	10	80	8.0	-	-	-	0.6	400	2.4	10.4-14.8	9
	G18	Ton	79	5	4.0	11	25	2.8	8	40	3.2	0.9	350	3.2	13.2	18
	G17	Qmd	84	5	4.2	-	-	-	12	70	8.4	1.7	300	5.1	13.5-17.7	17
	G13	Gd	76	5	3.8	17	35	6.0	6	95	5.7	0.4	600	2.4	14.1-17.9	17
	G12	Ton	82	5	4.1	6	70	4.2	10	130	13	1.2	350	4.2	25.5	18
Andean Batholith	G30	Qmd	85	5	4.3	-	-	-	13	90	11.7	1.3	500	6.5	18.2-22.5	30
	G22	Gd	81	5	4.1	3	70	2.1	12	80	9.6	1.5	500	7.5	19.2-23.3	41
	G25	Qmd	85	5	4.3	7	75	4.3	6	85	5.1	1.0	600	6.0	15.4-19.7	22
	G29	Qmd	89	5	4.1	-	-	-	17	90	15.3	1.4	700	9.8	25.1-29.2	33
	G26	Gd	81	5	4.1	7	70	4.9	8	65	5.2	1.6	400	6.4	16.5-20.6	18
	G27	Gd	83	5	4.2	7	75	5.3	6	90	5.4	1.3	400	5.2	15.9-20.1	17

M = Mineral Model Abundance Expressed in wt%

A = Ni Abundance in the Mineral

C = Ni Contribution of the Mineral to the Ni Content of the Whole Rock

NOTE: The data were obtained by Atomic Absorption except for the data in the last column.

This was obtained by INAA.

TABLE 17

PETROGENETICALLY SIGNIFICANT ELEMENT RATIOS

	COASTAL BATHOLITH						CENTRAL BATHOLITH				
	<u>G3</u>	<u>G10</u>	<u>G11</u>	<u>G6</u>	<u>G5</u>	<u>G2</u>	<u>G15</u>	<u>G18</u>	<u>G17</u>	<u>G13</u>	<u>G12</u>
	<u>Qd</u>	<u>Ton</u>	<u>Ton</u>	<u>Gd</u>	<u>Gd</u>	<u>Gd</u>	<u>Gd</u>	<u>Ton</u>	<u>Qmd</u>	<u>Gd</u>	<u>Ton</u>
Eu/Eu*	0.91	0.68	0.77	0.67	0.67	0.72	0.60	0.83	0.68	0.66	0.79
K/Rb	290	326	367	258	208	483	204	309	280	127	333
Rb/Sr	0.09	0.11	0.10	0.24	0.22	0.20	0.35	0.10	0.18	0.20	0.03
K/Sr	26.1	35.9	36.7	61.9	45.8	96.6	71.4	30.9	50.4	25.4	10.0
K/Cs x 10 ⁻⁴	0.78	0.66	0.69	0.74	1.14	3.87	0.95	0.48	1.19	0.24	0.37
K ₂ O/K ₂ O + Na ₂ O	0.23	0.30	0.25	0.41	0.44	0.38	0.48	0.30	0.43	0.26	0.10
K ₂ O/CaO	0.18	0.42	0.53	0.83	0.95	0.78	1.42	0.26	0.67	0.41	0.06
Na ₂ O/CaO	0.60	0.99	1.63	1.19	1.20	1.27	1.57	0.59	0.89	1.14	0.52
K ₂ O/Na ₂ O	0.31	0.42	0.33	0.70	0.79	0.62	0.91	0.44	0.75	0.36	0.11
Na ₂ O + K ₂ O/CaO	0.78	1.41	2.16	2.02	2.15	2.05	2.99	0.85	1.56	1.55	0.58
Na ₂ O + K ₂ O/FeO	0.84	2.31	1.34	3.34	3.25	1.95	5.11	1.54	2.52	1.01	2.42
MgO/MgO + ΣFeO	0.31	0.43	0.27	0.38	0.43	0.17	0.40	0.46	0.40	0.27	0.67
Th/U	4.1	5.4	5.1	1.9	6.4	3.9	10.6	4.4	5.1	5.4	4.1
La/Yb	8.4	7.0	5.4	18.4	16.6	3.8	21.2	5.8	6.4	7.7	3.5
Ba/Rb	6.6	8.7	11.5	4.9	5.5	4.1	4.6	8.1	10.4	6.1	15.0
Ba/Sr	0.6	1.0	1.2	1.2	1.2	0.8	1.6	0.8	1.9	1.2	0.4

TABLE 17 (continued)

PETROGENETICALLY SIGNIFICANT ELEMENT RATIOS

	COASTAL BATHOLITH						CENTRAL BATHOLITH				
	<u>G3</u>	<u>G10</u>	<u>G11</u>	<u>G6</u>	<u>G5</u>	<u>G2</u>	<u>G15</u>	<u>G18</u>	<u>G17</u>	<u>G13</u>	<u>G12</u>
	<u>Qd</u>	<u>Ton</u>	<u>Ton</u>	<u>Gd</u>	<u>Gd</u>	<u>Gd</u>	<u>Gd</u>	<u>Ton</u>	<u>Qmd</u>	<u>Gd</u>	<u>Ton</u>
Kr/Ca	83	133	169	157	240	94	232	71	154	186	82
Ra/Cs	177	178	216	141	302	330	213	126	440	114	167
R/Na	0.35	0.47	0.37	0.78	0.88	0.69	1.02	0.49	0.84	0.40	0.12
$\Sigma\text{FeO}^*/\text{MgO}$	3.78	2.4	5.52	3.12	2.68	6.15	3.61	2.20	2.84	5.24	0.74
$\text{Fe}_2\text{O}/\text{SiO}_2$	0.02	0.03	0.02	0.04	0.04	0.03	0.05	0.03	0.05	0.02	0.01

ΣFeO^* equal total iron expressed as FeO.

TABLE 17 (continued)

PETROGENETICALLY SIGNIFICANT ELEMENT RATIOS

	ANDEAN BATHOLITH					
	<u>G30</u>	<u>G22</u>	<u>G25</u>	<u>G29</u>	<u>G26</u>	<u>G27</u>
	<u>Qmd</u>	<u>Gd</u>	<u>Qmd</u>	<u>Qmd</u>	<u>Gd</u>	<u>Gd</u>
Eu/Eu*	0.66	0.50	0.60	0.60	0.69	0.48
K/Rb	457	239	217	266	193	216
Rb/Sr	0.08	0.19	0.21	0.13	0.19	0.45
K/Sr	36.6	45.4	45.6	34.6	36.7	97.2
K/Cs x 10 ⁻⁴	1.76	0.86	0.29	0.85	0.57	0.37
K ₂ O/K ₂ O + Na ₂ O	0.32	0.39	0.39	0.39	0.35	0.45
K ₂ O/CaO	0.61	1.05	0.96	1.47	1.94	1.10
Na ₂ O/CaO	1.30	1.63	1.48	2.31	3.63	1.33
K ₂ O/Na ₂ O	0.47	0.64	0.65	0.64	0.54	0.83
Na ₂ O + K ₂ O/CaO	1.77	2.27	2.13	2.95	4.17	2.16
Na ₂ O + K ₂ O/FeO	2.71	3.43	3.42	3.65	3.65	3.16
MgO/MgO + Σ FeO	0.50	0.40	0.44	0.30	0.36	0.29
Th/U	2.3	3.2	3.4	3.4	3.9	3.3
La/Yb	13.8	21.2	15.0	14.0	15.3	8.0
Ba/Rb	13.0	5.7	5.0	5.6	4.7	4.2
Ba/Sr	1.1	1.1	1.0	0.7	0.9	1.9

TABLE 17 (continued)

PETROGENETICALLY SIGNIFICANT ELEMENT RATIOS

	ANDEAN BATHOLITH					
	<u>G30</u>	<u>G22</u>	<u>G25</u>	<u>G29</u>	<u>G26</u>	<u>G27</u>
	<u>Qmd</u>	<u>Gd</u>	<u>Qmd</u>	<u>Qmd</u>	<u>Gd</u>	<u>Gd</u>
Sr/Ca	186	266	245	495	603	131
Ba/Cs	500	203	67	179	138	72
K/Na	0.53	0.72	0.73	0.72	0.60	0.93
$\Sigma\text{FeO}^*/\text{MgO}$	1.86	2.42	2.22	3.92	5.86	3.78
$\text{K}_2\text{O}/\text{SiO}_2$	0.04	0.05	0.05	0.04	0.04	0.04

ΣFeO^* equals total iron expressed as FeO.

TABLE 18

MINERALOGICAL RELATIONSHIPS BETWEEN SAMPLES G10 (TONALITE)
AND G6 (GRANODIORITE)

	<u>G10(%)</u>	<u>Subtracting(%)</u>	<u>Result(%)</u>	<u>G6</u>
Quartz	18.6	.	29.9	29.6
Feldspar	56.7	20	59.0	59.2
Biotite	12.0	55	10.5	10.6
Amphibole	12.0	12	0	0
Magnetite	0.6	0.23	0.6	0.6

TABLE 19

FRACTIONAL CRYSTALLIZATION MODEL (MAJOR ELEMENTS) FOR THE
TRANSITION G10 (TONALITE) TO G6 (GRANODIORITE)

	<u>G10(%)</u>	0.2 <u>An30(%)</u>	0.06 <u>BiO</u>	0.12 <u>Hb</u>	0.005 <u>Mt</u>	0.001 <u>Ap</u>	<u>Result(%)</u>	<u>G6</u>
SiO ₂	61.4	61.0	38.8	48.0			67.4	67.8
Al ₂ O ₃	17.1	24.7	22.1	8.7			16.2	15.7
FeO*	5.4		19.4	15.3	100		3.1	3.3
MgO	2.3		7.6	12.9			0.5	1.1
CaO	5.2	6.0	0.6	12.2		54.0	3.9	3.5
Na ₂ O	5.1	8.3	0.3	1.3			5.2	4.2
K ₂ O	2.2		7.4	0.5			2.8	2.9
TiO ₂	0.65		2.7	1.0			0.6	0.5
P ₂ O ₅	0.23		1.0	0.1		46.0	0.18	0.18

FeO* is total Fe expressed as FeO. The sources of the chemical composition for plagioclase (An 30) biotite and hornblende are given in the text. The number preceding each mineral (for example, 0.2 for An 30) indicates the weight fraction of the initial magma that must fractionate as that mineral. The column Result(%) contains the major element composition predicted by the model. This table also contains the composition of sample G6 approximated to the first decimal.

TABLE 20

FRACTIONAL CRYSTALLIZATION MODEL (MAJOR ELEMENTS)
FOR THE TRANSITION G10 (TONALITE) TO G15 (GRANITE)

	<u>G10(%)</u>	0.26 <u>An30(%)</u>	0.12 <u>Hb</u>	0.064 <u>BiO</u>	0.01 <u>Mt</u>	0.001 <u>Ap</u>	<u>Result(%)</u>	<u>G15</u>
SiO ₂	61.4	61.0	48.0	38.8			69.0	73.0
Al ₂ O ₃	17.1	24.7	8.7	22.1			15.1	14.3
FeO*	5.4		15.3	19.4	100		2.4	2.4
MgO	2.3		12.9	7.6			0.6	0.6
CaO	5.2	6.0	12.2	0.6		54.0	3.7	2.4
Na ₂ O	5.1	8.3	1.3	0.3			5.2	3.8
K ₂ O	2.2		0.5	7.4			3.1	3.4
TiO ₂	0.65		1.0	2.7			0.66	0.40
P ₂ O ₅	0.23		0.1	1.0		46.0	0.18	0.16

FeO* is total Fe expressed as FeO. The sources of chemical composition for plagioclase (An 30), biotite and hornblende are given in the text. The number preceding each mineral (for example 0.26 for An 30) indicates the weight fraction of the initial magma that must fractionate as that mineral. The column Result(%) contains the major element composition predicted by the model. This table also contains the composition of sample G15 approximated to the first decimal.

TABLE 21

CHEMICAL COMPARISON BETWEEN COASTAL BATHOLITH TONALITES AND TEMUCO ANDESITES

	COASTAL BATHOLITH TONALITES			TEMUCO ANDESITES			
	G3	G10	G11	T2	T3	T9	T13
SiO ₂	58.70	61.44	67.35	58.56	60.53	60.39	61.35
Al ₂ O ₃	19.18	17.14	16.24	17.21	17.74	17.99	17.37
Fe ₂ O ₃	0.40	2.54	1.84	2.69	2.89	4.13	3.31
FeO	6.18	3.15	4.02	3.61	2.75	1.92	2.43
MgO	1.73	2.27	1.03	4.75	3.38	3.43	3.62
CaO	6.65	4.14	2.48	6.89	6.86	5.93	5.48
Na ₂ O	3.98	5.12	4.06	3.79	3.35	4.05	4.10
K ₂ O	1.22	2.15	1.32	1.42	1.59	1.25	1.43
TiO ₂	1.04	0.65	0.78	0.79	0.71	0.66	0.59
P ₂ O ₅	0.30	0.23	0.23	0.14	0.11	0.09	0.10
MnO	0.12	0.12	0.12	0.15	0.08	0.14	0.22
ΣFe as FeO	6.54	5.44	5.69	6.03	5.35	5.64	5.41
Sc	26.7	15.7	17.9	22	19	22	17
Cr	18	11	11	73	32	56	73
Co	15.3	12.6	10.2	23	13	24	16
Ni	10	12	9	20	-	-	20
Rb	35	55	30	35	-	-	35
Sr	395	490	300	350	-	-	420
Ba	230	480	345	269	556	217	322
Hf	4.1	5.8	5.3	2.8	5.1	2.6	3.8
Ta	0.88	0.38	0.41	0.3	0.5	0.2	0.4
Th	6.2	13.0	3.6	3.1	6.2	2.6	3.1

TABLE 21 (continued)

CHEMICAL COMPARISON BETWEEN COASTAL BATHOLITH TONALITES AND TEMUCO ANDESITES

	<u>COASTAL BATHOLITH TONALITES</u>			<u>TEMUCO ANDESITES</u>			
	<u>G3</u>	<u>G10</u>	<u>G11</u>	<u>T2</u>	<u>T3</u>	<u>T9</u>	<u>T13</u>
U	1.5	2.4	0.7	1.1	1.7	1.0	0.7
La	21.0	18.2	15.8	9.96	21.78	9.49	11.17
Ce	47.5	43.0	32.2	23.11	41.63	21.89	26.21
Nd	23.8	26.1	19.4	13.22	21.77	11.70	13.38
Sm	4.53	5.01	4.05	2.78	4.37	2.46	2.82
Eu	1.61	1.18	1.09	0.84	1.22	0.77	0.75
Gd	6.6	5.7	4.7	2.68	5.35	2.64	3.12
Ho	1.1	1.0	1.1	0.71	0.90	0.60	0.60
Yb	2.5	2.6	2.9	1.84	2.4	1.54	1.45
Lu	0.41	0.40	0.45	0.30	0.38	0.23	0.24
K/Rb	290	326	367	338	-	-	340
Rb/Sr	0.09	0.11	0.10	0.10	-	-	0.08
K/Sr	26.1	35.9	36.7	33.8	-	-	27.2
MgO/MgO + Σ FeO	0.31	0.43	0.27	0.58	0.53	0.52	0.54
K ₂ O/K ₂ O + Na ₂ O	0.23	0.30	0.25	0.27	0.32	0.24	0.26
Th/U	4.1	5.4	5.1	2.8	3.6	2.6	4.4
Ni/Co	0.7	1.0	0.9	0.9	-	-	1.3
K/Na	0.34	0.47	0.36	0.42	0.53	0.35	0.39

TABLE 22

FRACTIONAL CRYSTALLIZATION MODEL (MAJOR ELEMENTS) FOR THE
TRANSITION T2 (TEMUCO ANDESITE) TO T3 (TEMUCO ANDESITE)
AND G10 (COASTAL BATHOLITH TONALITE)

	<u>T2</u>	<u>0.10 Cpx</u>	<u>0.10 An40</u>	<u>Result(%)</u>	<u>T3</u>	<u>G10</u>
SiO ₂	58.6	52	58.5	60.0	60.0	61.4
Al ₂ O ₃	17.2	2.1	26.4	18.0	17.0	17.1
FeO*	6.0	7.3		6.6	5.3	5.4
MgO	4.8	19.5		3.6	3.5	2.3
CaO	6.9	18.6	8	5.3	5.4	5.2
Na ₂ O	3.8		7.1	3.9	4.0	5.2
K ₂ O	1.4			1.8	1.4	2.2
TiO ₂	0.8	0.2		1.0	0.6	0.7
P ₂ O ₅	0.1			0.13	0.2	0.2
MnO	0.2	0.3		0.21	0.1	0.1

FeO* is total Fe expressed as FeO. The source of the chemical composition used for clinopyroxene (Cpx) and plagioclase (pl) are given in the text. The number preceding each mineral (0.10 for Cpx and 0.10 for Pl) indicates the weight fraction of the initial magma that must fractionate as that mineral. The column Result(%) contains the major element composition predicted by the model. This table also contains the major element composition of sample T2 and G10 approximated to the first decimal. The FeO*/MgO of the clinopyroxene was modified according to the following relation $(\text{FeO}^*/\text{MgO})_{\text{cpx}}/(\text{FeO}^*/\text{MgO})_{\text{T2}} = 0.3$ (Roeder and Emslie, Contr. Minera Petrol., 29 (1970) 275-289).

TABLE 23

COMPARISON BETWEEN MAJOR AND REE OF THE TUPUNGATO SAMPLE (ANDEAN VOLCANIC, LATITUDE~33°15'S) AND SAMPLE G30 (ANDEAN PLUTONIC, LATITUDE~33°07')*

	<u>797 Tupungato</u>	<u>G30</u>		<u>797 Tupungato</u>	<u>G30</u>	<u>Marmolejo</u>
SiO ₂	61.23	61.35	La	19.1	20.7	26.4
Al ₂ O ₃	16.61	16.88	Ce	36.4	46.7	51.8
FeO*	4.71	4.60	Nd	17.9	23.0	26.9
MgO	3.25	2.47	Sm	3.51	4.33	4.74
CaO	4.48	4.51	Eu	0.98	1.00	1.04
Na ₂ O	5.05	5.85	Gd	4.6	4.9	6.1
K ₂ O	2.11	2.74	Ho	0.5	0.8	0.6
TiO ₂	0.79	0.92	Yb	1.1	1.5	1.6
MnO	0.09	0.09				
P ₂ O ₅	0.21	0.27				

*Note: This table also includes the REE for a sample from the Marmolejo Volcano (latitude~33°40'). The Marmolejo sample was analyzed only for REE.

TABLE 24

COMPARISON BETWEEN COASTAL BATHOLITH GRANODIORITES AND
ANDEAN BATHOLITH GRANODIORITES

	<u>Coastal bath. Gd.</u>	<u>Andean bath. Gd.</u>		<u>Coastal bath. Gd.</u>	<u>Andean bath. Gd.</u>
SiO ₂	67.8 - 68.8	66.1 - 69.7	Sc	5.9 - 6.4	7.5 - 8.7
Al ₂ O ₃	15.7 - 16.3	14.8 - 16.5	V	32 - 37	70 - 120
FeO*	2.9 - 3.3	3.7 - 4.7	Cr	16 - 19	17 - 41
MgO	1.05 - 1.08	0.8 - 1.7	Co	5 - 7	6.6 - 10
CaO	3.2 - 3.5	1.4 - 3.2	Ni	6	9 - 14
Na ₂ O	3.8 - 4.2	3.8 - 5.2	Rb	95 - 120	115 - 120
K ₂ O	2.9 - 3.0	2.7 - 3.3	Cs	2.2 - 3.3	3.2 - 7.0
TiO ₂	0.48	0.53 - 0.70	Sr	395 - 540	265 - 600
P ₂ O ₅	0.16 - 0.18	0.11 - 0.23	Ba	465 - 665	505 - 650
MnO	0.08 - 0.12	0.06 - 0.12	La	25.7 - 26.5	17.6 - 25.4
			Ce	44.3 - 49.5	33.4 - 40.6
			Nd	18.4 - 23.4	16.8 - 18.9
			Sm	3.16 - 3.72	3.16 - 3.52
			Eu	0.79 - 0.95	0.62 - 0.73
			Gd	4.1 - 5.1	3.3 - 4.7
			Ho	0.6 - 0.8	0.6 - 0.8
			Yb	1.4 - 1.6	1.2 - 2.2
			Lu	0.19 - 0.22	0.18 - 0.35
			Hf	3.9 - 4.1	4.1 - 5.9
			Ta	0.7 - 1.1	0.35 - 0.69
			Th	12.2 - 9.6	10 - 12.1
			U	6.3 - 1.5	2.9 - 3.8

TABLE 25

TRACE ELEMENT COMPARISON BETWEEN CENTRAL-CHILE GRANITOIDS,
 AVERAGE CIRCUMPACIFIC ANDESITES (Taylor, 1969),
 SIERRA NEVADA PLUTONIC ROCKS (Dodge, 1972)
 AND AVERAGE CIRCUMPACIFIC GRANODIOTITES (Taylor, 1969)

	Average Coastal Batholith Tonalites	Average Coastal Batholith Granodiorites	Average Central Batholith (G2 not included)	Average Andean Batholith	Average Circumpacific Andesites	Average Sierra Nevada Plutonic	Average Circumpacific Granodiorites
Sc	20	6.2	19	9	30	5-100	14
V	75	35	100	110	175	10-1500	75
Cr	13	18	17	27	56	1-1500	30
Co	13	6	14	10	24	5-100	10
Ni	10	6	11	14	18	5-700	15
Rb	40	108	68	102	31	20-270	110
Cs	2	2.8	3	5	0.5-1	-	4
Sr	395	470	435	550	385	10-2000	440
Ba	350	570	570	570	270	20-3000	500
La	18	26	18	20	12	30-150	36
Ce	41	47	38	40	24	200-700	47
Nd	23	21	22	19	13	100-150	26
Sm	4.5	3.4	4.5	3.5	2.9	-	6.8
Eu	1.3	0.9	1.1	0.8	1.0	-	1.2
Gd	6.0	4.6	5.3	4.0	3.3	-	7.4
Ho	1.1	0.7	1.1	0.7	0.7	-	1.6
Yb	2.7	1.0	2.7	1.4	1.9	1-7	3.6
Lu	0.4	0.7	0.4	0.2	-	-	-
Ta	0.6	0.9	0.6	0.5	-	-	-
Hf	5.1	4.0	5.2	5.2	2.3	-	3
Th	8	11	10	11	2.2	0.2-50.1	10
U	1.5	3.9	2.0	3.4	0.7	0.3-29.6	2.7

TABLE 26

COMPARISON BETWEEN CRETACEOUS AND TERTIARY ANDESITES*

	<u>Lower Cretaceous</u>	<u>Upper Cretaceous</u>	<u>Lower Tertiary</u>
SiO ₂	54.19	56.78	58.16
Al ₂ O ₃	17.90	17.89	18.15
Fe ₂ O ₃	5.05	5.14	3.84
FeO	4.51	3.92	3.60
CaO	6.10	5.28	6.08
MgO	3.66	2.89	3.02
Na ₂ O	4.22	4.76	4.27
K ₂ O	2.56	1.15	1.54
TiO ₂	0.99	0.95	0.79
MnO	0.24	0.19	0.34
P ₂ O ₅	0.34	0.27	0.14
	<u>Cretaceous</u>	<u>Tertiary</u>	
Ni (ppm)	24	18	
Co (ppm)	18	18	
Rb (ppm)	70	63	

* Data from Oyarzun (1971), and Vergara (1972).

TABLE 27
COUNTING SCHEDULE

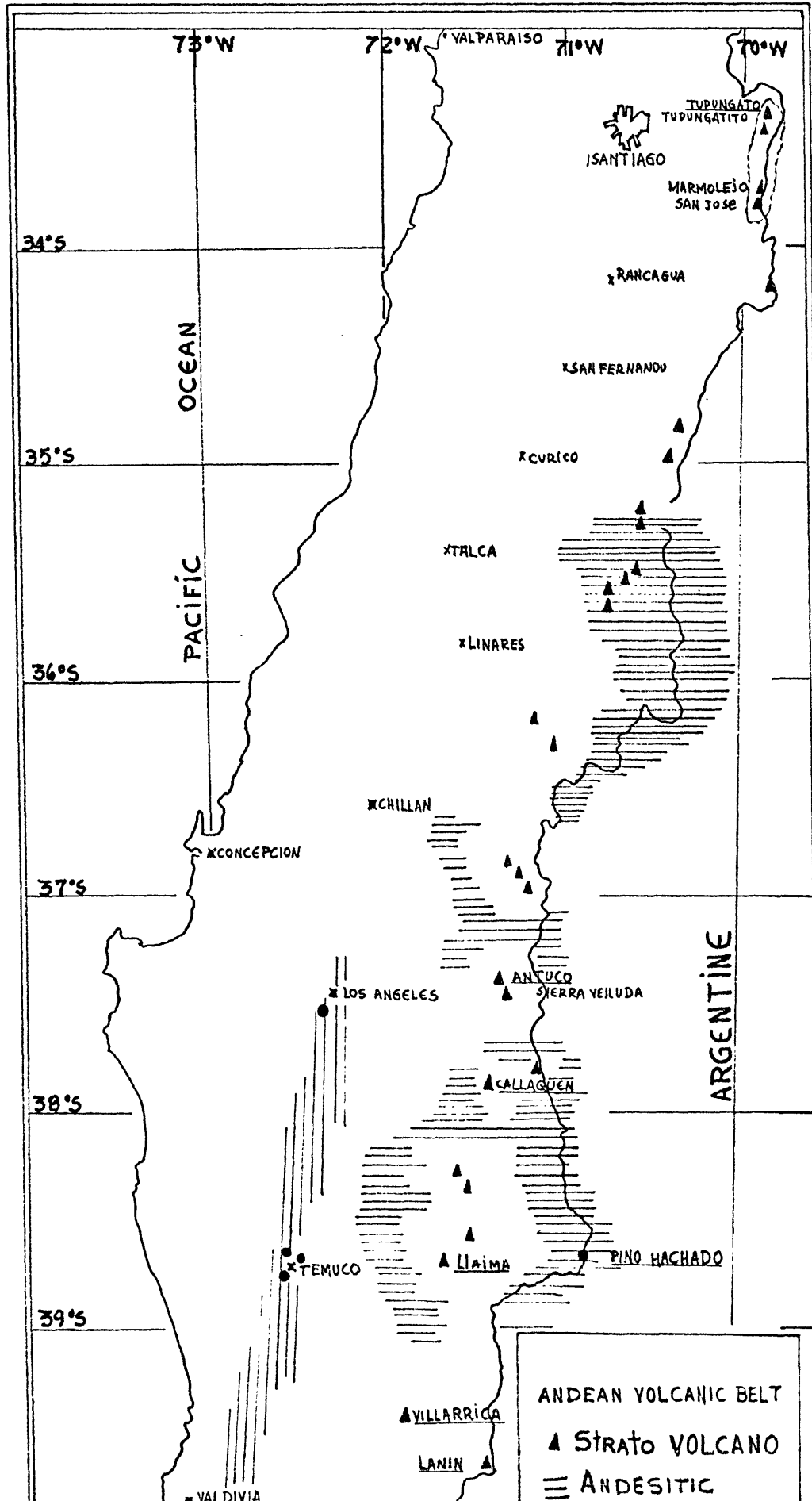
<u>Decay Time</u>	<u>Detector</u>	<u>Element</u>	<u>Photopeak Used (KeV)</u>
5ds	LEPS	Ho	80.6
		Sm	103.2
		U	106.3
8ds	18cc	Lu	208
		Yb	283
		La	328.8;487.0;1596.5
		Ba	496.3
15ds	LEPS	Nd	91.1
		Gd	97.4
		Ta	100.1
		Eu	121.9
		Hf	133.0
		Ce	145.5
30ds	18cc	Th	312.9
		Cr	320.1
		Cs	604.6
		Sc	889.3
		Ta	1221.4
		Co	1332.5
		Eu	1407.9

TABLE 28
CALIBRATION PEAKS USED IN INAA

<u>Detector</u>	<u>Standard</u>	<u>E(keV)</u>	<u>(Rel. Int)</u>	
LEPS	^{241}Am	13.90	(2.75)	
		17.75	(49.5)	
		20.80	(12.8)	
		26.36	(7.5)	
		59.57	(100)	
18 cc	^{152}Eu	121.9		
		244.7		
		344.4		
	^{137}Cs	661.6		
		^{152}Eu	121.8	
			244.7	
			344	
			444.2	
			965	
			1087	
	1113			
	1408			
	^{54}Mn	843.8		
^{139}Ce		165.8		

Figure 1: Sample localities on a sketch map of Upper Cenozoic volcanics in central-south Chile, modified from Vergara (1974) and Moreno (1974a).

FIGURE 1 (TOP)



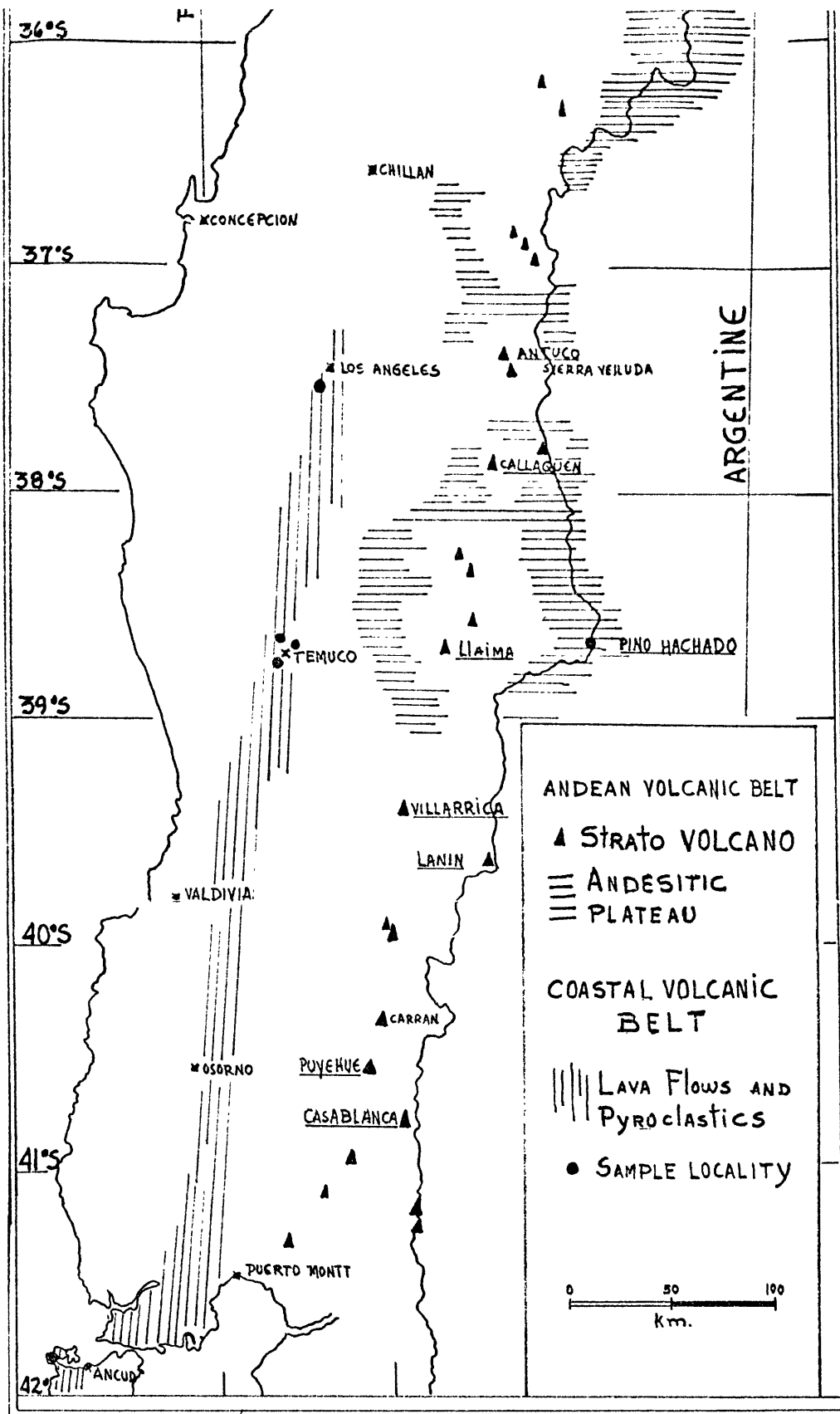


Figure 1 (BOTTOM)

Figure 2: FMA diagram (wt%) with total iron calculated as FeO. Solid lines represent general limits of Japanese hypersthene (calc-alkaline) series (Kuno, 1968a). Open circles are for calc-alkaline rocks from central-south Chile (Klerkx, 1965; Vergara and Katsui, 1969; Oyarzun, 1971). Other symbols represent samples of this study.

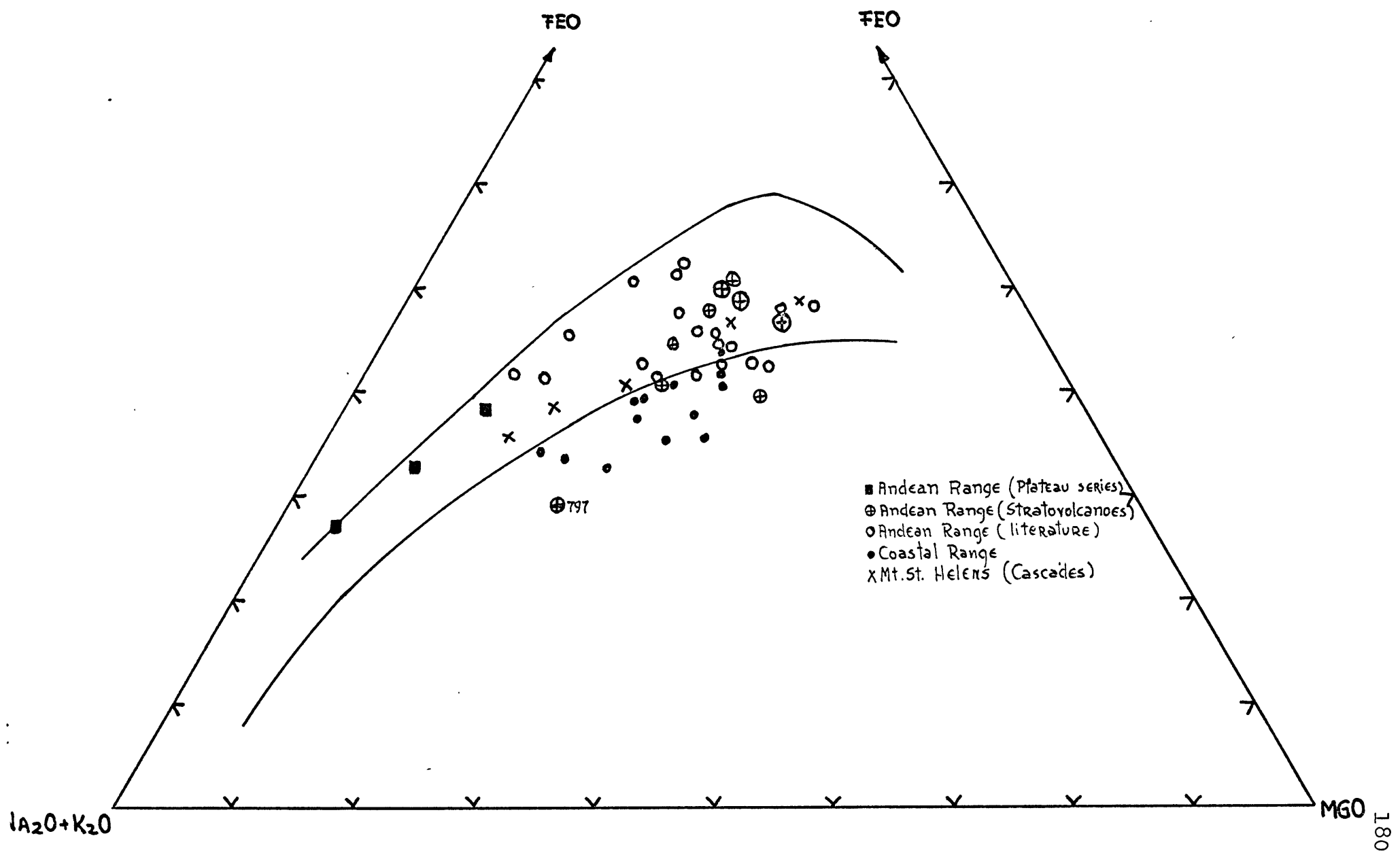


Figure 2

Figure 3: Total alkalis versus silica plot. Dotted lines represent boundaries of high-alumina basalt series (Kuno, 1966). Solid lines are proposed boundaries between alkaline and subalkaline suites (Irvine and Baragar, 1971; MacDonald, 1968). Data symbols as in Figure 2.

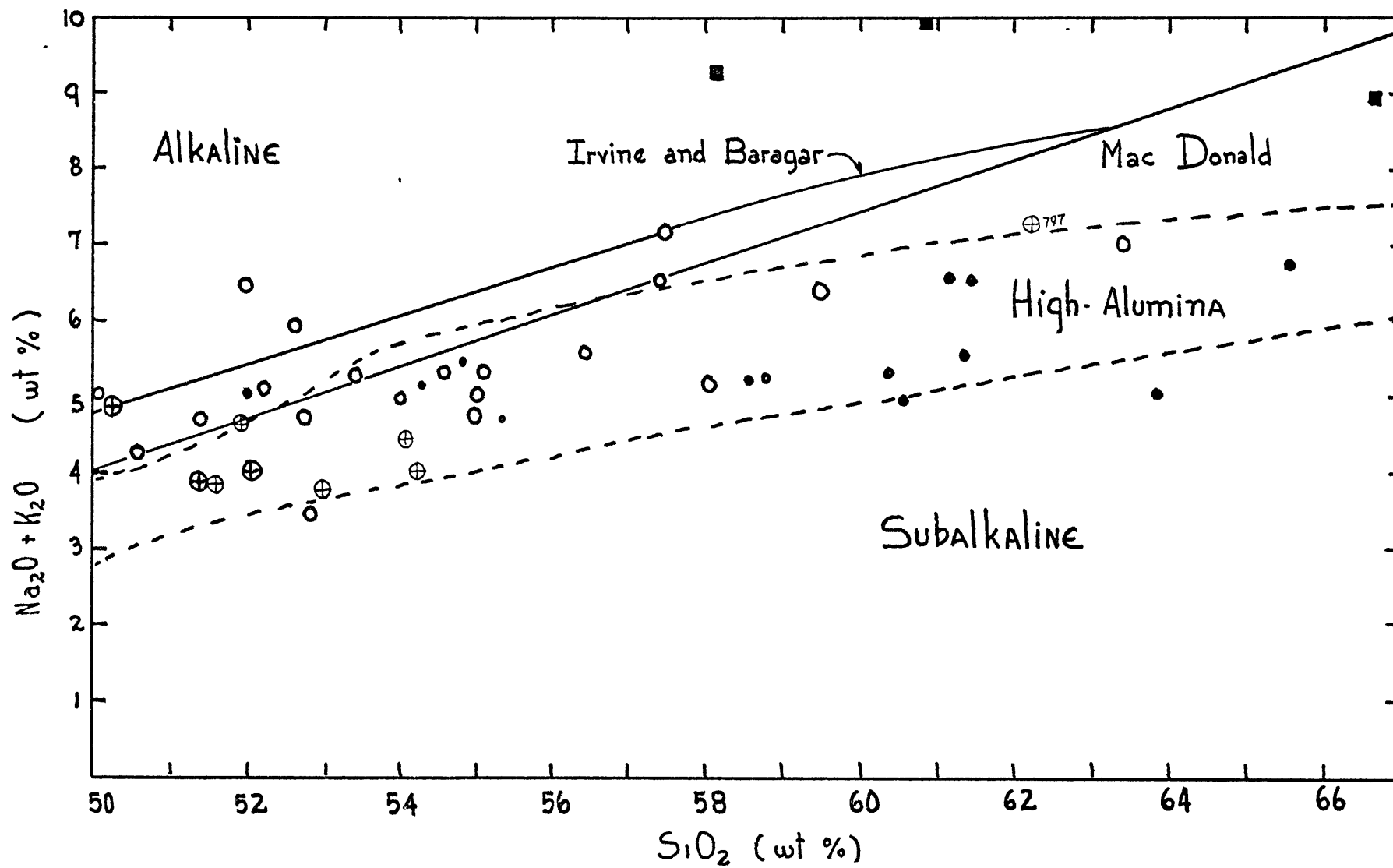


Figure 3

Figure 4: Al_2O_3 versus normative plagioclase composition (% An). Solid line from Irvine and Baragar (1971) separates volcanic rocks into tholeiitic field (below line) and calc-alkaline field (above line). Symbols for calc-alkaline rocks as in Figure 2. Data for Nazca Plate and Chile Rise from Paster (1968) and Hekinian (1971). Dotted lines connect data for core (C) and altered margin (M) pairs from basalt fragments (Hekinian, 1971). Abundances from central Chile plutonic rocks are also included (Lopez-Escobar and Oyarzun, 1974)

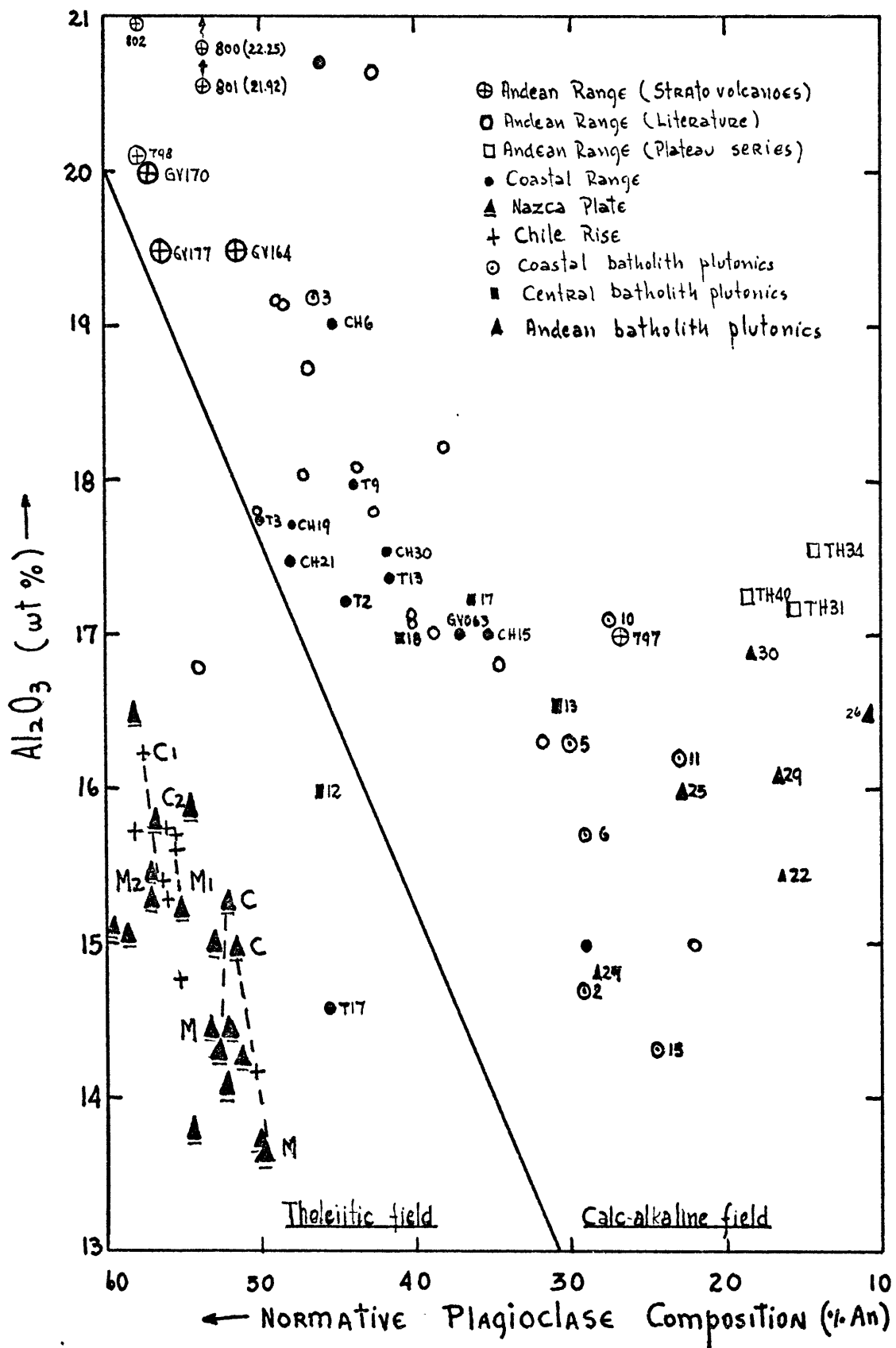


Figure 4

Figure 5: Normative color index (sum of normative pyroxene + olivine + opaques) versus normative plagioclase composition (% An) illustrating subdivision of calc-alkaline rocks into basalts, andesites and dacites. Field boundaries from Irvine and Baragar (1971). Data symbols as in Figure 2.

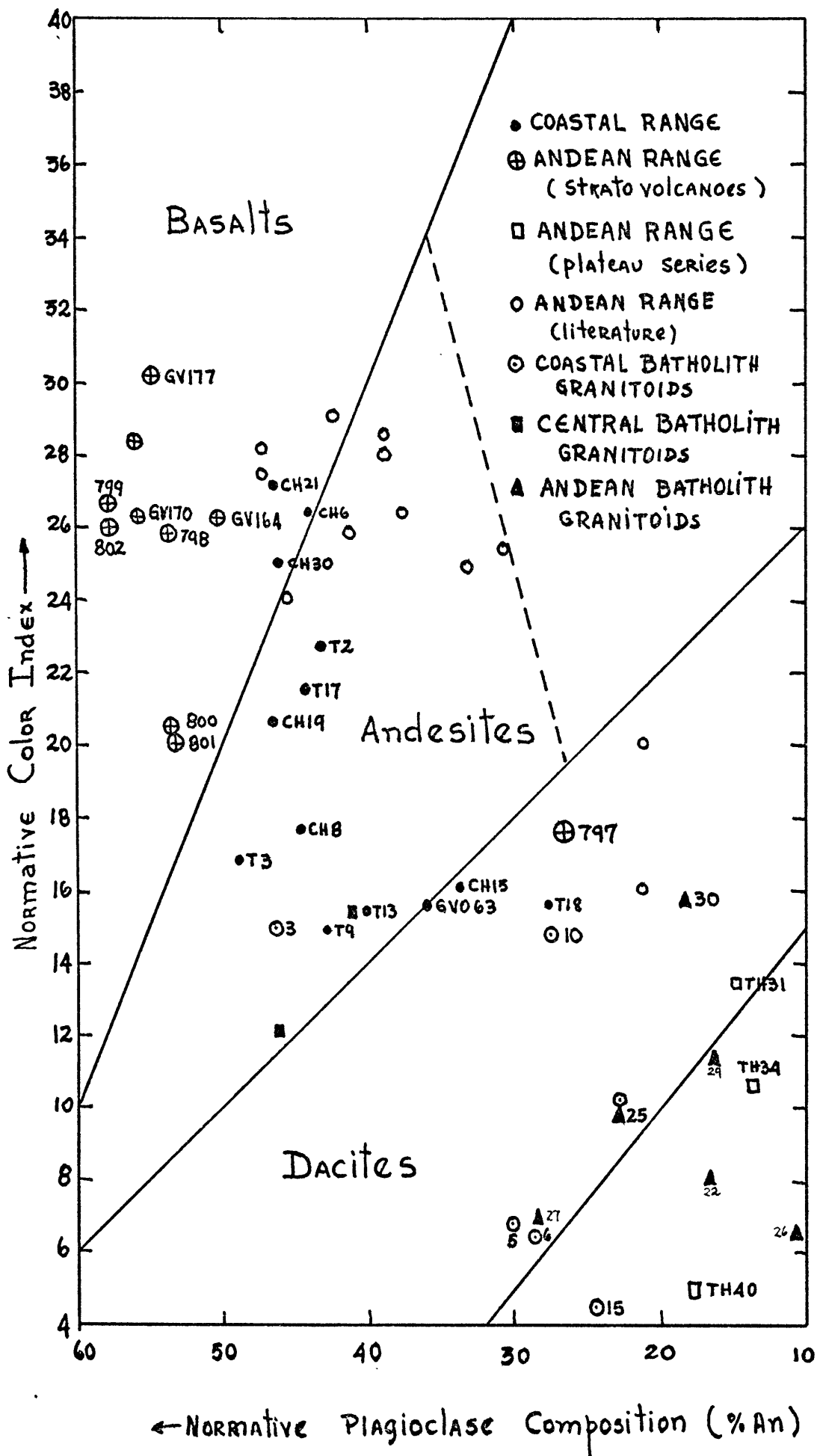


Figure 5

Figure 6: Rare-earth element abundances normalized to a chondritic average (Frey et al., 1968). Average circumpacific andesite and average low-silica andesite from Taylor (1969). a) Ancud samples. b) Temuco samples. Data for rare-earth element range in Nazca Plate and Chile Ridge from Schilling (1971), Schilling and Bonatti (1974), and Frey (unpublished). T3 is the most differentiated Temuco andesite. c) Los Angeles dacite samples.

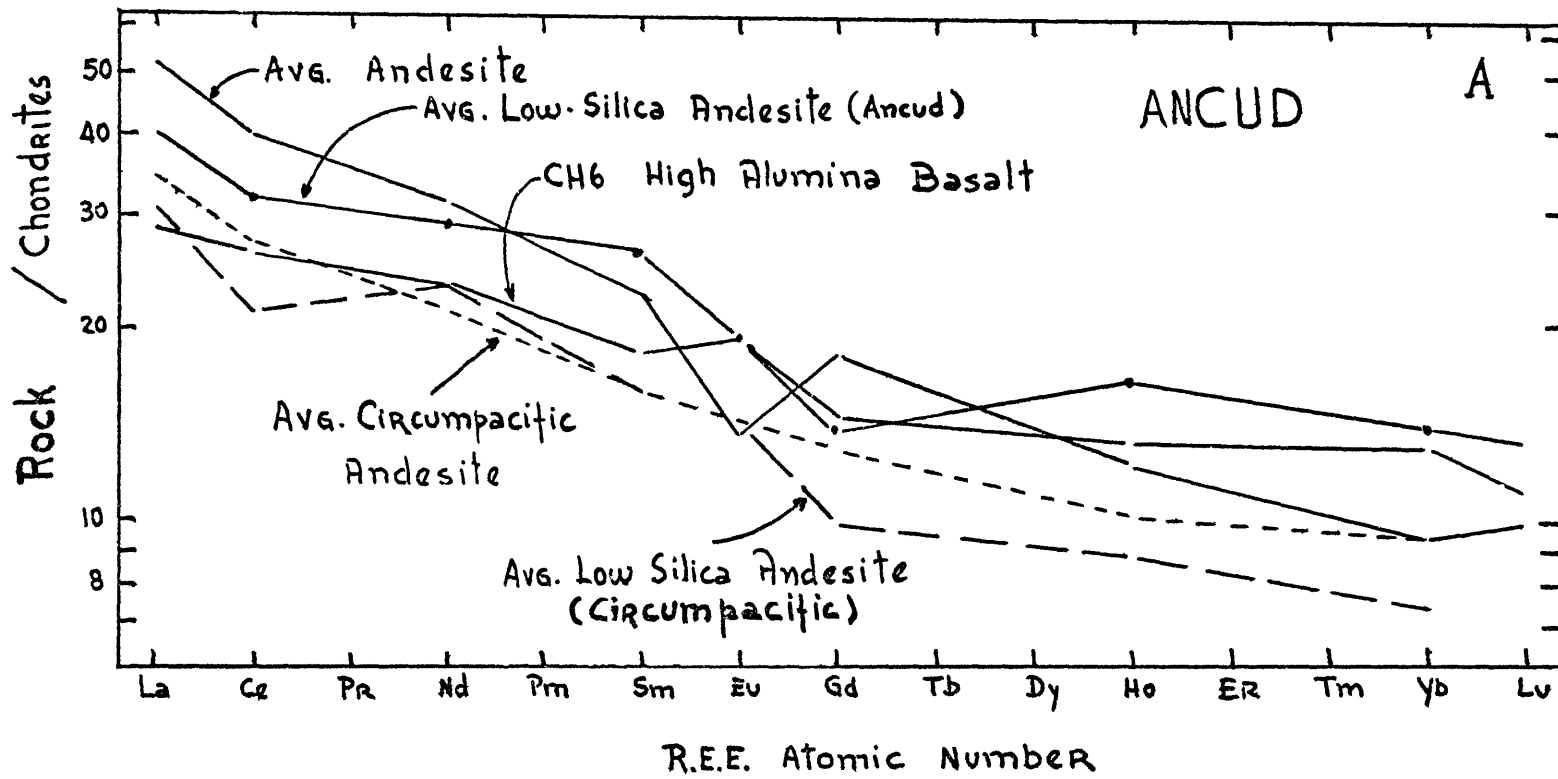


Figure 6

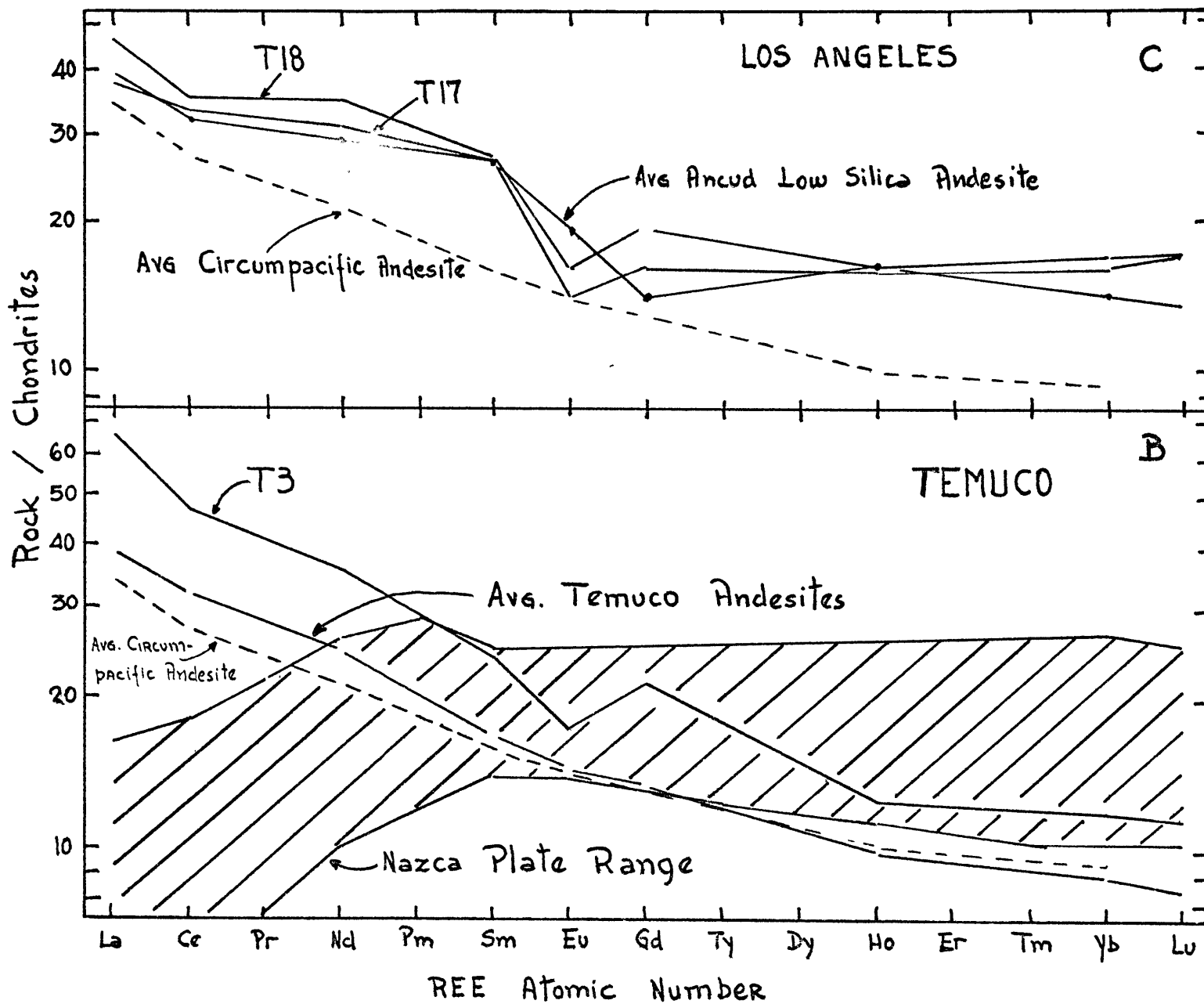


Figure 6 (continued)

Figure 7: Rare-earth element abundances normalized to a chondritic average (Frey et al., 1968). CH6 (high-alumina basalt from Ancud, this study), Warner Basalt, California (Philpotts et al., 1971), and range for high-alumina basalts from Japan and New Zealand (Masuda, 1968; Taylor, 1969; Philpotts et al., 1971).

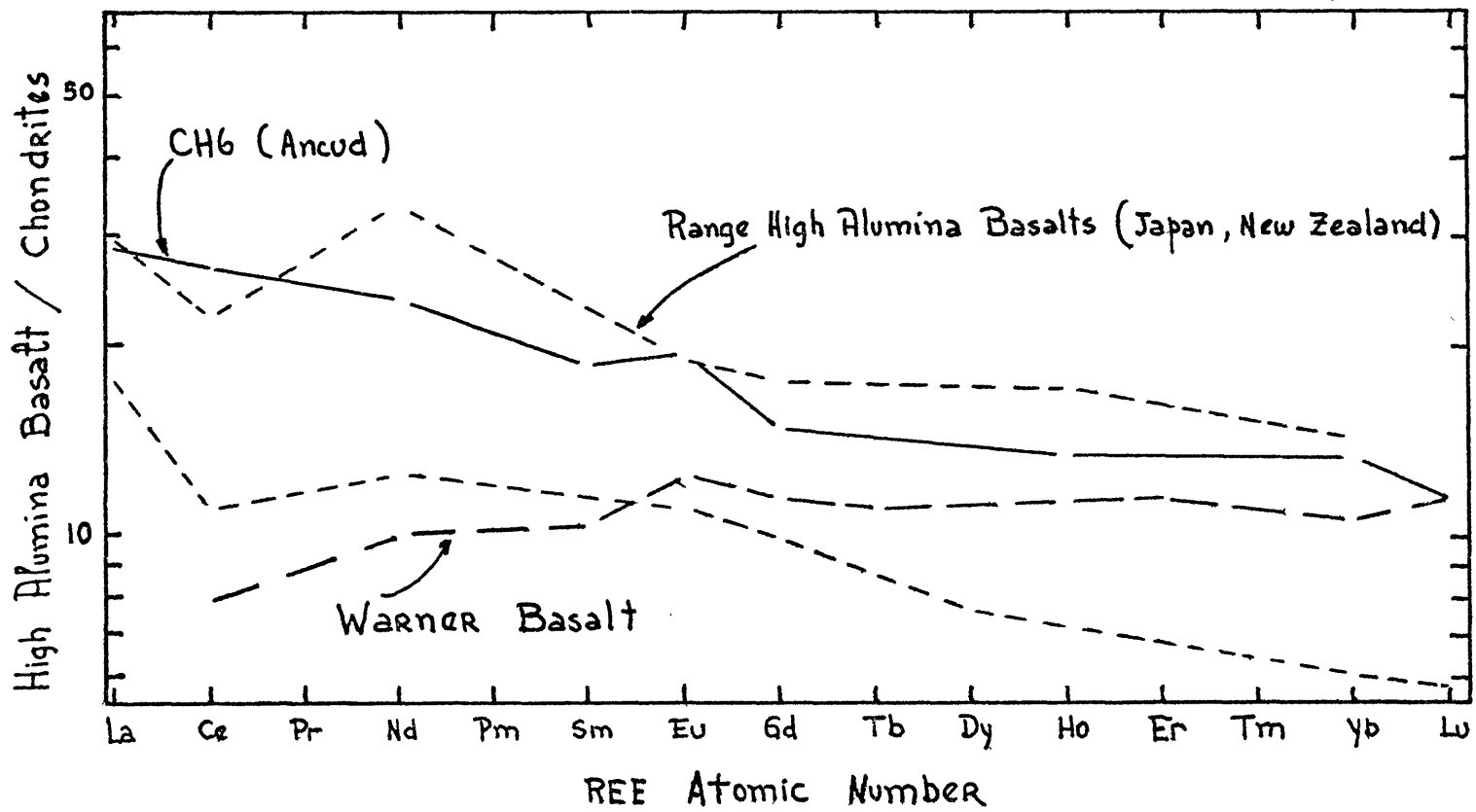


Figure 7

Figure 8: K_2O versus SiO_2 plot. X symbols represent calc-alkaline rocks from northern Chile (Siegers et al., 1969). Other symbols are for central-south Chile as indicated in Figure 2.

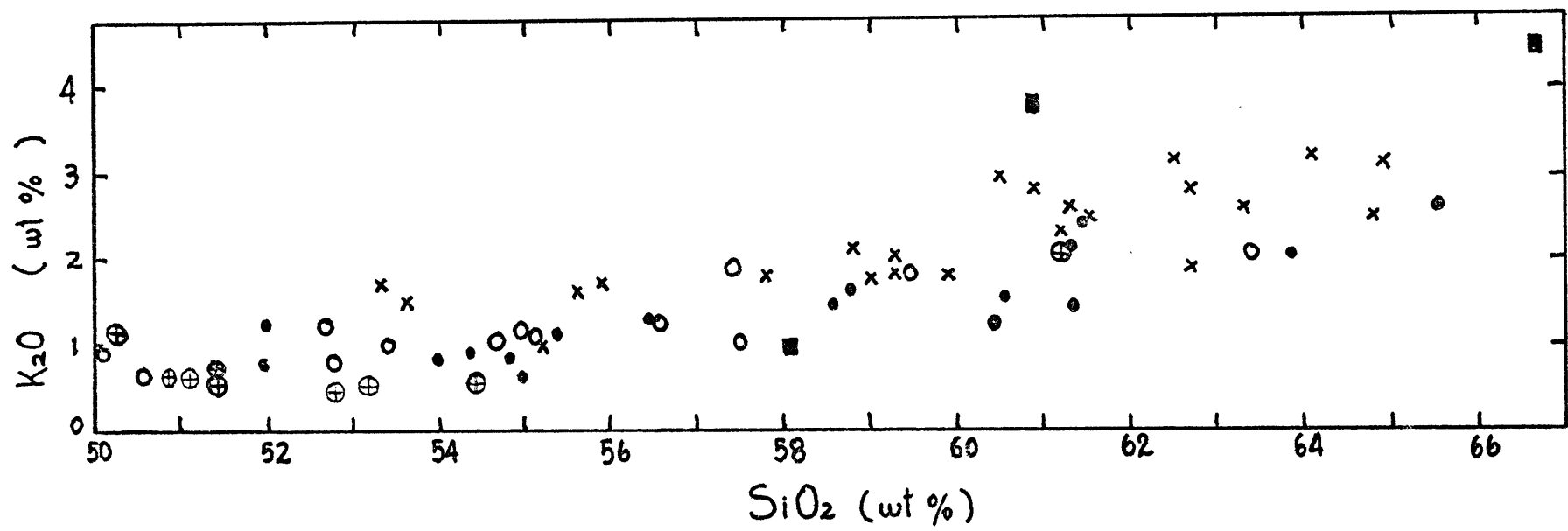


Figure 8

Figure 9: Values of C^l/C_0 for various elements. For Temuco, C^l is average of andesites T2, T9, and T13 and for Ancud, C^l is average of low-silica andesites. C_0 for Temuco and Ancud are estimated average values (ppm) of Nazca Plate basalt (Sc=40, Cr=300, Co=50, Ni=100, La=3.2, Ce=11.4, Nd=9.6, Sm=3.6, Eu=1.3, Ho=0.98, Yb=2.6, Lu=0.42, K=1160, Rb=1.1, Sr=135 and Ba=10). Values of C^l/C_0 for 40% modal fractional melting of amphibole (100%), amphibole (50%) plus clinopyroxene (50%), and eclogite (50% garnet plus 50% clinopyroxene) were calculated using eqn. 14 of Shaw (1970), and the partition coefficients of Table 4. Star symbols are values of garnet granulite model from DeLong (1974).

Figure 9: Open squares for REE are data obtained for
(continued) a liquid derived experimentally by melting
a Hawaiian tholeiite at 5kb and 2000°C
(Holloway and Burnham, 1972). The REE
abundances in this liquid have been normalized
to those of the parent Hawaiian tholeiite.

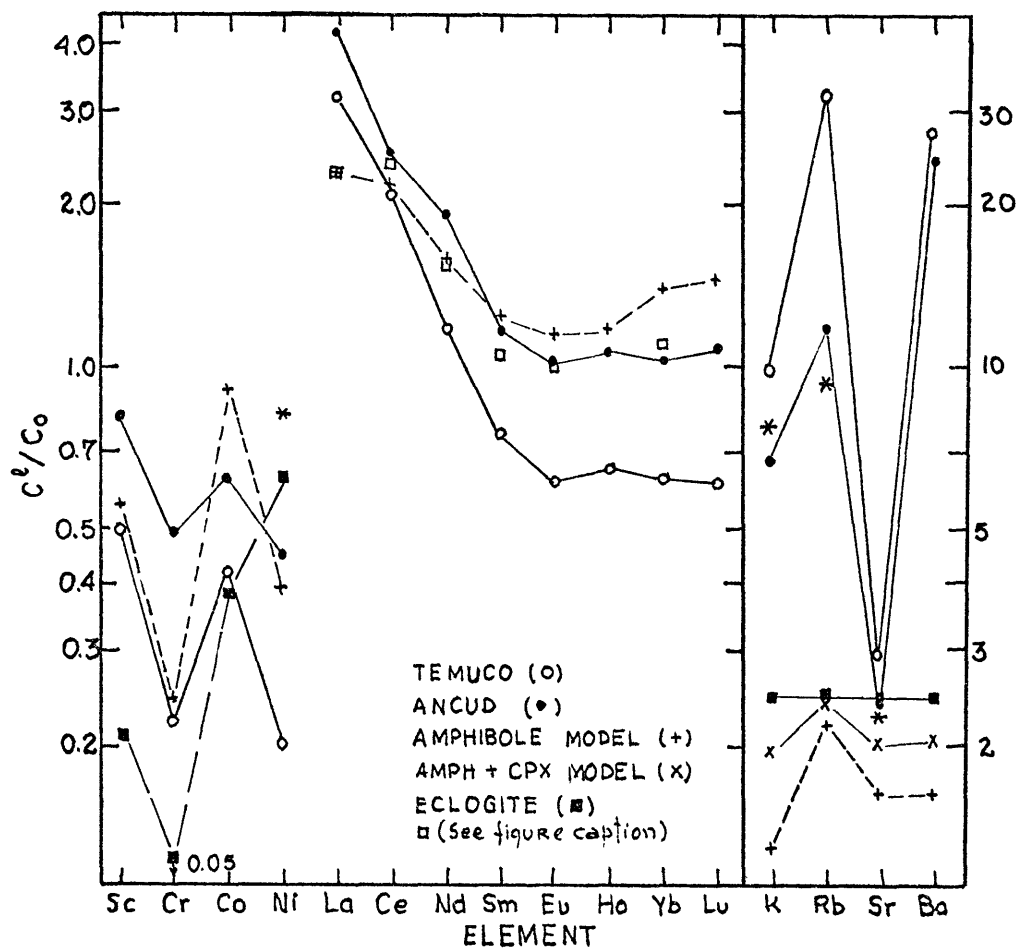


Figure 9

Figure 10: Chondrite normalized rare-earth abundances in theoretical liquids derived by fractional melting (Shaw, 1970). Amphibole and eclogite modal melting models as in Figure 9 with initial solid concentrations (C_0) abundances equal to Nazca Plate basalt estimates (see Figure 9 caption). Initial rare-earth element concentrations for the peridotite clinopyroxene (15%), orthopyroxene (25%), and olivine (60%) are twice chondritic abundances (Frey and Green, 1974). The 5% fractional melt of peridotite was formed from a cpx:opx:oliv melting ratio of 2:1:1. Chilean Coastal Belt range from Temuco and Ancud andesites. Nazca plate average from Schilling and Bonatti (1974) and Frey (unpublished).

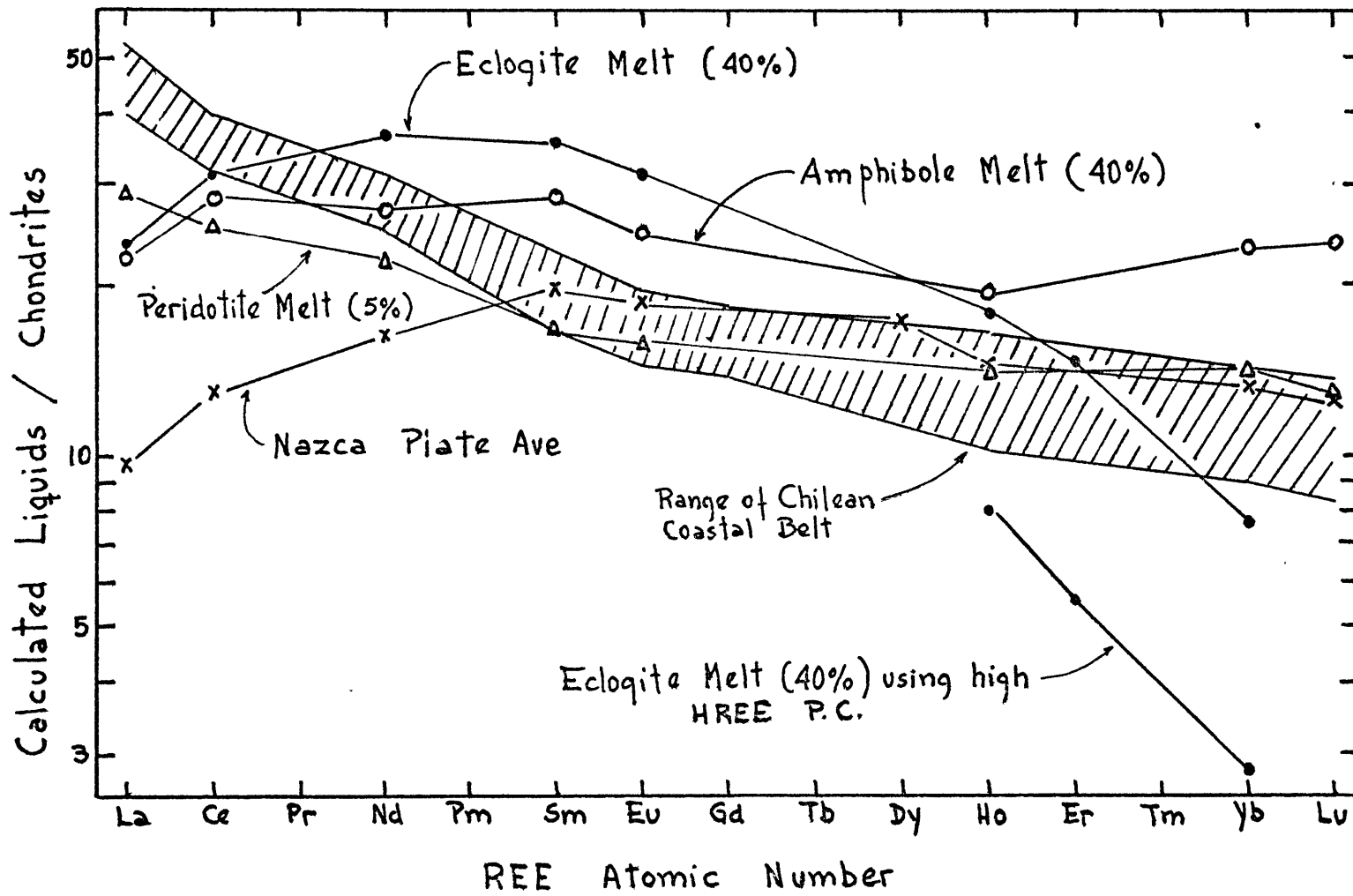


Figure 10

Figure 11: Rare-earth abundances in Mt. St. Helens (Cascades) calc-alkaline rocks normalized to a chondritic average (Frey et al., 1968). Franciscan (Tiburon) eclogite data from Frey (unpublished.) Range of Juan de Fuca and Gorda Ridge values from Kay et al. (1970), and Schilling (1971). Star symbols are an average of 19 Juan de Fuca Ridge basalts from Corliss (1970).

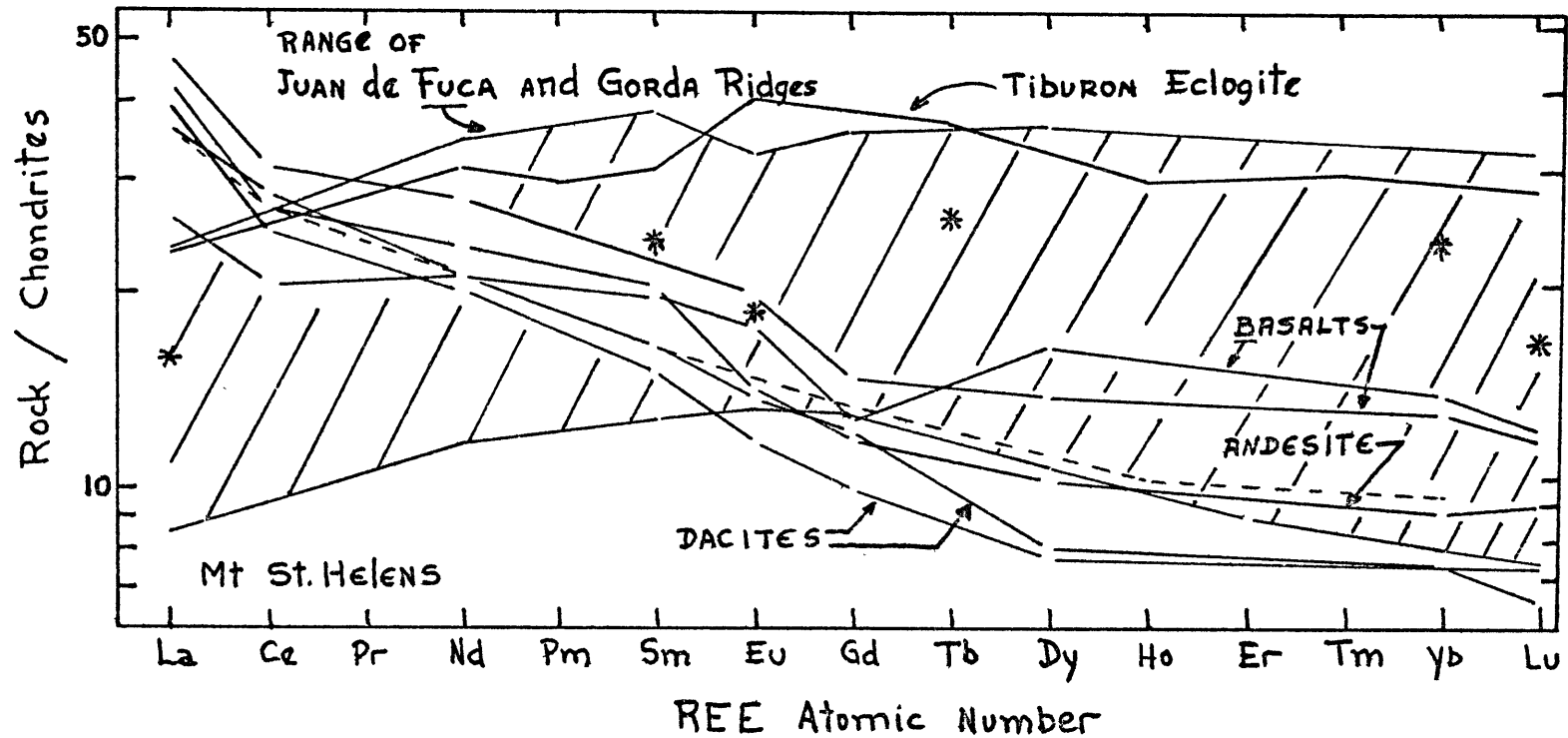


Figure 11

Figure 12: ratios of abundance in 5% non-modal peridotite fractional melt (see Figure 10 caption) to Temuco andesites (average of T2, T9, and T13) and Ancud low-silica andesite average. Initial peridotite concentrations (C_0) in ppm are Sc=16, Cr=2200, Ni=1500, Co=110, K=500, Rb=1, Sr=20, and Ba=20.

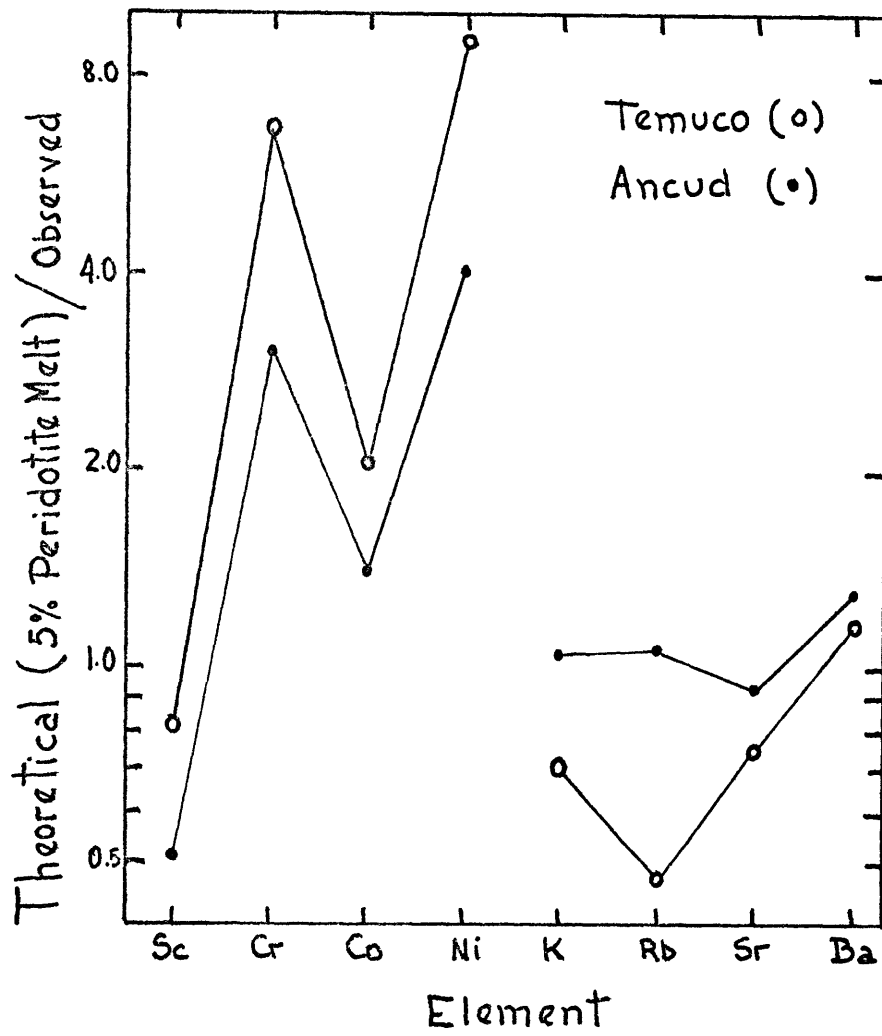


Figure 12

Figure 13: Rare-earth element abundances of the Pino Hachado samples (Plateau series) normalized to a chondritic average (Frey et al., 1968). Circumpacific andesite average from Taylor (1969).

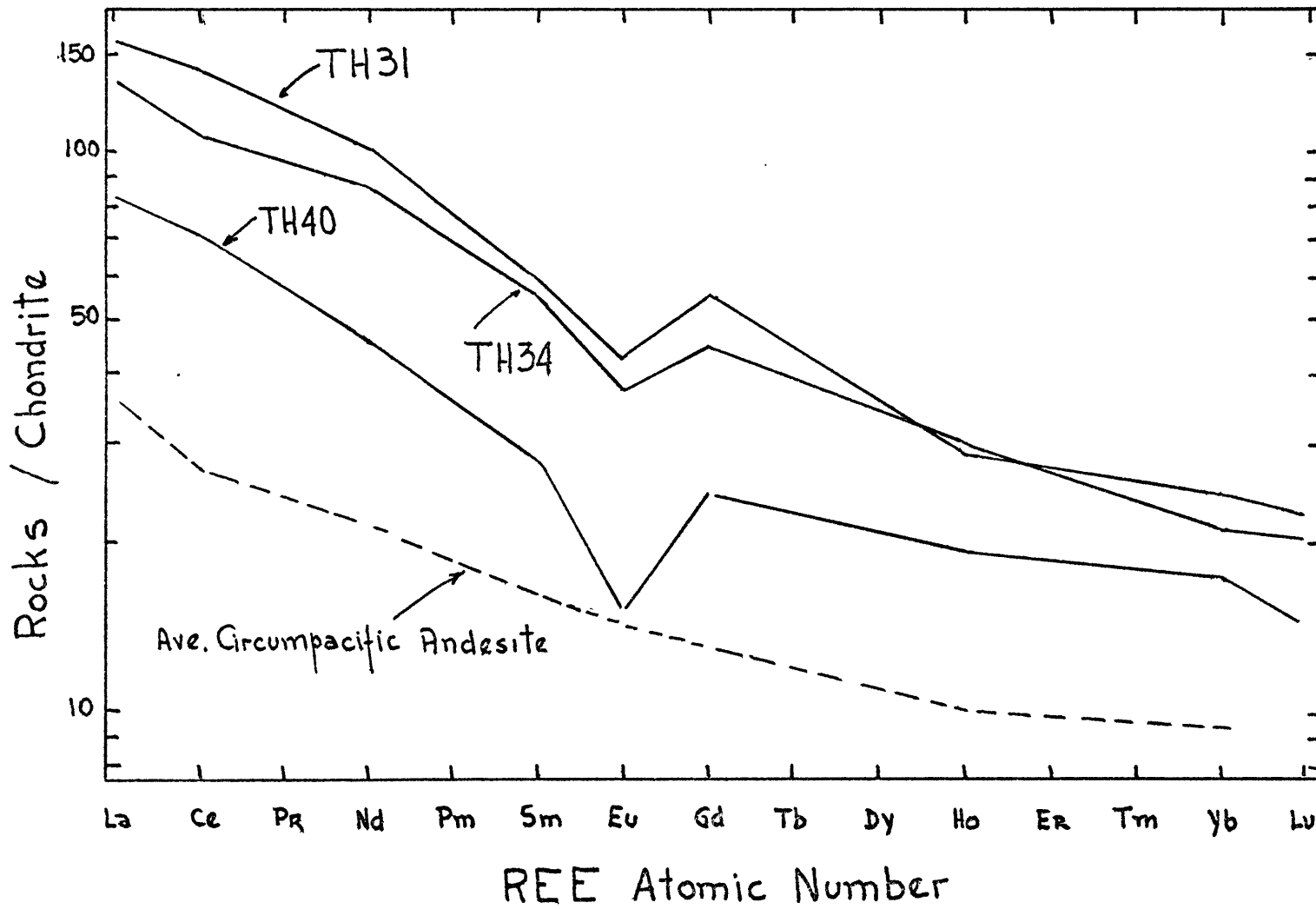


Figure 13

Figure 14: Rare-earth element abundance of the Tupungato sample (797, high Andean andesite from latitude $33^{\circ}15'S$) normalized to a chondritic average (Frey et al., 1968). Circumpacific andesite average from Taylor (1969).

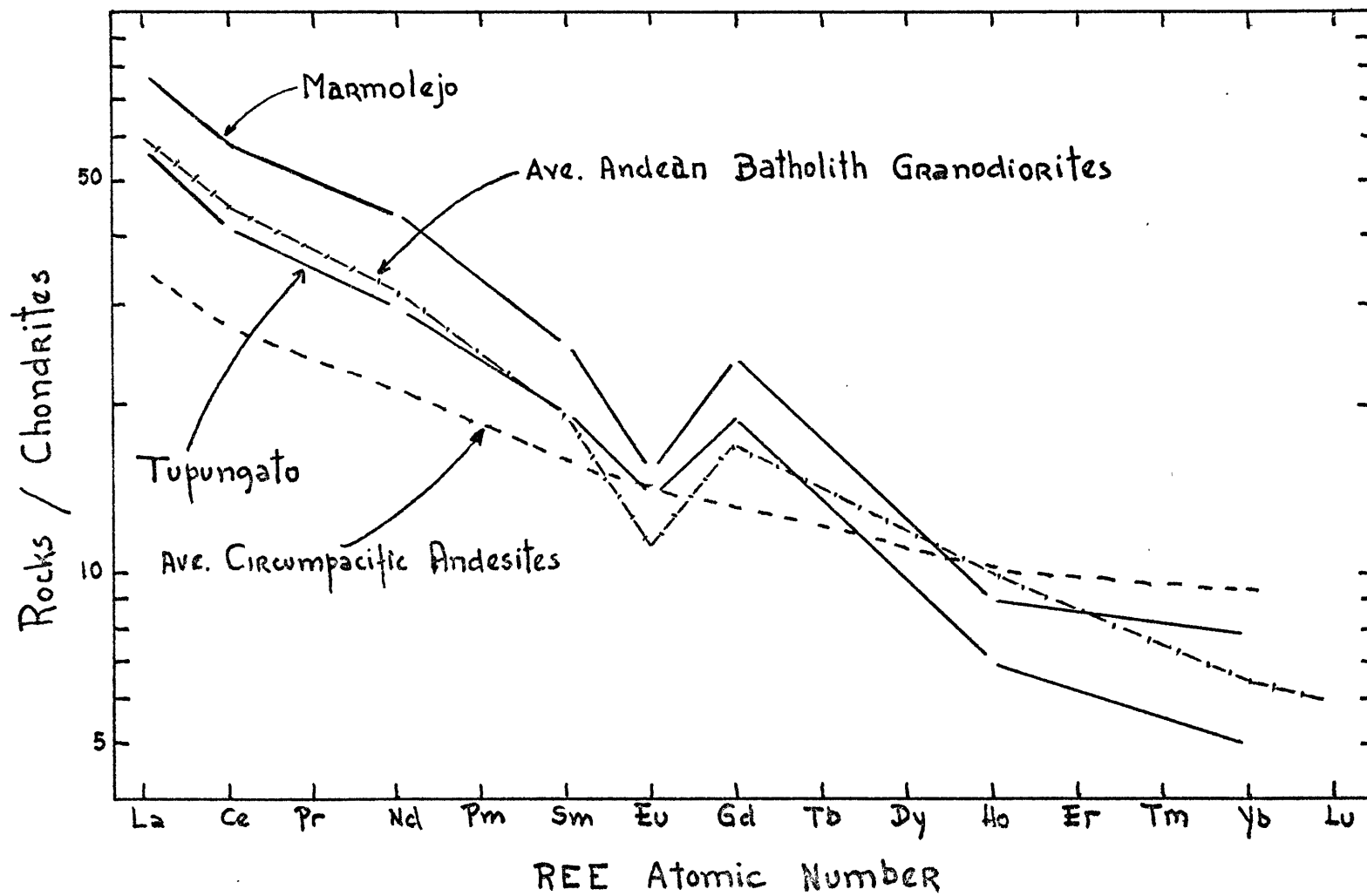


Figure 14

Figure 15: Rare-earth element abundances normalized to a chondritic average (Frey et al., 1968).
a) Samples with La/Yb \sim 2-3 (Antuco, Llaima, Villarrica, Puyehue and Casablanca). b) Samples with La/Yb \sim 5 (GV164 and 800 from Lanin and 799 from Callaquen).

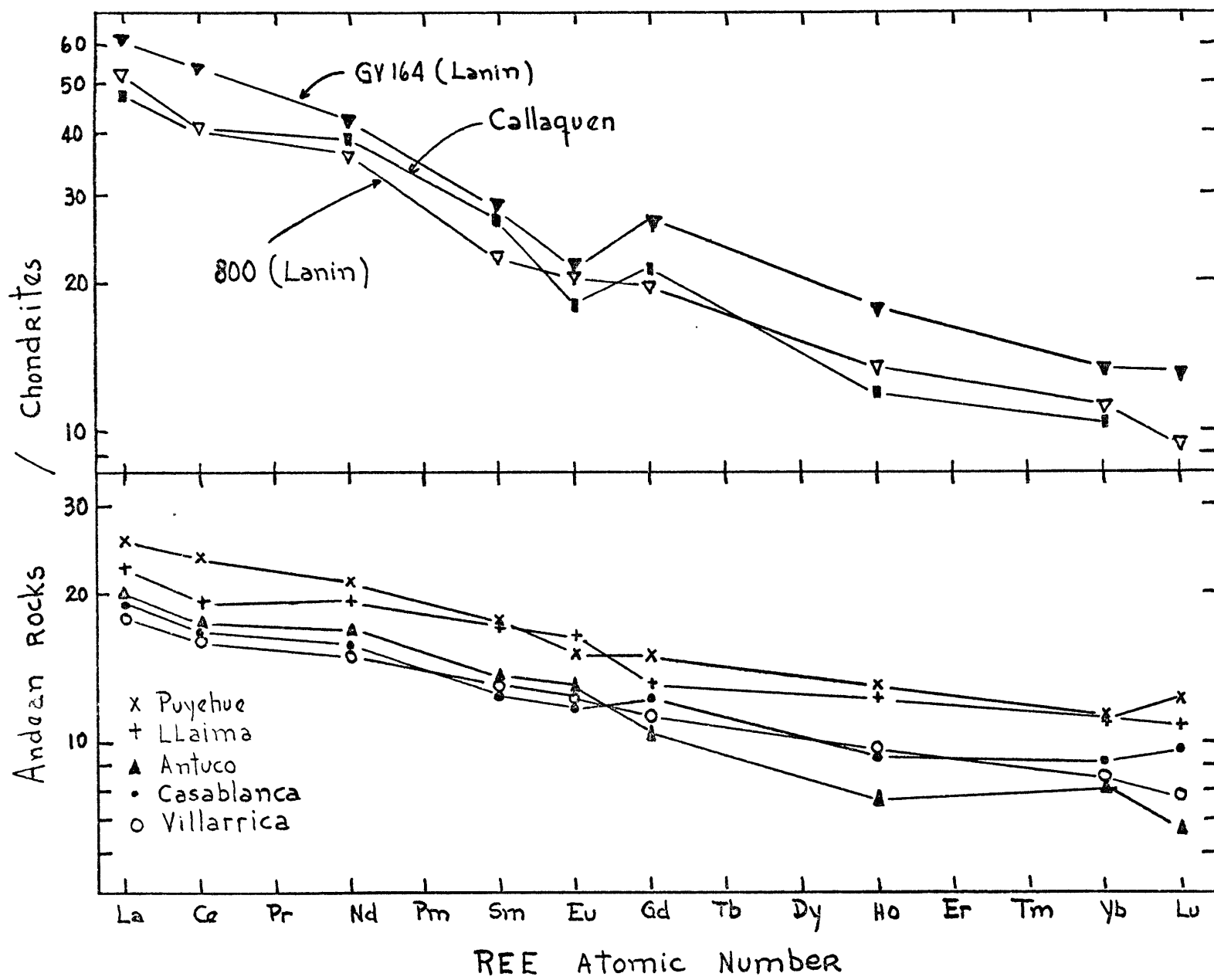


Figure 15

Figure 16: Comparison of the REE abundances of the samples with $\text{La/Yb} \sim 2-3$ with chondritic normalized REE abundances in theoretical liquids derived by fractional melting (Shaw, 1970). Amphibole and eclogite model melting models as in Figure 9 with initial solid concentrations (Co) abundances equal to Nazca Plate basalt estimates (see Figure 9 caption). Initial REE concentrations for the peridotite clinopyroxene (15%), orthopyroxene (25%), and olivine (60%) are twice chondritic abundances (Frey and Green, 1974). The 10% fractional melt of peridotite was formed from a cpx:opx:olv melting ratio of 2:1:1.

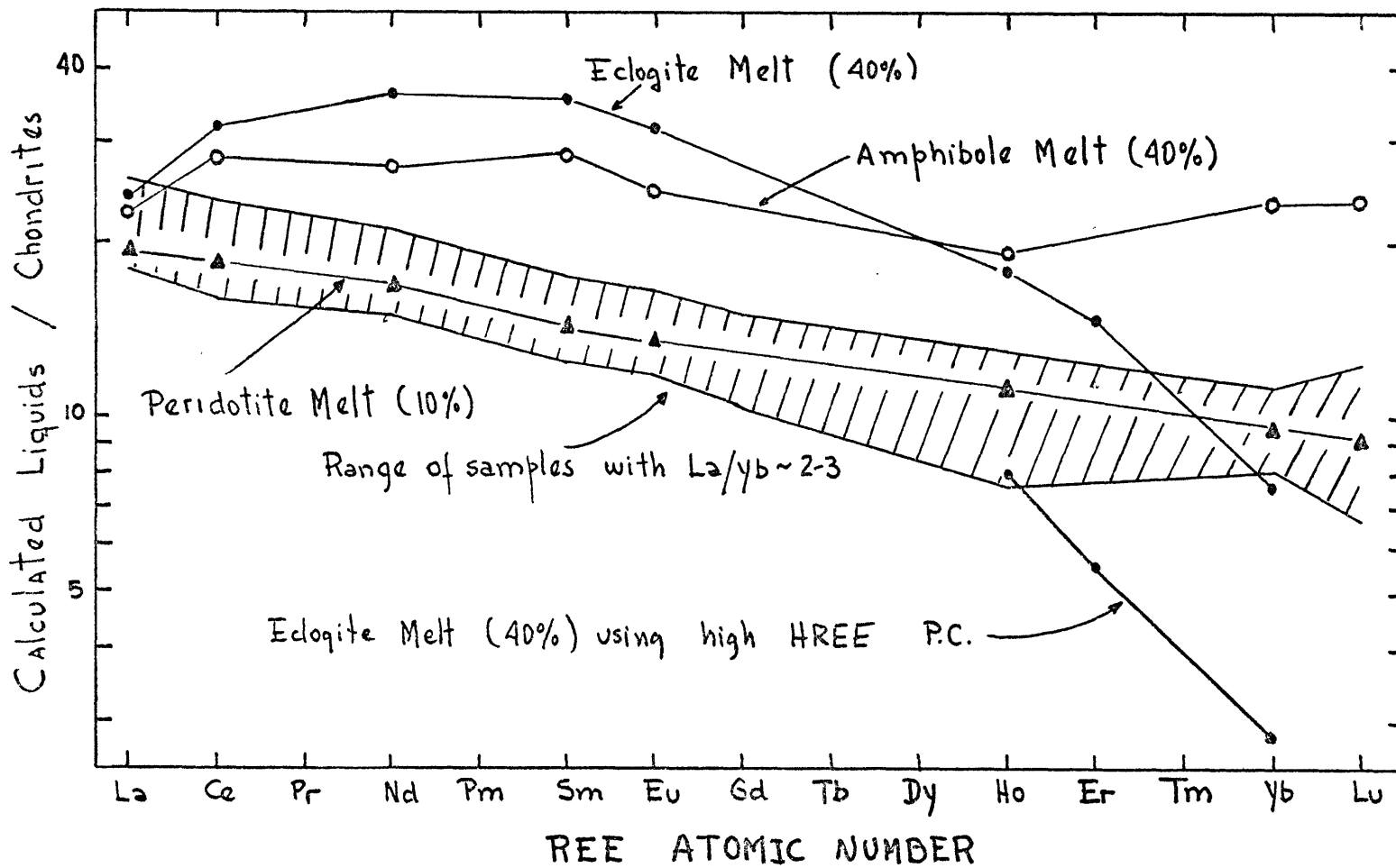


Figure 16

Figure 17: Comparison of REE abundances of the samples with $\text{La/Yb} \sim 5$ with chondritic normalized REE abundances in theoretical liquids derived by fractional melting (Shaw, 1970). Initial solid concentrations abundances as in Figure 16. The 2% fractional melt of peridotite was formed from a cpx:opx:olv melting ratio of 2:1:1. The REE pattern that results by fractionation of plagioclase (30%) and clinopyroxene (5%) from sample 800 is also included.

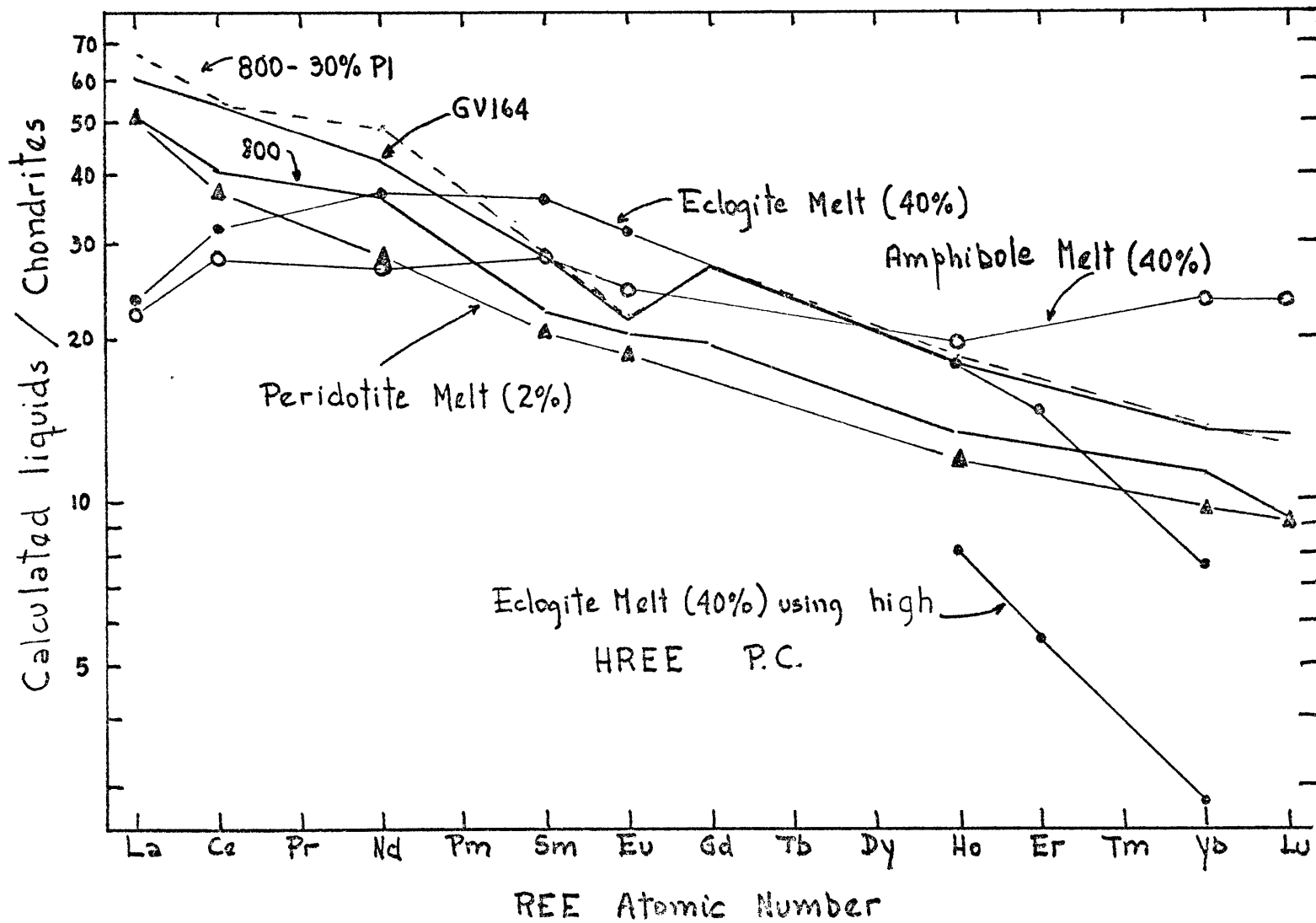


Figure 17

Figure 18: Comparison of REE abundance of the Tupungato sample ($\text{La/Yb} \sim 11.6$) with chondritic normalized REE abundances in theoretical liquids derived by fractional melting (Shaw, 1970). Initial solid concentrations abundances as in Figure 16. The 2% and 10% fractional melts of peridotite were formed from a cps:opx:olv melting ratio of 2:1:1.

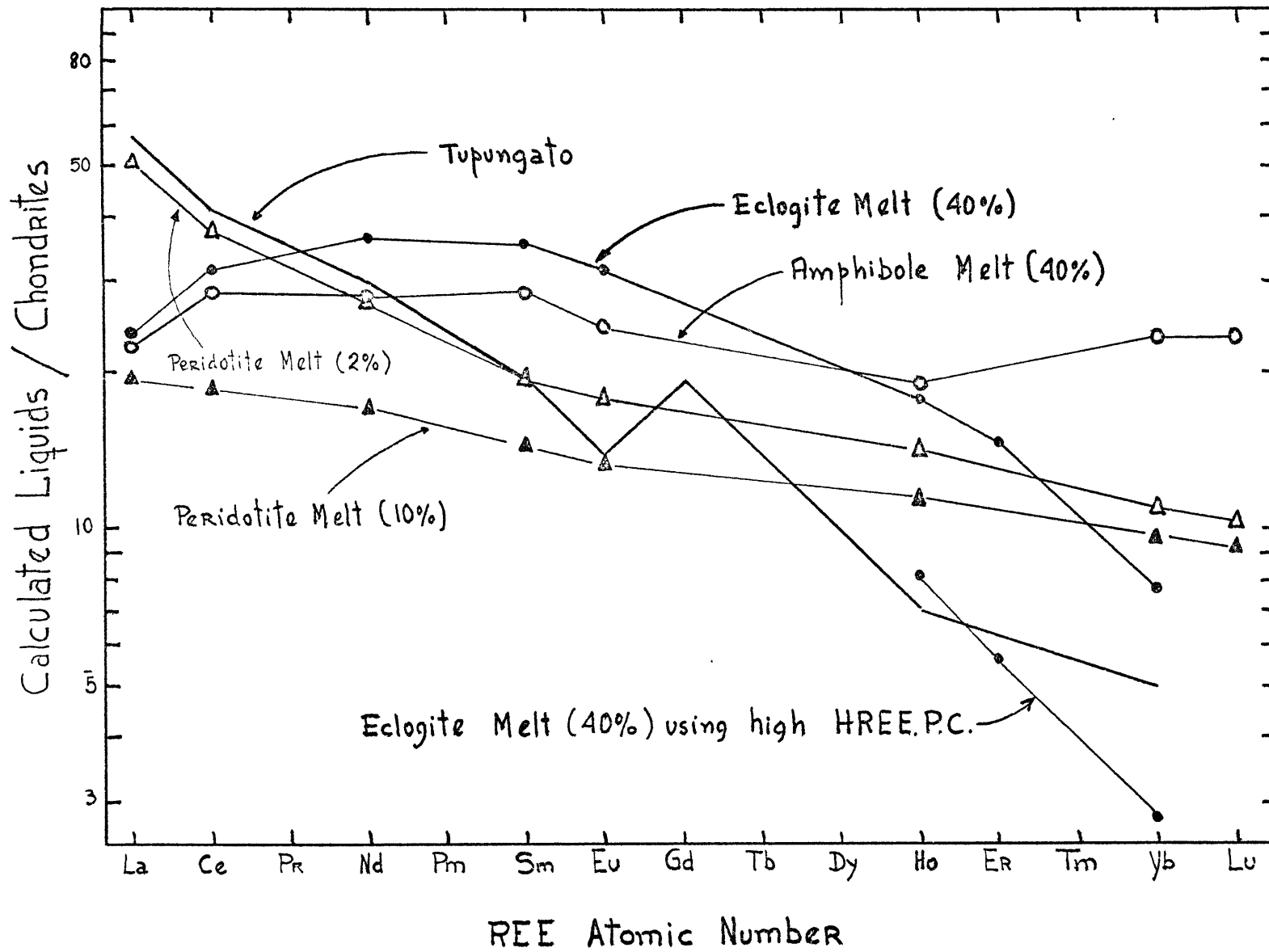
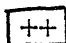




Figure 18

Figure 19: Sample localities on a sketch map of the central Chile (33° - 34° S) granitoids modified from the "Mapa Geológico de Chile" (1968).

 Upper Paleozoic (Coastal) batholith;
 Upper Cretaceous (Central) batholith;
and  Tertiary (Andean) batholith.

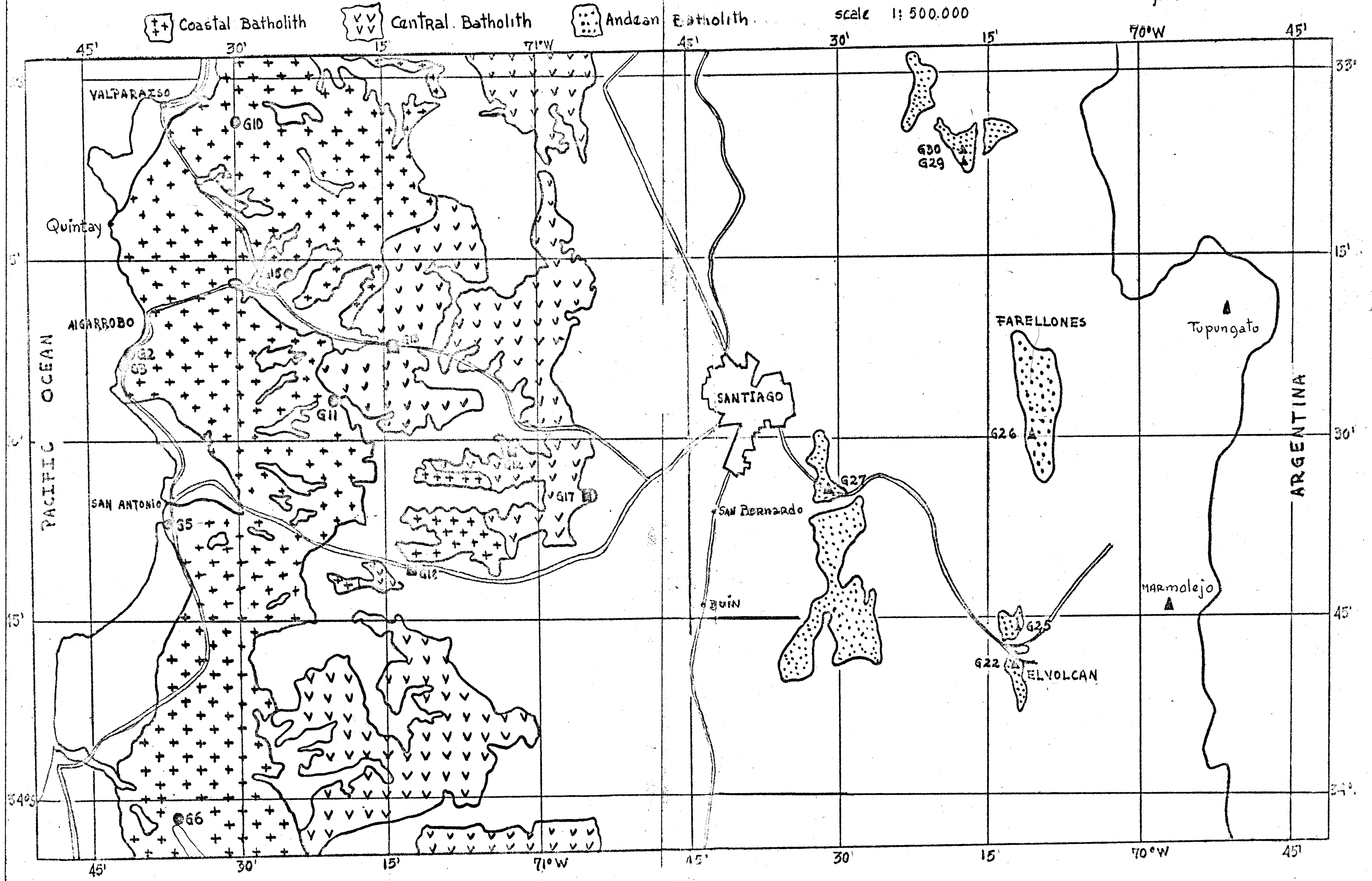


Figure 20: Modal abundance of the central Chile granitoids plotted on the APQ (alkali feldspar, plagioclase and quartz) diagram. Classification of plutonic rocks (Streckeisen, 1973).

Figure 20

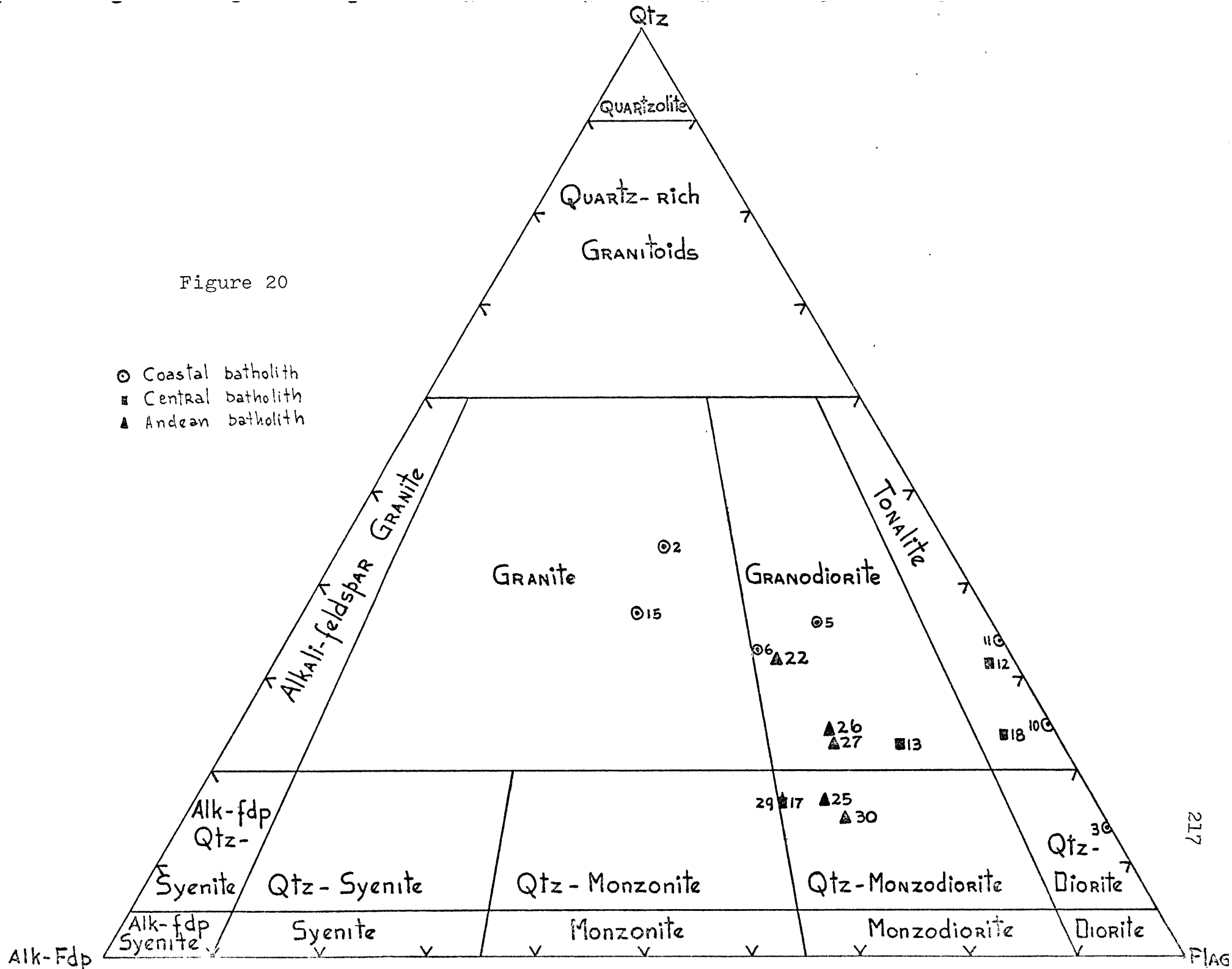


Figure 21: Ab-Q-Or normative diagram (wt%) for the central Chile granitoids. Solid lines represent isobaric cotectic lines for 0.5, 5, and 10 kb respectively for the system Ab-Q-Or water saturated. Dotted line joins the minimum points and eutectics between 0.5 and 10 kb.

Figure 21

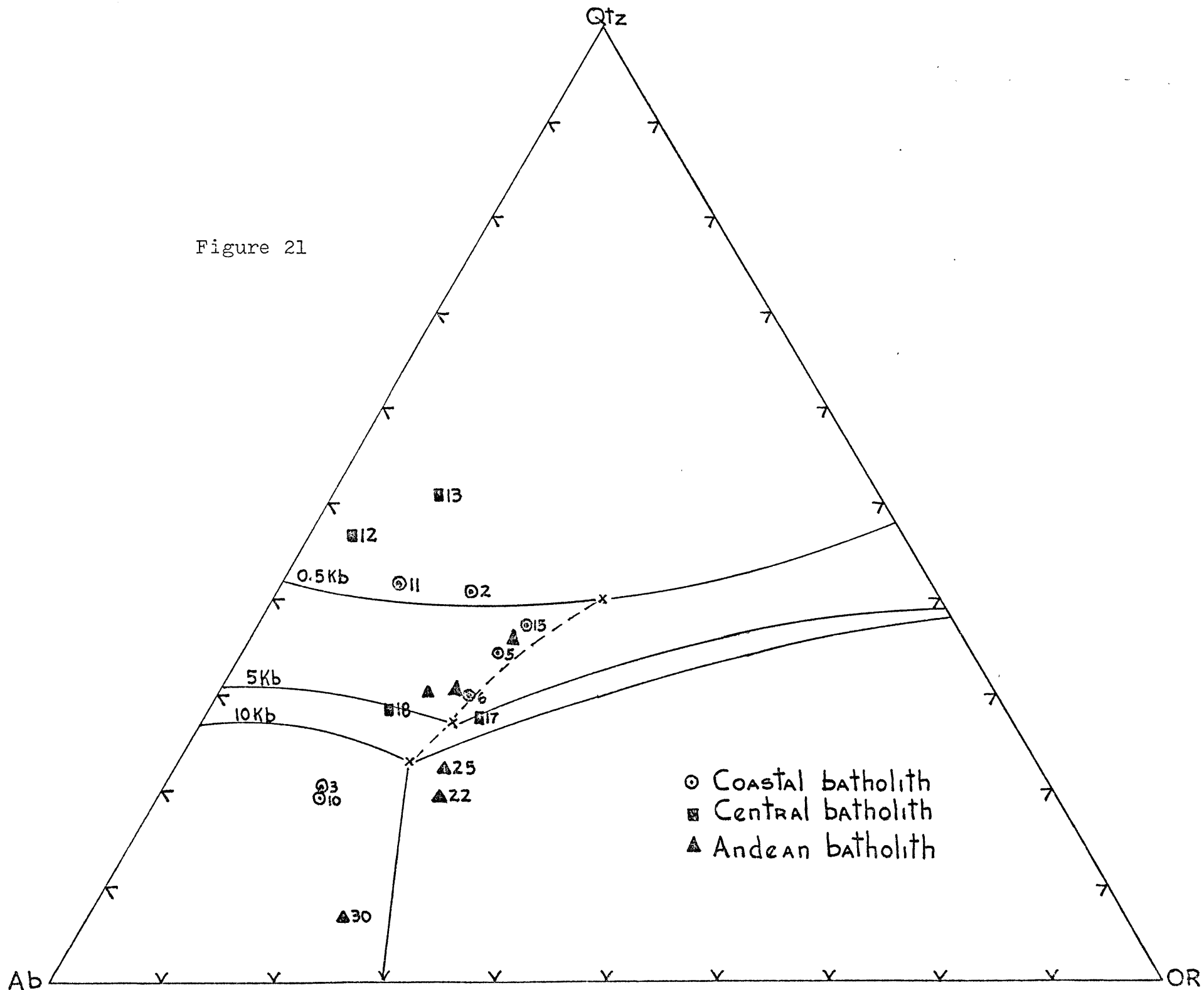


Figure 22: FMA diagram (wt%) with total iron calculated as FeO. Solid lines represent general limits of Japanese hypersthene (calc-alkaline) series (Kuno, 1968a) \odot are for Coastal batholith granitoids, \blacksquare are for Central batholith granitoids and \blacktriangle are for Andean batholith granitoids. As comparison, this diagram also includes volcanic rocks from central-south Chile (x) and from Mt. St. Helens (Cascades \otimes).

Figure 22

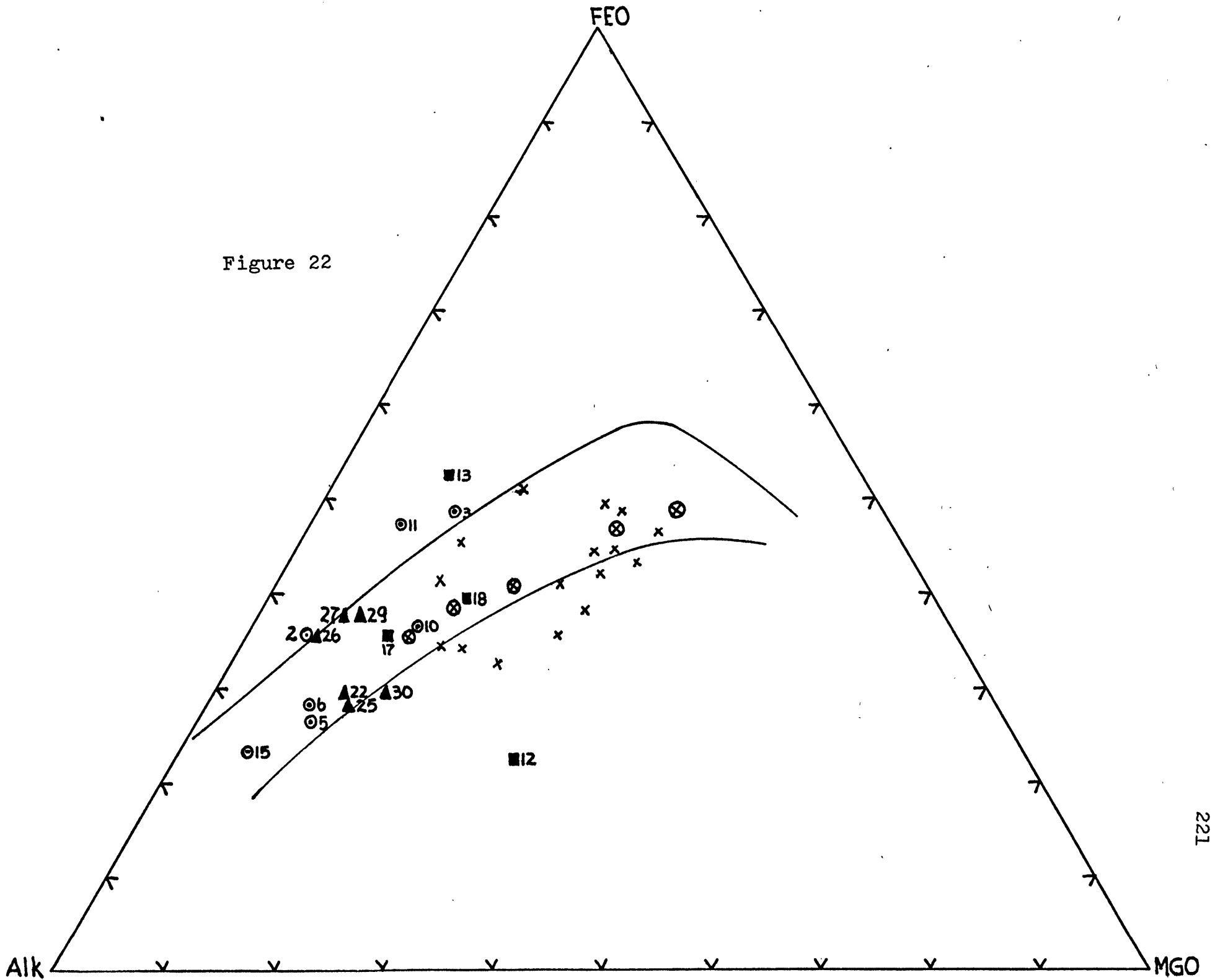


Figure 23: Major and minor elements and K_2O/SiO_2 ratio plotted as a function of the longitude of the samples. Encircled in dotted lines are those samples with similar SiO_2 abundances (67.3 ± 0.5 wt%). Data symbols as in Figure 22. Sample G12 is not circled because of its unusual geochemistry.

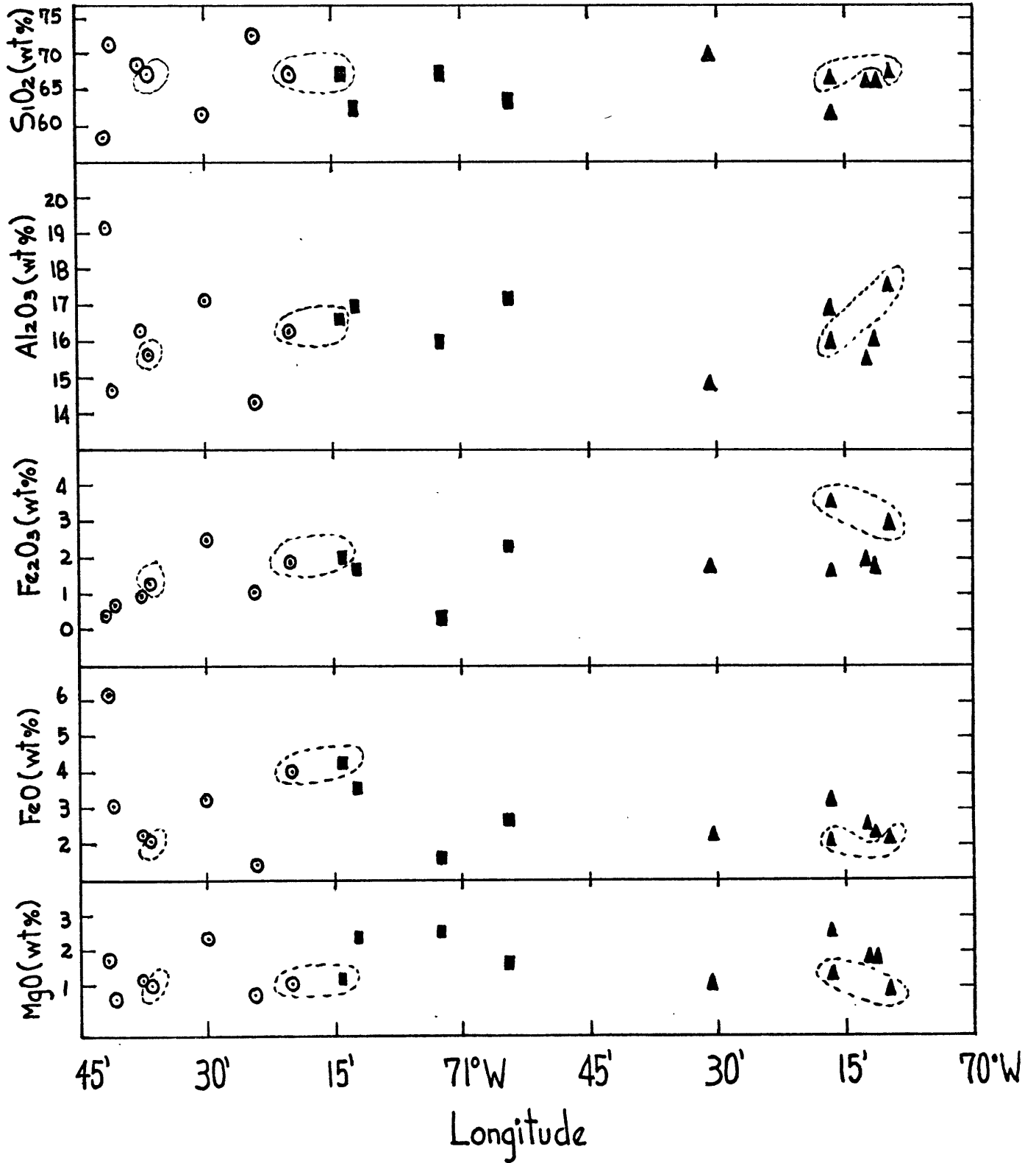


Figure 23

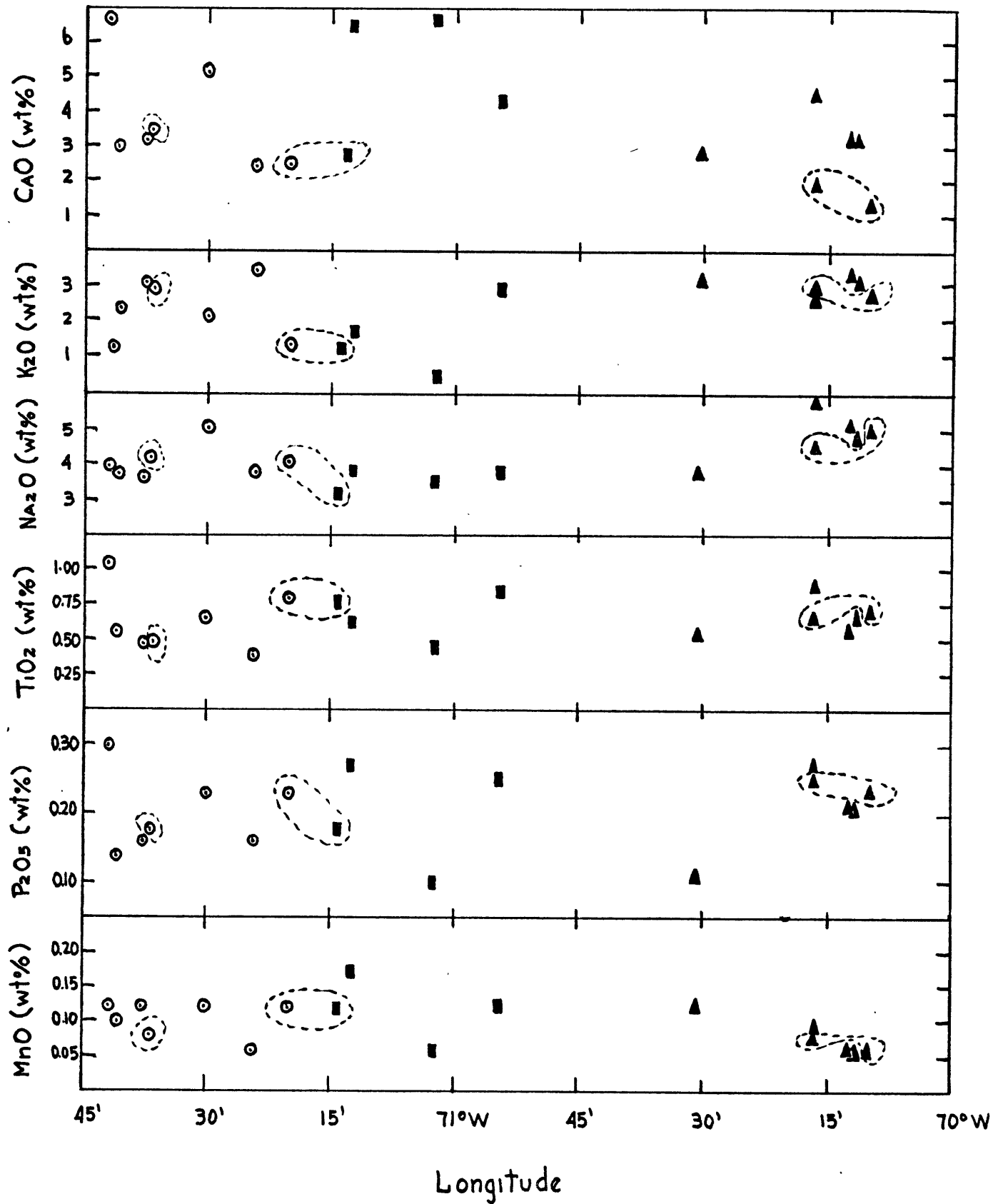


Figure 23 (continued)

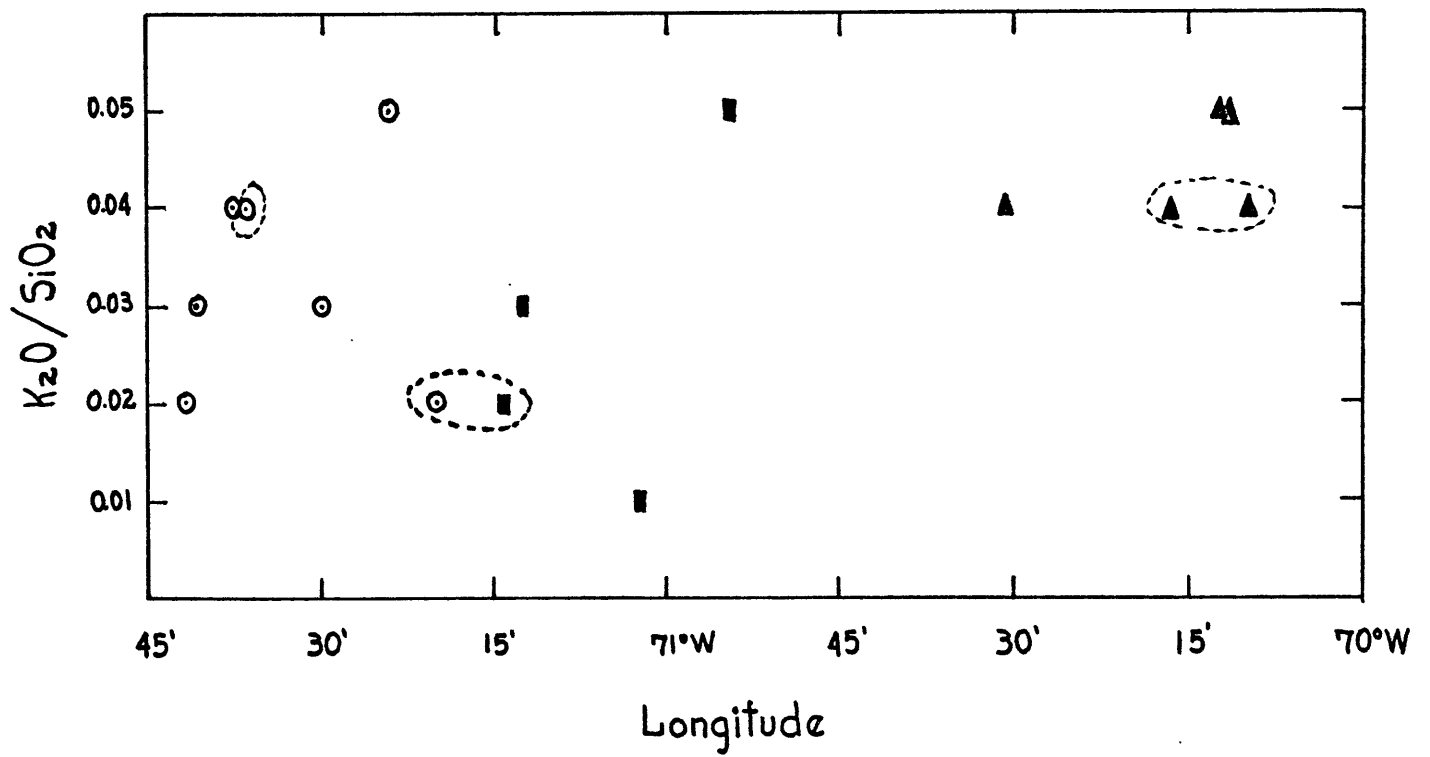


Figure 23 (continued)

Figure 24: Major elements of the Chilean volcanic and plutonic rocks plotted as a function of the SiO_2 content. Data symbols for plutonic rocks as in Figure 22, (+) are for Andean volcanic rocks, (this work; Klerkx, 1965; Vergara, 1969), (x) are for Coastal range volcanic rocks (this work), (∇) are for central Chile andesites (Oyarzun, 1971) (o) are for northern Chile andesites and (●) are for northern Chile ignimbrites.

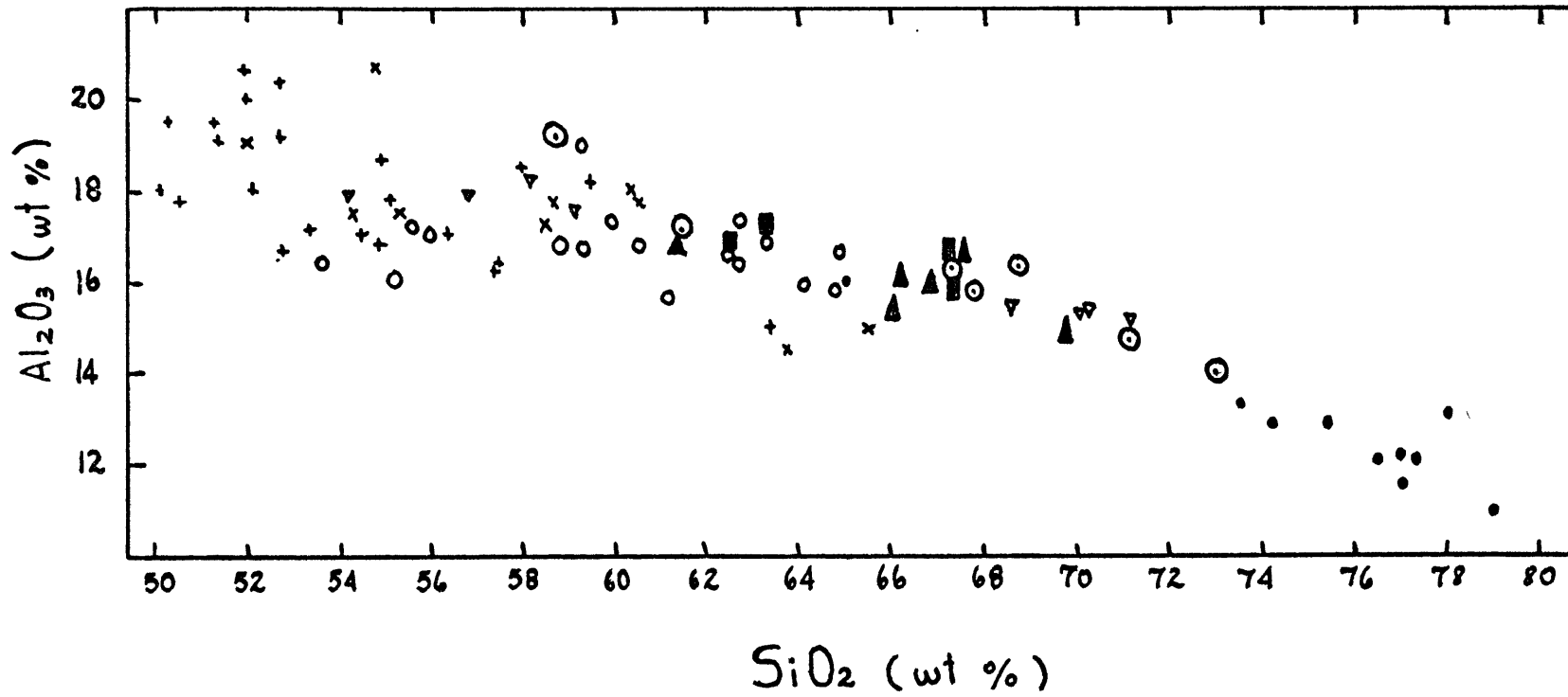


Figure 24

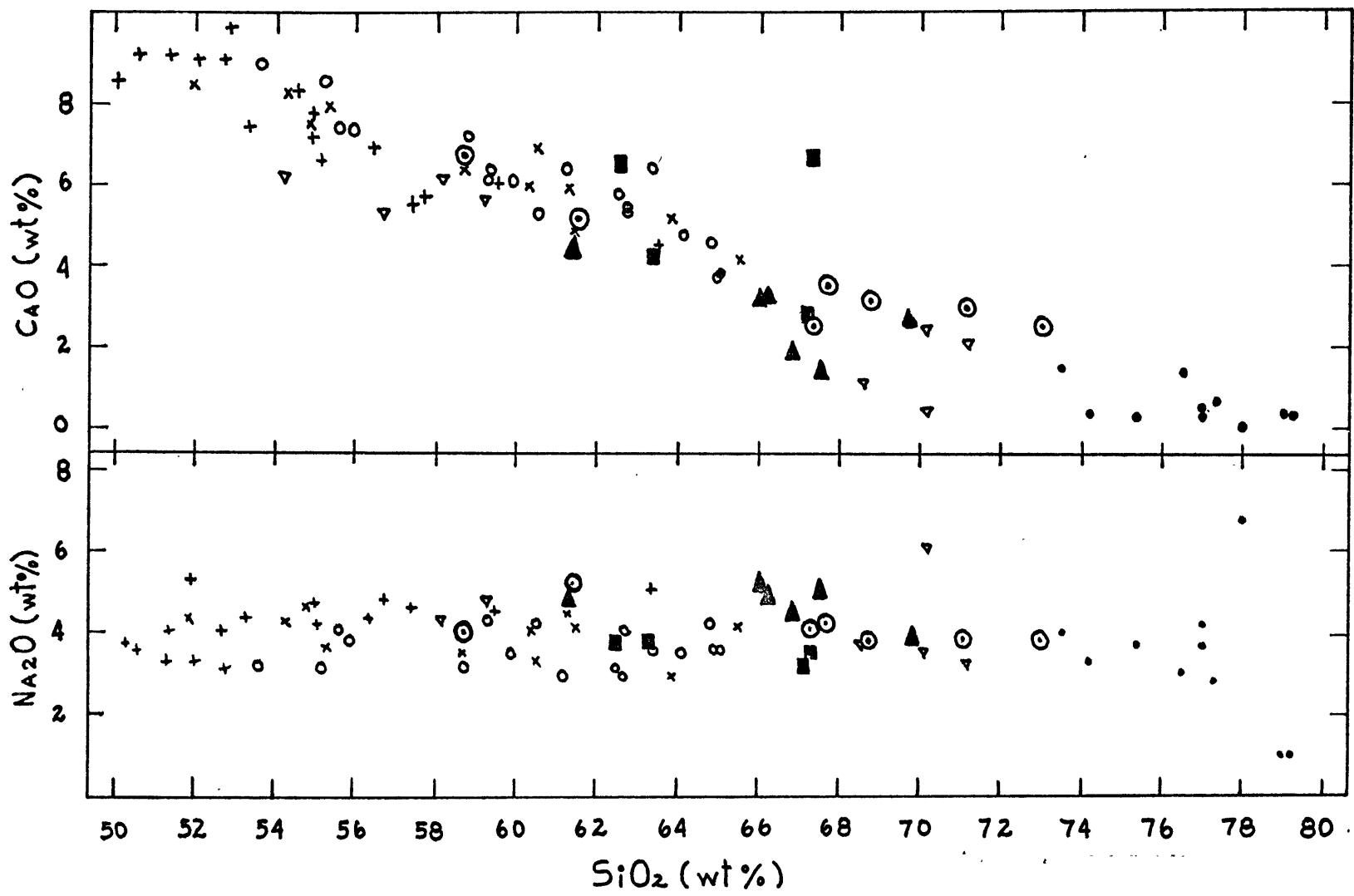


Figure 24 (continued)

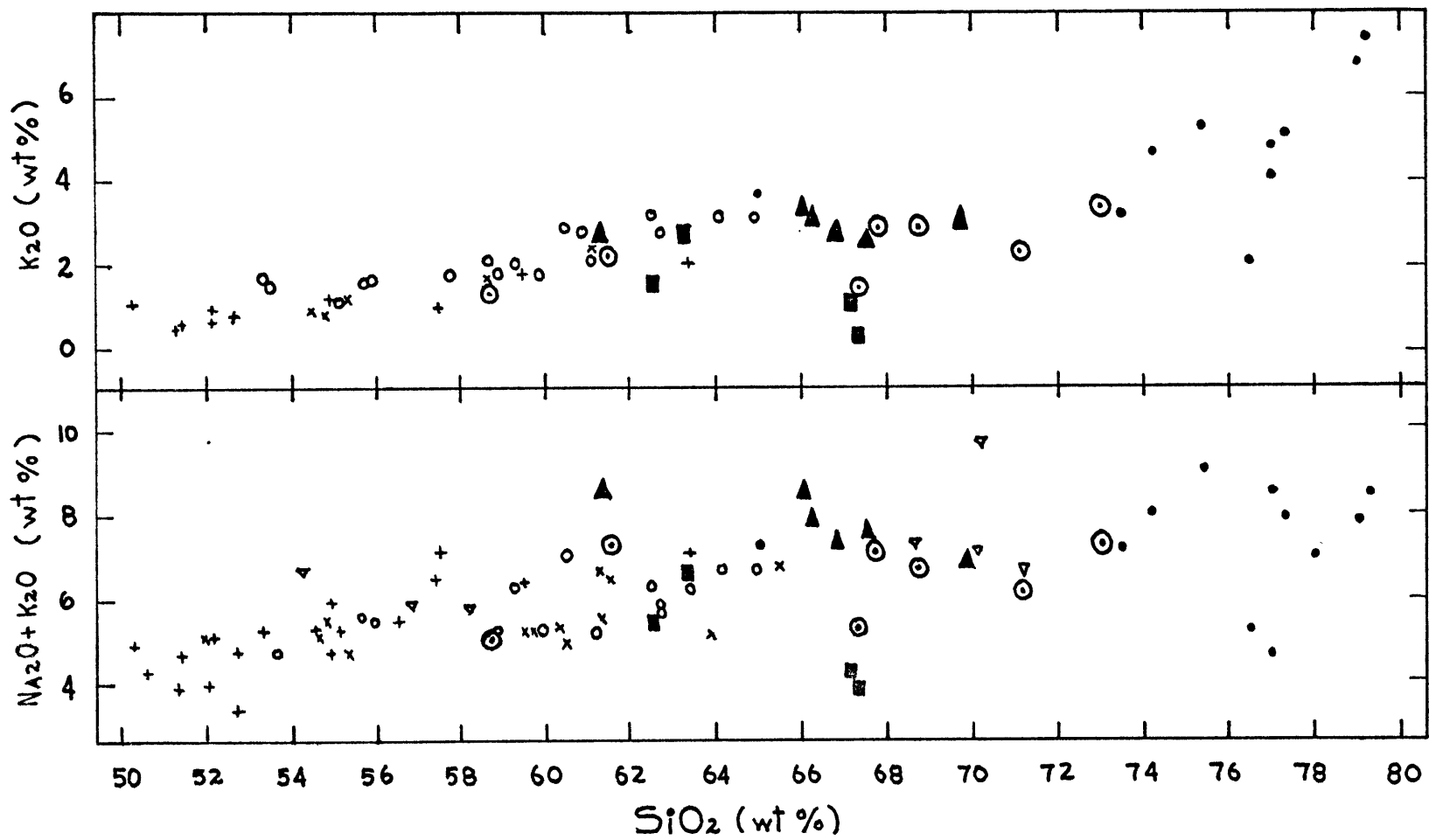


Figure 24 (continued)

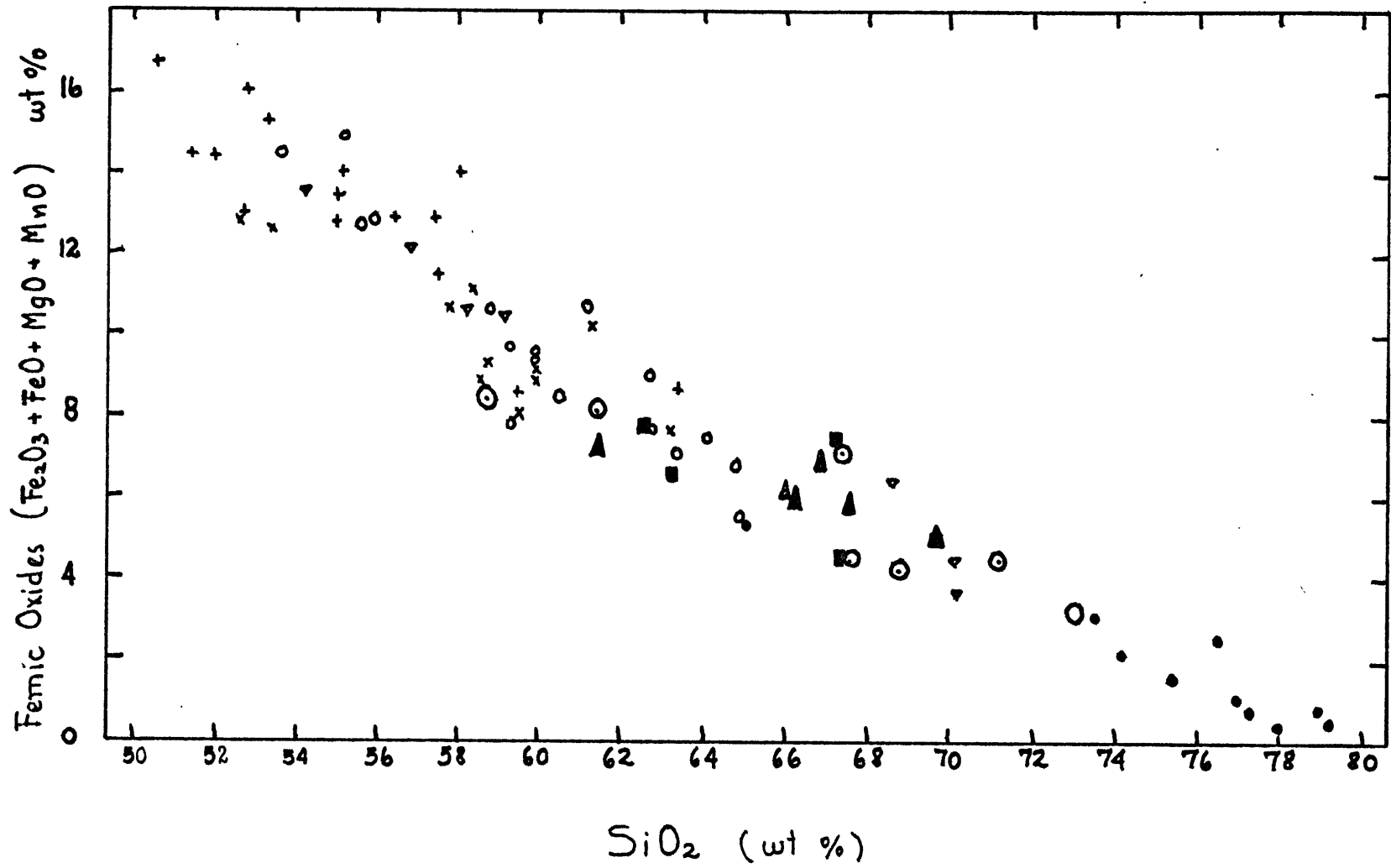


Figure 24 (continued)

Figure 25: Trace element abundances in central Chile granitoids plotted as a function of the longitude of the samples. Encircled in dotted lines are these samples with similar SiO_2 abundances (67.3 ± 0.5 wt%). Data symbols as in Figure 22. Sample G12 is not circled because of its unusual geochemistry.

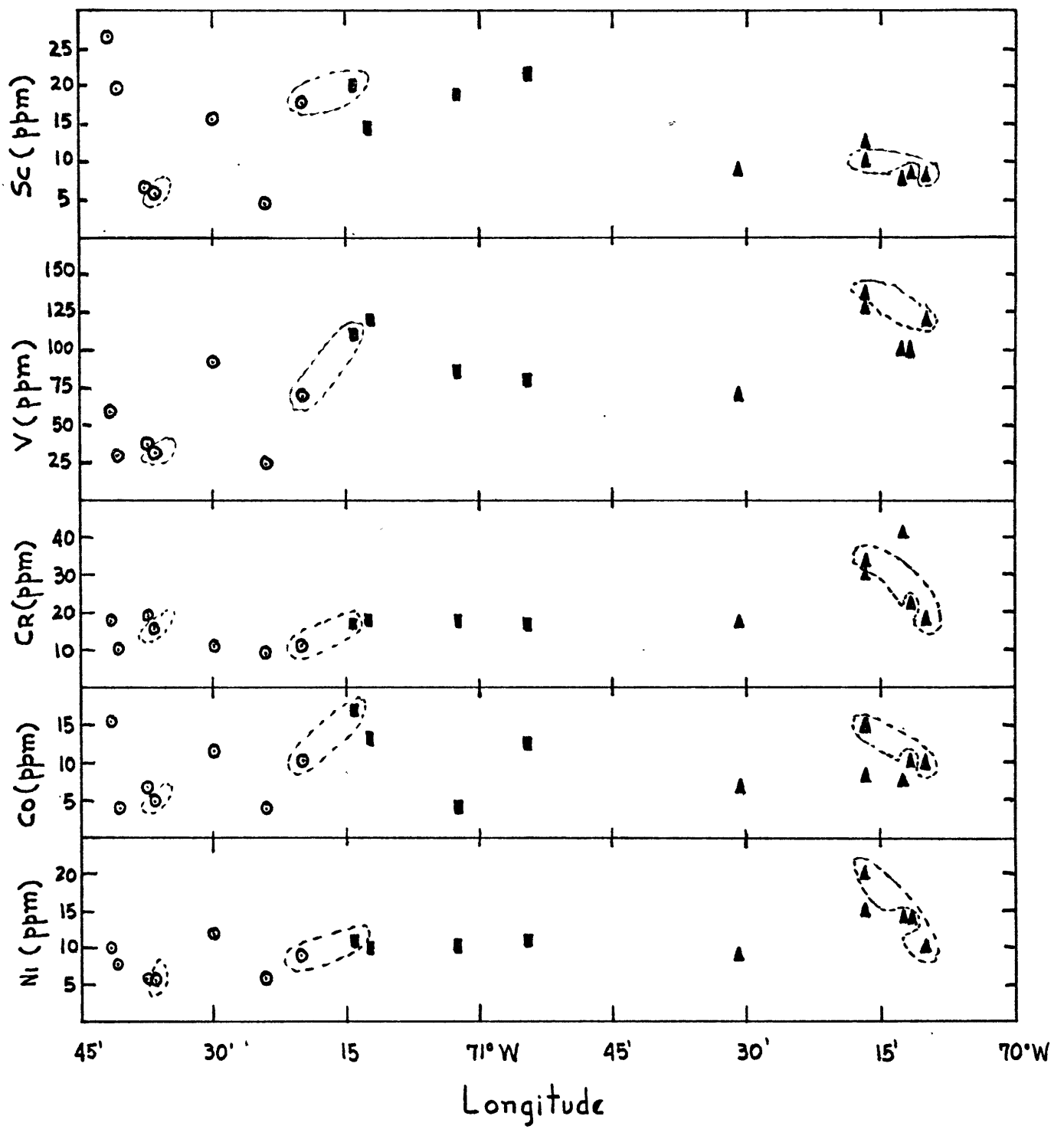


Figure 25

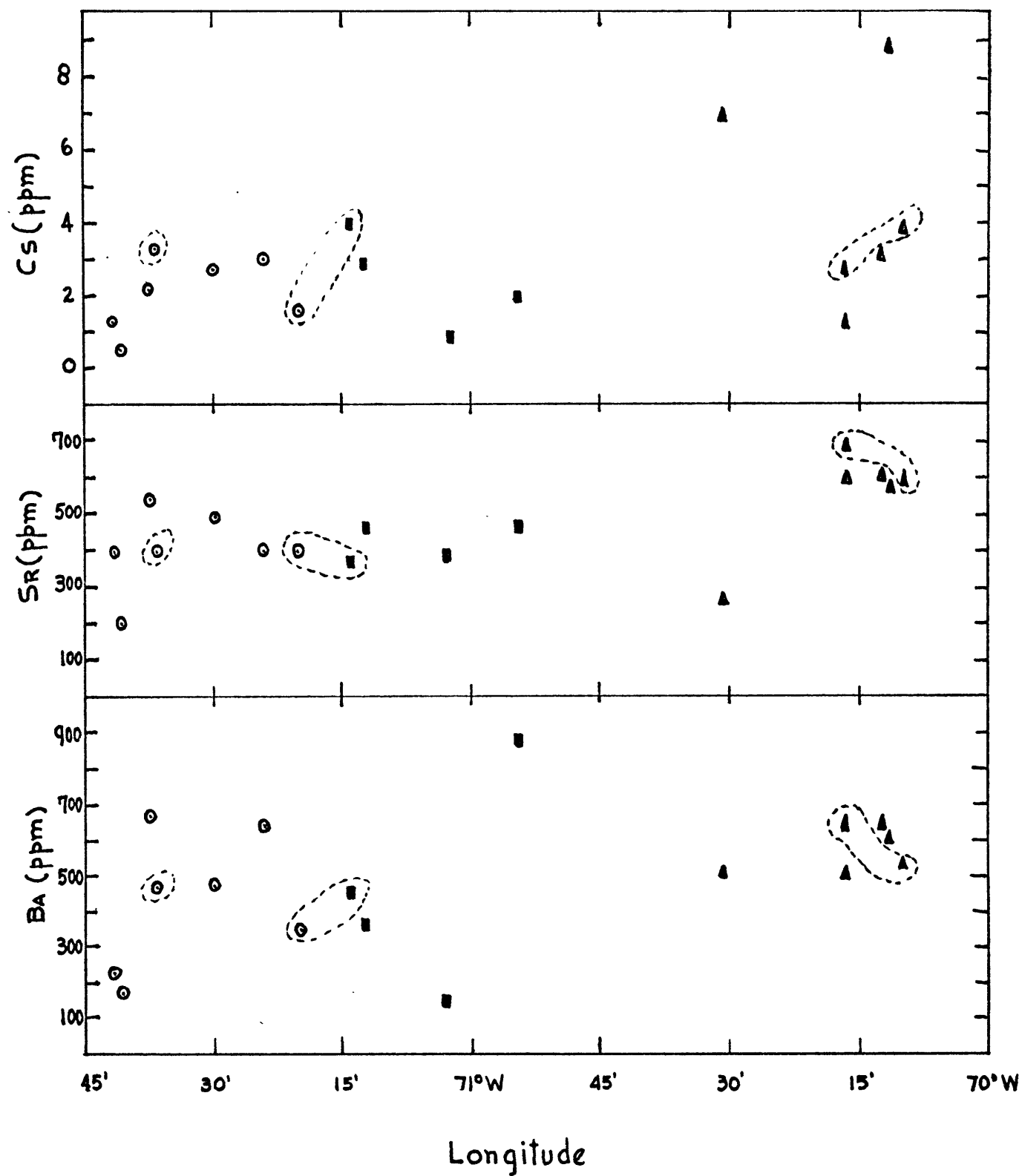


Figure 25 (continued)

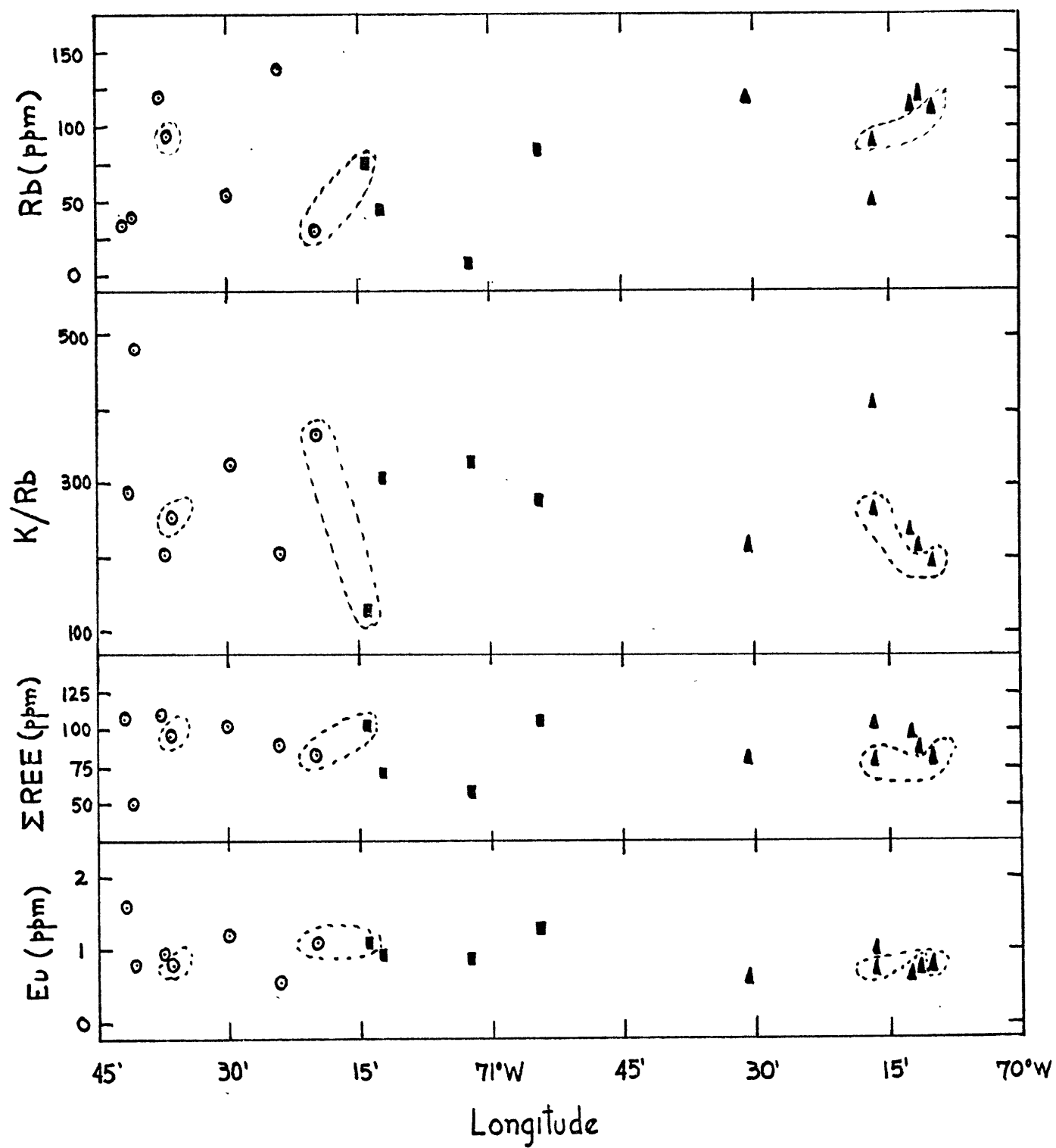


Figure 25 (continued)

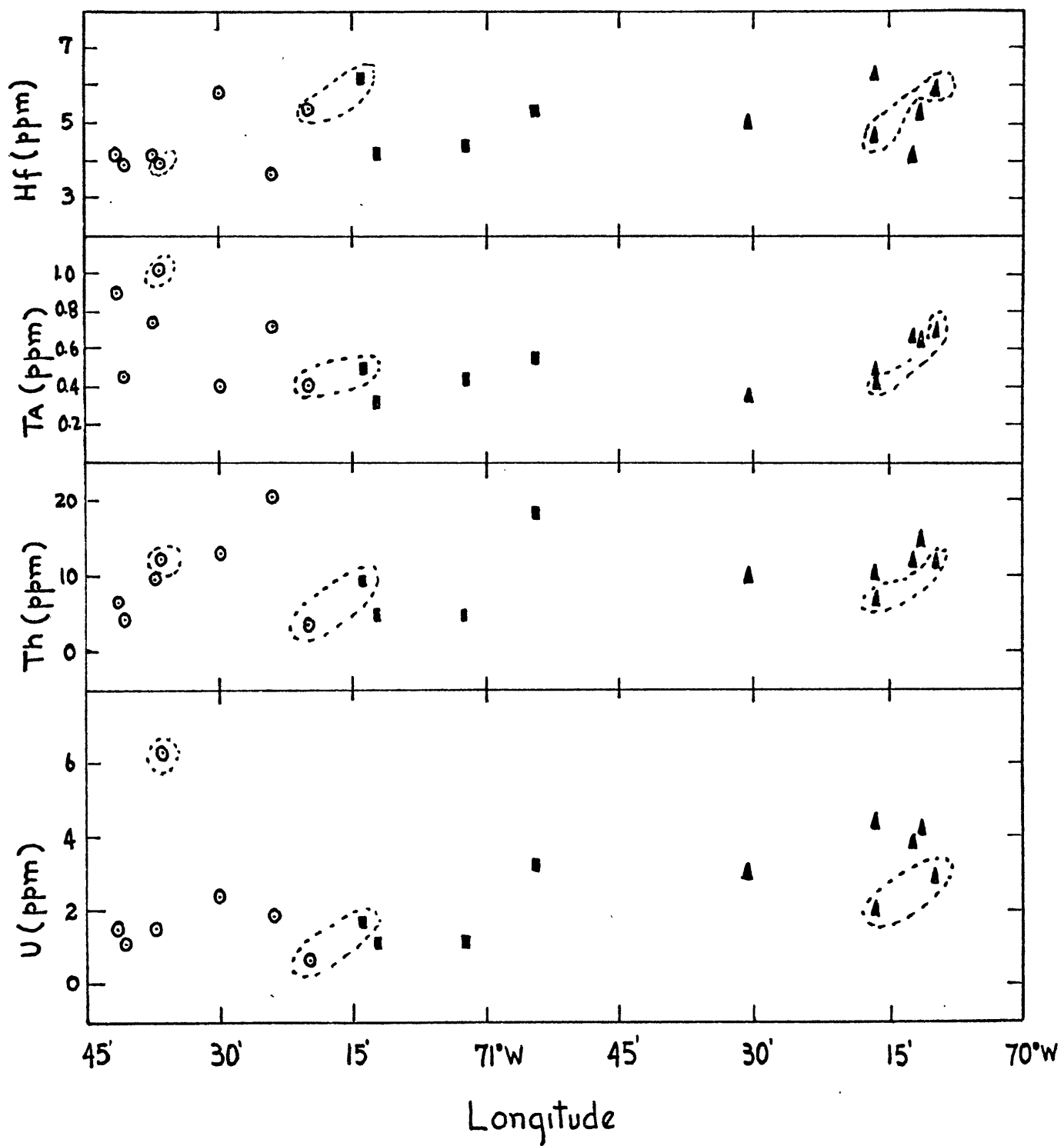


Figure 25 (continued)

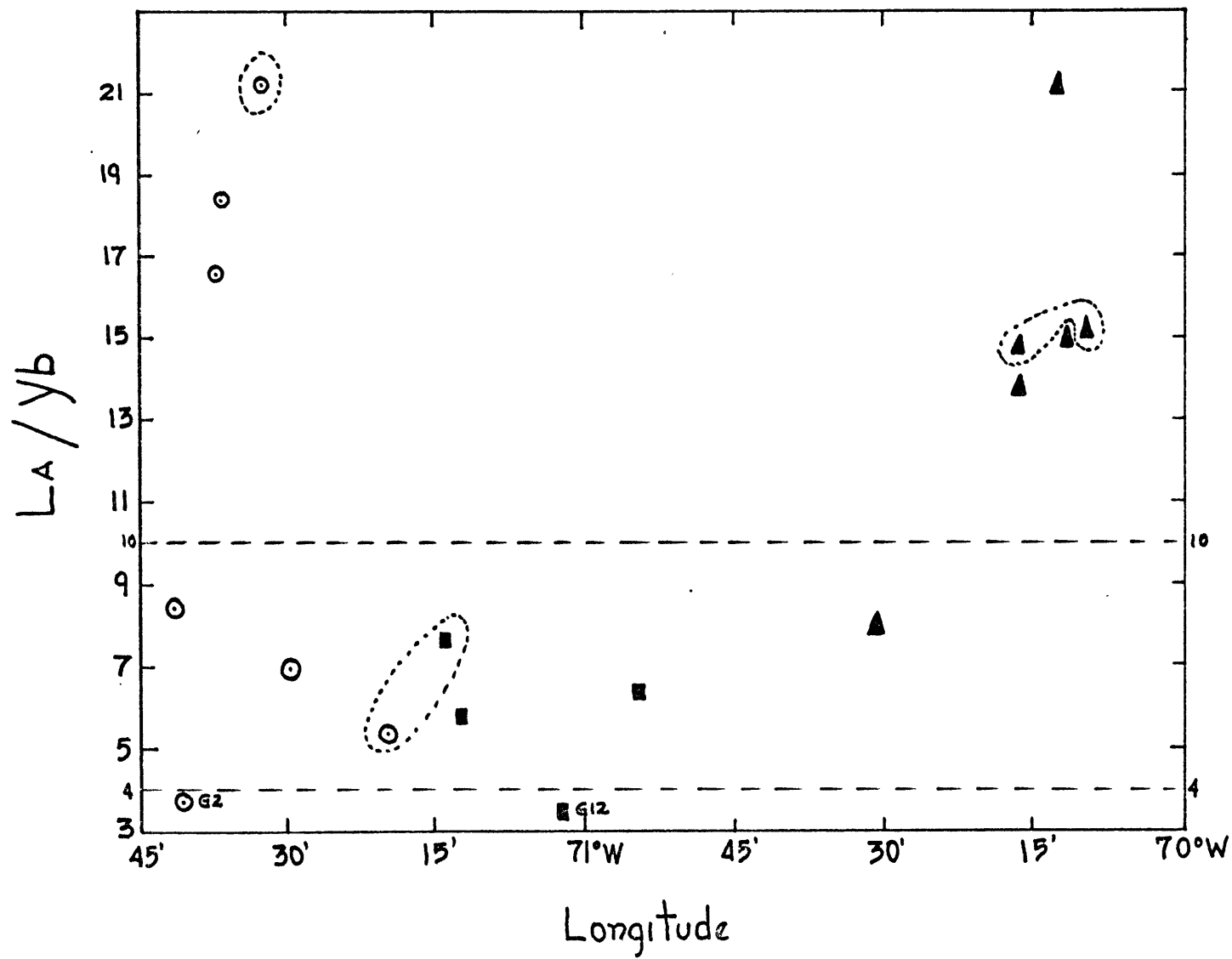


Figure 25 (continued)

Figure 26: REE abundances of the central Chile granitoids normalized to a chondritic average (Frey et al., 1968) a) Coastal batholith tonalites, b) Coastal batholith granodiorites c) Central batholith plutonic rocks d) Andean batholith plutonic rocks.

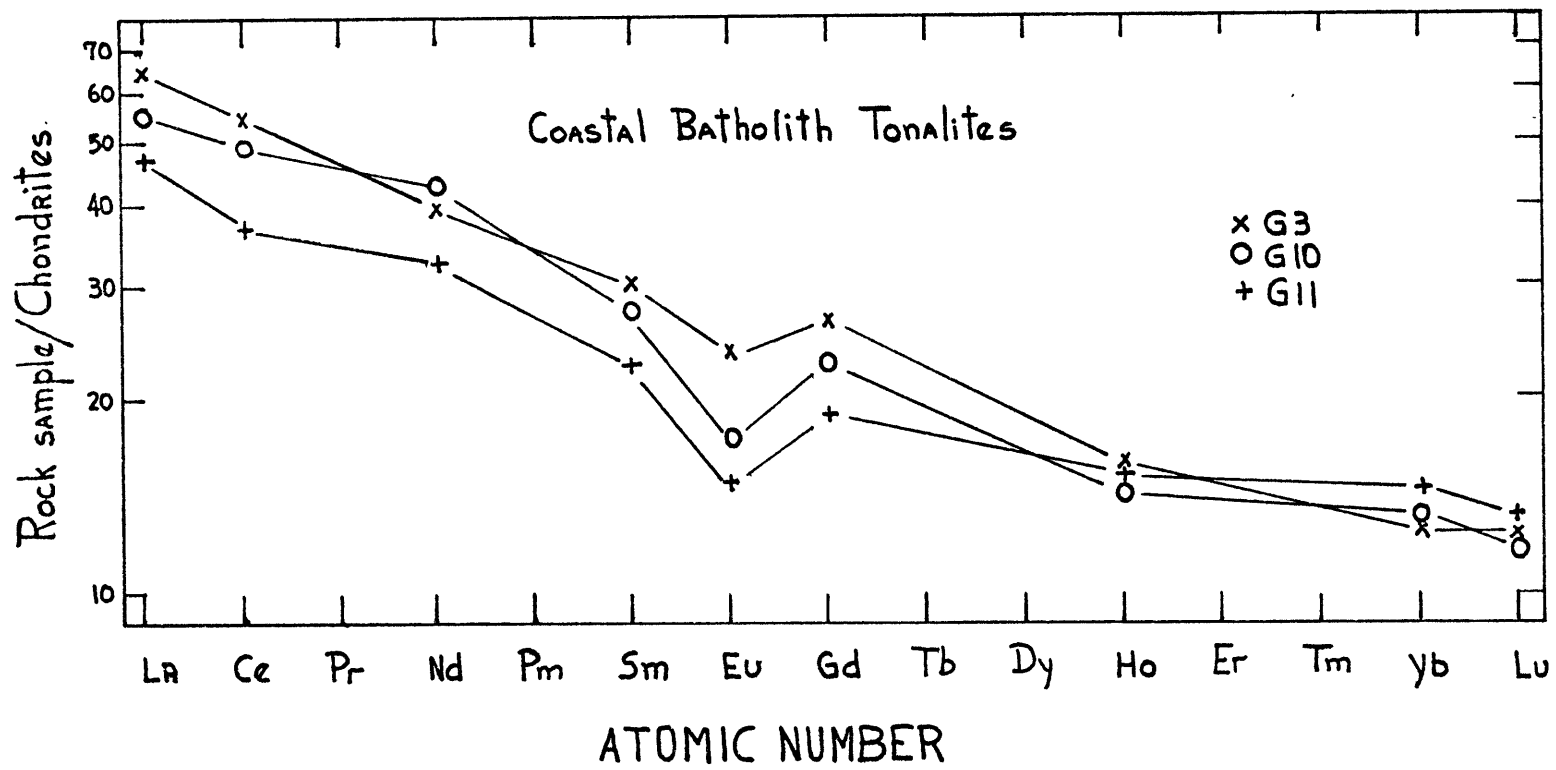


Figure 26

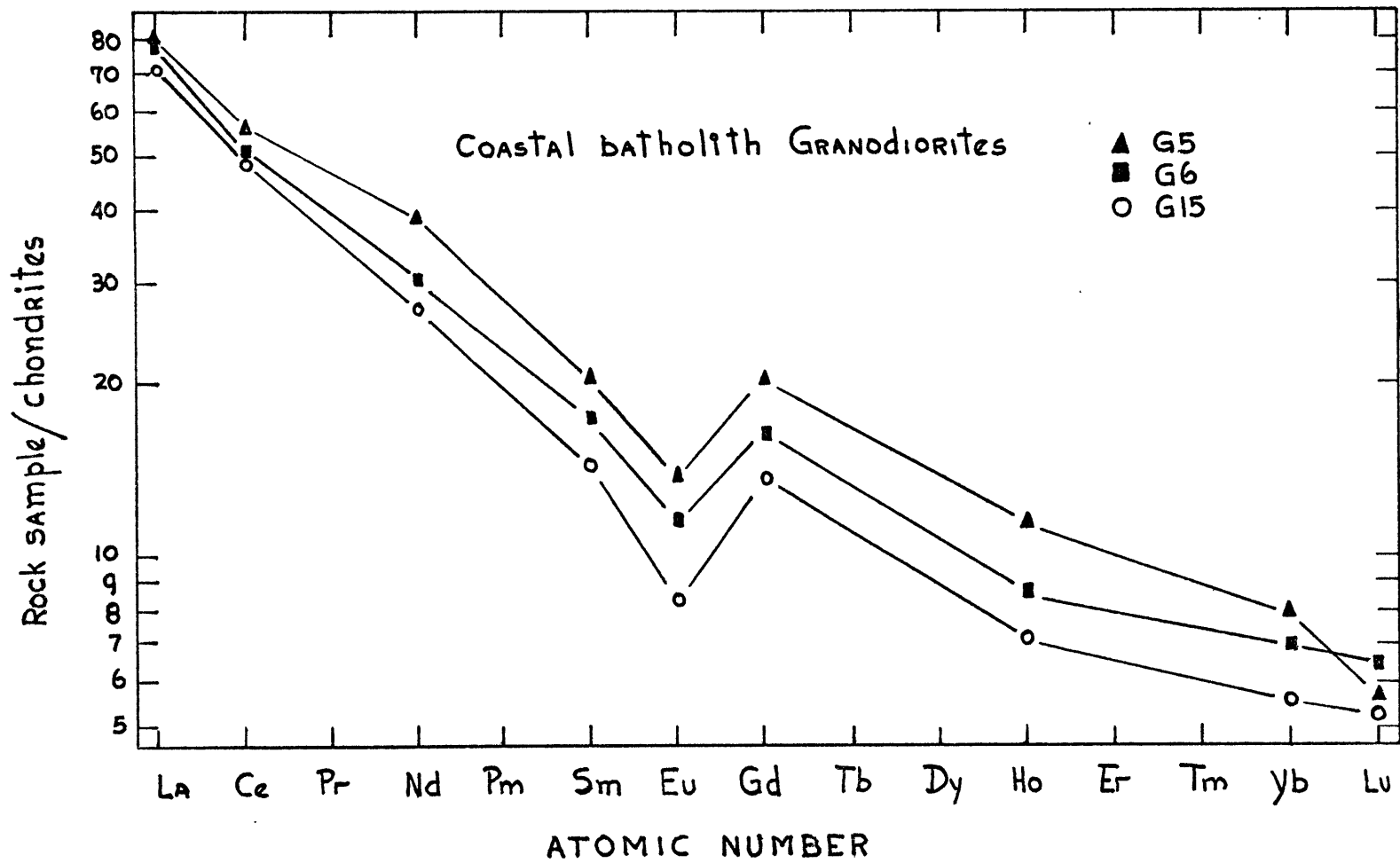


Figure 26 (continued)

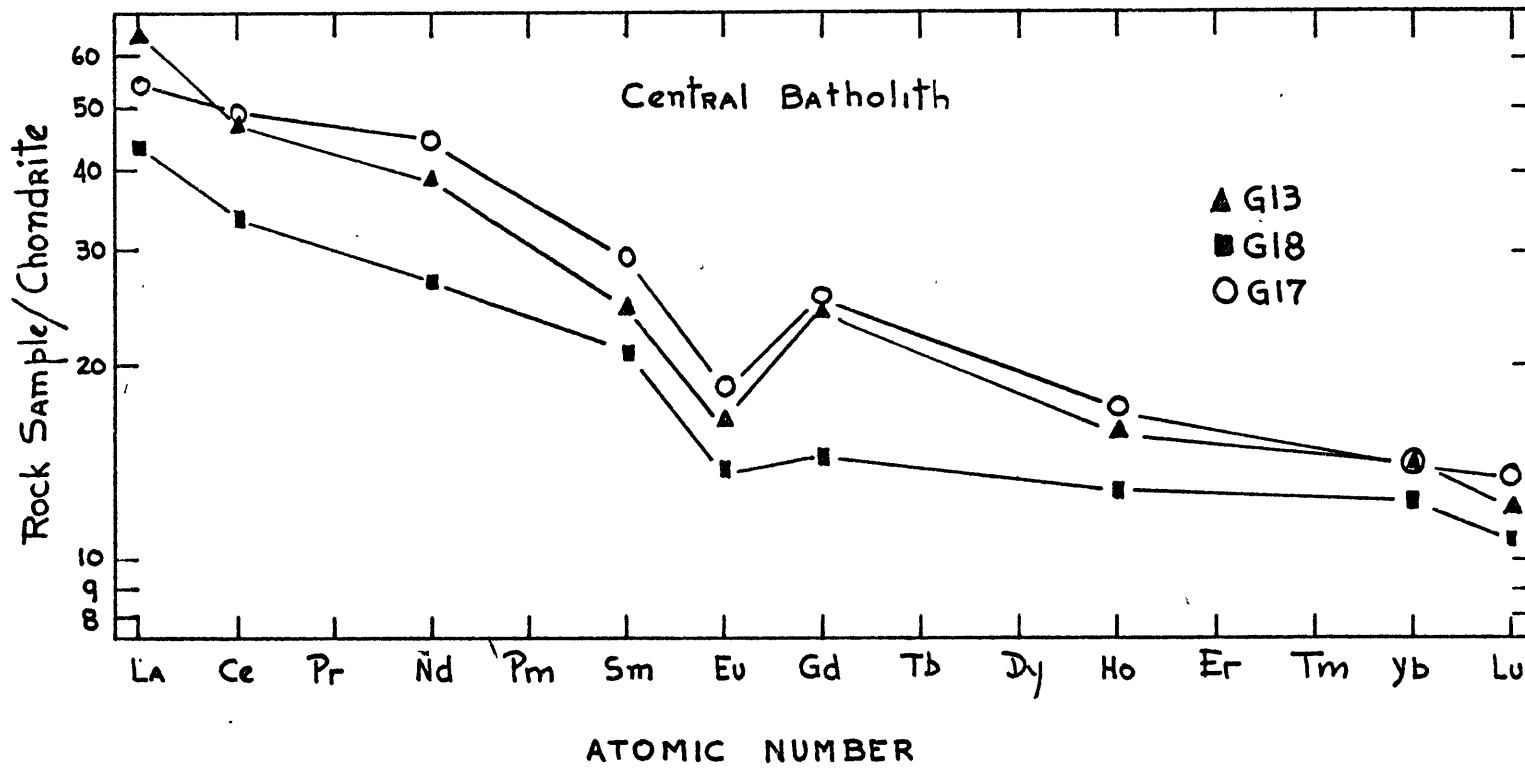


Figure 26 (continued)

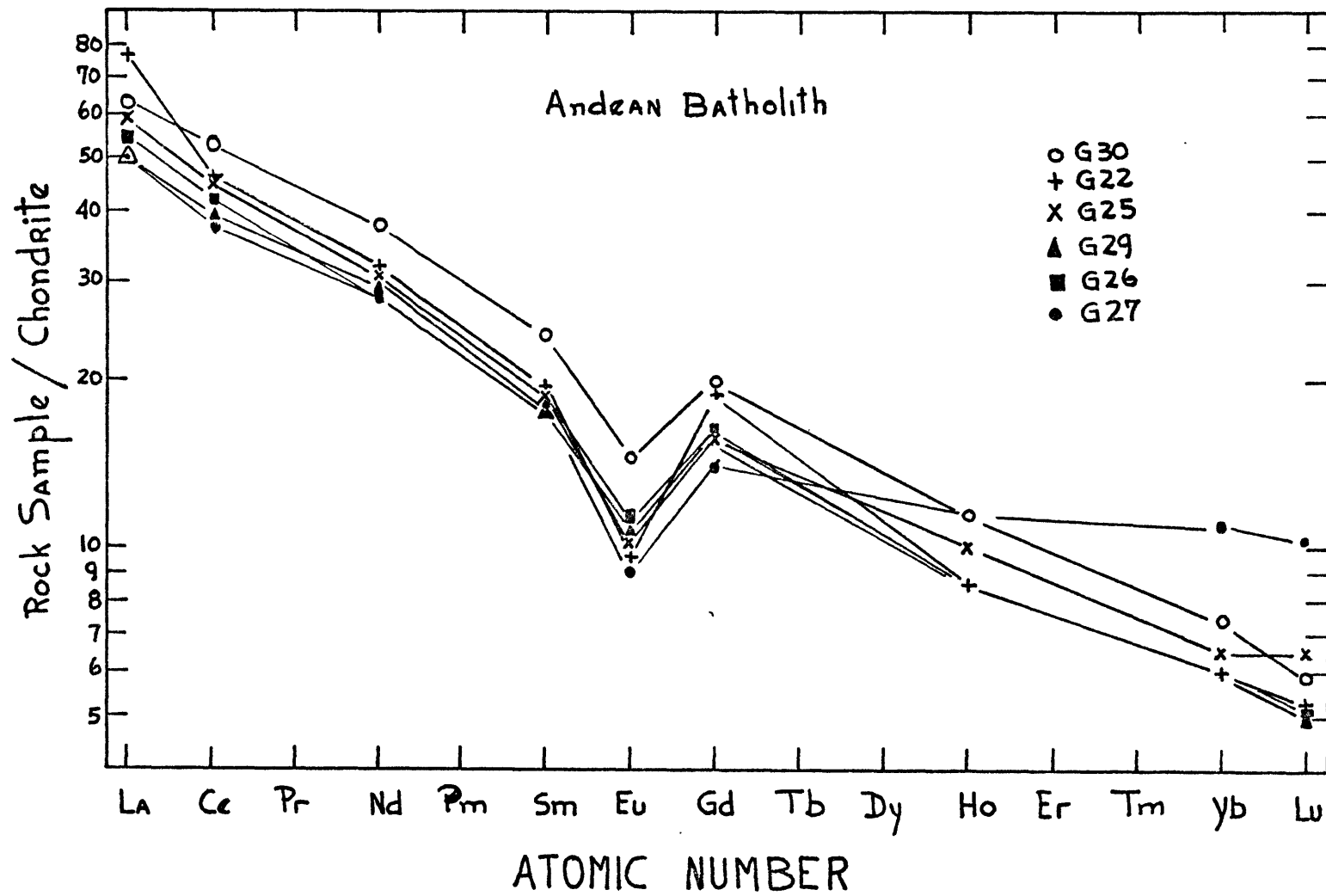


Figure 26 (continued)

Figure 27: REE abundances normalized to a chondritic average (Frey et al.; 1968). Average of the Coastal batholith granodiorites. Average of the Andean batholith granodiorites and average of some granitoids from Sierra Nevada (H. Noyes, personal communication).

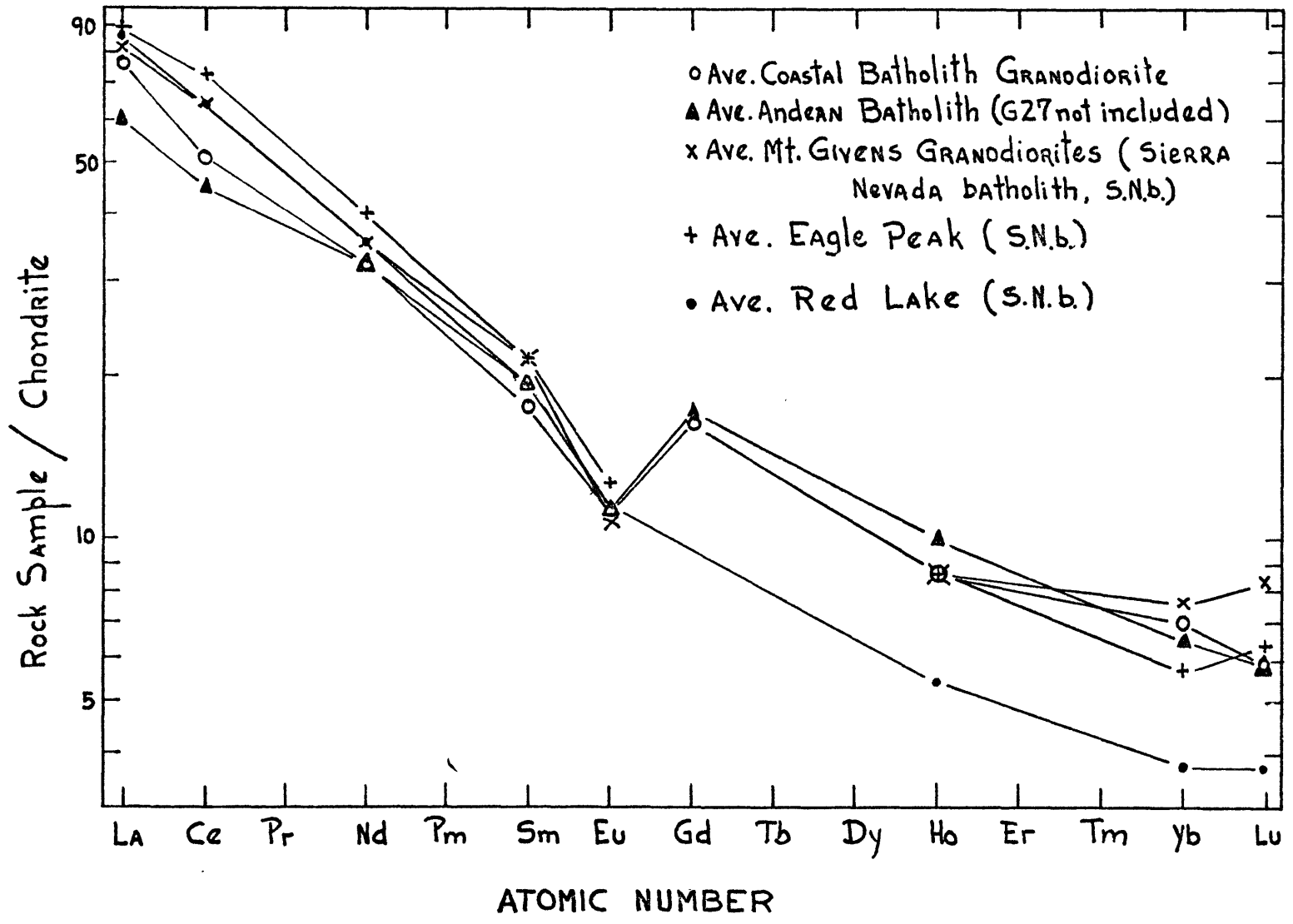


Figure 27

Figure 28: REE abundances normalized to a chondritic average (Frey et al., 1968). Average of the Coastal batholith tonalites. Average of samples G13 and G17 (from Cental batholith). Average of the Central batholith rocks analyzed. Average circumpacific granodiorites (Taylor, 1969). Bonsall tonalite (Southern California batholith, Towell et al., 1965). Woodson Mt. granodiorite (Southern California batholith, Towell et al., 1965).

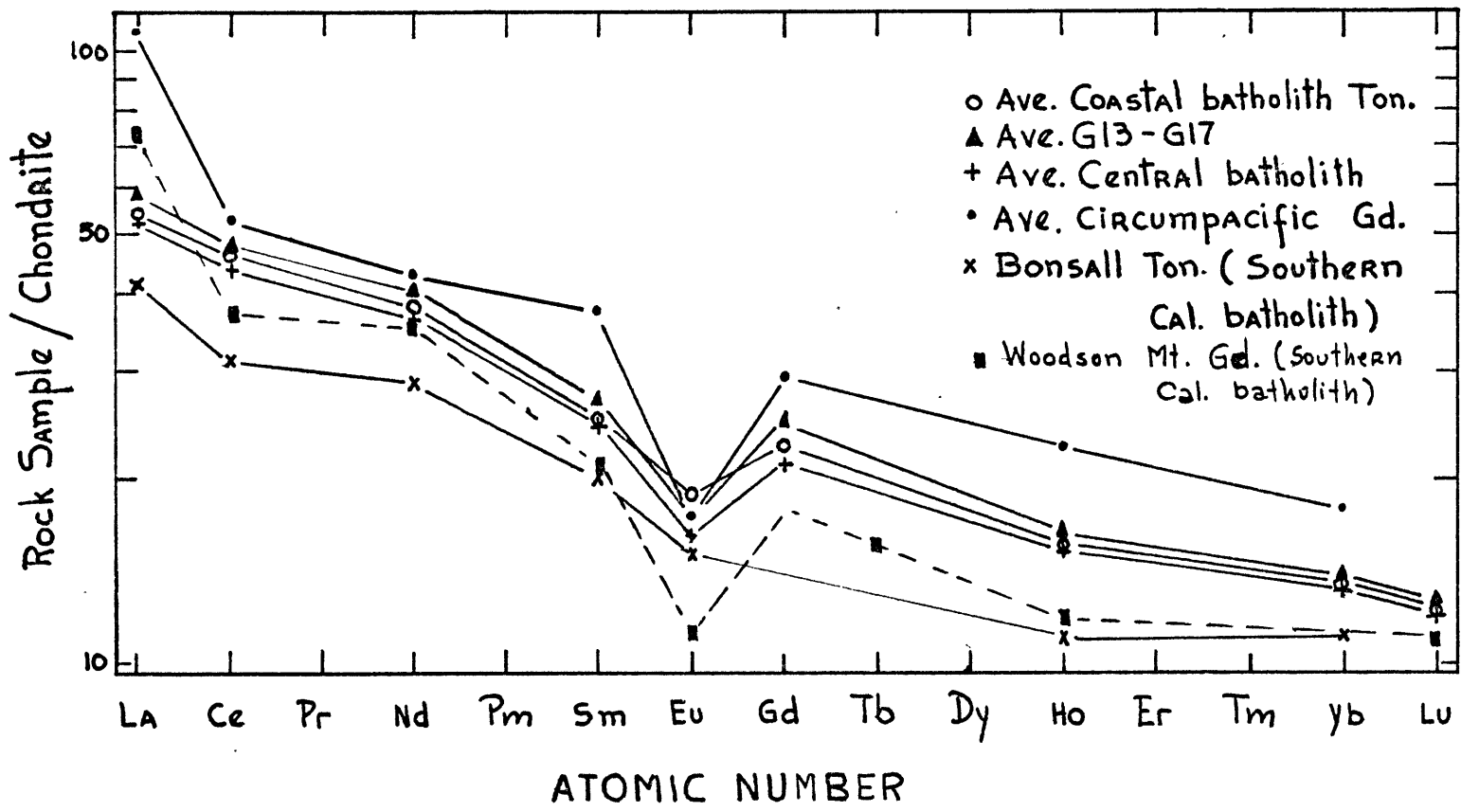


Figure 28

Figure 29: REE abundances normalized to a chondritic average (Frey et al., 1968). Sample G2 (Coastal batholith granite), sample G12 (Central batholith tonalite), Average Coastal batholith tonalite and sample T3 (the most differentiated andesite from Temuco).

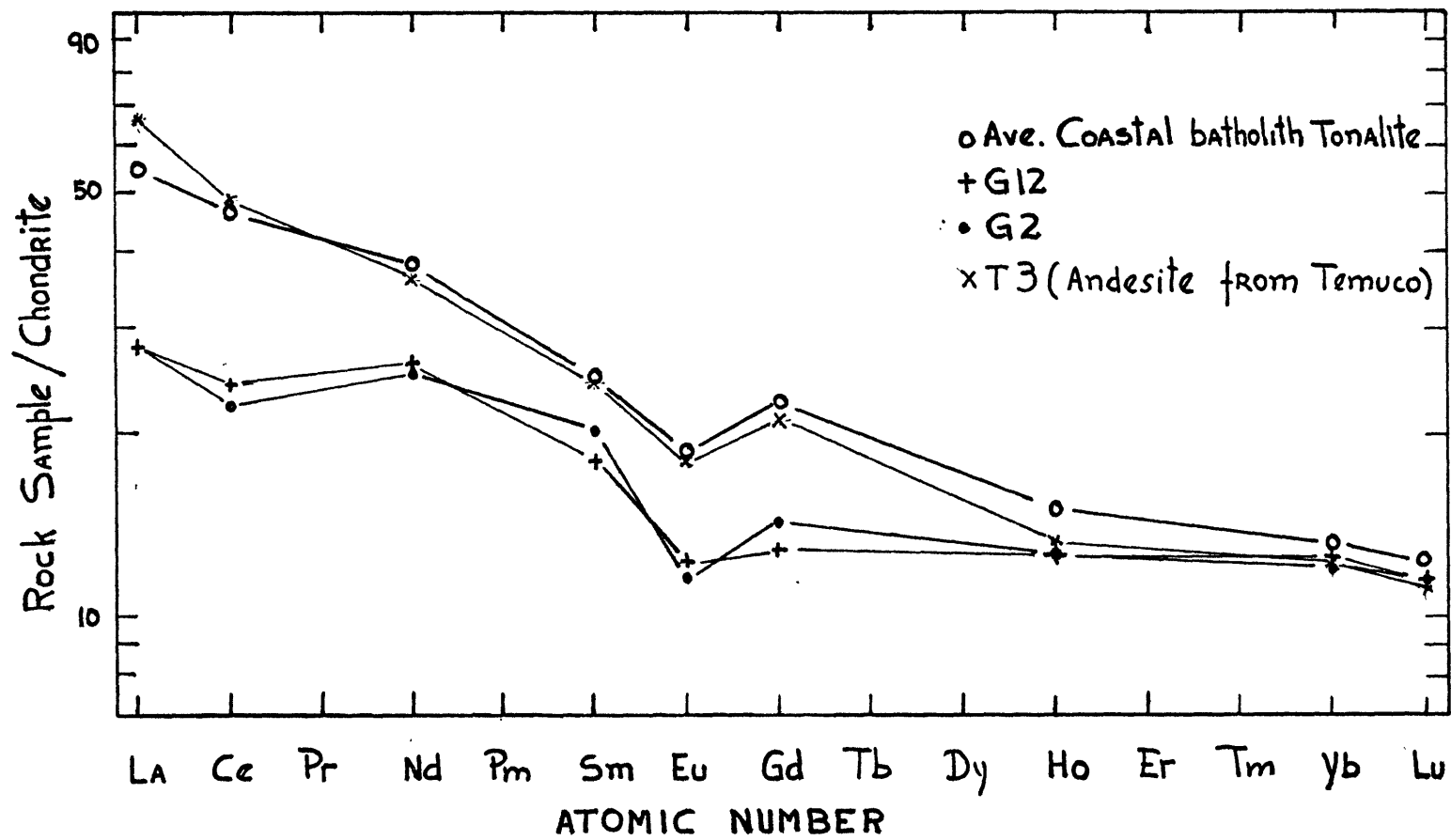


Figure 29

Figure 30: Solid/liquid rare-earth partition coefficients for amphiboles. Data for 2Hb, 3Hb and 8Hb from Nagasawa and Schnetzler, 1971.

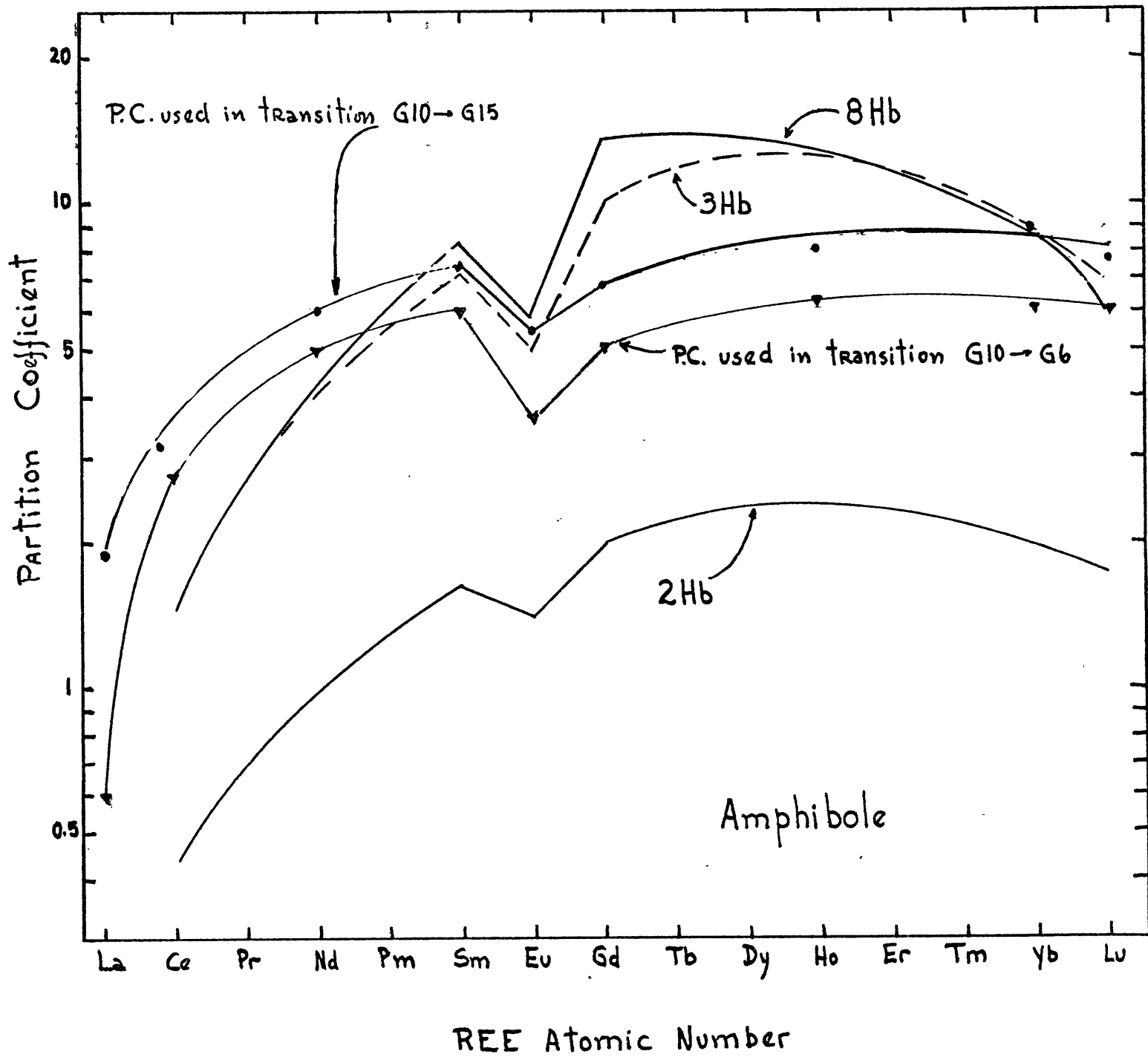


Figure 30

Figure 31: Solid/liquid rare-earth partition coefficient for plagioclases. Data from Schnetzler and Philpotts, 1970.

Figure 31

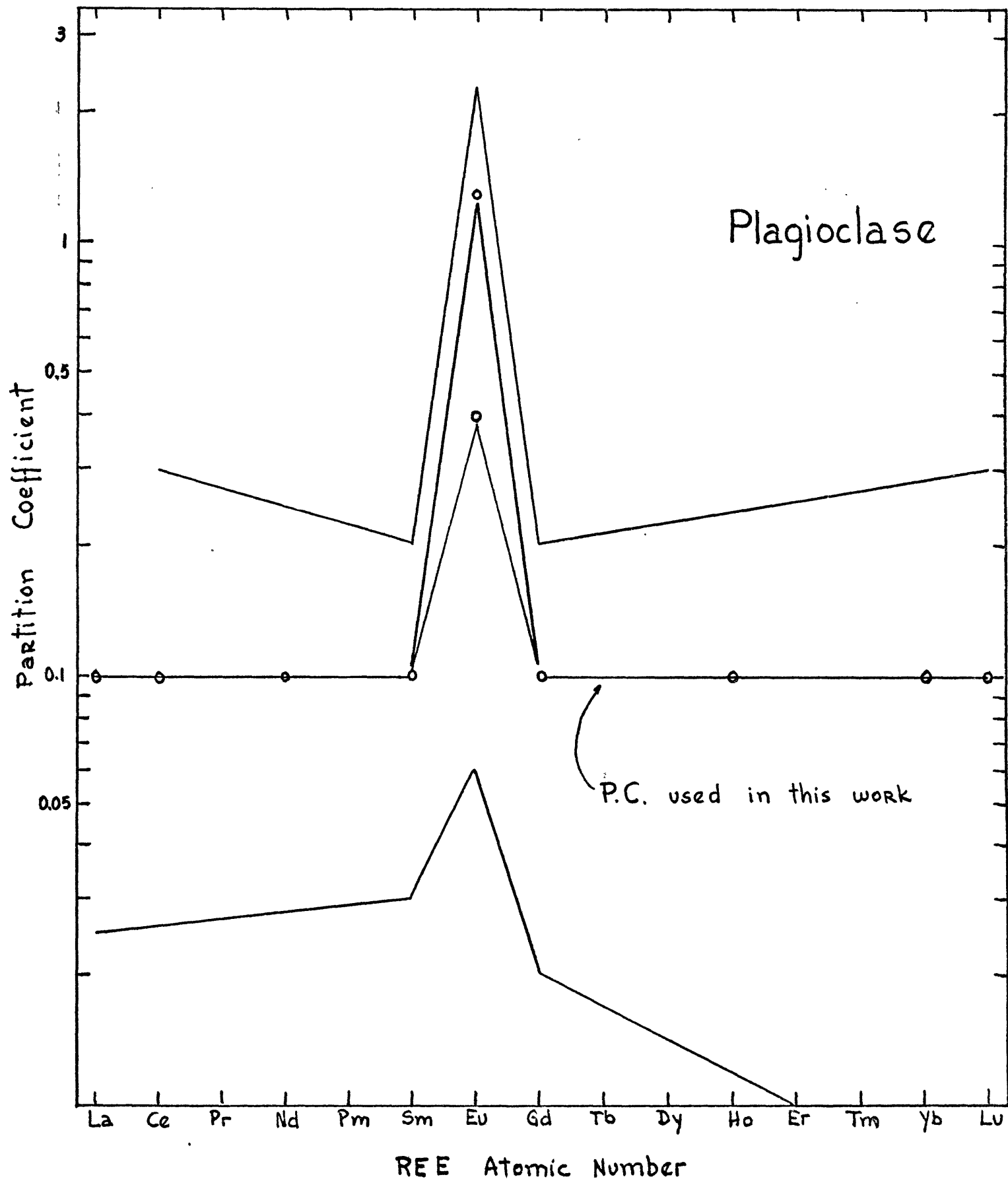


Figure 32: Eu partition coefficients as a function of the plagioclase composition. \odot are from Schnetzler and Philpotts, 1970. \blacktriangle are from Dudas et al., 1971. \blacksquare are from Nagasawa and Schnetzler, 1971. \times is a value in K-feldspar from Schnetzler and Philpotts (1970). \bullet value used in this work.

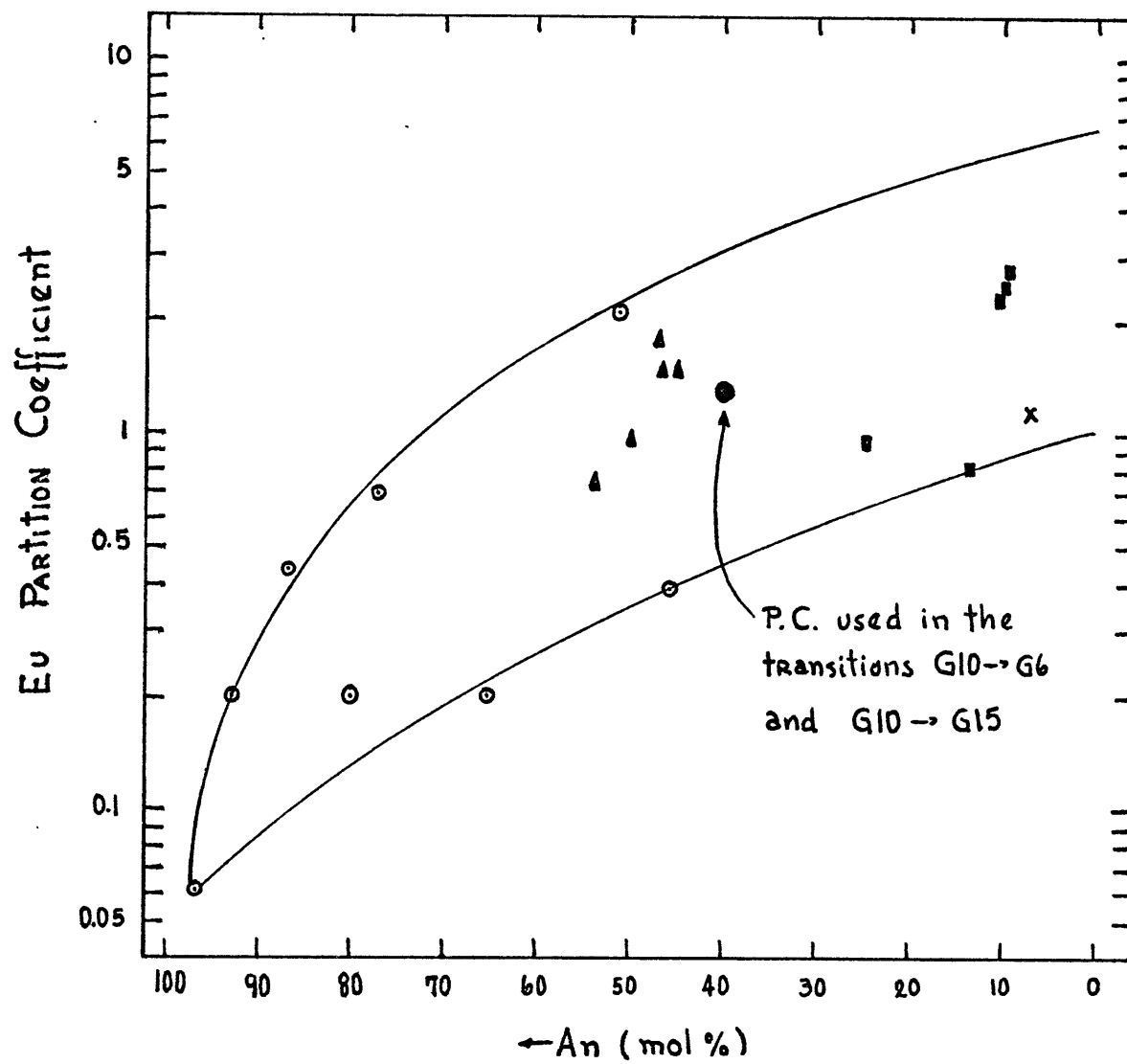


Figure 32

Figure 33: Solid/liquid rare-earth partition coefficients for a biotite. Data from Schnetzler and Philpotts, 1970.

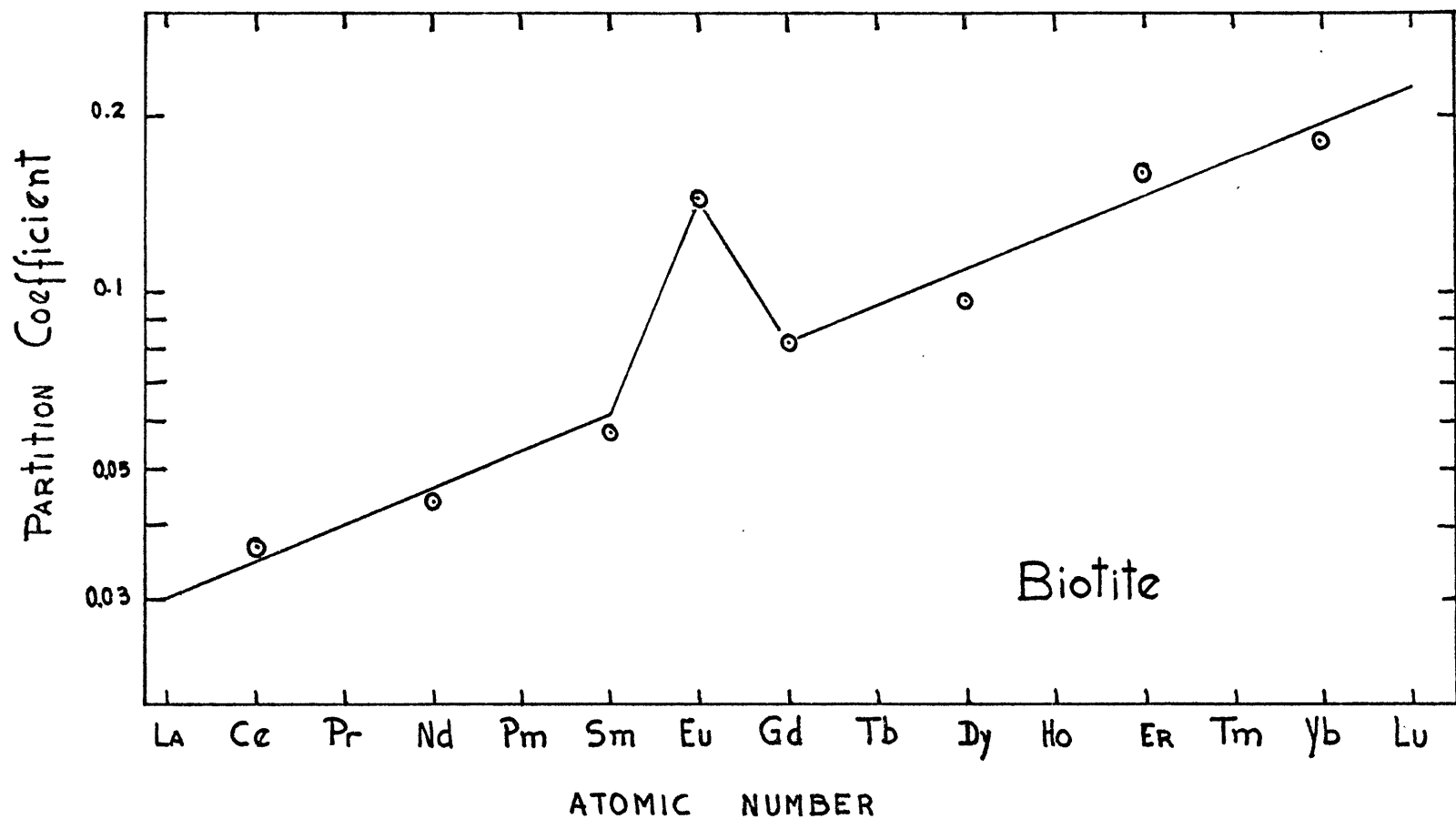


Figure 33

Figure 34: Solid/liquid partition coefficients for clinopyroxene. Data from Table 4.

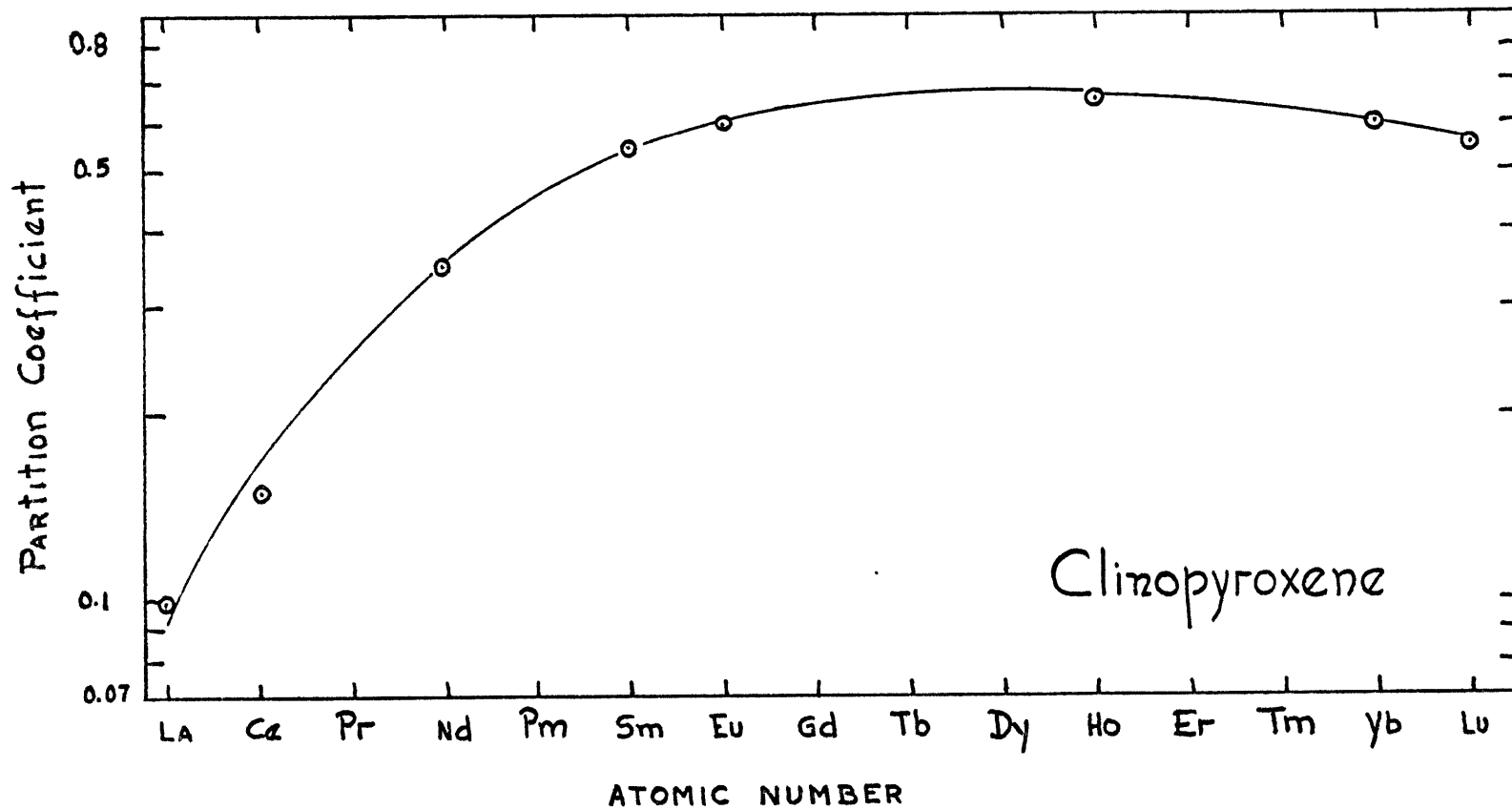


Figure 34

Figure 35: REE abundances normalized to a chondritic average (Frey et al., 1968). Sample T2 (andesite from Temuco), average circumpacific andesite T3 (andesite from Temuco, more differentiated than T2), G10 (Coastal batholith tonalite). REE pattern that results by subtracting from T2, 25% cpx and 25% plag.

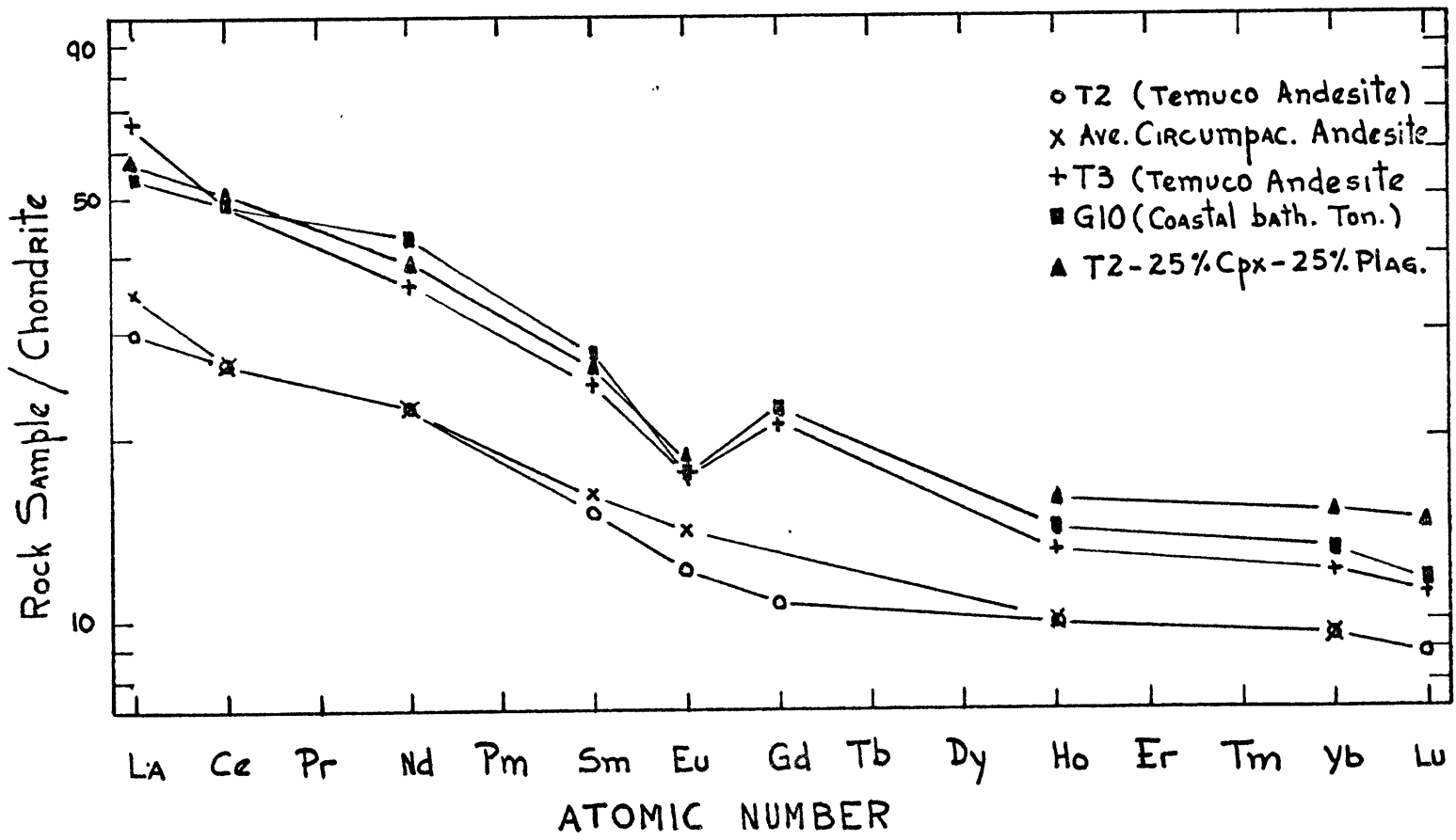


Figure 35

Figure 36: Sr partition coefficients as a function of the plagioclase composition. Source of the data is the same as for Figure 32.

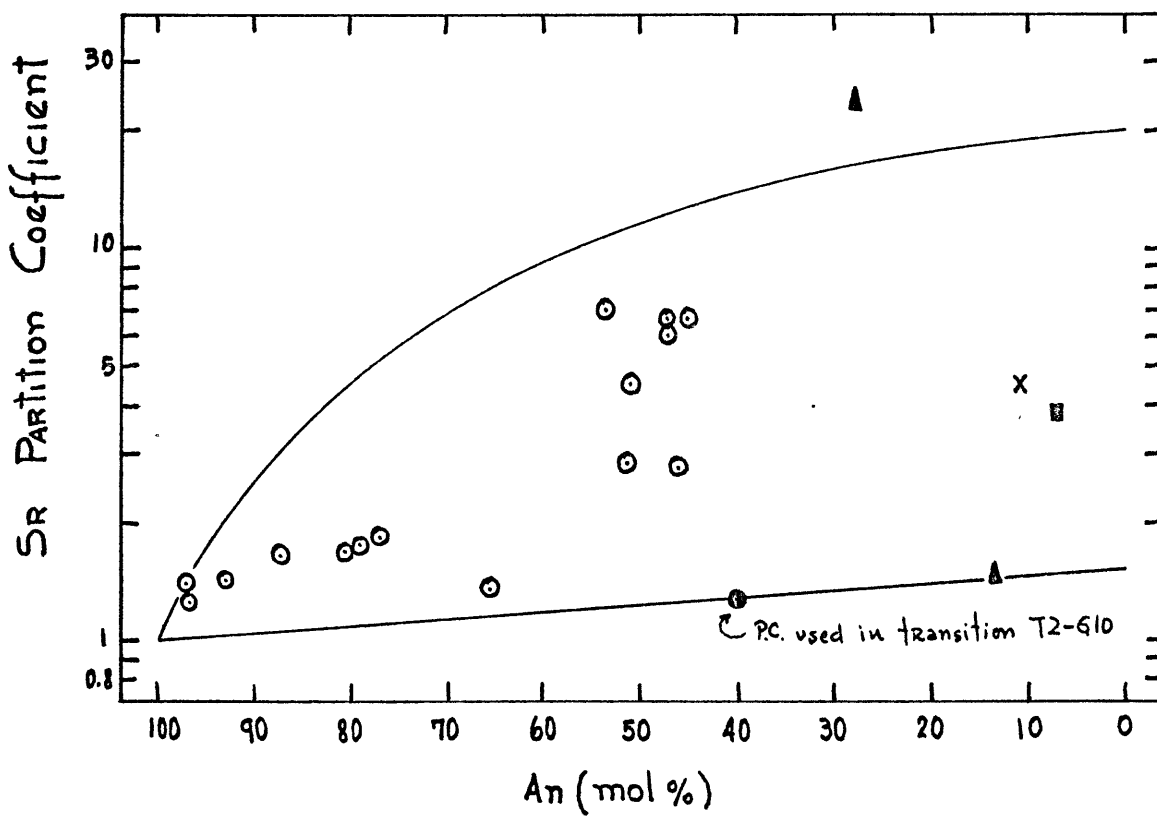


Figure 36

Figure 37: Ba partition coefficients as a function of the plagioclase composition. The source of the data is the same as for Figure 32.

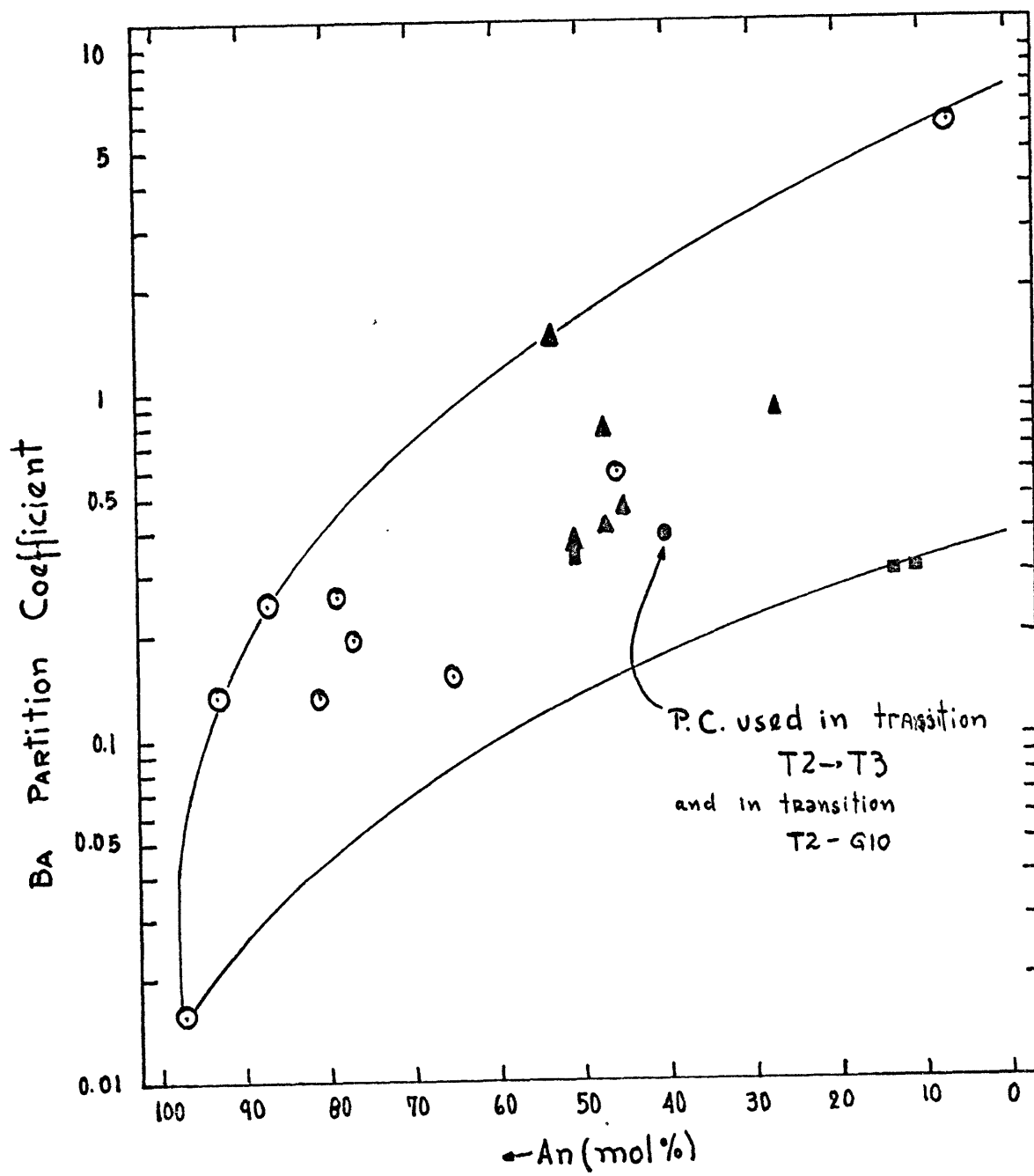


Figure 37

Figure 38: Comparison of REE abundances of samples G6 and G15 with chondritic normalized REE abundances in theoretical liquids derived by fractional crystallization (Gast, 1968). The parent rock is G10. REE partition coefficients for plagioclase are 0.1, except for Eu that is 1 for the transition G10 to G6, and 1.3 for the transition G10 to G15. REE partition coefficients for clinopyroxene are shown in Table 5 and in Figure 30. REE partition coefficients for biotite are shown in Figure 33.

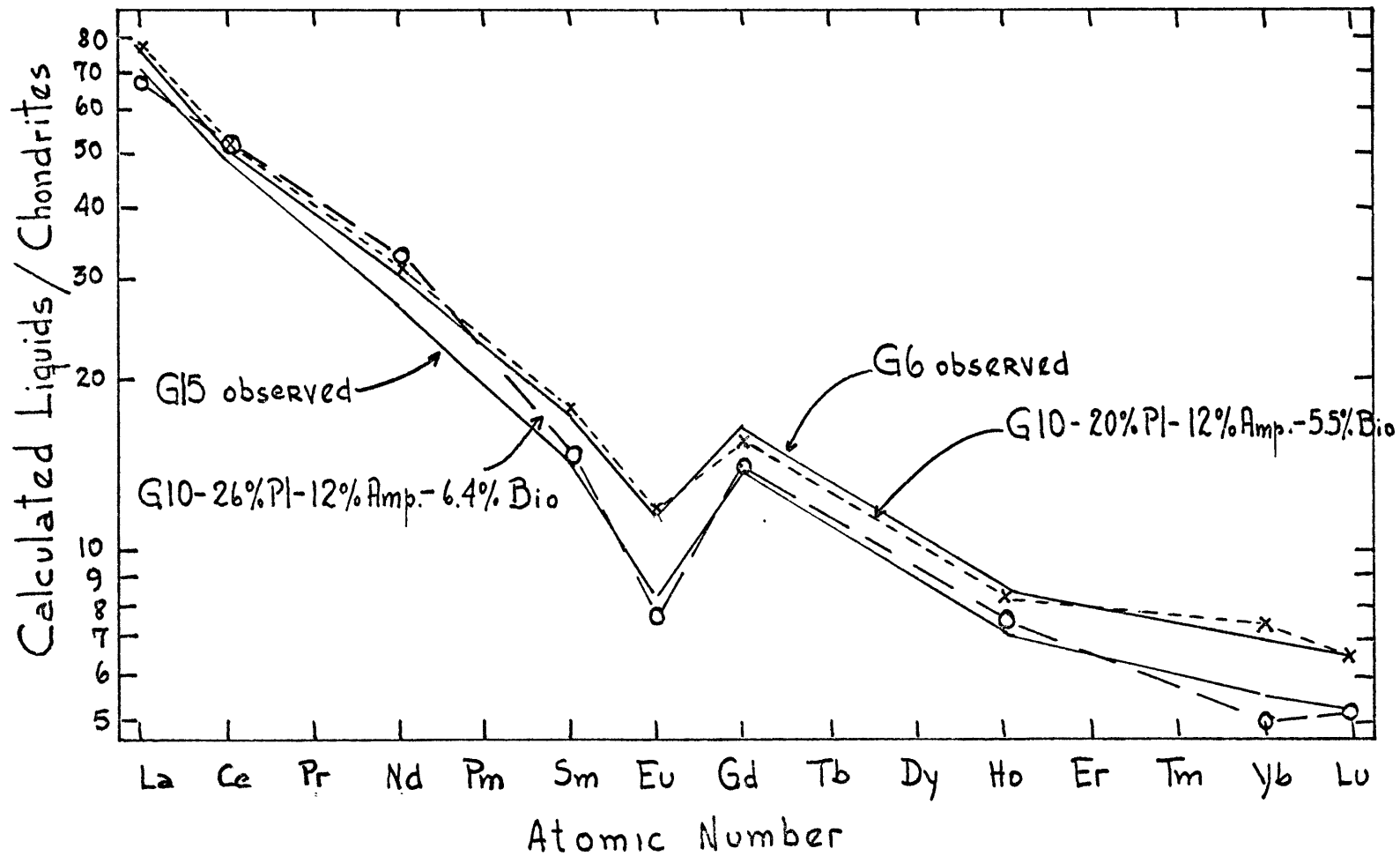


Figure 38

Figure 39: Schematic diagram of the gamma ray spectrometry equipment used.

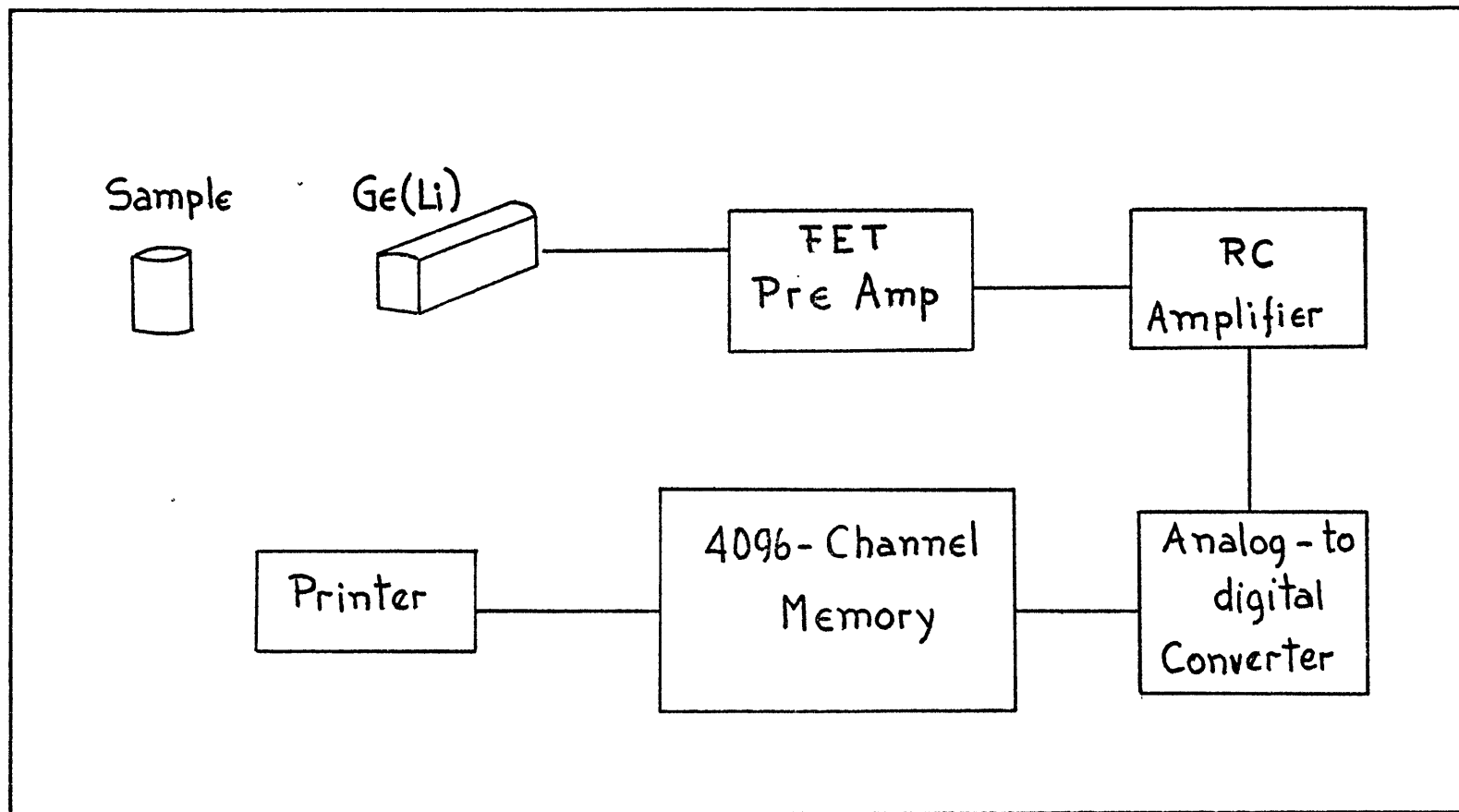


Figure 39

ACKNOWLEDGEMENTS

I am grateful to Professor F. A. Frey who inspired and supported this study, for his valuable comments and discussions. I am indebted to Professor J. Oyarzun of the Universidad del Norte (Chile) and to Professor M. Vergara of the Universidad de Chile for all the collaboration they rendered to me during the development of this work. I am grateful to Dr. A. J. Irving and to my fellows Beverly Carroll, Don Skibo, Harry Noyes, Rudolf Hon, Chien Ming Sung, John Suen for their collaboration and discussions. I thank Dr. A. Parkes for his collaboration in the electron microprobe determinations. Finally, I am grateful to Mrs. Linda Ingham who kindly collaborated in typing this thesis.

BIOGRAPHICAL INFORMATION

Leopoldo Lopez-Escobar

Born: 1940. Santiago, Chile

Education: B.A. Biology and Chemistry. Catholic University of Chile, 1963

M.S. in Earth and Planetary Sciences, MIT

Thesis: "Appalachian Rhyolites: Geochemical Data Concerning their Origin", 1972

M.S. in Chemistry, MIT, 1972

Thesis: "Determination of Trace Mercury in Organic Matrices by Flameless Atomic Absorption"

Professional Positions:

Teaching Assistant, Catholic University of Chile, 1961

Assistant Professor, Chemistry. Austral University of Chile (1963-1966)

Associate Professor, Chemistry. Austral University of Chile (1967-1969)

Graduate Student, Chemistry. MIT, 1969-1972

Graduate Student, Geochemistry, MIT, 1970 to present.

Professional Societies:

Geological Society of America

Sigma xi

The American Association for the Advancement of Science

Research Interests:

Petrogenesis and geochemistry of igneous rocks with emphasis on abundance and geochemical significance of trace elements, applications of nuclear chemistry to geochemistry; study of geological material in lung tissue.